GEOLOGY, GEOCHEMISTRY, AND GEOCHRONOLOGY OF OLIGOCENE MAFIC DIKES NEAR RILEY, NEW MEXICO

by
Melissa I. Dimeo

Submitted in Partial Fulfillment of the
Requirements of the Degree of
Masters of Science in Geochemistry
May 2008

Department of Earth and Environmental Science
New Mexico Institute of Mining and Technology
Socorro, New Mexico, USA

ABSTRACT

Mafic dikes near Riley, New Mexico are a subswarm of the large-diameter Magdalena Radial Dike Swarm (MRDS). The MRDS radiates from the westward-younging Oligocene Socorro-Magdalena caldera cluster of the Mogollon-Datil volcanic field. The Riley dikes form the north-central portion of the MRDS and lie on the southeast corner of the Colorado Plateau. The dikes trend between NNW and NNE, perpendicular to the regional extension direction of the early Rio Grande rift. The Riley dikes are more numerous and closely spaced than elsewhere in the MRDS. This study examines the age, mineralogy, petrology, and geochemistry of the Riley dike swarm. The dikes have a lithospheric mantle source and show age correlations with local caldera-forming eruptions.

Eight Riley dikes were dated by the $^{40}Ar/^{39}Ar$ method as between 25.21±0.30 Ma and 29.19±0.26 Ma. Seven dated dikes appear to radiate northward from the coeval Sawmill Canyon, Hardy Ridge, and Mt. Withington calderas. The two youngest dated dikes trend NNW and the older dikes trend NNE, which contradicts a simple radial pattern of emplacement from a deep westward-migrating source under the local calderas. Cross-cutting relationships of the dikes in the field also contradict a simple radial emplacement pattern. The dominant northward strike of the dikes and their coeval age relationships to the calderas are permissible of a relatively fixed magma source under the migrating caldera-forming eruptions.

Based on field occurrences, thin section textures, and mineral chemistry dikes are subdivided into: basaltic, basaltic with significant biotite, minette, analcime-bearing, and analcime-bearing speckled texture. Basaltic dikes contain phenocrystic clinopyroxene, olivine, and groundmass plagioclase ± olivine ± fine biotite. Some basaltic dikes contain phenocrystic biotite, K-feldspar ± plagioclase ± clinopyroxene ± olivine. Minettes are recognizable in the field by the presence of biotite clots. Minettes also contain K-feldspar ± clinopyroxene. Analcime-bearing dikes contain high-calcium clinopyroxene, olivine, sparse biotite, and intergrown analcime and potassium feldspar after leucite. Analcime-bearing speckled texture dikes contain partially assimilated xenoliths of sanidine, biotite, and pyroxene mixed with analcime within a groundmass of plagioclase and clinopyroxene , as observed in thin section. Electron backscatter images show speckled texture dikes contain intersertal analcime and laths of K-feldspar and plagioclase and lack apparent xenolithic or mixing textures. Magnetite is an abundant minor phase in all the dikes and apatite is common in minettes and analcime-bearing dikes.

Most dikes near Riley probably did not reach the Oligocene land surface. About two-thirds of the basaltic and minette dike samples are autometasomatized by magmatic CO_2 ($\delta^{13}C$ = -3 to -9‰). The CO_2 autometasomatized dikes contain calcite pseudomporphs after pyroxene and olivine(?). Some dikes, usually minettes, contain finely disseminated groundmass carbonate. Analcime-bearing dikes contain little to no carbonate and contain the freshest pyroxenes. One holocrystalline basaltic dike contains little to no carbonate and is bounded by a significant (<20 m-wide) baked wallrock aureole. This dike is interpreted as a lava flow feeder dike that degassed as it vented.

All the dike samples are potassic and most are potassic trachybasalt or shoshonite. Analcime-bearing and minette samples have higher alkali and lower silica contents than basaltic samples. Trace element spiderdiagrams show similar patterns with extreme negative Nb and Ta anomalies and more subtle negative Ti anomalies. These anomalies, coupled with high LILE/HFSE ratios, are consistent with a magma source of partial melt of subduction-modified lithospheric mantle with some crustal contamination. Other lavas in the Mogollon-Datil volcanic field share a similar magma source.

ACKNOWLEDGEMENTS

I want to thank my committee: Richard Chamberlin, Bill McIntosh, Phil Kyle, and Nelia Dunbar. They have been a great source of knowledge, ideas, and enthusiasm.

Lisa Peters, Rich Esser, Matt Heizler, Virgil Lueth, Lynn Heizler, Andrew Campbell, Mike Timmons, Lewis Gillard, and Lara Owens assisted with sample preparation, data interpretation, presentation, organization, funding, printing, and reviewing. A big Thank You! to them and to everyone else I met along the way.

Funding over the years was provided by the Earth and Environmental Science Department, New Mexico Bureau of Geology and Mineral Resources, New Mexico Geological Society Grant-in-Aid, and New Mexico Tech Graduate Student Association Research Grants.

TABLE OF CONTENTS

LIST OF FIGURES

LIST OF TABLES

LIST OF PLATES

This Thesis is accepted on behalf of the faculty
of the Institute by the following committee:

Philip R Kyle
Academic Adviser

Richard M Chamberlin
Research Advisor

Nelson W. Dunbar
Committee Member

William C McIntosh
Committee Member

Committee Member

16 June 2008
Date

I release this document to New Mexico Institute of Mining and Technology

Melissa Bineo 6/16/08

Students Signature Date

1. INTRODUCTION

Dikes are magma-filled fractures that have proved useful in many areas of geologic research and in understanding several crustal processes. For example, Laughlin et al. (1983) used the orientation of parallel dikes of the approximately the same age to infer the regional extension direction at the time of dike emplacement. The age and distribution of dikes have been used to reconstruct volcanic edifices (Ancochea et al., 2008) and giant radial dike swarms (>300 km) have been used to locate mantle plumes (Ernst and Buchan, 2001). Dike swarms are commonly associated with volcanic centers and are considered an integral part of the magmatism (Sigurdsson, 1987).

A large radial mafic dike swarm (~250 km diameter) in central New Mexico surrounds an Oligocene cluster of westward-younging calderas (Chamberlin et al., 2002). Giant radial dike swarms (radii > 300 km) of basaltic composition are often believed to represent mantle plumes (Morgan, 1971) but the dikes of this study are much shorter than those in giant swarms (≥150 km). It is unlikely the region was underlain by a magma source as large as a mantle plume, but a significant heat source must have existed to induce caldera-forming eruptions. The mafic dikes near Riley may represent periodic tapping of this basaltic heat source which may be a lithospheric upwelling due to documented regional extension (Chamberlin, 1983; Aldrich, et al., 1986; Chamberlin and Osburn, 1986; Baldridge et al., 1989 and others) or a “mini-plume” (Chamberlin et al., 2003).

In this study, a subswarm of a larger radial dike swarm, in the vicinity of Riley, New Mexico, was examined. The purpose was to characterize the mineralogy, texture, and chemistry of the Riley dike swarm and relate the dike ages to local caldera eruptions, and to determine the dike magma source. Insight into the formation of the Riley dike swarm involves investigation of several questions: Is there a pattern in trend versus age? Do dike trends correlate with chemistry or petrography? Is there a correlation between dike ages and ignimbrite eruptions? What is the dike magma source and did the source migrate westward with caldera activity? This thesis seeks to address these questions using a combination of field mapping, petrography, mineral chemistry, geochemistry, and geochronology.

1.1 Geologic Setting

The Riley area is located on the southeastern Colorado Plateau near the northern boundary of the Mogollon-Datil volcanic field (MDVF) and is bordered to the east and south by extensional basins of the Rio Grande rift that are superimposed on the volcanic structures of the MDVF (Fig. 1). The dikes near Riley are a subswarm of the large-diameter Magdalena radial dike swarm (MRDS). The MRDS spans 220° of arc (Chamberlin et al., 2002) around the Oligocene Socorro-Magdalena caldera cluster (SMCC) on the northern margin of the MDVF. Dikes of the Riley subswarm are oriented NNE to NNW and were emplaced perpendicular to the tectonic extensional direction of the early Rio Grande rift in late Oligocene time (Chamberlin et al., 2007). The high density (close spacing) of mafic dikes at Riley is attributed to a coaxial relationship between tectonic extension and outward directed (northward) magmatic pressures, from under the caldera cluster.

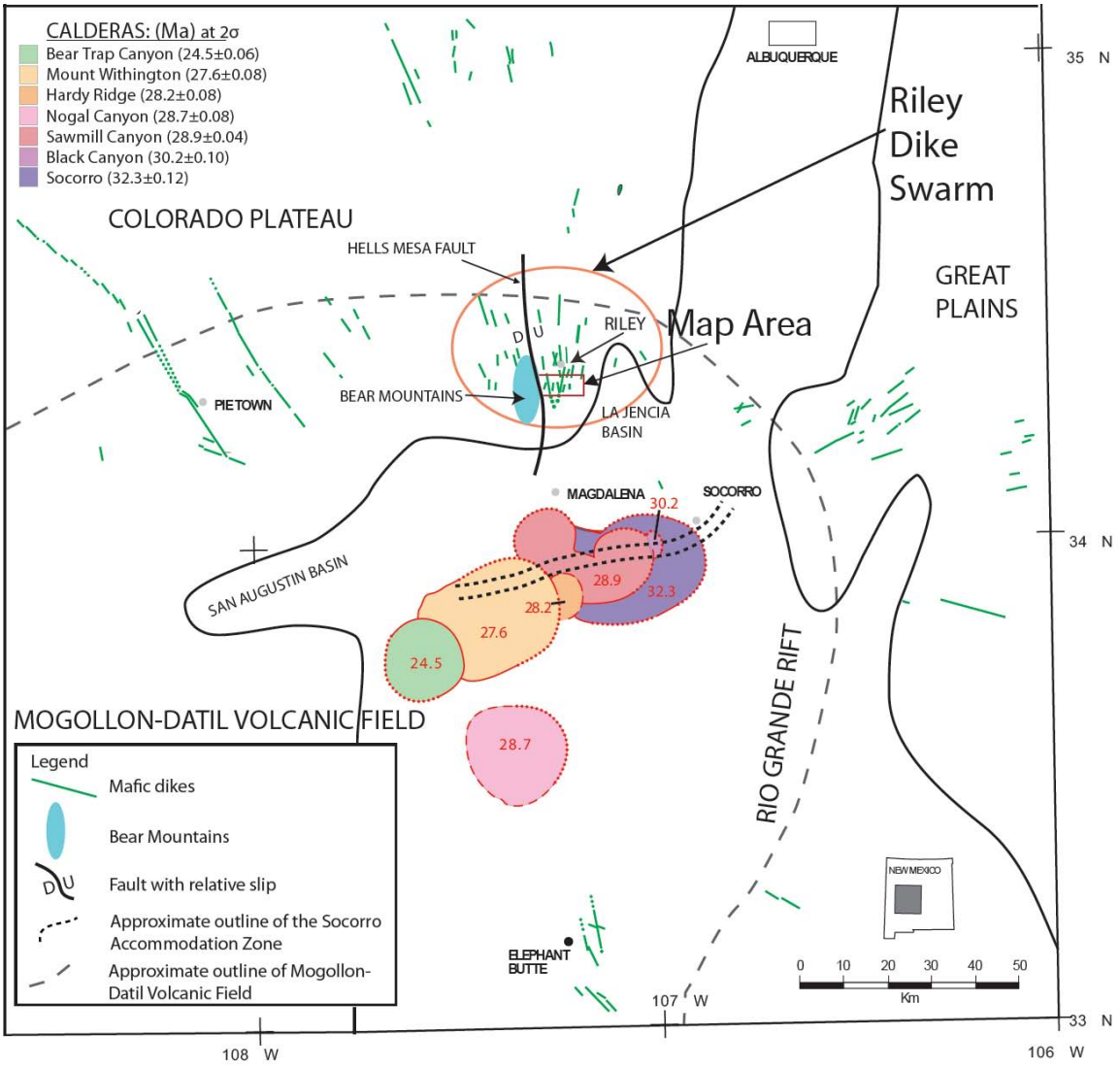

Figure 1. Generalized tectonic map of the Riley area. Note how mafic dikes of the Magdalena radial dike swarm are concentrated in subswarms. Modified from Chamberlin, et al. (2002), Chapin and Seager (1975), and Woodward et al. (1975).

1.2 Regional extension

The Rio Grande rift consists of a system of asymmetrical grabens of Neogene age bounded by steep faults (Baldridge et al., 1989) that extend from Colorado to Texas. The crust of the rift is ~22% thinner (10-15 km) than that of the neighboring Colorado Plateau and Great Basin (Wilson et al., 2005). Rift-forming extension occurred during middle to late Cenozoic time (Baldridge et al., 1989). The exact timing of the onset of extension is controversial (Chapin et al., 2004) although most authors agree that extension began in different places along the rift between 36-31 Ma (eg. Aldrich et al., 1986; Cather, 1990) and the rate of extension increased at ~29 Ma (eg. Chamberlin, 1983; Cather et al., 1994).

The northeast-trending Socorro Accommodation Zone (SAZ) accommodates a widening of the Rio Grande rift in south-central New Mexico. The SAZ is superimposed along the pre-rift crustal weakness called the Morenci lineament and the SAZ now separates domains of oppositely-tilted normally faulted blocks (Chapin, 1989; Chapin and Cather, 1994). This domino-style faulting (Chamberlin, 1978, 1983) began shortly after the onset of ignimbrite volcanism (Chamberlin, 1983; Chapin, 1989). Riley is approximately 5 miles north of the moderate to strongly extended terrane associated with domino-style faulting.

1.3 Volcanism

The MDVF is located south of the Colorado Plateau and its eastern margin has been locally distended along the western margin of the Rio Grande rift. Volcanism of intermediate composition dominated the Mogollon-Datil volcanic field prior to the onset of rifting (40-36 Ma) (McIntosh et al., 1992). Mafic lava eruptions began at about 36 Ma but increased after initiation of ignimbrite volcanism (Chapin, 1989) at 32 Ma. The

MRDS surrounds six overlapping calderas (and one peripheral caldera), termed the Socorro-Magdalena caldera cluster (SMCC), that lie in a westward-younging trend (~32 to 24 Ma) along the SAZ (McIntosh et al., 1992; Chapin et al., 2004). Episodic bimodal volcanism continued into the Miocene after ignimbrite volcanism ceased ~24 Ma (eg. Bobrow et al., 1983; Baldridge et al., 1989).

1.4 Relationship between extension and volcanism

The mechanical relationship between rifting and volcanism is unknown (McIntosh et al., 2004), but rhyolitic magma ascent has apparently been focused along the Morenci Lineament (Bobrow et al., 1983) and accommodation zones tend to "leak" magmas (Chapin and Cather, 1994). Volcanism in the MDVF between 40-20 Ma may represent back-arc or intra-arc magmatism related to changes in subduction angle of the Farallon plate beneath the North American plate (Baldridge et al., 1991; McIntosh et al., 1992) rather than being related to extension of the Rio Grande rift.

1.5 Geology of the Riley area

The Riley area consists of dominantly gently SW- to SE-dipping Cretaceous and Tertiary strata (Fig. 2) originally described by Tonking (1957) and mapped in further detail by Massingill (1979). Strata are cut by numerous moderate displacement (< 100 m) normal faults that are locally superimposed on Laramide thrust faults (Tonking, 1957; R. Chamberlin, pers. commun.). The largest normal fault is the Hells Mesa fault, which accommodated relative uplift of the Riley area by several hundred feet compared to the western fault block (Tonking, 1957), which includes the adjacent northern Bear Mountains. Subsequent erosion left the Bear Mountains topographically higher than the uplifted Riley block and exposed the dikes near Riley.

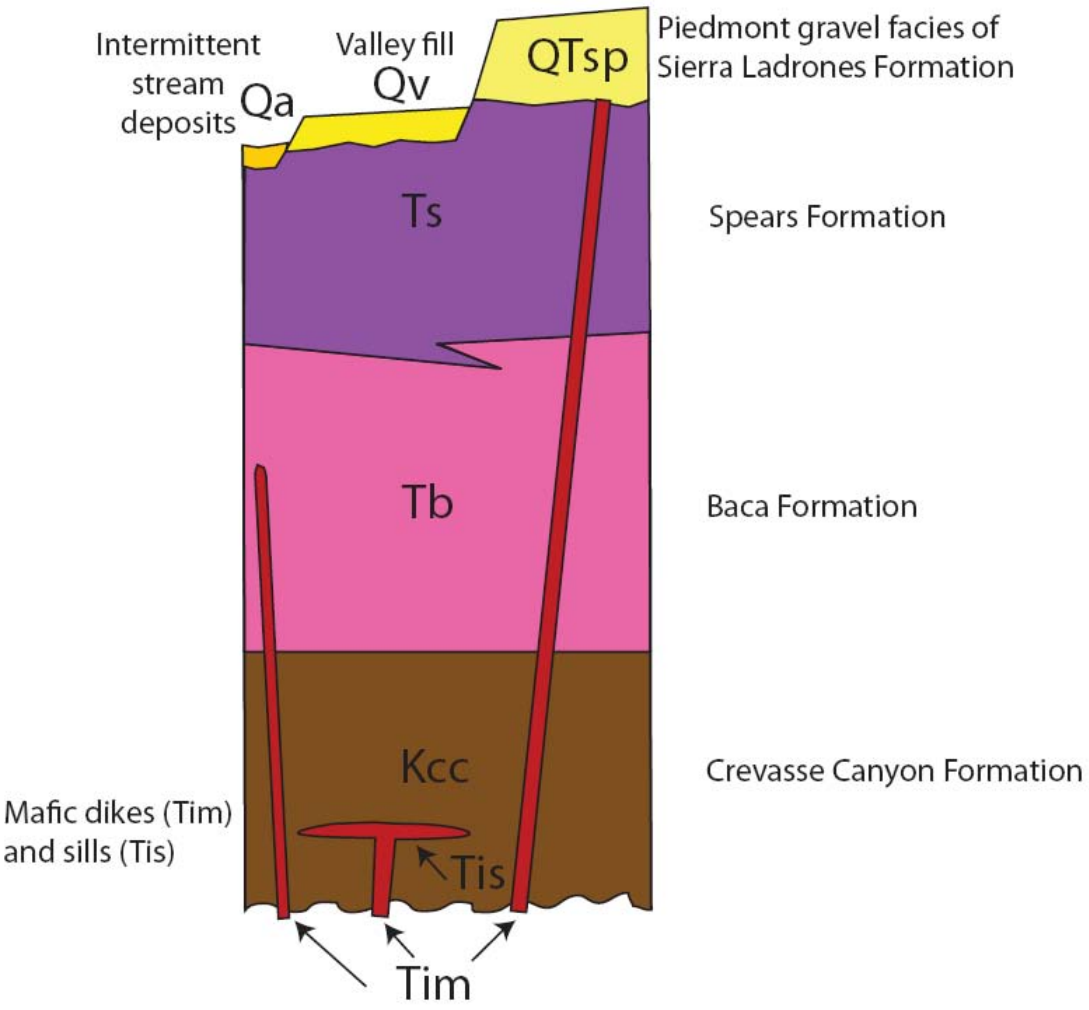

Figure 2. Stratigraphic column of the Riley area.

Additional strata found in the northern Bear Mountains include three regional ignimbrites from the SMCC. Cobbles of the Oligocene Hells Mesa, La Jencia, and Vicks Peak tuffs are common in the alluvial and fluvial gravels that mantle the Riley area. The Tertiary Spears Formation, also found at the west margin of the field area, is comprised of volcaniclastic rocks. Several volcanic units are interlayered with middle and upper portions of the Spears Formation (Cather et al., 1994). Volcanic necks are present northwest of the town of Riley, and over 2000 feet of lava flows of the La Jara Peak basaltic andesite, apparently fed by some dikes of the MRDS (Tonking, 1957), are also found in the Bear Mountains.

2. FIELD STUDIES

A geologic map was constructed at a scale of 1:12,000 using standard USGS topographic maps as a base (Plate 1) and supplemented by aerial photographs. The map covers portions of the Carbon Springs and Mesa Cencerro Quadrangles. Stratigraphic nomenclature used here follows previously established stratigraphic frameworks of Tonking (1957), Massingill (1979), and Osburn and Chapin (1983), but details in the following sections are based on the current mapping of the study area.

Samples collected for petrographic and geochemical analyses and $^{40}Ar/^{39}Ar$ geochronology are discussed in later chapters. One to two one-quart bags of material were collected from the freshest portions of the dikes. In addition to sample collection within the mapped area, some samples were collected north of the mapped area including the locations within the adjacent La Jara Peak and Riley Quadrangles. All sample locations were assigned UTM coordinates using a handheld GPS unit and are listed in Appendix A. All UTM coordinates listed in the text refer to Plate 1.

2.1 Stratigraphy

2.1.1 Quaternary sedimentary deposits (Qa, Qv, Qco, QTsp)

Quaternary sedimentary deposits are divided into four map units according to relative age and stratigraphic position. Active alluvium (Qa) fills streambeds and consist of sand to boulders derived from the Hells Mesa and La Jencia tuffs shed from the Bear Mountains as well as minor amounts of material from Tertiary and Cretaceous map

units. Middle to late Pleistocene valley fill alluvium (Qv) covers dikes in a large portion in the west of the map area. Valley fill sediments consist of sand and gravel from the Bear Mountains to the west; mostly cobbles of the Hells Mesa and La Jencia tuffs. Piedmont gravels of the Sierra Ladrones Formation (QTsp) also consist of volcanic-rich gravels shed from the Bear Mountains. This piedmont facies unit caps several small mesas and covers many dikes south of the map area. The Sierra Ladrones Formation predates incision of the Rio Salado, which flows across the Riley dike swarm north of the current study area. Three mapped piles of dike material (dike colluvium, Qco; near UTM 13S 0292216(E), 3800680(N)) apparently fell from a neighboring dike (named the Spears Ranch Dike). The collapse material is probably of late Pleistocene age and predates erosion of the Spears Ranch Dike to its present topographic position, which is lower than the collapse material. Qco is coeval with Qv.

2.1.2 Tertiary Spears Formation (Ts)

The Spears Formation (Ts) consists of andesitic and dacitic volcaniclastic sediments that form prominent reddish-purple to purple-gray ledges. The Spears formation has a gradational contact with the underlying Baca formation (Tonking, 1957; Osburn and Chapin, 1983). Only the lower portion of the Spears Formation is present in the map area.

2.1.3 Tertiary Baca Formation (Tb)

The Baca Formation (Tb) typically consists of reddish sandstones, conglomerates, and mudstones that unconformably overlie the Cretaceous Crevasse Canyon Formation. The basal Tb consists of conglomerate that includes clasts of limestone, quartzite, granite, and pegmatite. In the central portion of the map area, where the Cretaceous-Tertiary

contact crosses Forest Road 354 (UTM 13S 0294540(E), 3800833(N)), a ~30 m thick weathering zone (Kcco; not mapped on Plate 1) of anomalously colored (pale red, white, to purple) Crevasse Canyon sediments underlies the basal Baca conglomerate. Large hematite masses, often botryoidal, interpreted as fragments of an early Tertiary lateritic soil (Chamberlin, pers. commun.) are locally found as float near the top of this zone. Uranium mineralization is known to be associated with this weathering zone in the Datil Mountains-Pie Town region (Chamberlin, 1981). The weathering zone is locally absent on an upthrust block of Crevasse Canyon Formation exposed about 2 km west of FR 354.

Above the basal conglomerate are pink coarse-grained arkosic sandstones with a few large (meter-scale) cross beds. Much of the middle Baca Formation contains red to reddish-purple sandstones and siltstones. Thin, broad channel deposits are common. One tan, cross-bedded shale layer outcrops near the southern border of the map area. The upper portion consists of red, green, and yellow siltstones and mudstones and red to pink sandstones. Petrified wood fragments and large portions of silicified tree trunks are common in the upper siltstones and mudstones.

2.1.4 Cretaceous Crevasse Canyon Formation (Kcc)

The Crevasse Canyon Formation (Kcc; Mesaverde Group of Massingill 1979; Chamiso Formation of Winchester, 1920) consists of multiple beds of fine-grained sandstone and dark gray to black shale. Massingill (1979) separated the formation into 3 units: a basal sandstone; a middle section of sandstone, siltstone, and minor coal; and an upper unit of interbedded sandstone and shale.

The lower Crevasse Crevasse Canyon is exposed north of the study area. The middle section contains tan silty shale and tan to yellow-green cross-bedded sandstones

with thin (~10-25 cm) beds of coal. Limonite concretions ranging from a few cm to greater than one meter in diameter are common in some of the pale tan sandstones. Lignite nodules are common in the shale.

Sandstone and shale beds in the upper unit are commonly 10 cm to 1 m thick. Light tan colored sandstones are often structureless. Dark brown, cross-bedded, and well-indurated sanstone layers locally form prominent north-trending linear ridges that can be confused with mafic dikes on aerial photos.

2.2 Structure

The map area consists of numerous gently tilted fault blocks with a regional westerly dip of ~5-15°. Massingill (1979) notes several "gentle" folds resulting from Laramide compression. There is, however, evidence of significant folding and contractional and extensional faulting. Throw of a west-dipping thrust fault exposed on the southern arroyo wall at UTM 13S 0293855(E), 3800248(N) is estimated to be ~100 m (Fig. 3). Other significant structures of the study area include several folds, a monoclinal thrust, two normal faults, and several uncertain faults (Plate 1).

2.3 Intrusive rocks

Numerous dikes and a few sills are exposed (Fig. 4) within the Cretaceous and Tertiary strata. The following section describes field observations of textural and mineralogical characteristics of the dikes, geometry and physical relationships among dikes, between dikes and wallrock, and between dikes and faults. Due to the minor number of sills, they are mentioned only briefly.

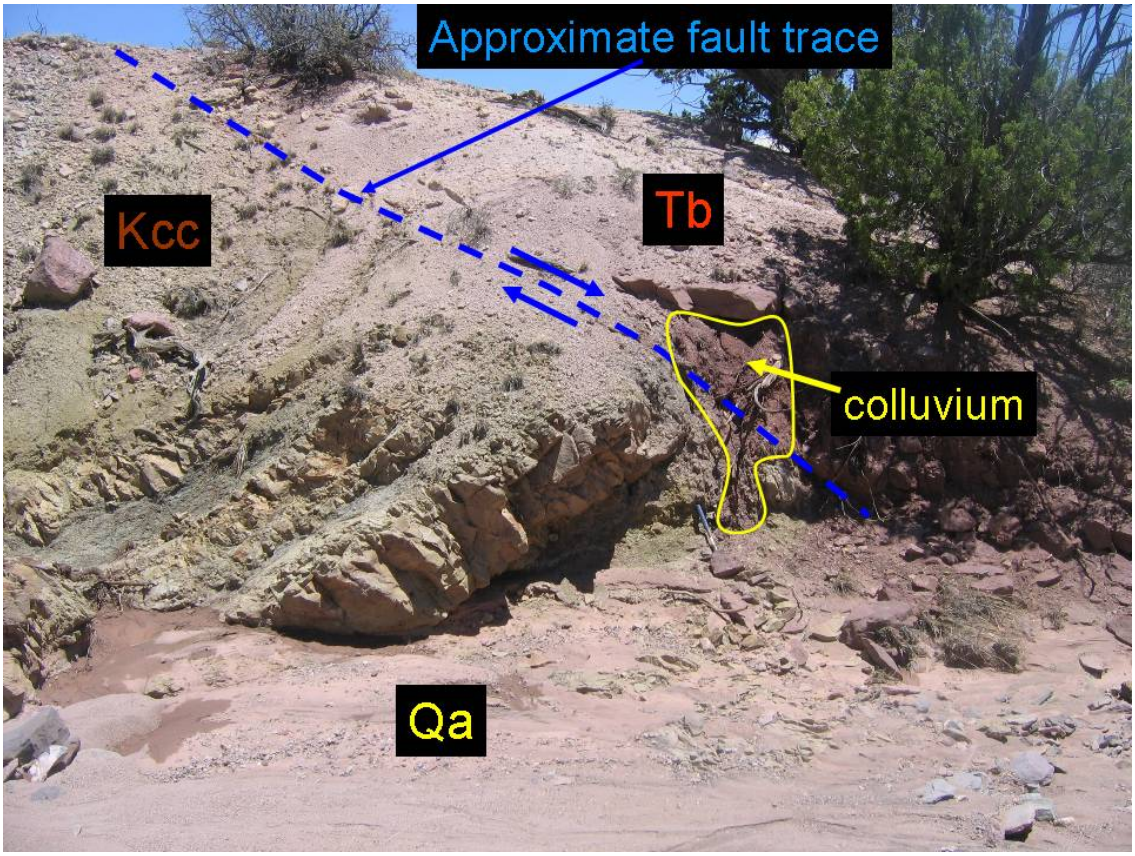

Figure 3. Normal fault that juxtaposes Crevasse Canyon Formation (Kcc, brown and gray) against to the Baca Formation (Tb, red). Looking ENE at NNE-striking fault. Photo taken at UTM 13S 0294359(E), 3801199(N). Hammer is 41 cm long.

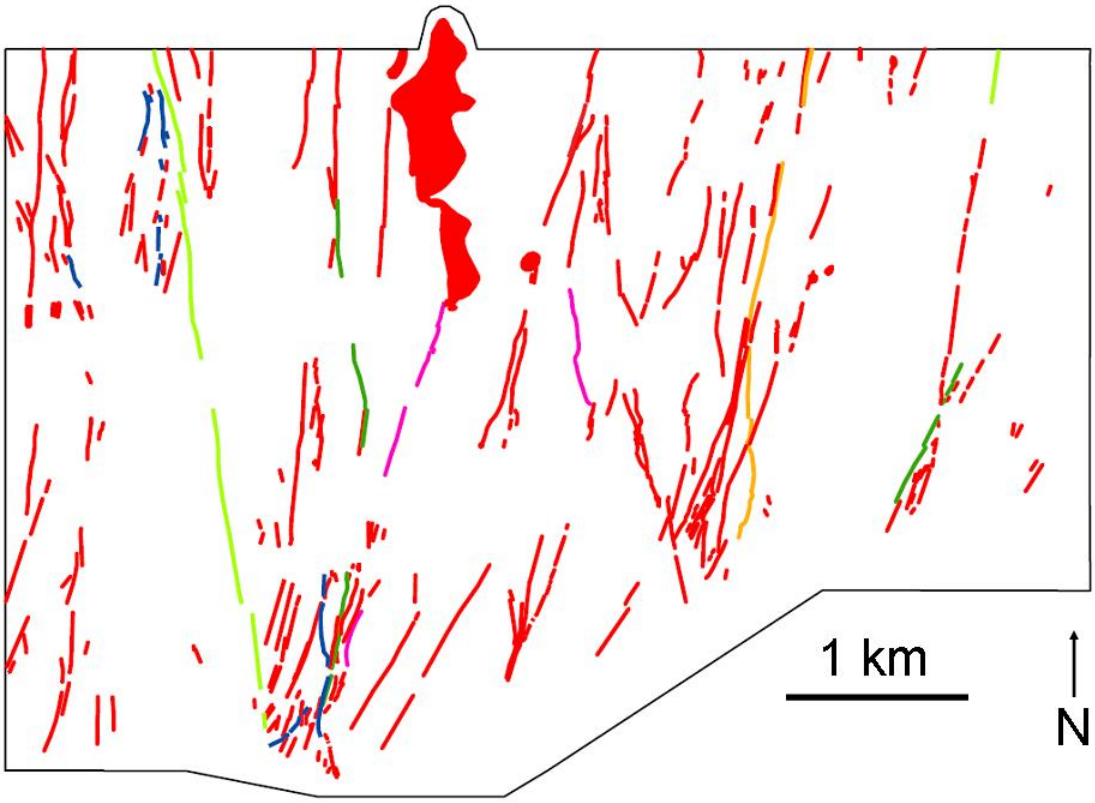

Figure 4. Map showing the numerous dikes (colored lines) and few sills (red shapes) within the study area. Colors represent different types of dikes that are discussed in Chapters 2 and 3.

2.3.1 Field classification of texture and mineralogy

Two main types of intrusive rocks were recognized based on field mineralogy: basaltic and minette. All sills and most of the dikes are basaltic, characterized by small yellowish-brown olivine and black pyroxene phenocrysts, groundmass plagioclase (occasionally phyric), ± biotite. Plagioclase was usually only identified with a hand lens, but could be seen with the naked eye in rare coarse grained dikes or portions of dikes. Minettes also have pyroxene phenocrysts but are primarily recognized by their rare to common biotite clots. These clots are as large as several cm in diameter (Fig. 5). Biotite crystals in some basaltic dikes can be seen with a hand lens, but these dikes lack biotite clots that are characteristic of the minettes.

Two special subcategories of basaltic dikes are 1) pyroxene porphyry and 2) "speckled." One pyroxene porphyry dike was recognized, shown in orange on Plate 1. The pyroxene phenocrysts in this dike are commonly several mm, up to 1 cm, much larger than in any other dike. Speckled dikes were recognized by their abundant black pyroxene phenocrysts and white spots a few mm in size. Many of the white spots are subhedral to euhedral (Fig. 6a) and are abundant in the weathered surfaces of speckled dikes but are not visible in fresh surfaces (Fig. 6b), suggesting that they are bleached or altered primary phases. The thin section prepared from a fresh sample of a speckled dike (RDS-013A) contains no apparent white spots (Chapter 3 and Appendix C). The white spots visible on weathered surfaces may be bleached phenocrysts (of feldspar or feldspathoid?).

Figure 5. Large biotite clot mostly weathered out of a minette dike.

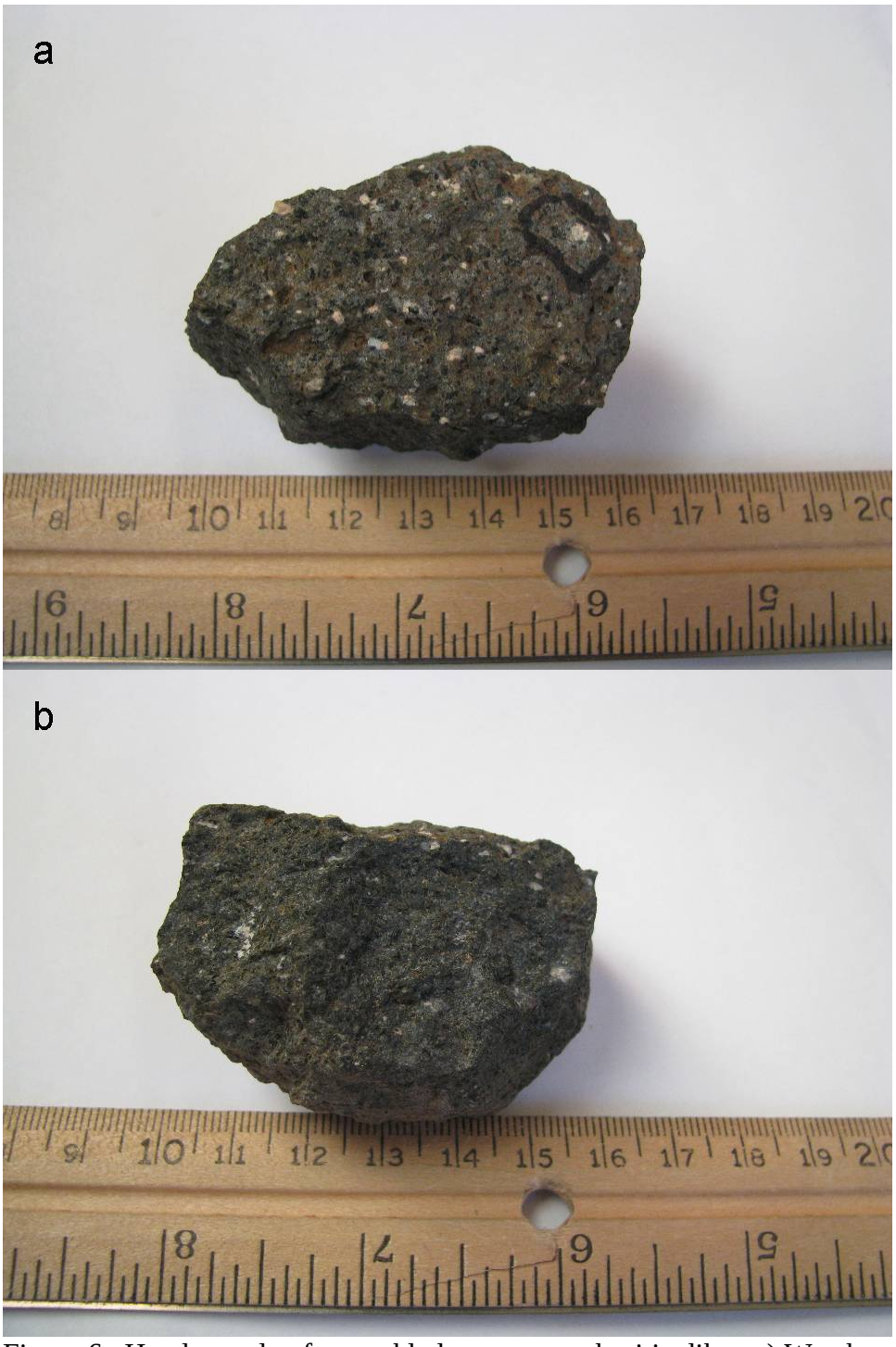

Figure 6. Hand sample of a speckled texture porphyritic dike. a) Weathered surface of the dike shows dark pyroxene phenocrysts and subhedral white spots. Black circle surrounds one of these white spots. b) Profile of sample from weathered surface (top) into fresher dike material. Note the white spots are more abundant (or more visible) at the weathered surface. White spots may be bleached phenocrysts of feldspar or feldspathoid. Even the black pyroxene phenocrysts are less apparent on the fresher surface.

2.3.2 Dike widths and sill thicknesses

Dikes range from less than a meter to 10 m wide, but most are 1-4 m wide. Mapped dikes were generally at least 1 m wide. The width of some dikes also varies along strike by 1-2 m, sometimes doubling their width. Dike lengths also vary greatly between a few meters to several kilometers. Many mapped dikes are continuously exposed for 0.5-2 km.

Most sills (all but one) are relatively thin and small, 1-2 m thick and extend ≤ 15 m laterally, and appear to be sill-like portions of dikes. The largest sill is probably 10-20 m thick and its largest dimension is ~1.5 km. East of the largest sill, at UTM 13S 0293900(E), 3801800(N), is a hill capped by sill material. The two sills were likely laterally continuous prior to erosion and exhumation. The large sill occurs in the Crevasse Canyon Formation and as Massingill (1979) notes, most sills occur in the Crevasse Canyon Formation and Mancos shale, a unit that is north of the map area. Massingill (1979, p. 139) suggests that depth affected the location of sill emplacement because "equally ductile" layers are stratigraphically above and below the level of the sills. He estimates the sills were emplaced at a depth of 3000-3800 ft. A few minor sills are present in the Baca Formation and none were observed in the Spears Formation.

2.3.3 Weathering characteristics

Many dikes exhibit topographically positive, finer-grained chilled margins, each ~25 cm wide, and coarser-grained recessive cores (Fig. 7). The chilled margins must be broken with a hammer but the cores are crumbly and may texturally resemble the weathered host rock. Dikes with widths between 1-2 m are typically topographically

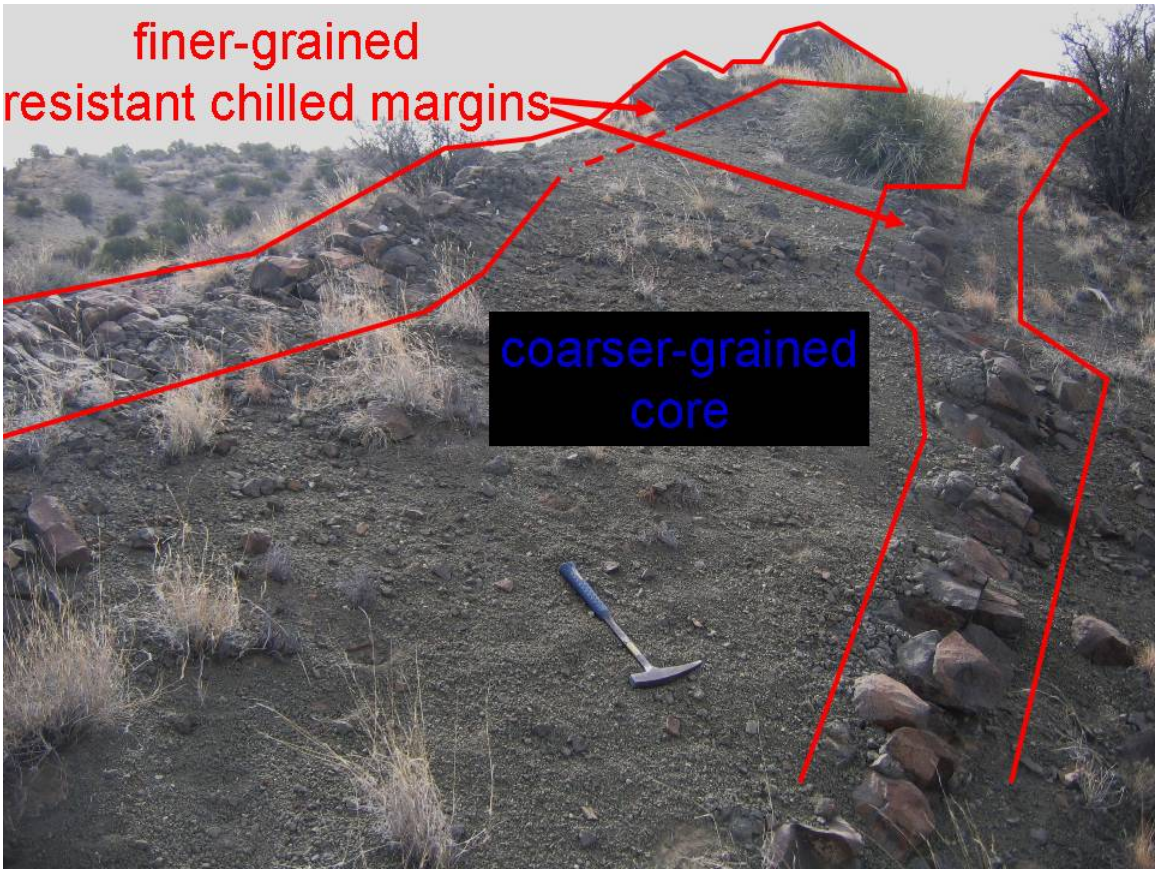

Figure 7. Dike with chilled margins and a recessive, coarser grained core. Hammer is 41 cm long.

positive with no recessive core. Dikes with no chilled margins are rare but can be several meters wide and are usually coarse-grained.

Occasionally dikes will have more than two chilled margins, i.e. they have more resistant, finer-grained ribs within coarser-grained recessive zones. Resistant internal ribs are usually discontinuous and only several meters long. These most likely represent multiple pulses of magma (composite dikes).

Many dikes display spheroidal weathering patterns (Fig. 8a). This spheroidal weathering sometimes follows the pattern of columnar jointing with columns perpendicular to the dike walls to produce outcrops that look like cobblestone walls (Fig. 8b).

2.3.4 Color

Fresh surfaces of all dikes are usually medium to dark gray and most dikes weather to one of two colors: dark reddish-brown or greenish-gray. The greenish dikes are coarser-grained and less resistant than reddish-brown dikes. Massingill (1979) notes that the type and water content of host rock may influence the weathering pattern of dikes, and that the greenish dikes tend to be more common in the Baca Formation. The formation of greenish dikes may be influenced by the type and water content of host rock, but green dikes tend to be coarser grained than other dikes and contain abundant serpentinized olivine (Chapter 3) and likely chlorite and epidote. Coarse-grained recessive cores of reddish-brown dikes also tend to be greener than the more resistant margins, suggesting that color has more to do with grain size and alteration mineralogy than host rock.

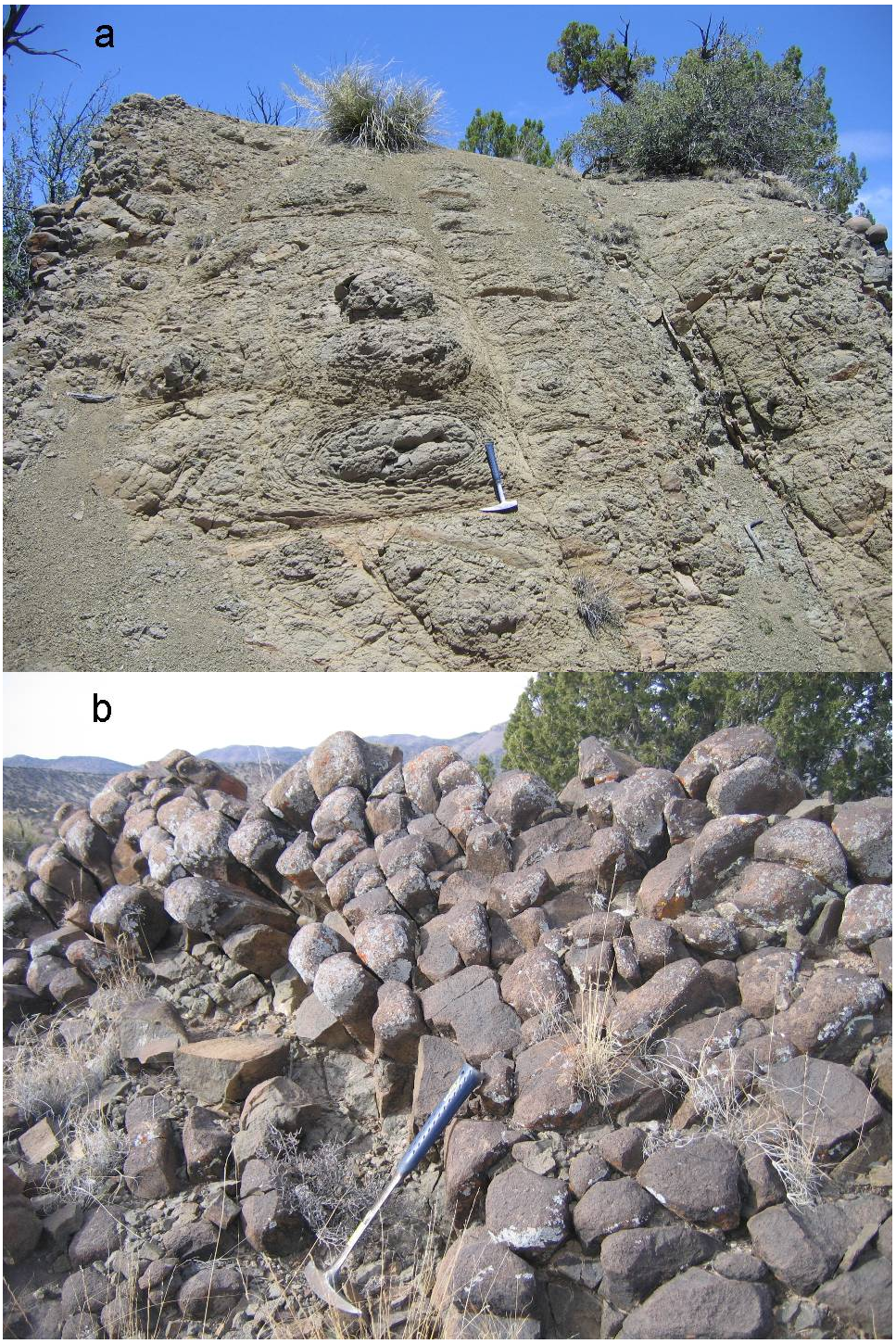

Figure 8. Spheroidal weathering patterns exhibited by dikes. a) Spheroidal weathering of the coarse grained core of a dike. Hammer is 41 cm long. b) Columnar joints perpendicular to dike walls. This portion of the dike tilts significantly to the east. This particular dike is "famous" among NM geologists for the rounded column ends resembling a cobblestone wall bordering Forest Road 354 (Chamberlin, et al., 1983a, Second day road log Fig. 2-53.5). Photo taken at UTM 13S 0294515(E), 3800918(N). Hammer is 41 cm long.

The color difference between chilled margin and core is often subtle, but in one dike the color difference is extreme. This dike looks like two dikes from the side because it has black chilled margins and green core (Fig. 9).

3.3.5 Dike branching

Several dikes have small (<1 m wide) branches that often extend only several meters from the trunk. One dike displays multiple branches that thin northward (Fig. 10). This dike parallels Forest Road 354 in the center of the map area. The intrusion exposure begins at the southern end as a 15 m-wide sill at UTM 13S 0294600(E), 3800500(N). The dike extending north from the sill is 10 m wide. The dike bifurcates into 3 m-wide and 4 m-wide branches, trending NNW and N, respectively. The 4 m-wide NNW-trending branch continues north and bifurcates into 1 m and 3 m wide branches which are exposed for another ~200 m to the north. The branching pattern suggests northward propagation of this dike (Dimeo and Chamberlin, 2006).

2.3.6 Cross-cutting relationships

Age relationships at intersections of dikes are often unclear because of vegetation, sediment cover, or similar textures of the dikes. At well exposed intersections, examining continuity of chilled margins can help decipher the dikes' relative ages. Chilled margins reveal the cross-cutting relationship between two dikes with similar colors and textures just west of FR 354, at UTM 13S 0294675(E), 3800400(N). A 10 m-wide dike with continuous chilled margins and a recessive core cuts a 1 m-wide dike with no recessive core. There is a notable dilatational offset in the trace of the narrower dike (Fig. 10, Plate 1).

Figure 9. Dike with a dark gray chilled margin and green core. Hammer is 38 cm long. Photo taken at UTM 13S 0291919(E), 3802576(N), looking east.

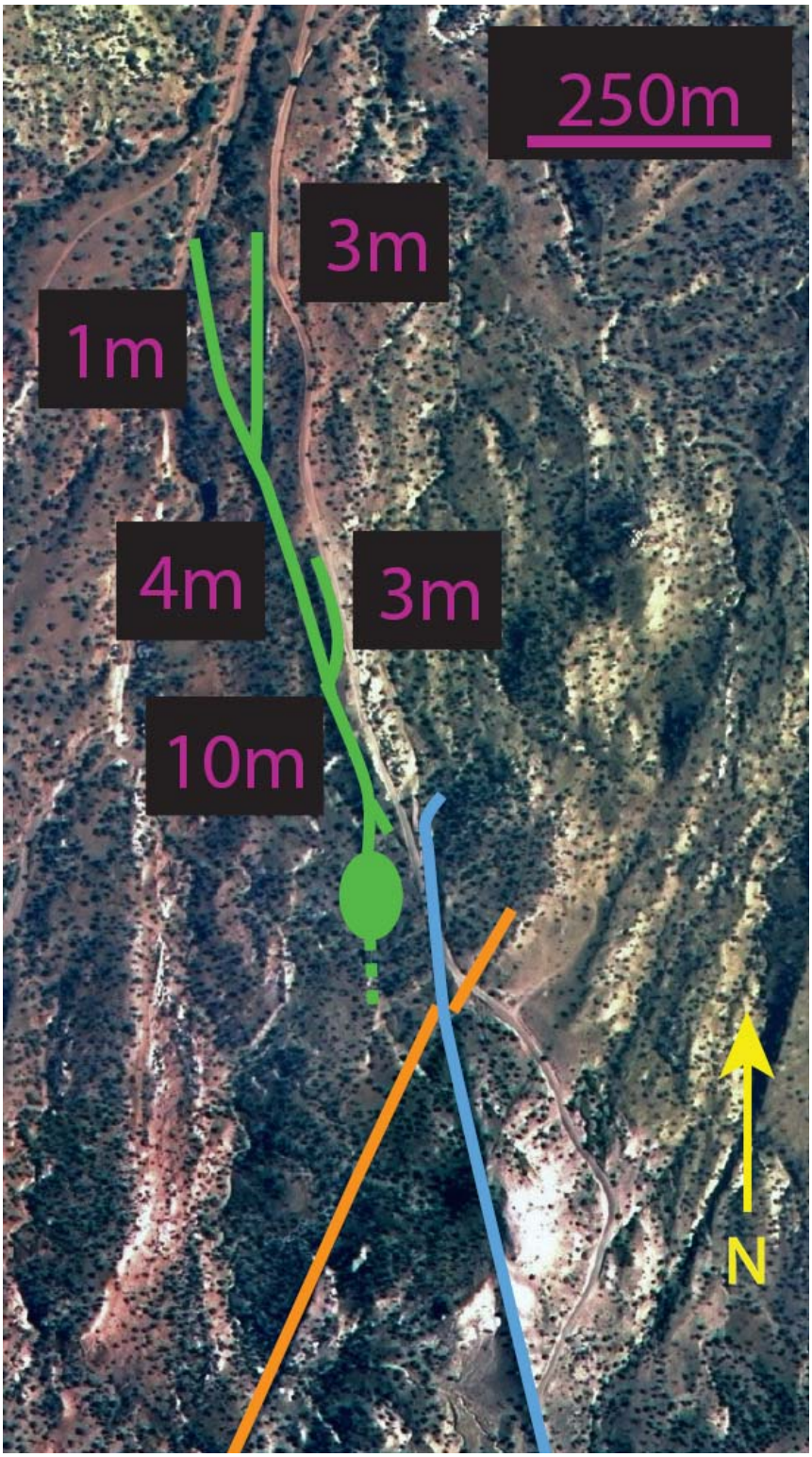

Figure 10. A map of branching dike and a simple dilation cross-cutting relationship along FR 354. Trunk of northward-branching dike (green) extends north from a 15 m-wide sill. Each successive branch of the dike is thinner than its trunk. A younger 10-m wide dike (blue) cuts an older 1-m wide dike (orange). Lengths refer to adjacent dikes and dike branches.

Another intersection is complicated by a local poor exposure of chilled margins (UTM 13S 0295100(E), 3800800(N)). North and south of the intersection, chilled margins are visible. South of the intersection, the western dike is 3 m wide and the eastern dike is 8 m wide (Fig. 11). North of the intersection, the dikes become contiguous and there are three chilled margins. The central chilled zone is only 3m from the east side of the composite dike, which indicates a cross-cutting relationship. Fortunately, the 8 m-wide dike is readily distinguished by abundant large black pyroxene phenocrysts (the pyroxene porphyry dike). An east-west traverse at the intersection reveals that the pyroxene phenocryst porphyry dike is continuous, indicating that it is the younger, cross-cutting dike.

A minette dike is involved in intersections with two other dikes, as well as having the most abrupt change in trend seen anywhere in the field area. As the minette dike trends 059 and approaches an older, coarse-grained greenish basaltic dike, it abruptly changes trend by 69° (Fig. 12; UTM 13S 0292550(E), 3799650(N)). It then steps over several meters to the northwest. The southern end of the northwestern step-over tapers to a sharp point, which is rarely observed at most dike terminations. The dike continues northeast along the same trend (035) as before the bend and clearly cuts the 011-trending green dike, producing a dilational offset of the latter. The “bent” tip of the minette dike southwest of the intersection suggests the minette dike propagated to the northeast. Farther north, the minette dike curves gently northward and is cut by a basaltic dike that trends 005 (UTM 13S 0292657(E), 3799283(N)).

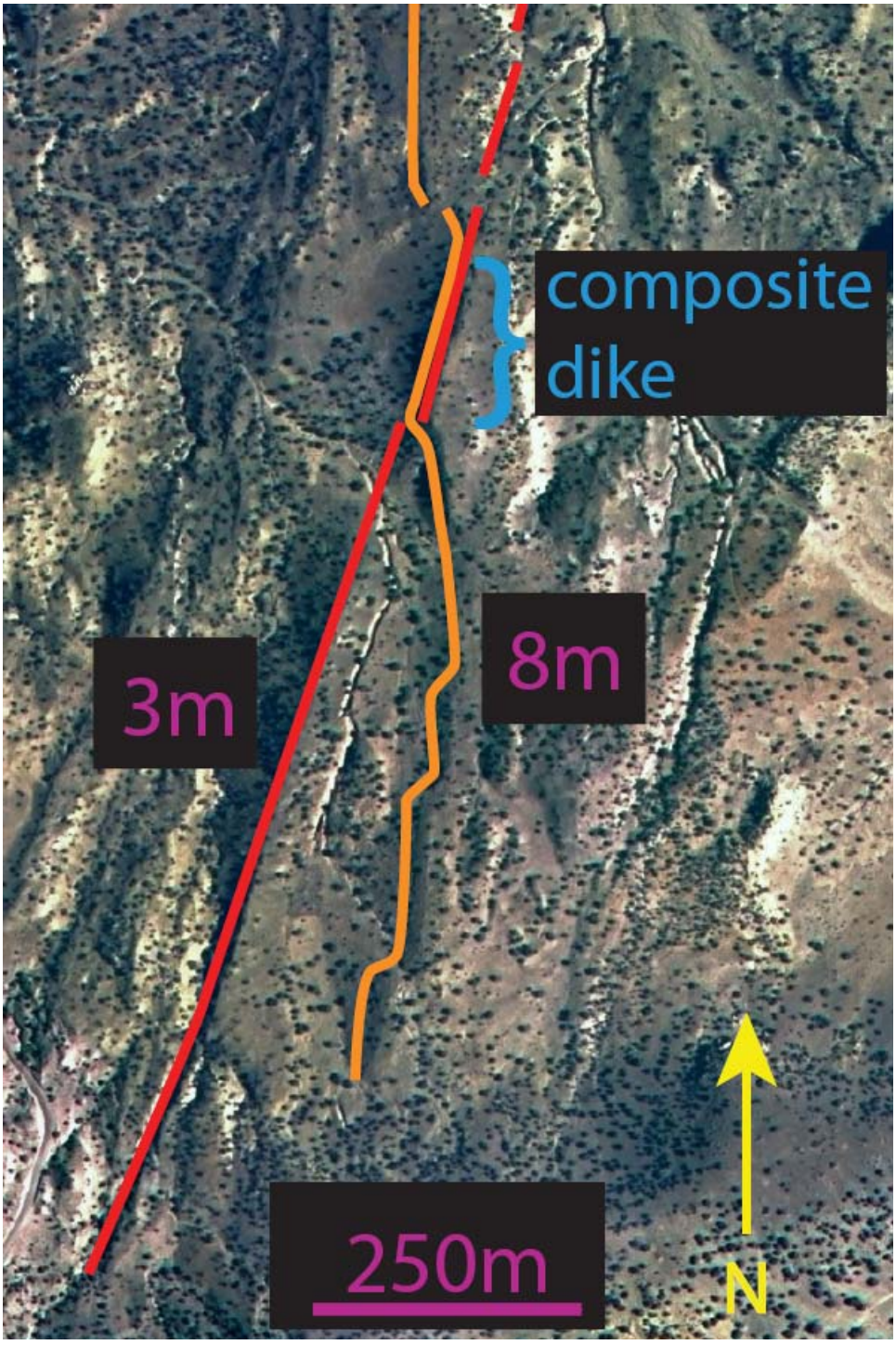

Figure 11. A younger dike deviated by an older dike. The younger dike (orange) jogs and bends several times as it approaches the older dike (red) from the south. The younger dike is emplaced alongside the older dike for ~35m before continuing northward along its original trend.

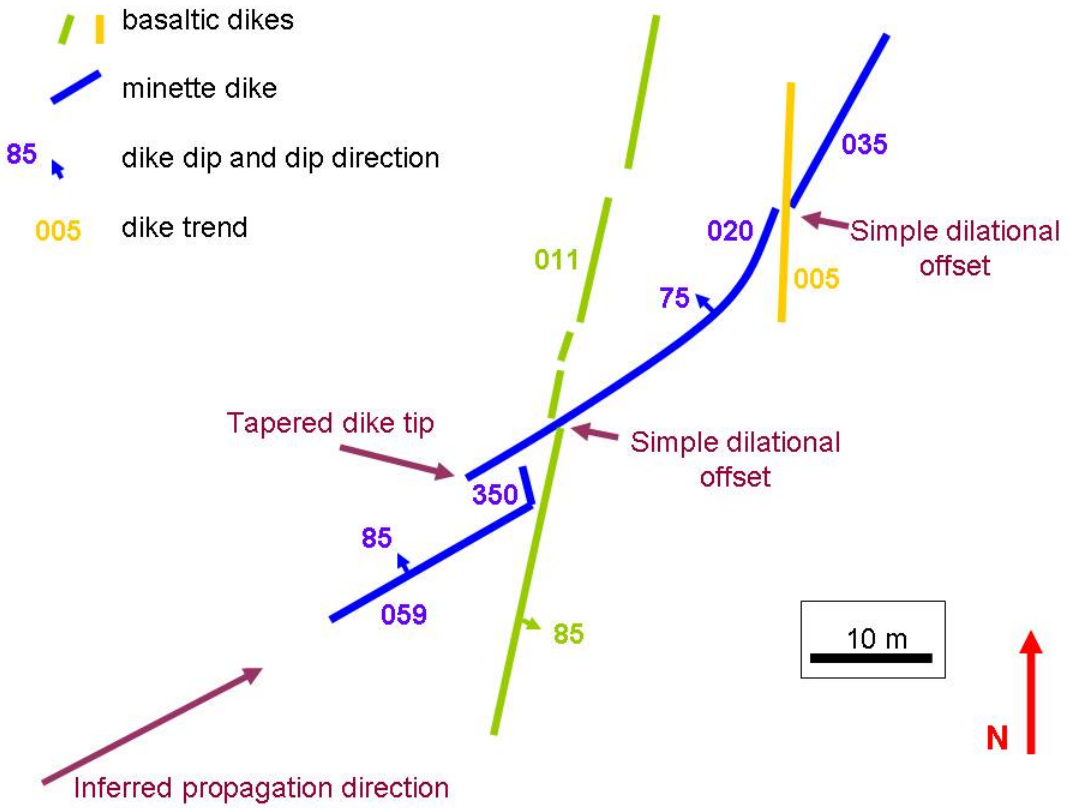

Figure 12. Cross-cutting dikes. The minette dike (blue) appears to have been deflected by an older basaltic dike (green), then stepped over and cut the older dike. Farther north, the minette dike is offset by another basaltic dike (yellow). The geometric relationships suggest that the minette dike was propagating to the northeast when it "bounced off" the older basaltic dike at an oblique angle. Abrupt change in trend (sharp bend) of the minette dike is located at UTM 13S 0292550(E), 3799650(N).

2.3.7 Relationships between dikes and wallrock

At some bends in dikes, neighboring wallrock is upturned as though it was pushed aside during dike emplacement. Near UTM 13S 029228(E), 3799728(N), upturned mudstone beds are quite apparent (Fig. 13). The general dip of the area is 5° WSW, but locally it is greater than 40° to the northeast. The dike made an abrupt turn to the left (west) during emplacement and presumably pushed aside wallrock on its right (northeast) as it continued northward.

Wallrock bordering dikes is occasionally baked or discolored. Baked or discolored wallrock rarely extends more than several cm from a dike. Baked Crevasse Canyon Formation is often slightly darker brown and more cemented within a few cm of dikes. Conglomerates of the Baca Formation locally form <1 m wide, topographically high ridges bordering dikes (Fig. 14). The Spears Formation is more resistant to erosion than most dikes and is less commonly baked. Unlike dikes in other formations, nearly all dikes cropping out in the Spears formation are more recessive than both their baked or unbaked host rock.

At UTM 13S 292508(E), 3800006(N) a ~6 m-wide dike has a 20 m-wide baking aureole on its eastern side and a ~5 m-wide baking aureole on the west side. Figure 15 shows the discoloration of the baked wallrock compared to the same fresh layers of the Baca Formation 30 m away. The dike has no resistant margins and is coarse grained throughout. The lack of finer-grained chilled resistant margins and the presence of the large baking aureole suggests this dike was long-lived and possibly fed a lava flow.

Some small dikes exposed in arroyo walls in Baca Formation mudstones are plume-shaped (Fig. 16) and imply that some dikes never reached the Oligocene land

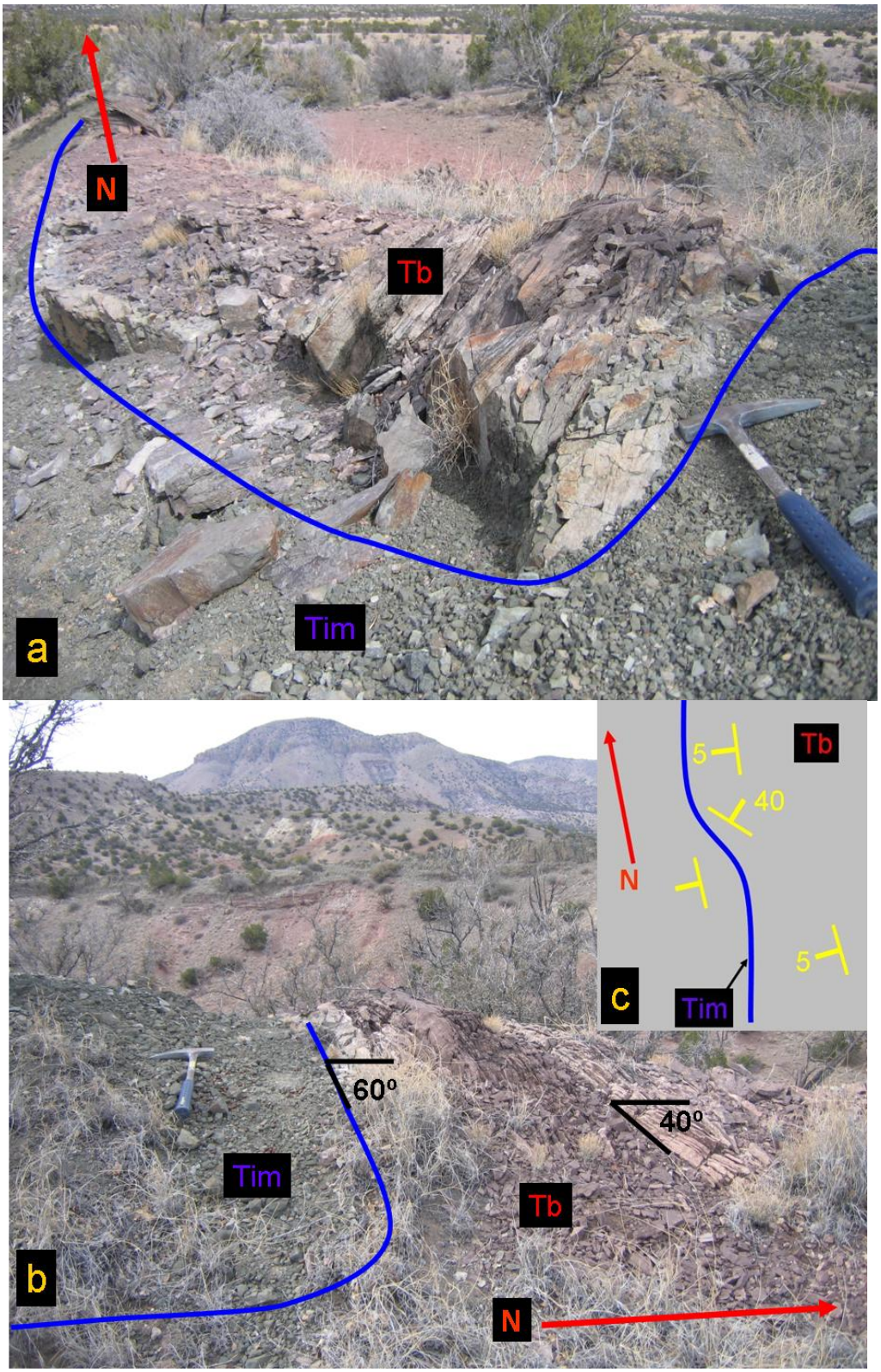

Figure 13. Upturned bedding at bend in dike. Dike outlined in blue. Hammer is 41 cm long. a) View looking NNE. b) View looking west. c) Map view schematic of dike trend and bedding dips.

Figure 14. Locally baked conglomerate of the Baca Formation is more resistant than the dike that caused the baking. Dike is poorly exposed in the photo. It lies to the right of the baked Baca and beneath the hammer handle. Hammer is 41 cm long.

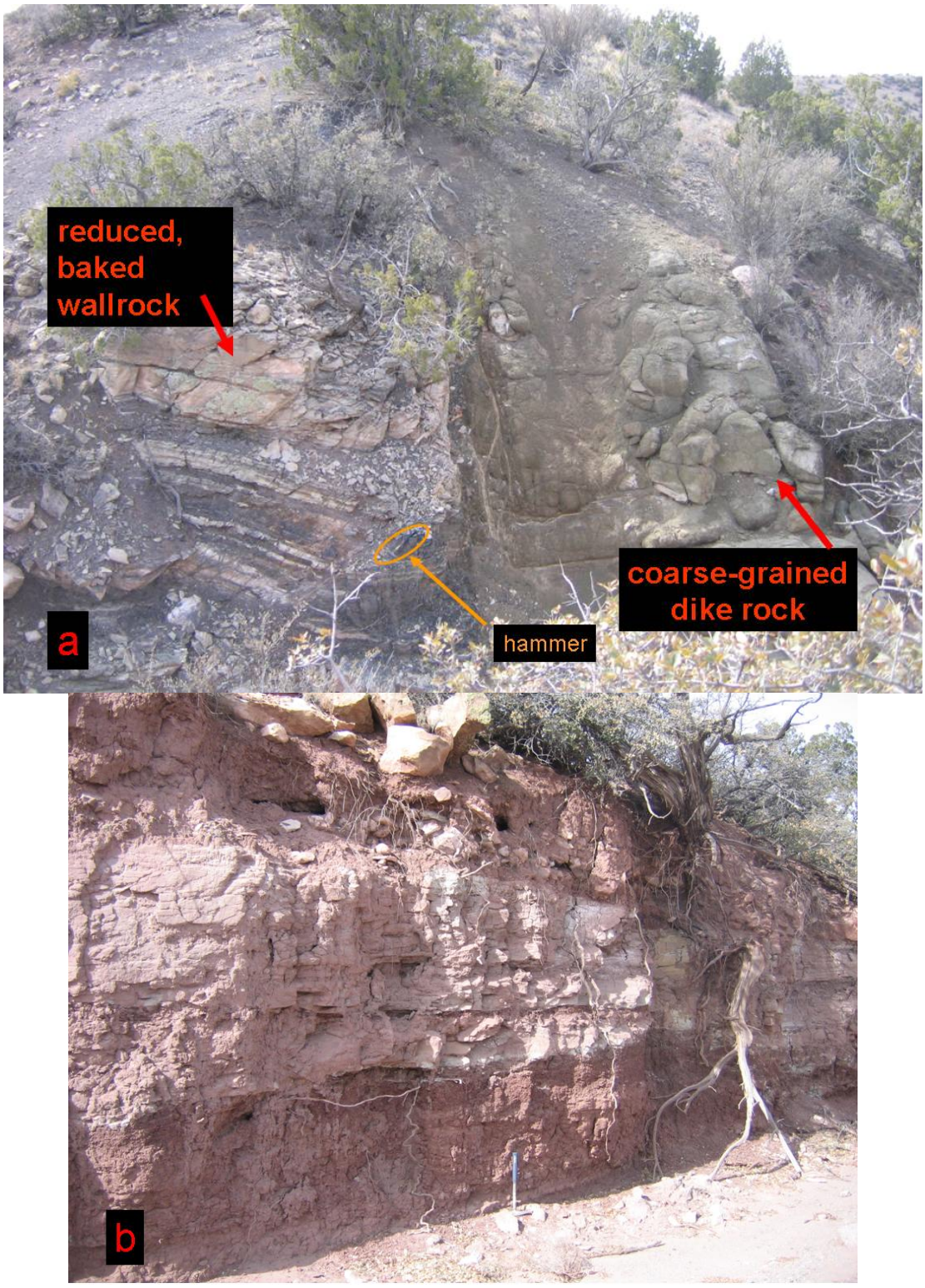

Figure 15. Coarse-grained dike and a 20 m-wide aureole of baked wallrock. a) Numerous small offsets in the discolored baked Baca formation accommodate several meters of dike width. Photo taken at UTM 13S 292508(E), 3800006(N). b) The same layers of the Baca Formation, unbaked, ~30 m east of photo a. Hammer in both photos is 41 cm long.

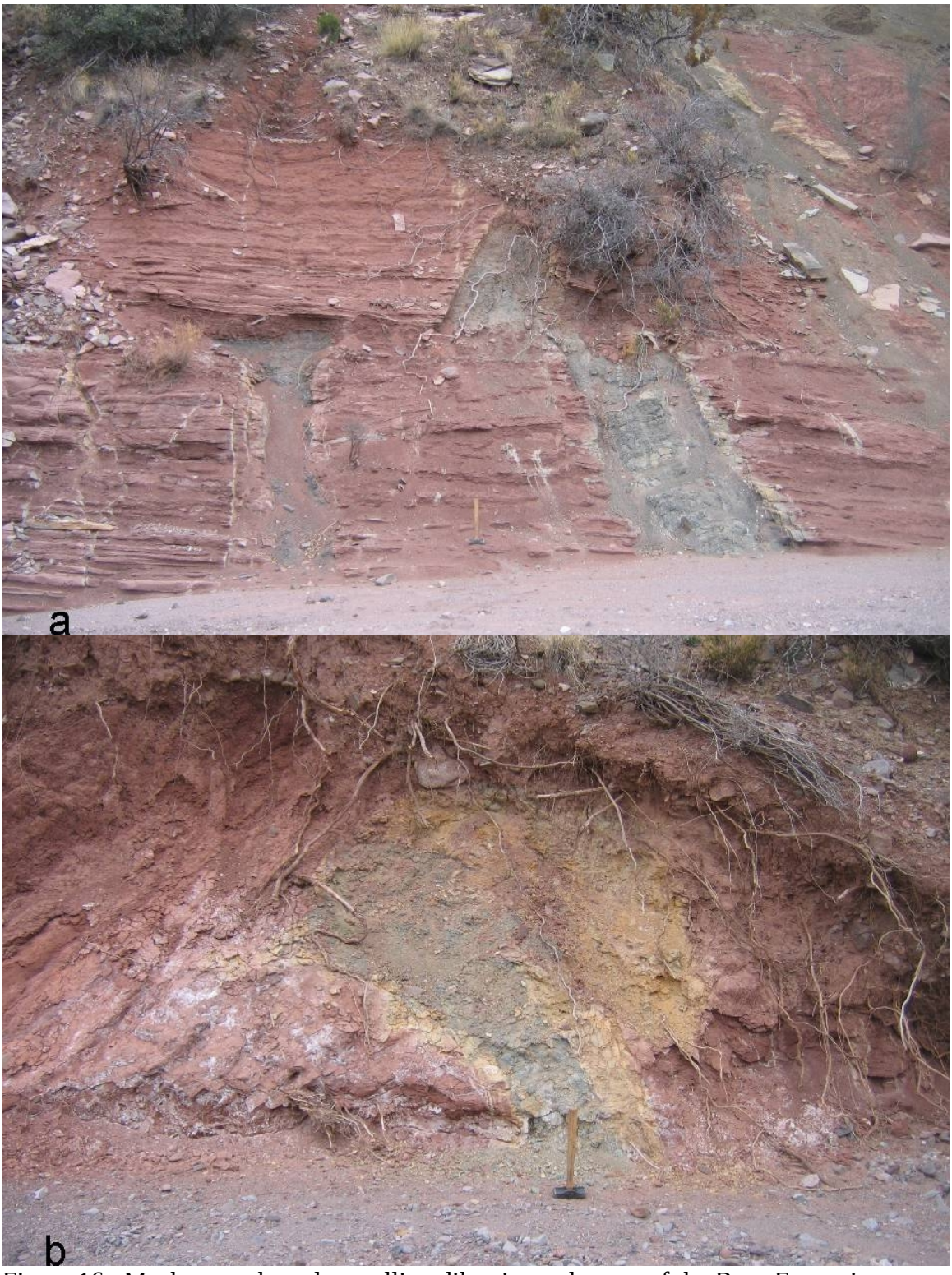

Figure 16. Mushroom-shaped upwelling dikes in mudstones of the Baca Formation. Hammer in both photos is 39 cm long. a) Some baking is apparent as whitened strata. Baca beds do not appear to be deformed due to dike emplacement. b) Baked (reduced) Baca beds are white to yellow. Photos taken at approximately UTM 13S 0291088(E), 3799599(N). Apparently some dikes did not reach the Oligocene land surface.

surface. Some baking of wallrock is apparent due to discoloration of Baca to white and yellow along the contacts of the dikes. Folding or microfaulting of Baca beds due to dike emplacement is not apparent.

2.3.8 Xenoliths

Xenoliths are moderately common but are not ubiquitous, being found only in parts of some dikes. Quartzite is the most common xenolith and locally occurs in xenolith-rich zones several meters long along strike. Quartzite xenoliths are typically ≤ 25 cm. Rare sandstone xenoliths are only a few cm in diameter and are likely clasts of host rock. Dikes that outcrop in Baca Formation conglomerate often contain mm-sized xenoliths of the wallrock. A granitic xenolith was found in a minette dike.

2.3.9 Relationships between dikes and faults

Slickensides are found on the margins of some dikes. Obvious large offset of bedding by dike emplacement is not seen, suggesting that the slickensides are the result of the wallrock shifting to accommodate the dike width. Few dikes are obviously in or adjacent to faults, and there is usually no significant offsetting of beds on opposite sides of dikes. One dike that appears to be in a fault or a fault zone has an unusual layered texture that is possibly the result of shearing after dike emplacement (Fig. 17), but differential shear between flowing magma and stationary dike walls can result in a similar texture.

Figure 17. Dike with an unusual platey fracture pattern. This dike is in or adjacent to a fault. This layered fracturing may have resulted from shearing of the dike by fault movement after emplacement, but differential shear between flowing magma and the stationary dike walls can result in a similar texture. Photo is looking SSW and taken at UTM 13S 0291351(E), 3799952(N). Hammer is 38 cm.

3. PETROGRAPHY AND MINERAL CHEMISTRY

Thin section petrography and electron microprobe analyses were used to characterize and categorize the dikes using primary and alteration mineralogy, mineral chemistry, and textural relationships between phases. The two types of dikes recognized in the field, basaltic and minette, were refined and new dike types were recognized using laboratory techniques. The goal of characterizing and categorizing the dikes is to investigate relationships among and between the dike categories in regard to magma sources and relative timing of emplacement.

The five categories of dikes based on amount and size of biotite, the types and texture of feldspar, and the presence of analcime in the dikes are basaltic, basaltic with significant biotite, minette, analcime-bearing, and speckled texture analcime-bearing. Most dikes are basaltic and contain groundmass plagioclase, groundmass and phenocrystic pyroxene, olivine, and sparse to common fine biotite. Minettes contain groundmass and phenocrystic biotite and pyroxene and groundmass alkali feldspar. Minettes are recognizable in the field because the phenocrystic biotite is often found in "clots" a few cm in diameter. Basaltic dikes with significant biotite contain biotite phenocrysts but lack the clots present in minette dikes. They also contain sanidine, ± plagioclase, and possibly clinopyroxene. Analcime-bearing dikes contain analcime (after leucite), groundmass and phenocrystic pyroxene, one to two groundmass feldspars, biotite, and olivine. The black (pyroxene) and white (feldspar?) speckled texture of some

dikes was recognized in the field but the dikes were categorized as basaltic. Laboratory analyses revealed that the dikes contain analcime, clinopyroxene, feldspar, and biotite. Table 1 lists samples by category.

Minor and alteration phases are found in all three categories of dikes. Minor phases observed include magnetite and common apatite. Common alteration phases include clays, epidote, chlorite, and zeolites. Many dikes contain abundant carbonate that resulted from autometasomatism of the dikes by undegassed magmatic CO_2.

Sample preparation and methods of analysis are presented in Appendix B. Thin section petrography is presented in Appendix C and electron microprobe data are presented in Appendix D.

3.1 Feldspar

Feldspar is an essential mineral in all the dikes and is generally confined to groundmass. Representative feldspar analyses are shown in Table 2. Feldspars of all compositions are present but labradorite and sanidine are the most common. Compositions between labradorite and sanidine are likely the result of mixing between the dike magma and granitic xenoliths recognized in thin section and electron backscatter images. Albite analyses likely represent alteration of feldspar.

3.1.1 Basaltic dikes

Most basaltic dikes contain essential fresh groundmass plagioclase with polysynthetic twinning and common trachytic texture (Fig. 18). Microprobe analyses reveal that all basaltic dikes with fresh plagioclase contain labradorite (Fig. 19).

Some samples contain alkali feldspar and plagioclase more sodic than labradorite. Andesine analyses of some samples may represent albitization (or normal zoning) but the

Table 1. List of samples according to dike type. Dike types based on mineralogy and mineral chemistry.

Sample			
Basaltic samples			
RDS-1			
RDS-4	heavily altered		
RDS-6	heavily altered		
RDS-8			
RDS-013B			
RDS-013C	same dike as RDS-013B, not the same dike as RDS-013A		
RDS-027			
RDS-005			
MDS-14		**Basaltic samples with significant biotite**	
MDS-15		RDS-7	
MDS-16		RDS-13	
RDS-031		RDS-159	
RDS-031B		RDS-206	
RDS-204		RDS-209	
RDS-207			
RDS-188		**Analcime-bearing samples**	
RDS-189A		RDS-5	
RDS-189B		RDS-211	
RDS-190	same dike as RDS-15		
RDS-198		*Spears Ranch Dike*	
		RDS-2	
RDS-15A	core	RDS-10	
RDS-15B	between core and margin	RDS-19	
RDS-15C	margin	RDS-203A	east margin
		RDS-203B	between west margin and core
Pyroxene porphyry dike		RDS-203C	between west margin and core
RDS-16A	core	RDS-203D	core
RDS-16B	between core and margin	RDS-203E	west margin
RDS-16C	margin	MDS-11	
02-77-11-1		MDS-31	
RDS-191		MDS-32	
RDS-199			
RDS-202A		**Analcime-bearing, speckled texture**	
RDS-202B		RDS-013A	not the same dike as RDS-013B & C
		MDS-12	
Feeder(?) dike			
RDS-11	heavily altered	**Minette samples**	
RDS-12		RDS-3	
RDS-17		RDS-098X	same dike as RDS-3
RDS-130		RDS-009	
		RDS-102	
		RDS-106	

basaltic: samples contain plagioclase, clinopyroxene, ± olivine, ± fine biotite.
analcime-bearing: samples contain analcime (after leucite), clinopyroxene, biotite, K-feldspar, ± plagioclase.
analcime-bearing, speckled texture: samples with pyroxene phenocrysts and bleached feldspars/feldspathoids(?).
basaltic with significant biotite: samples contain sanidine, ± plagioclase, ± clinopyroxene
minette: samples with biotite clots

Table 2. Representative electron microprobe analyses of feldspar reported in wt% and samples are listed in order of increasing Or.

	1	2	3	4	5	6	7
	RDS-15A-07	RDS-17-21	RDS-7-22	RDS-8-25b	RDS-3-09	RDS-102-31	RDS-2-19
SiO_2	51.89	54.47	53.61	65.09	64.03	64.31	63.93
Al_2O_3	29.93	28.33	29.63	21.37	21.24	19.84	19.36
FeO	0.92	1.12	0.60	0.74	1.10	0.00	0.28
BaO	0.06	0.05	0.20	0.07	0.25	0.68	0.00
CaO	12.60	11.16	11.12	2.05	1.96	0.48	0.31
Na_2O	4.12	4.40	4.70	8.38	5.47	3.02	0.86
K_2O	0.21	0.25	0.76	3.05	7.44	11.87	15.56
SrO	0.44	0.22	0.43	0.03	0.34	0.24	0.05
Total	100.16	100.00	101.04	100.78	101.82	100.44	100.36
Numbers of ions on the basis of 32O							
Si	9.490	9.903	9.685	11.535	11.478	11.737	11.803
Al	6.451	6.070	6.308	4.463	4.487	4.267	4.212
Fe3+	0.070	0.085	0.045	0.055	0.082	0.041	0.022
Ba	0.004	0.004	0.014	0.005	0.018	0.049	0.000
Ca	2.469	2.174	2.152	0.389	0.376	0.094	0.061
Na	1.461	1.551	1.646	2.879	1.901	1.069	0.308
K	0.049	0.058	0.175	0.689	1.701	2.763	3.665
Sr	0.047	0.023	0.045	0.003	0.035	0.025	0.005
Total	20.040	19.867	20.071	20.018	20.079	20.045	20.077
Or	1.2	1.5	4.4	17.4	42.8	70.4	90.8
Ab	36.7	41.0	41.4	72.7	47.8	26.5	7.6
An	62.1	57.5	54.2	9.8	9.5	2.4	1.5

1: Petrographic group: basaltic.

2: Petrographic group: basaltic.

3: Petrographic group: basaltic with significant biotite.

4: Petrographic group: basaltic.

5: Petrographic group: minette.

6: Petrographic group: minette.

7: Spears Ranch Dike. Petrographic group: analcime-bearing.

Analytical methods are reported in Appendix B.

Uncertainties based on replicate analyses of standard reference materials are reported in Appendix E.

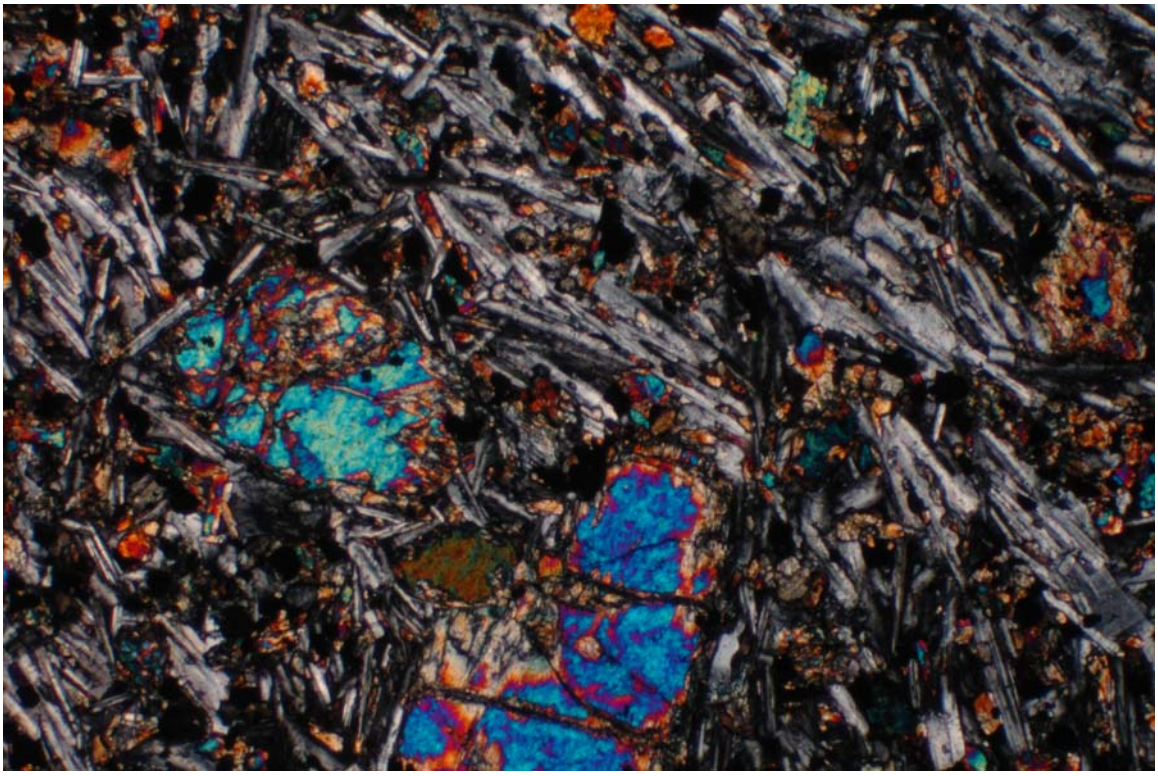

Figure 18. Trachytic alignment of plagioclase microlites in sample RDS-12. Petrographic group: basaltic. This sample is from the feeder(?) dike. The larger blue birefringent phenocrysts are fresh olivine and the small groundmass crystals with red to blue birefringence are clinopyroxene. Fresh olivine phenocrysts are rare in the Riley dikes. Field of view is 1.8 mm wide.

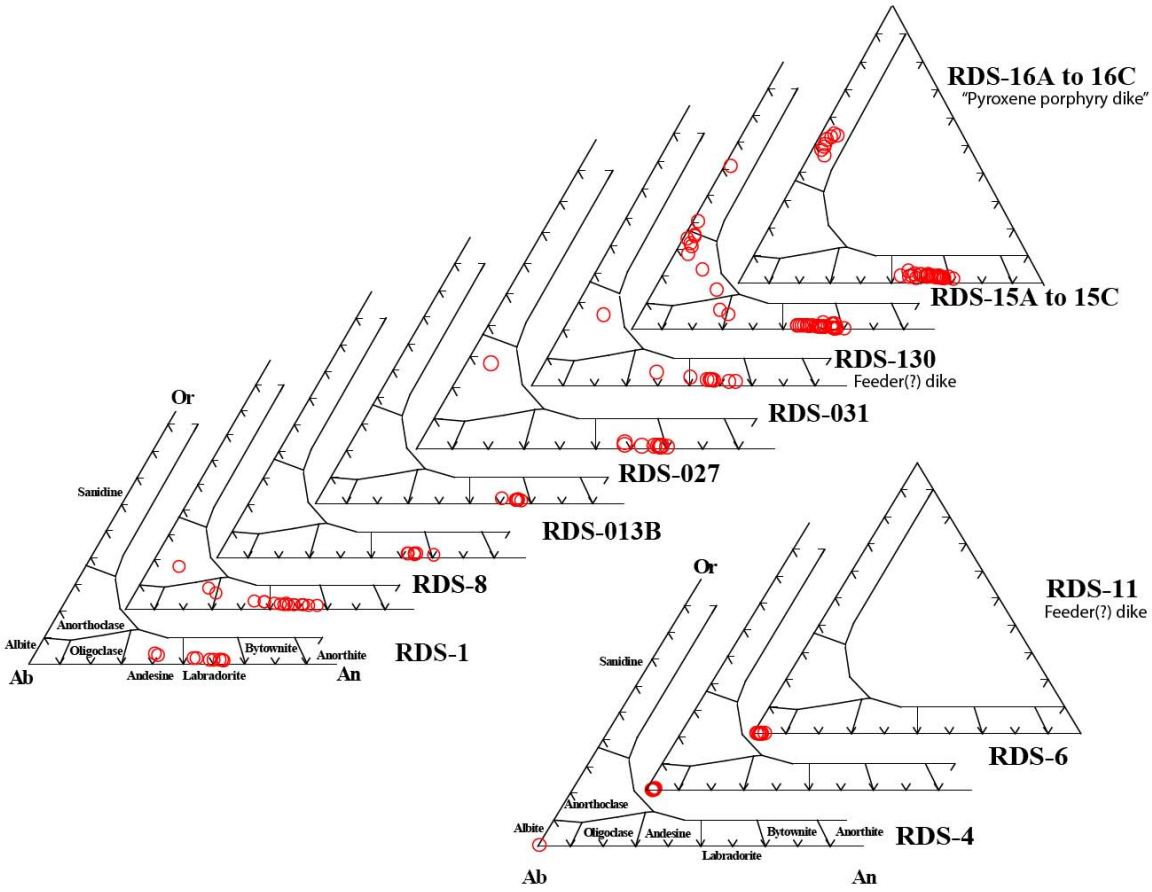

Figure 19. Feldspar ternary diagrams for basaltic samples. Feldspars of the three samples on the bottom, RDS-4, RDS-6, and RDS-11, are albitized.

trend of increasing K suggests evolution of the magma or incorporation of felsic material (i.e. xenocrystic contamination). The single anorthoclase analysis of RDS-031 appears to be part of a transition or alteration zone. Anorthoclase and andesine analyses of RDS-130 are rims of crystals that have labradorite cores and may represent overlap of the microprobe beam onto two chemical zones.

Samples RDS-15A, B, and C, RDS-16A, B, and C, were sampled to analyze textural and chemical differences across the width of dikes. RDS-203A, B, C, and D were also analyzed by petrographic microscope for textural differences across the dike. As expected, samples from near the dike margin are finer-grained than samples from the dike cores. Chemical differences across the dikes are discussed in the following paragraphs.

RDS-15 samples are from a basaltic dike. All three samples contain abundant labradorite and occasional smaller alkali feldspar (Fig. 20). Abundant quartz xenocrysts are apparent in all three samples suggesting that the alkali feldspar is the result of incorporation of xenolithic material. The sanidine analysis in RDS-15A is adjacent to one of these quartz grains.

RDS-16 samples are also from a basaltic dike. Samples RDS-16B and RDS-16C, collected from the midpoint between margin and core and from the margin, respectively, contain sanidine in addition to labradorite (Fig. 21). Sample RDS-16B contains crustal xenoliths observed in both thin section and the electron microprobe. Sanidine analyses of RDS-16B are within a xenolith. Sanidine analyses of RDS-16C are from relatively small crystals which are adjacent to quartz grains. No xenoliths were observed in RDS-16A, the sample from the dike core.

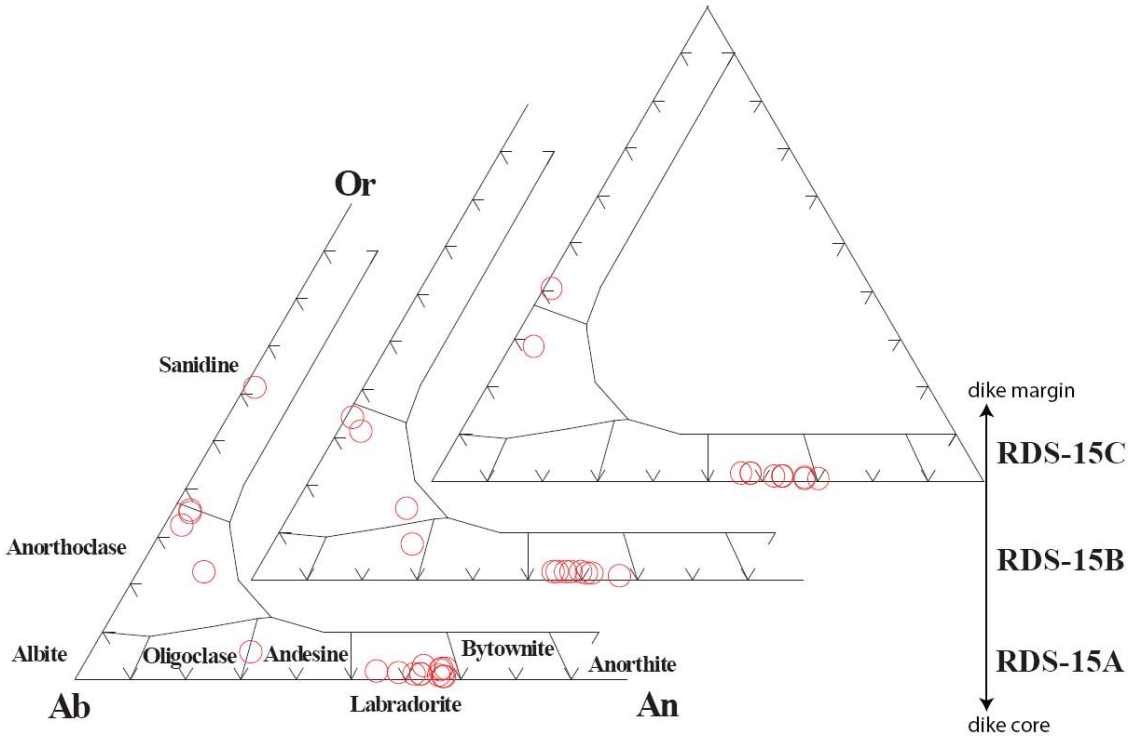

Figure 20. Feldspar ternary diagrams for basaltic samples RDS-15A, RDS-15B, and RDS-15C. Sample RDS-15A is from the center of the dike and RDS-15C is from the margin.

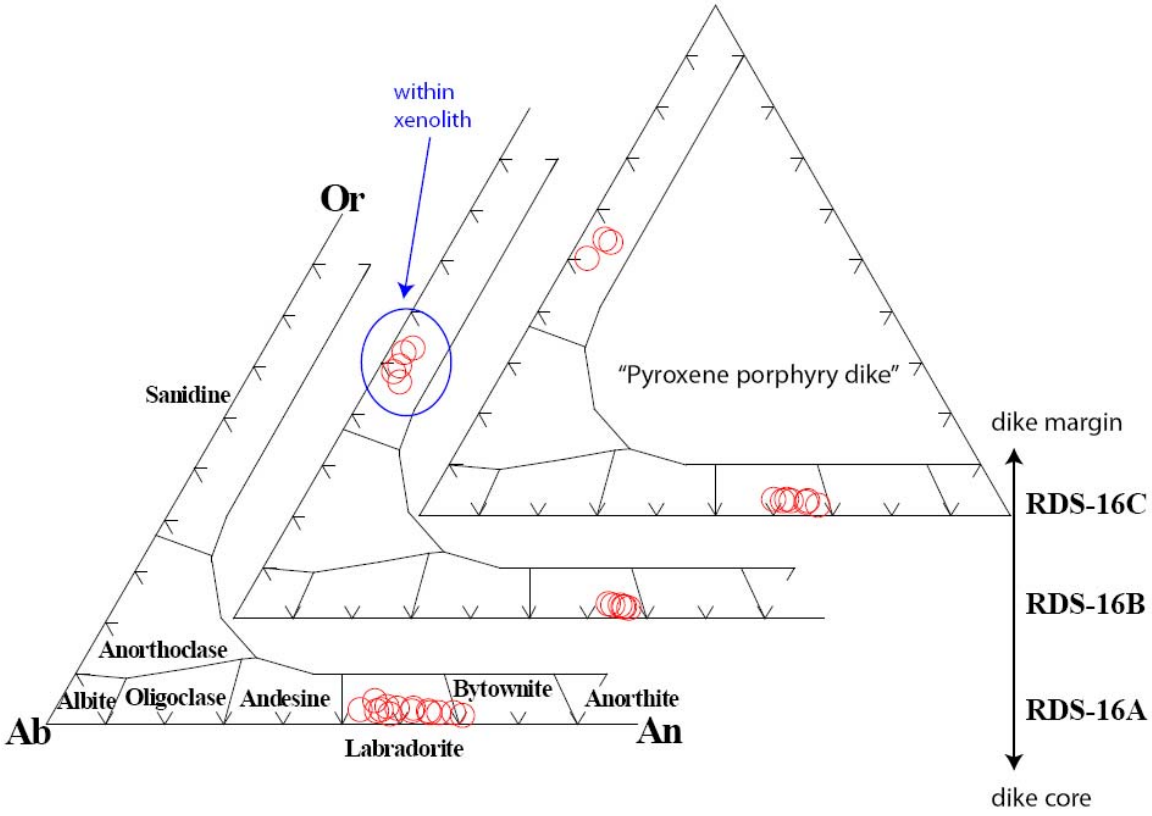

Figure 21. Feldspar ternary diagrams for samples from the pyroxene porphyry basaltic dike. Sample RDS-16A is from the center of the dike and RDS-16C is from the margin. RDS-16B was sampled between A and C.

Altered plagioclase is observed in few samples. Several samples considered basaltic based on their primary mineralogy of plagioclase, pyroxene, and minor biotite, contain albitized or altered plagioclase. The three samples (RDS-4, RDS-6, RDS-11) analyzed by electron microprobe that contain altered plagioclase contain albite and lack labradorite and alkali feldspar (Fig. 19).

Feldspar was rarely observed in sample RDS-4 using the microprobe. Only one feldspar point was analyzed using the electron microprobe. This sample contains abundant silicification observed in the microprobe which is possibly an alteration product of feldspar.

The large (~1mm) plagioclase crystals in sample RDS-6 are almost completely albitized (Fig. 22). Figure 23 shows plagioclase with a patchy texture. The darker patches are albite.

Feldspars in RDS-11 are also completely albitized, but another sample (RDS-130) from the same dike contains fresh feldspar (Fig. 24). Both samples are basaltic, holocrystalline, and coarse grained, but RDS-130 is the finer grained of the two (Fig. 25). Sample RDS-11 is from the altered dike margin and RDS-130 is from the fresher dike core.

3.1.2 Basaltic samples with significant biotite

Some basaltic samples have more abundant and larger biotite than the majority of basaltic samples. Unlike other basaltic samples, these dikes contain essential primary sanidine (Fig. 26).

Plagioclase was observed in two of the samples in thin section, but was only analyzed in one sample. This sample contains labradorite like the other basaltic samples.

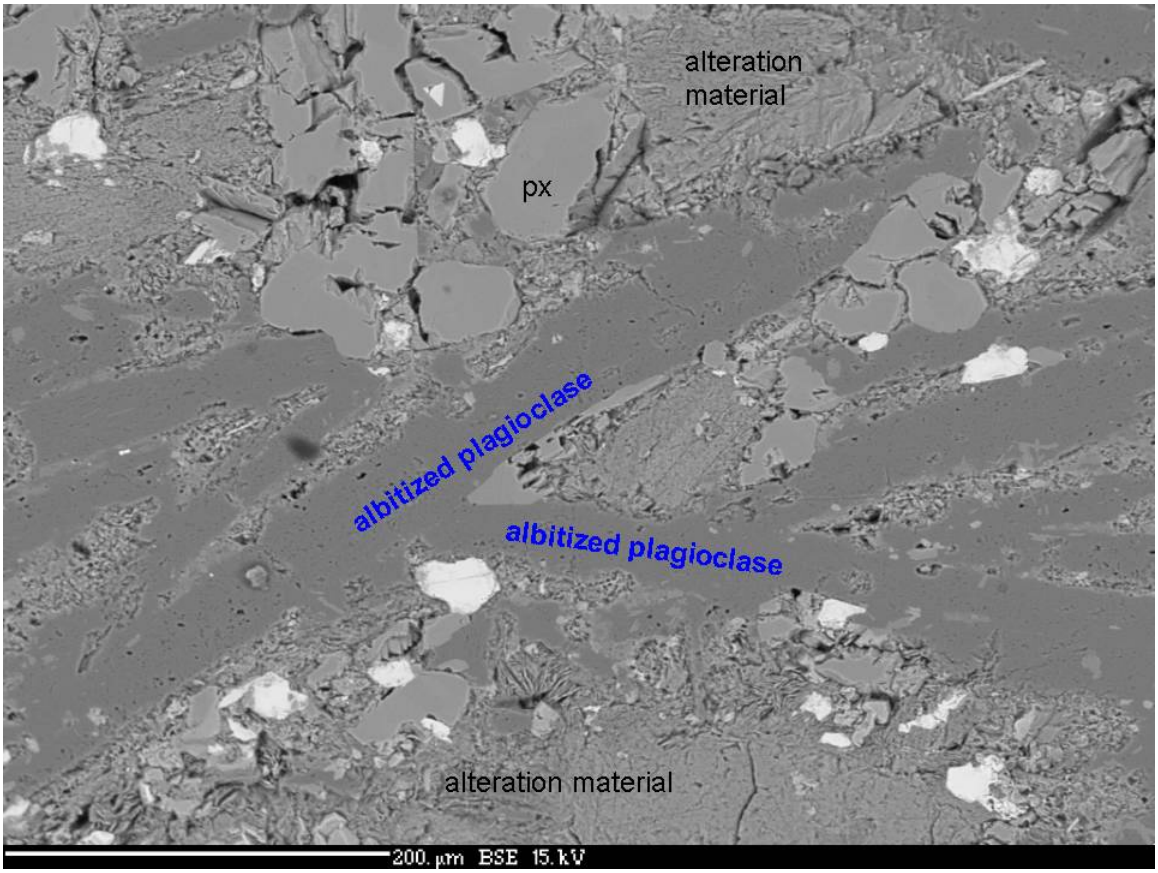

Figure 22. Backscatter electron image of sample RDS-6 showing completely albitized feldspar crystals. Px = pyroxene.

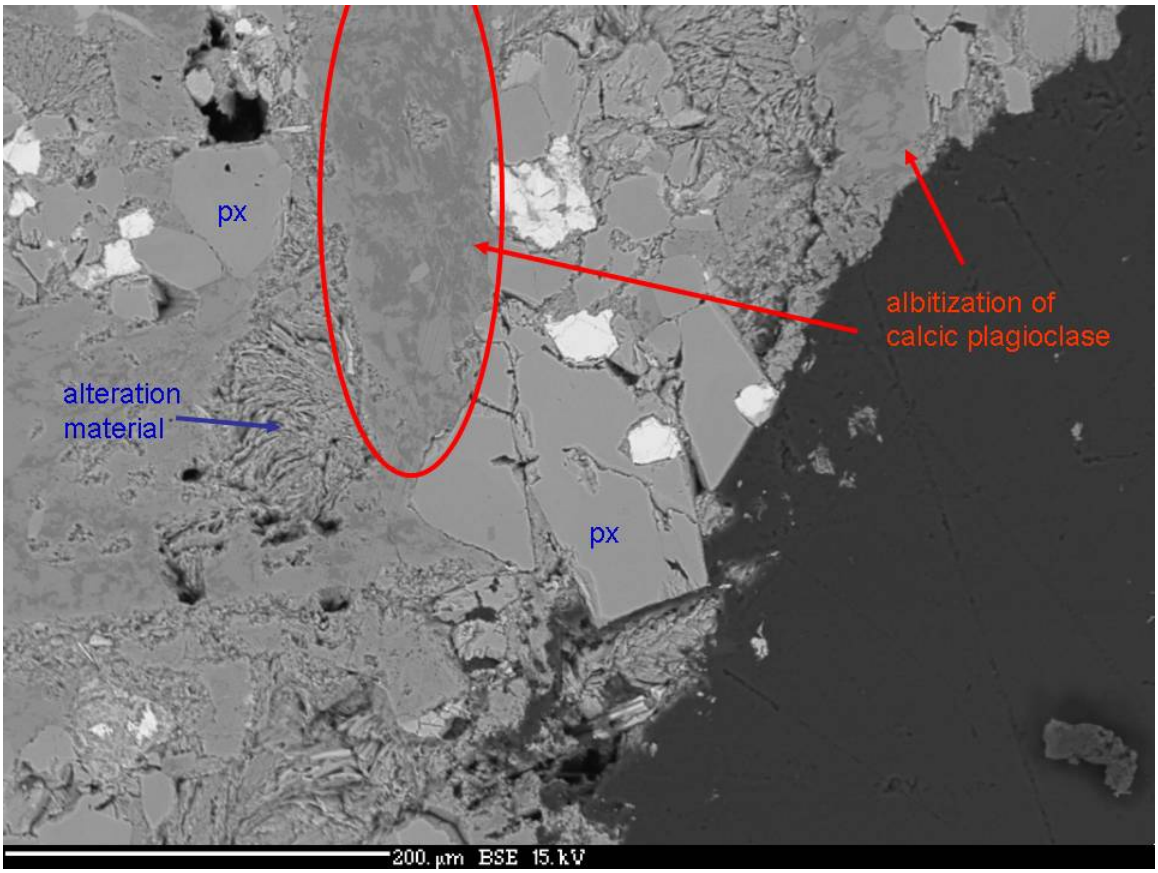

Figure 23. Patchy texture of a plagioclase crystal in the process of separation of albite and anorthite. Px = pyroxene.

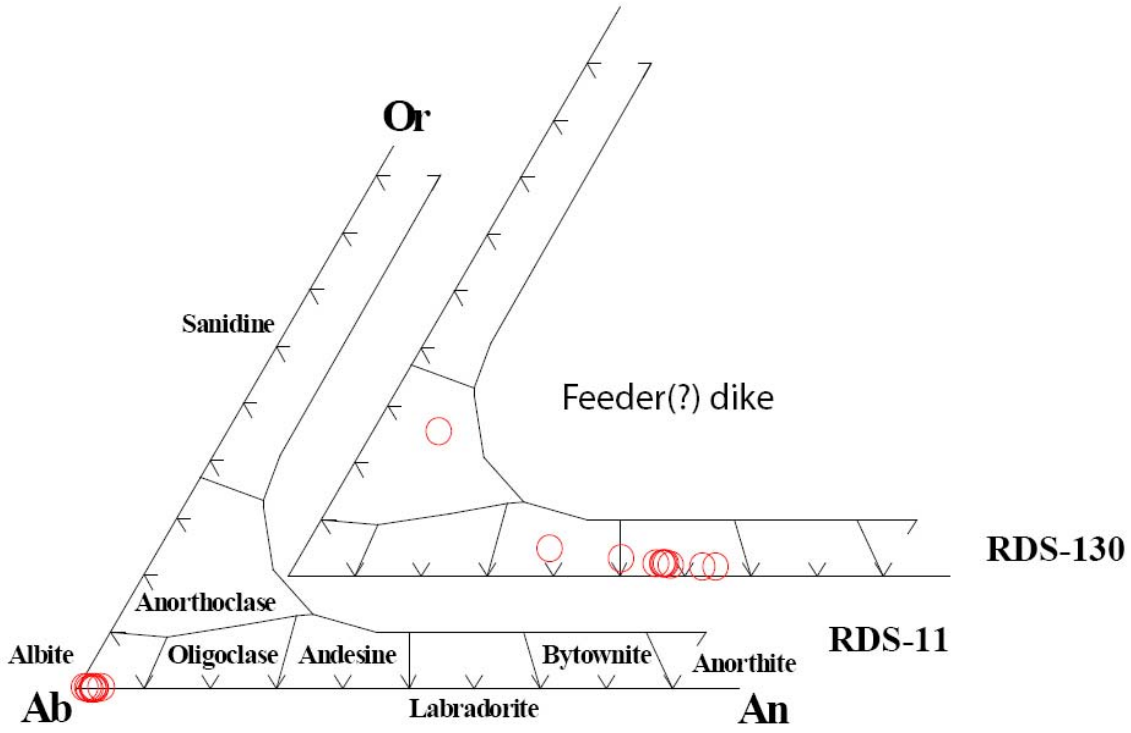

Figure 24. Feldspar ternary diagrams for two samples from the same dike. RDS-11 is from the altered dike margin and RDS-130 is from the fresher dike core.

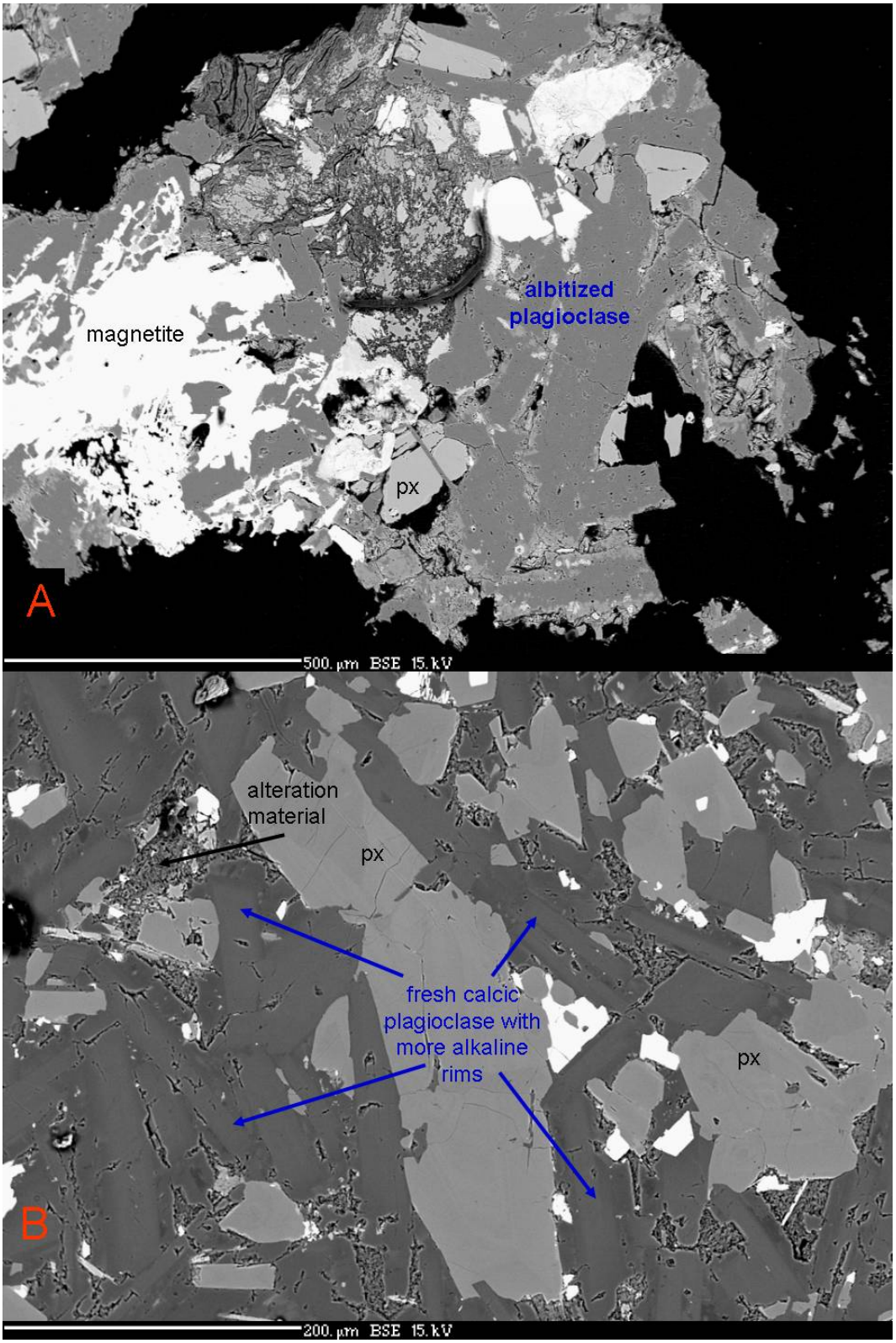

Figure 25. Backscatter electron images of two samples from the same dike. a) Completely albitized feldspar in sample RDS-11. b) Fresh plagioclase in sample RDS-130. Note different scales. Px = pyroxene.

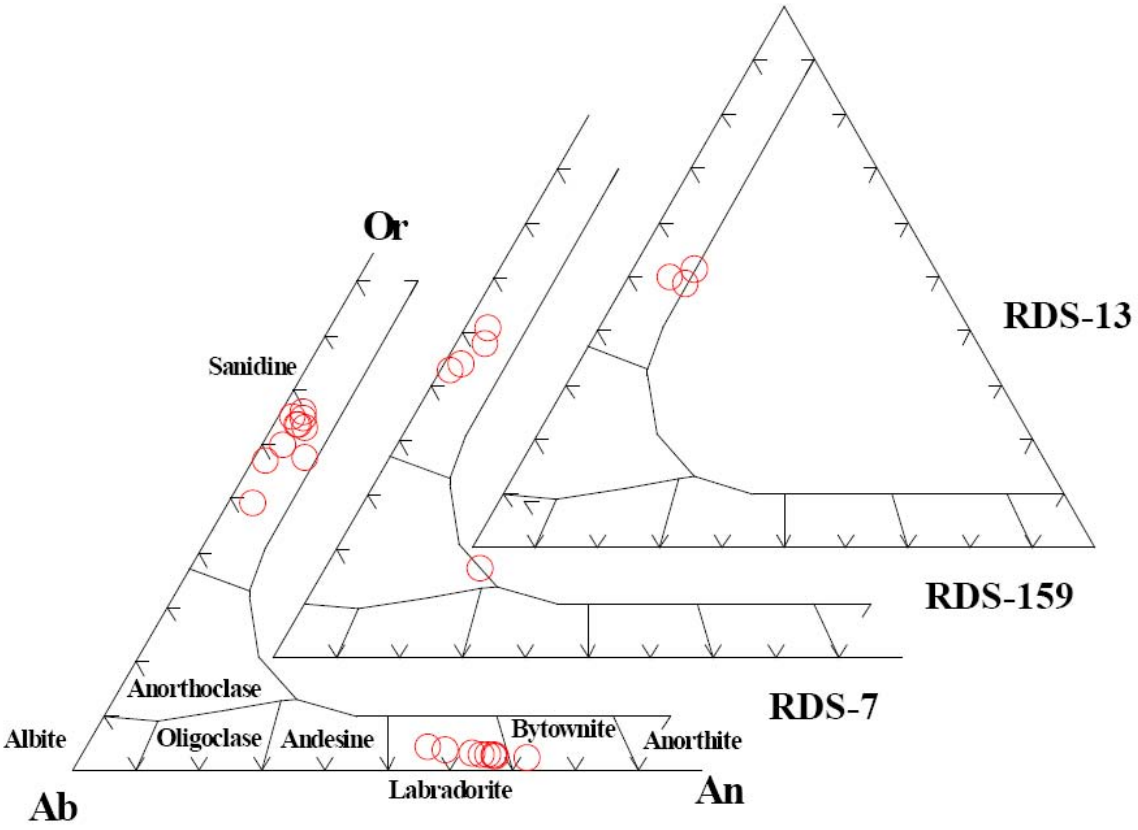

Figure 26. Feldspar ternary diagrams for basaltic samples that contain significant biotite.

There are no textural differences between the two feldspar populations. Some crystals appear to have a calcic core and alkali rim but there are crystals of similar size that are completely K-feldspar and do not appear to be xenocrystic.

There is no textural difference to explain the anorthoclase point in sample RDS-159, but plagioclase was observed in the thin section of this sample. There are also no textural differences between the samples to explain the higher-Ca sanidine in RDS-13.

3.1.3 Minettes

As stated in Chapter 2, minettes are recognizable in the field due to their common biotite clots up to several cm in size. In thin section, minettes contain a mottled groundmass. Feldspars are therefore difficult to identify. Some of the groundmass feldspar is altered to clay and zeolites.

Minettes contain essential sanidine (Figs. 27 and 28). Sanidine in sample RDS-106 is more sodic and the sample includes anorthoclase and plagioclase. The plagioclase analyses are along the margin of a xenolith and the more sodic alkali feldspars are probably the result of the xenolith melting and mixing with the dike magma. There are no obvious textural differences between the samples to explain the high-Ca sanidine in RDS-3.

3.1.4 Analcime-bearing dikes

Some dikes contain occasional plagioclase in a pervasive isotropic groundmass. All contain sanidine (Fig. 29). Backscatter images reveal the isotropic groundmass in non-speckled texture analcime bearing dikes to be intergrown K-feldspar and analcime, which is interpreted as an exsolution texture (Figs. 30 and 31). This groundmass texture and analcime are discussed in section 3.2.

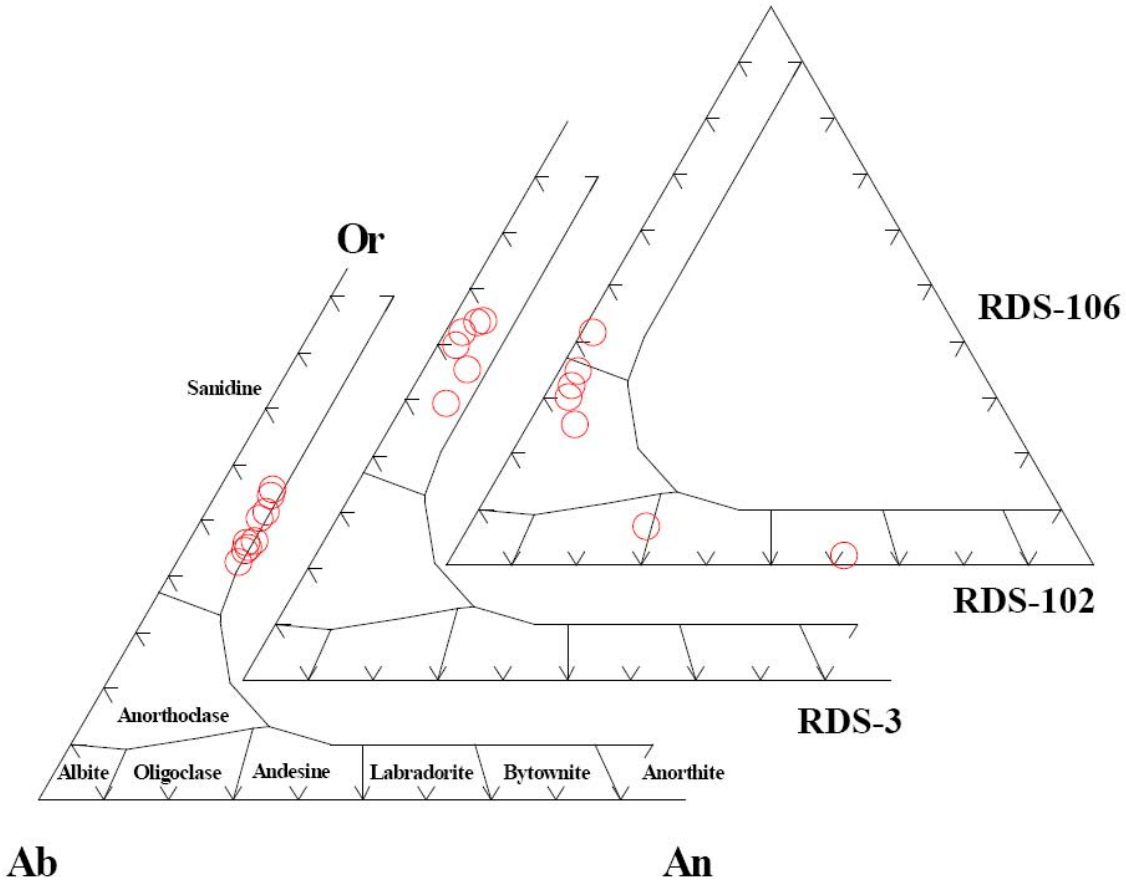

Figure 27. Feldspar ternary diagrams for minette samples.

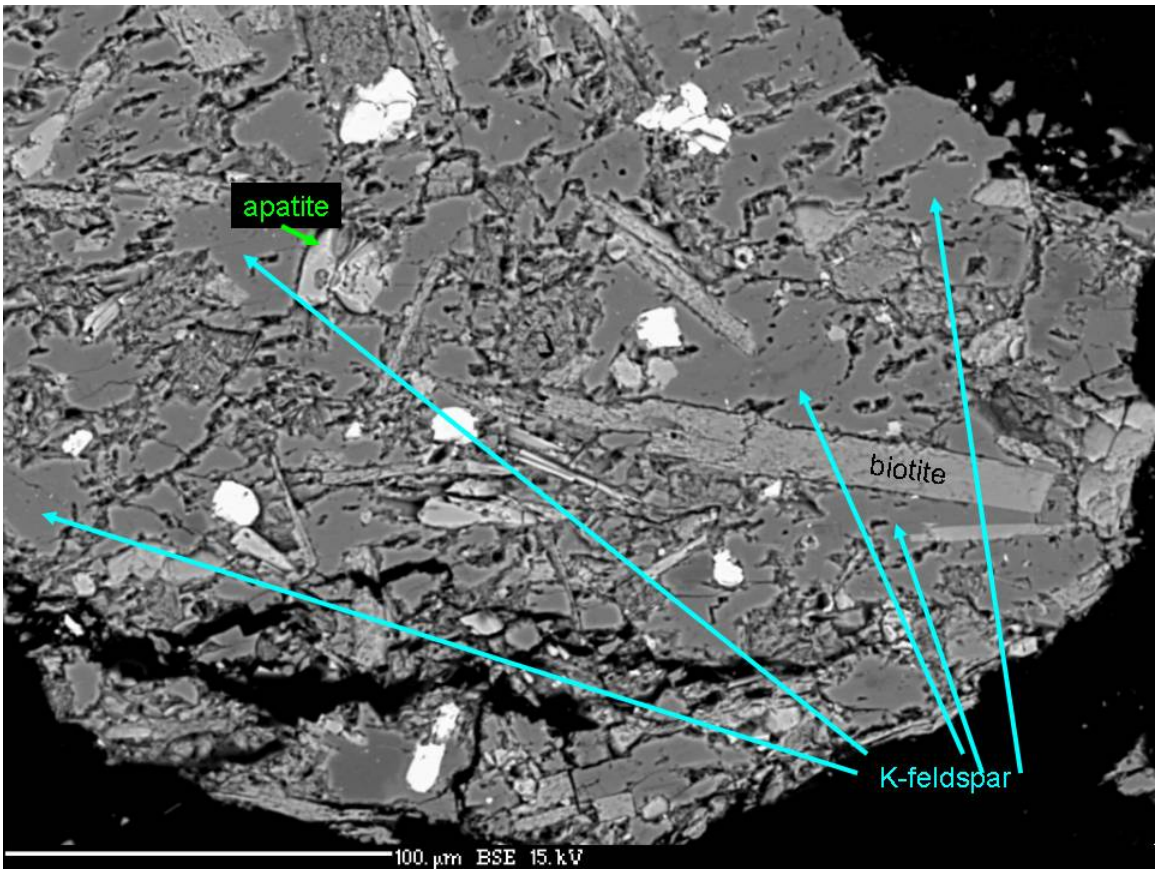

Figure 28. Minette sample RDS-3 with abundant K-feldspar.

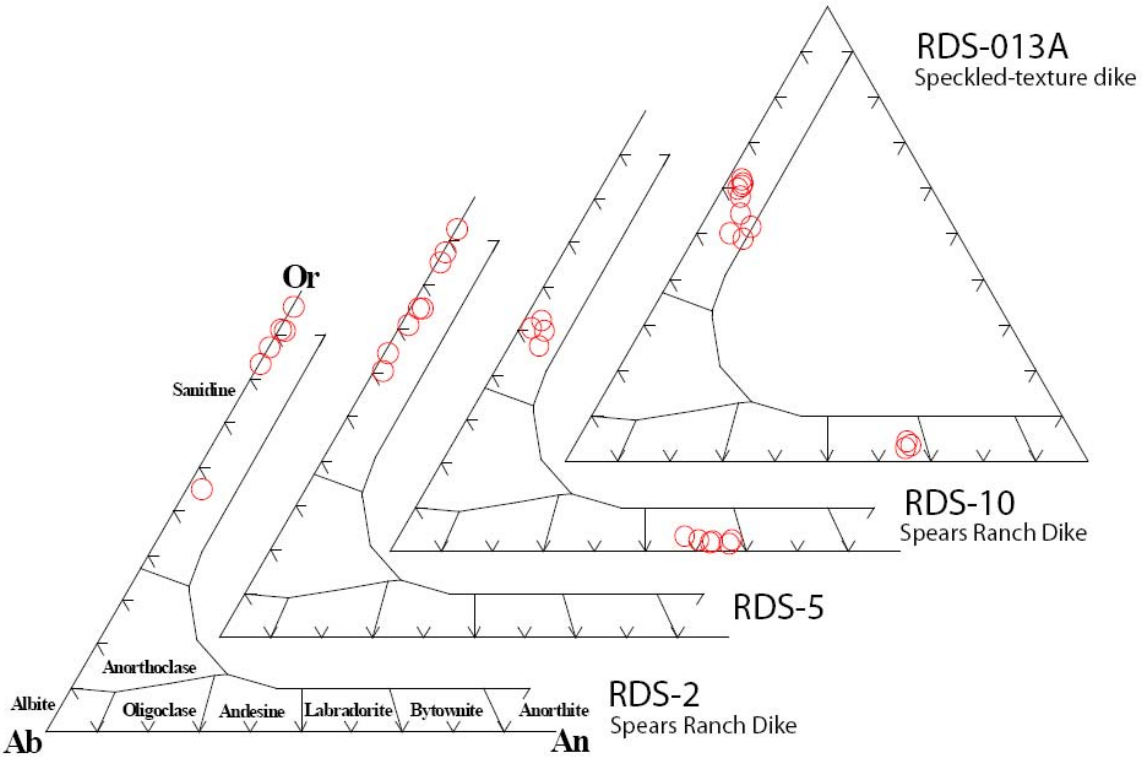

Figure 29. Feldspar ternary diagrams for analcime-bearing samples. RDS-2 and RDS-10 are from the Spears Ranch Dike.

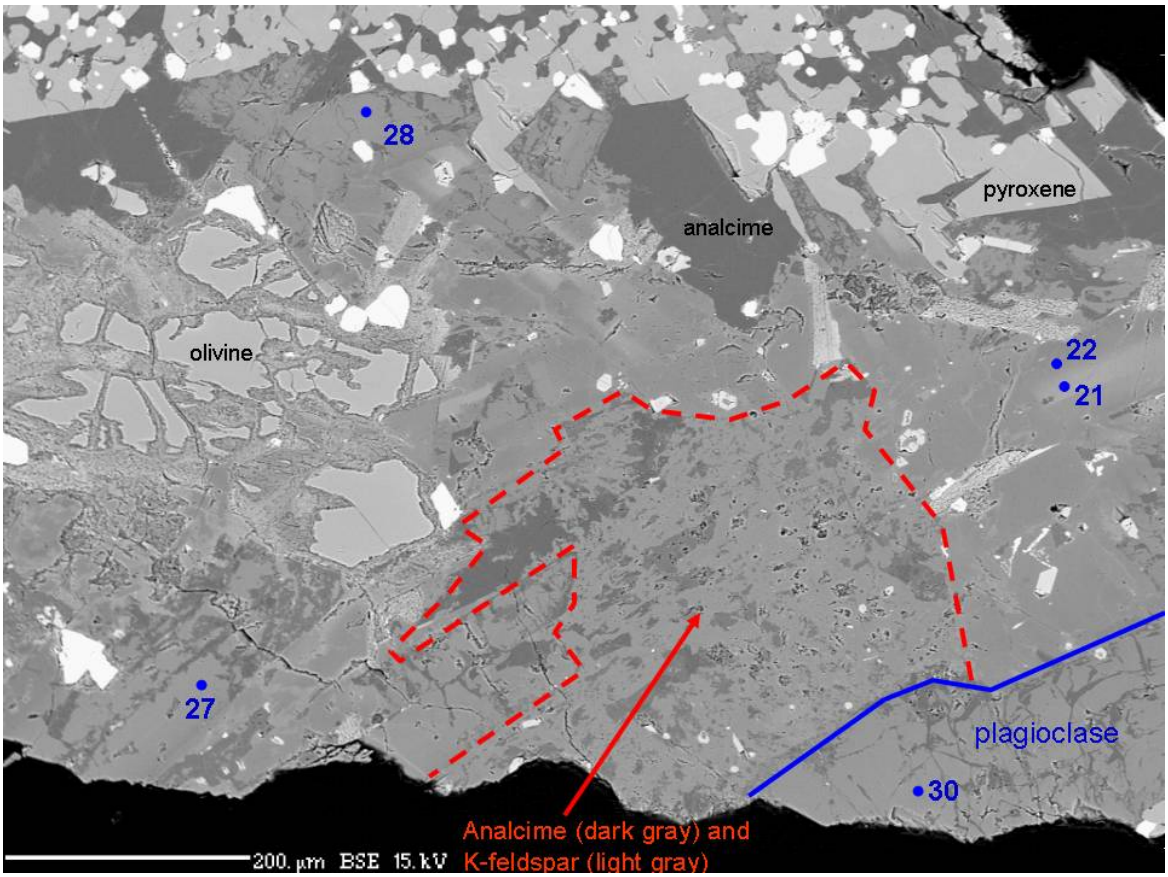

Figure 30. Analcime and K-feldspar groundmass in sample RDS-10. Points 21 and 22 are alkali felspar but point 21 is enriched in barium (Ba = 1.7 wt%). Points 27, 28, and 30 are plagioclase. For data refer to Appendix D.

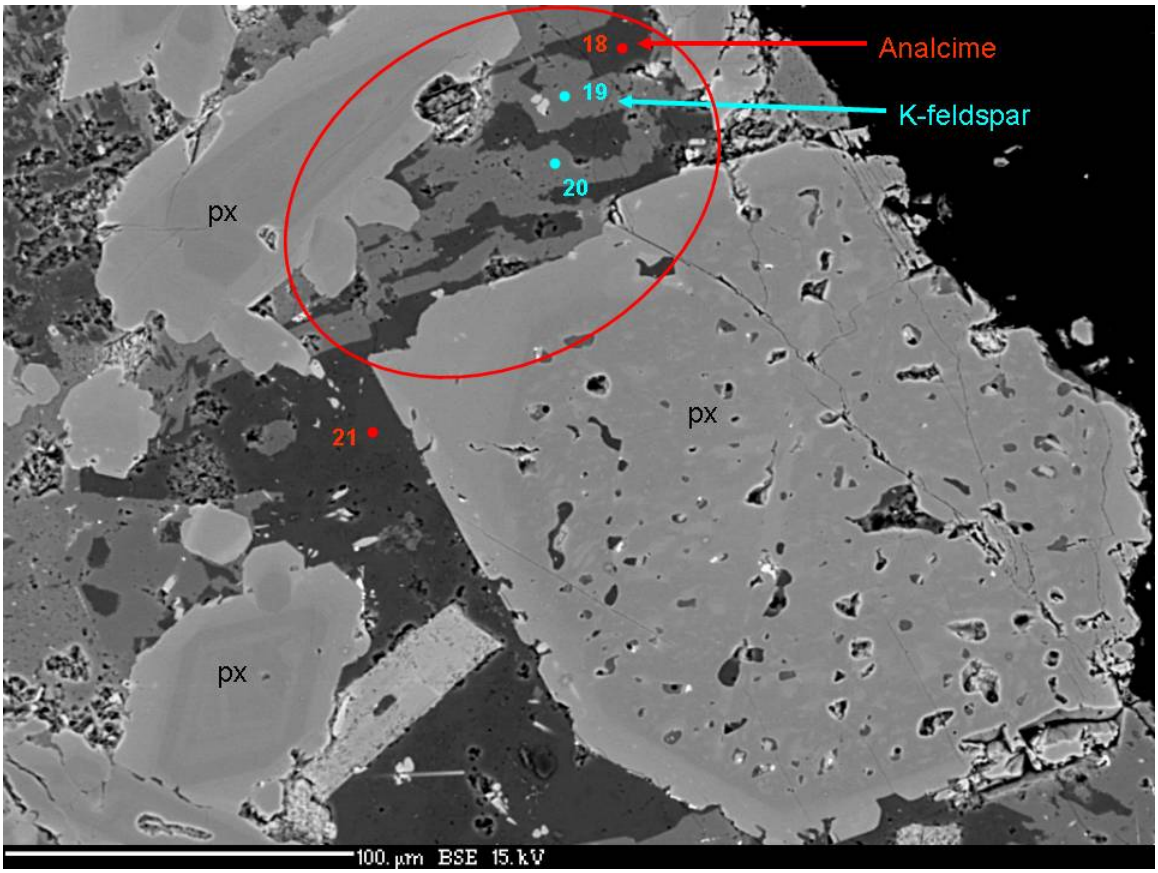

Figure 31. Analcime and K-feldspar groundmass in sample RDS-2. The pattern of interleaved analcime and K-feldspar may represent intergrowth or perthitic exsolution. Note zoned pyroxenes (px). Numbered points refer to data in Appendix D.

Labradorite is present in two analyzed samples, including the speckled texture sample RDS-013A. One sample with and one sample without labradorite, RDS-10 and RDS-2, are from the Spears Ranch Dike. The presence of labradorite and lower-K sanidine in RDS-10 reveals compositional variation along the strike of the dike.

3.2 Leucite and analcime

Analcime-bearing dikes display two textures. The first is a fine-grained texture that cannot be distinguished from other basaltic samples in the field. Analcime-bearing dikes with this field texture contain fresh pyroxene and an isotropic groundmass and contain rare to no plagioclase. Analcime-bearing dikes with the second texture are recognizable in the field. They are porphyritic, containing several mm-sized black phenocrysts of pyroxene and similar-sized white crystals.

Analcime-bearing dikes of texture #1 were first termed nephelinite (Dimeo, 2006) because of leucite trapezohedrons recognized in one thin section (Fig. 32), and the cloudy, low relief, low-birefringent to isotropic analcime in the groundmass was misidentified as nepheline, which is optically similar. Leucite trapezohedrons were only observed in one of five samples from the Spears Ranch Dike (RDS-2) and in none of the other samples with the same isotropic groundmass (RDS-5 and RDS-211). The leucite has altered to K-feldspar and muscovite. Leucite and muscovite were not observed in the electron microprobe.

Representative electron microprobe analyses of analcime are shown in Table 3. In some electron backscatter images analcime appears to be intergrown or exsolving in a perthitic texture with K-feldspar (Fig. 31) and in other samples intersertal analcime is common (Fig. 33). Analcime occasionally appears to have subhedral crystal shapes (Fig.

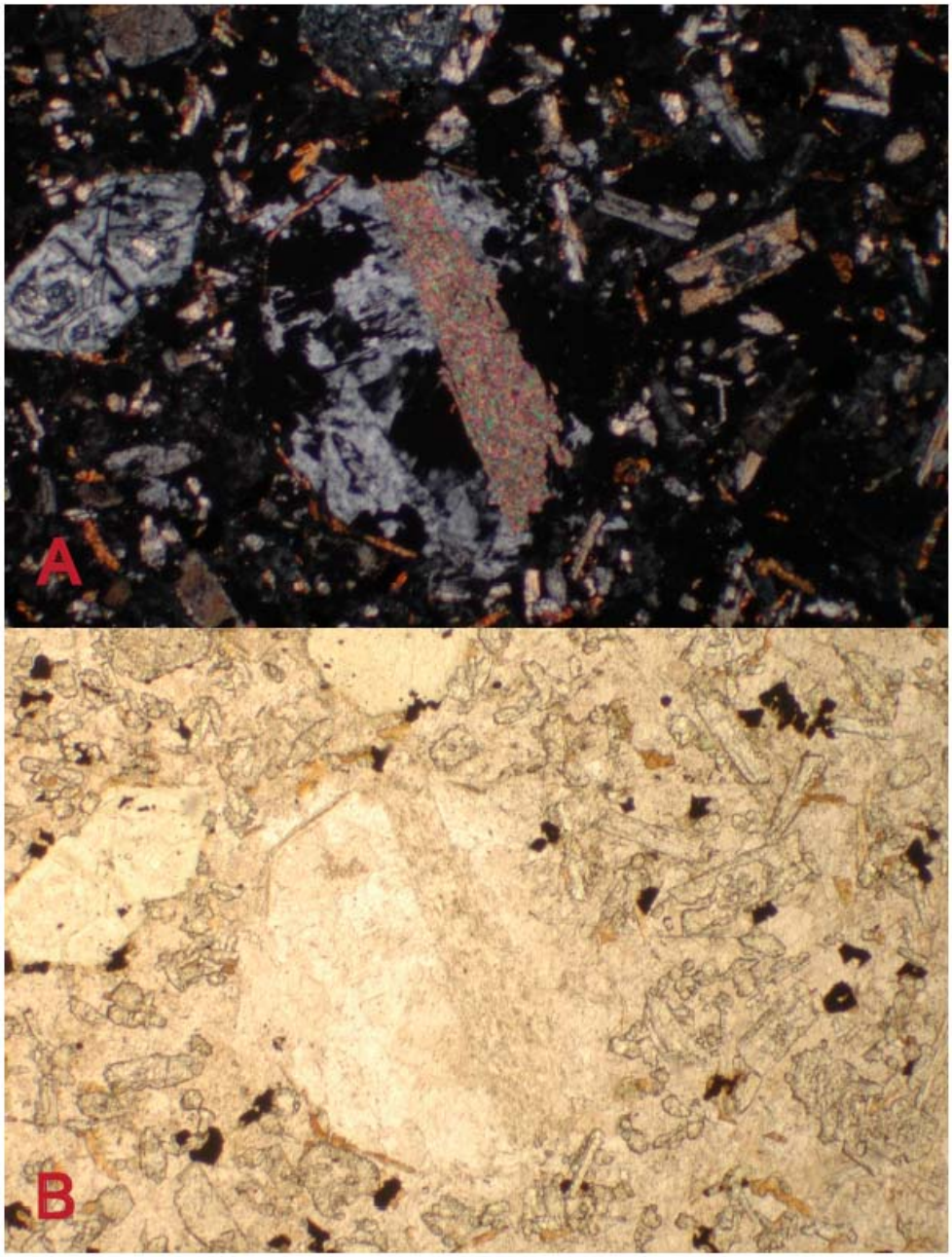

Figure 32. Muscovite within trapezohedron of a former leucite crystal. Leucite has been replaced by analcime and K-feldspar. Field of view is 1.8 mm wide. a) cross-polarized light, b) plane polarized light.

Table 3: Electron microprobe analyses of analcime. Values reported in wt% and samples are listed in order of decreasing Na_2O

	1 RDS-10-26	2 RDS-2-21	3 RDS-013A-19	4 RDS-5-25b
SiO_2	57.89	53.68	53.88	61.43
Al_2O_3	23.15	27.25	28.59	26.1
FeO	0.44	0.18	0.18	0.59
CaO	0.2	1.27	2.76	0.14
Na_2O	12.34	11.7	10.56	8.77
K_2O	0.44	0.03	0.27	0.1
SrO	0	0.07	0.23	0.02
BaO	0.01	0	0.05	0
Total	88.96	88.36	93.02	94.28
Numbers of ions on the basis of 96O				
Si	32.782	30.601	30.105	33.092
Al	15.449	18.307	18.826	16.570
Fe2+	0.208	0.086	0.084	0.266
Ca	0.121	0.776	1.652	0.081
Na	13.547	12.931	11.439	9.159
K	0.318	0.022	0.192	0.069
Total	62.426	62.722	62.298	59.237

1: Spears Ranch Dike. Petrographic group: analcime-bearing.

2: Spears Ranch Dike. Petrographic group: analcime-bearing.

3: Petrographic group: analcime-bearing, speckled texture.

4: Petrographic group: analcime-bearing.

Analytical totals are low because of water in the structure of analcime.

Analytical methods are reported in Appendix B.

Uncertainties based on replicate analyses of standard reference materials are reported in Appendix E..

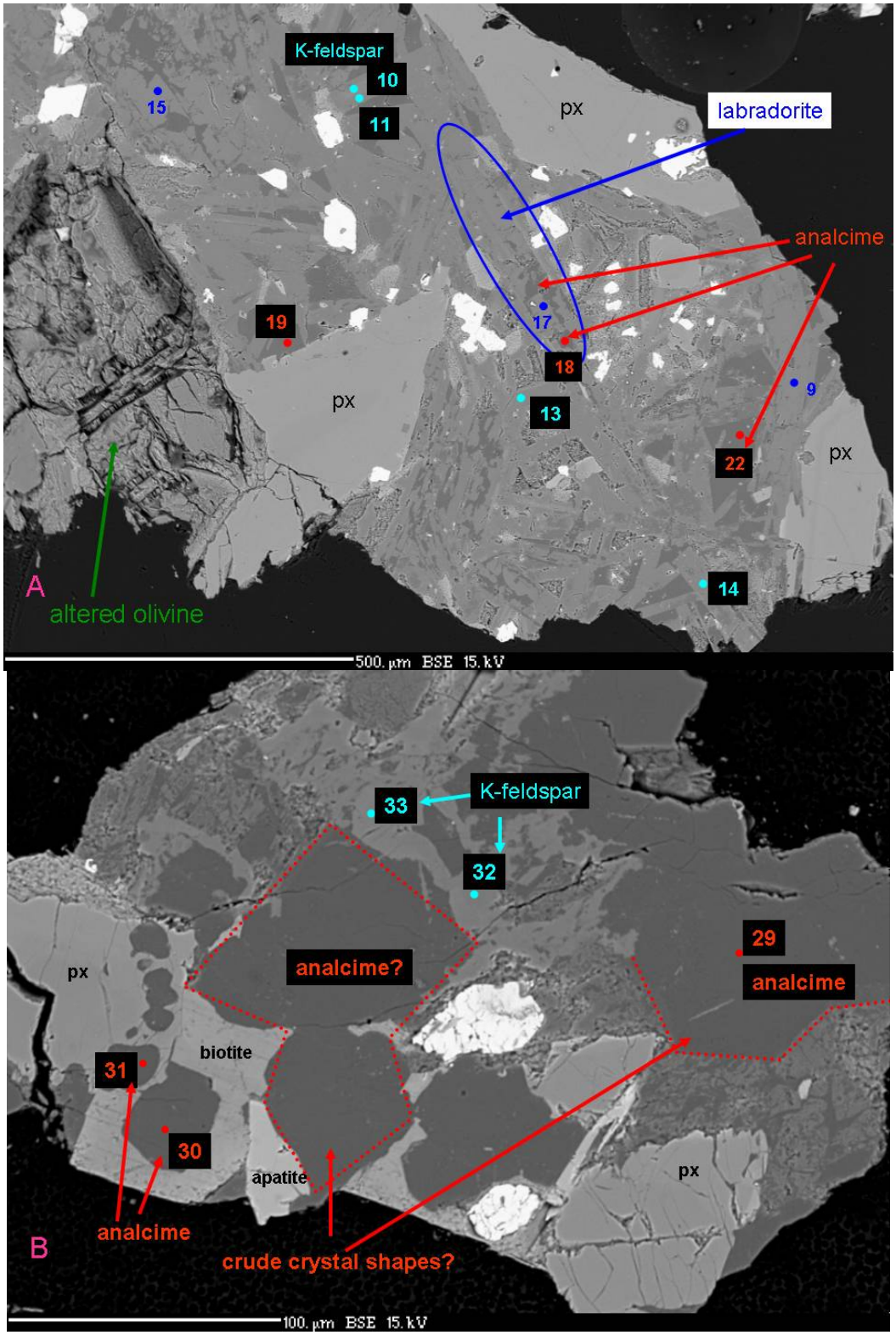

Figure 33. Analcime intergrown(?) with other phases. a) Backscatter image of RDS-013A showing two feldspars and analcime. b) Backscatter image of RDS-5 showing analcime within pyroxene and biotite. Larger areas of analcime appear to have a crude crystal shape. Numbers refer to point data in Appendix D.

33b). Sample RDS-013A contains analcime within a partially assimilated xenolith(?) observed in thin section which is discussed further in section 3.10.1. This analcime might not be co-magmatic with the (basaltic?) host magma. This sample contains both intersertal analcime and analcime within plagioclase laths (Fig. 33a) observed in the microprobe. The texture of the analcime within the plagioclase is similar to albitization seen in RDS-6 (Fig. 34) suggesting the analcime is secondary.

It is probable that the analcime in these dikes is a secondary product formed from alteration of leucite. Leucite is rarely found in rocks older than Tertiary age likely because it has been replaced by pseudomorphic analcime (Deer et al., 1992). Analcime is a well-documented alteration product of leucite (e.g. Prelevic et al., 2004 and Luth and Bowerman, 2004). An experimental study shows that the low-temperature reaction is fast and replacement of 20% of primary leucite by analcime can occur in about four years (in the presence of Na^{+}_{aq} at 40°C; Putnis et al., 2007). Another experimental study reports that groundmass analcime found in dikes is probably secondary due to pressure and temperature constraints, i.e. magmatic analcime is only stable at pressures equivalent to the middle and lower crust (15-30 km; Roux and Hamilton, 1976).

3.3 Clinopyroxene

Clinoyroxene (cpx) is an essential groundmass mineral in all the dikes. It is also commonly found as phenocrysts but some dikes, such as the feeder(?) dike, lack any phenocrystic pyroxene. No orthopyroxene has been analyzed or identified. In many samples, cpx is partially to completely replaced by carbonate (Fig. 35) occasionally mixed with epidote (and chlorite?). Analcime-bearing dikes have the freshest cpx.

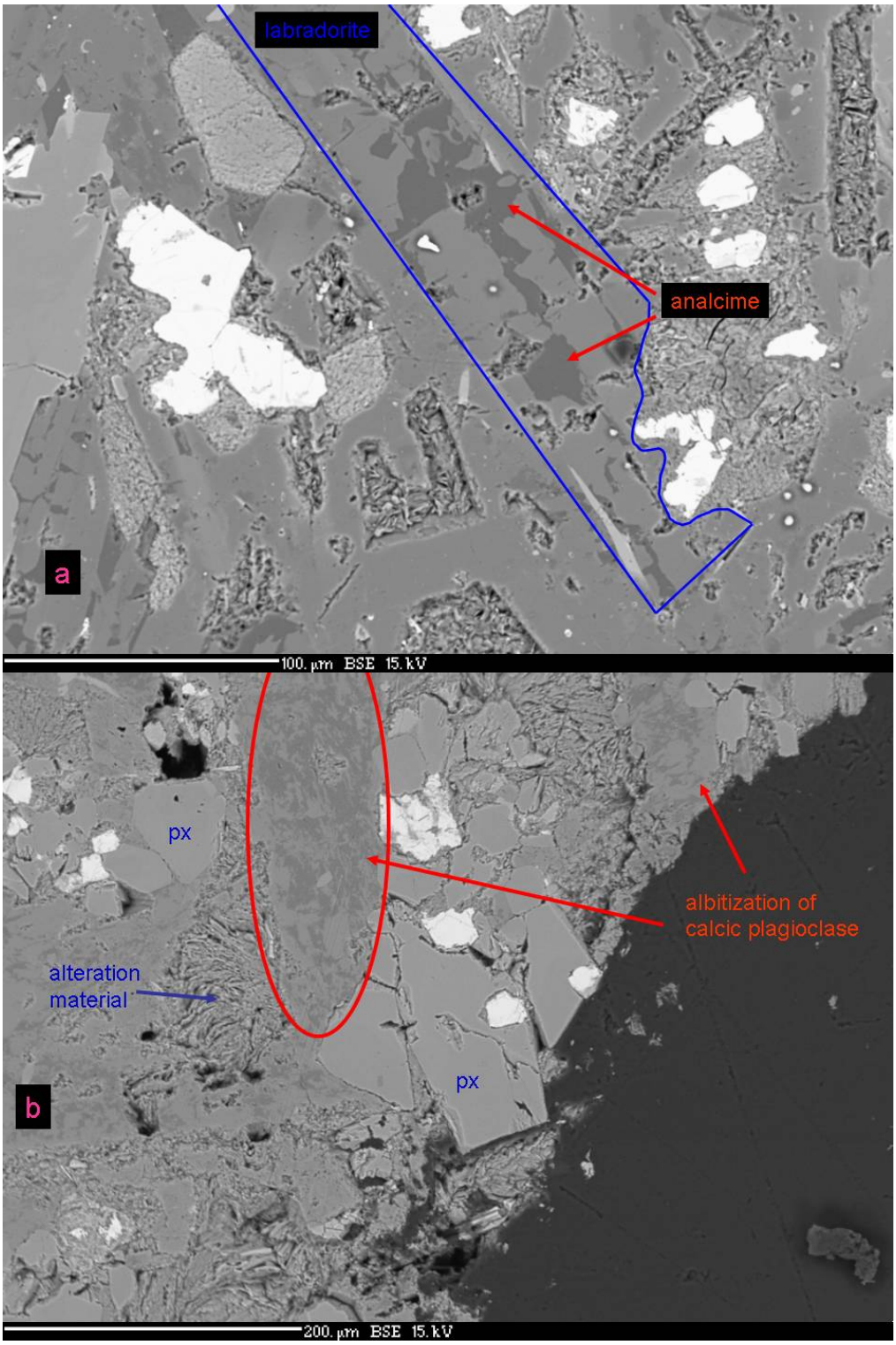

Figure 34. Comparison of compositional textures. a) Plagioclase with intergrown, exsolved, or intermixed analcime in sample RDS-013A. b) Albitizaiton of plagioclase in sample RDS-6.

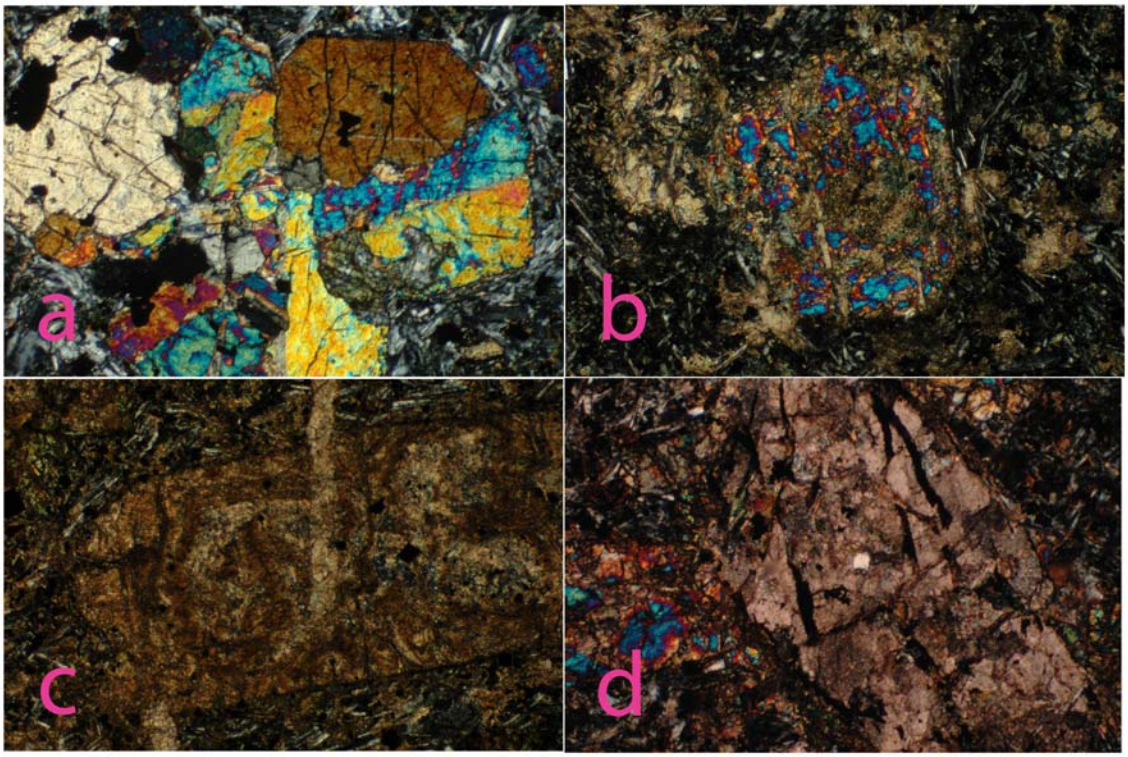

Figure 35. Fresh pyroxene and calcite pseudormorphs. Fields of view for all images is 1.8 mm wide. a) Fresh pyroxene in sample RDS-16A, b) pyroxene partially replaced by calcite in sample RDS-013B, c) pyroxene phenocryst completely replaced by calcite that is cut by a calcite vein in sample RDS-031B. d) Fresh pyroxene (blue, on left) juxtaposed next to a calcite psuedomorph of pyroxene (or olivine?).

Representative electron microprobe analyses of pyroxene are listed in Table 4. Cpx is diopside or high-Ca, high-Mg augite (Fig. 36). Cpx in analcime-bearing dikes are highly calcic, mostly falling in the diopside field. Cpx in the basaltic dikes are generally less calcic than those in analcime-bearing dikes, minettes, or biotite-rich basaltic dikes. A similar relationship is also displayed in a plot of CaO vs. SiO_2 in Figure 37. Cpx in minette dikes have higher CaO contents than most basaltic dikes. Analcime-bearing dikes that are indistinguishable from basaltic dikes in the field have higher pyroxene CaO contents than minettes and basaltic dikes. Pyroxenes from analcime-bearing dikes with a speckled texture in hand sample have CaO amounts similar to basaltic dikes, less than that of pyroxenes in both minette and basaltic dikes.

Some samples contain both fresh pyroxene and pyroxene replaced by carbonate. Figure 35d shows a fresh pyroxene abutting a pyroxene (or olivine?) crystal replaced by calcite. The calcite pseudomorph is larger than the fresh pyroxene demonstrating that it is not always the smallest crystals that are replaced first.

As stated above, analcime-bearing dikes contain the freshest pyroxene and higher-Ca pyroxene than other dikes. Calcite replacement of pyroxene was rarely noted in these dikes.

3.4 Biotite

Most samples contain biotite. Biotite in many basaltic samples is too fine to analyze in the electron microprobe. Biotite in minettes and in basaltic samples with significant biotite is often partially altered to clay. Biotite in some samples forms stellate formations (Fig. 38).

Table 4: Representative electron microprobe analyses of pyroxene. Values reported in wt%. Samples listed in order of decreasing mg#

	1 RDS-2-01	2 RDS-7-15	3 RDS-8-16	4 RDS-15C-11	5 RDS-106-05
SiO_2	52.7	52.61	51.72	48.95	48.26
Al_2O_3	2.1	2.45	2.72	4.15	5.26
TiO_2	0.46	0.5	0.69	1.29	1.34
MgO	16.59	16.27	15.66	14.82	14
FeO	5.26	5.75	6.68	8.08	7.93
MnO	0.14	0.09	0.17	0.21	0.14
CaO	22.85	23.01	22.73	21.43	22.3
Na_2O	0.25	0.28	0.29	0.48	0.39
Total	100.35	100.96	100.66	99.41	99.62
	Numbers of ions on the basis of 6O				
Si	1.9307	1.9205	1.9039	1.8399	1.8129
Al	0.0907	0.1054	0.1180	0.1838	0.2329
Ti	0.0127	0.0137	0.0191	0.0365	0.0379
Mg	0.9061	0.8854	0.8594	0.8304	0.7840
Fe^{2+}	0.1611	0.1755	0.2056	0.2540	0.2491
Mn	0.0043	0.0028	0.0053	0.0067	0.0045
Ca	0.8968	0.8999	0.8964	0.8629	0.8974
Na	0.0178	0.0198	0.0207	0.0350	0.0284
Total	4.0202	4.0230	4.0284	4.0492	4.0470
	Atomic percentages				
Mg	46.0	45.1	43.7	42.5	40.5
Fe+Mn	8.4	9.1	10.7	13.3	13.1
Ca	45.6	45.8	45.6	44.2	46.4
mg#	84.6	83.2	80.3	76.1	75.6

1: Spears Ranch dike. Petrographic group: analcime-bearing.

2: Petrographic group: basaltic with significant biotite.

3: Petrographic group: basaltic.

4: Petrographic group: basaltic.

5: Petrographic group: minette.

mg# = 100*Mg/(Mg+Fe+Mn)

Analytical methods are reported in Appendix B.

Uncertainties based on replicate analyses of standard reference materials are reported in Appendix E.

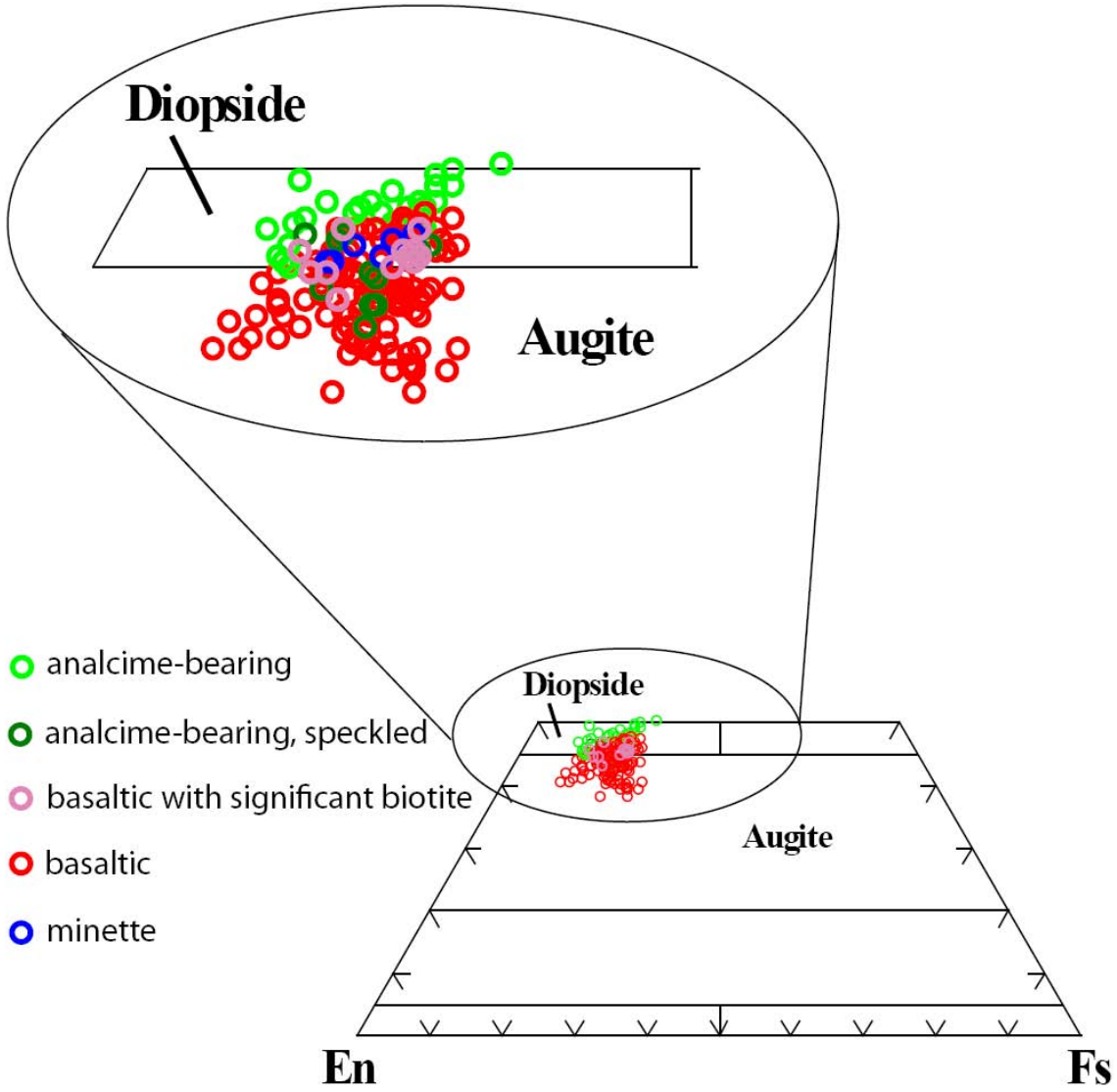

Figure 36. Composition of clinopyroxene in dike samples. Total Fe calculated as FeO. Nomenclature after Morimoto (1988).

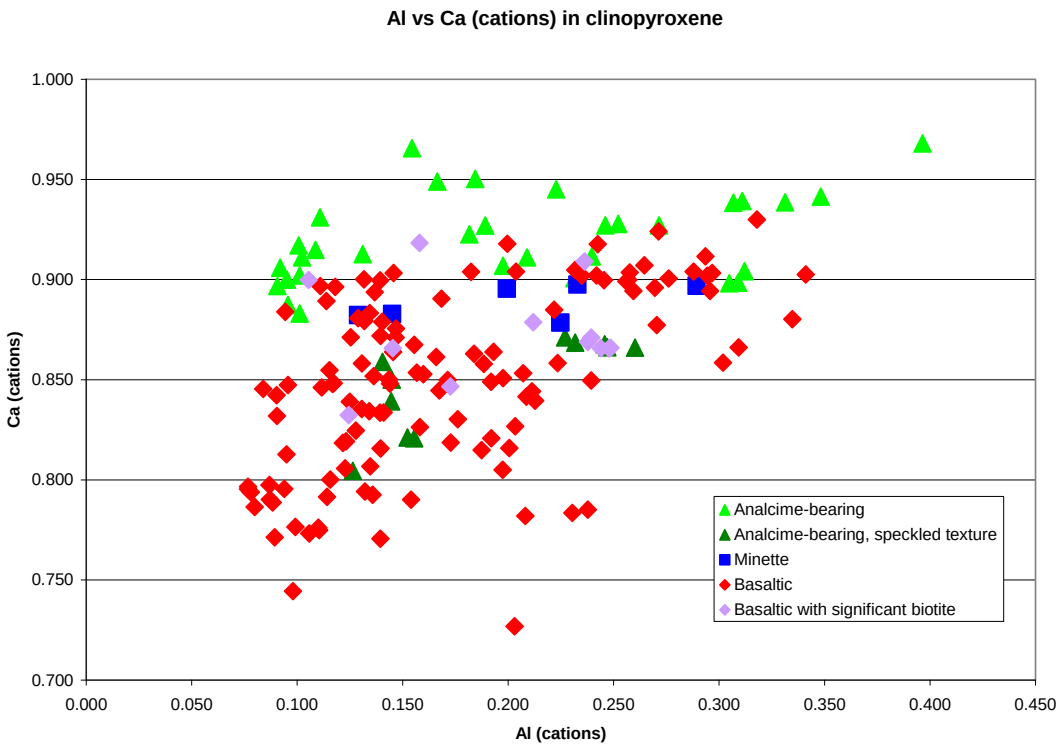

Figure 37. Plot of cations Al vs Ca in clinopyroxene. Pyroxenes in non-speckled analcime-bearing dikes have greater CaO contents than most other dikes. Pyroxenes in speckled-textured analcime bearing dikes contain less CaO than those in other analcime-bearing dikes. CaO contents in pyroxene of the basaltic dike with significant biotite (RDS-7) plot in the middle of the range of CaO contents of other basaltic dikes and are less than the contents of CaO in the minette dike (RDS-106).

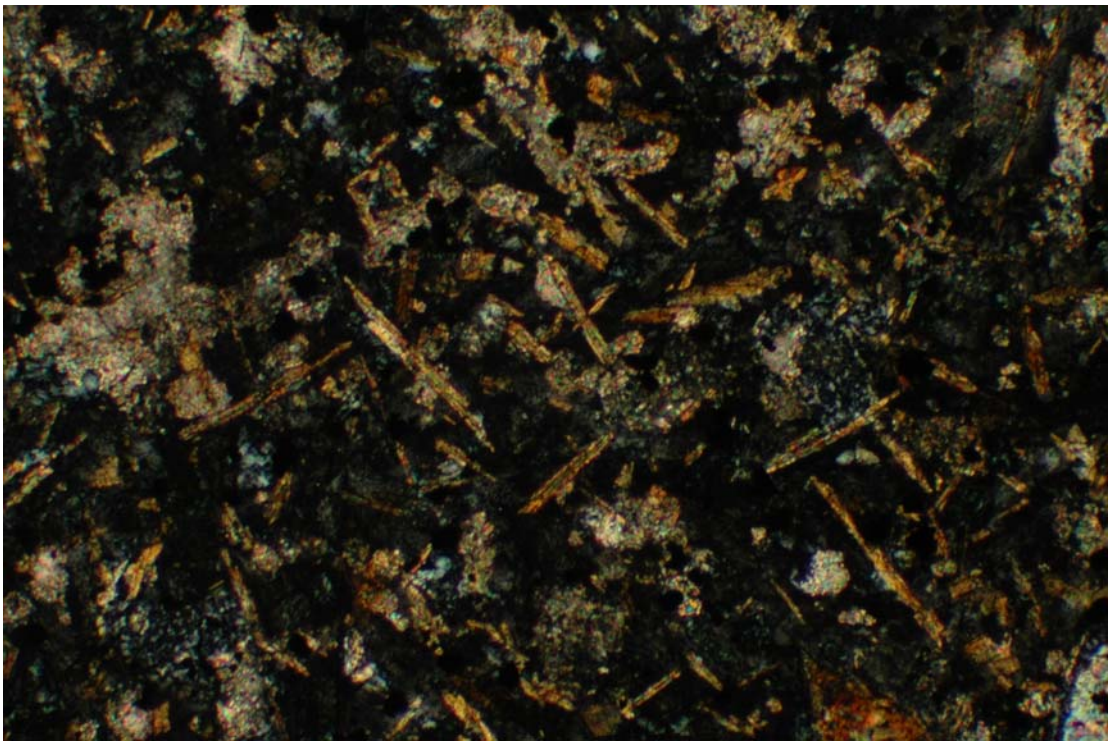

Figure 38. Biotite in sample RDS-7 form stellate formations.

Representative electron microprobe analyses of biotite are shown in Table 5. The biotite classification diagram (Fig. 39) shows crude compositional patterns among the groups. Biotites from minettes and basaltic samples with significant biotite generally group themselves around A1IV of 1 and Fe/(Fe+Mg) ≈ 0.25-0.35.

Biotite Cl and F (cation) contents are shown in Figure 40. Biotite in analcime-bearing dikes contains lower Cl and slightly higher F than most other dikes. Most biotite from minettes and basaltic samples with significant biotite contains high Cl and low F. The amount of Cl in biotite of basaltic dikes often falls between the levels of the two other groups.

3.5 Apatite

Apatite is a common minor accessory mineral in the dikes and it is seen in both thin section and electron microprobe (Fig. 41). Only two samples, one minette and one analcime-bearing dike, had crystals large enough to analyze with the electron microprobe. Electron microprobe analyses of apatite are found in Table 6.

The mineral chemistry shows two distinct populations (Fig. 42). Apatite in the minette sample contains higher Cl and lower F than the analcime-bearing sample. This is the same relationship seen in biotites of minette and analcime-bearing samples (see section 3.4) although the difference in F content of the biotites is less prominent.

3.6 Olivine

Fresh olivine is extremely rare in the dikes. However sparse (1-3%) small (1-2mm) euhedral phenocrysts, commonly completely replaced by serpentine and/or carbonate, are observed in most thin sections (Figure 43). These altered phenocrysts are often associated with fresh clinopyroxene in the same rock sample. Olivine was only

Table 5: Representative electron microprobe analyses of biotite. Values reported as wt%.

	1 RDS-2-17	2 RDS-3-13	3 RDS-10-33	4 RDS-13-10	5 RDS-16B-29	6 RDS-159-02
SiO_2	37.26	36.66	37.24	36.01	36.76	38.98
Al_2O_3	5.44	6.85	6.46	6.74	5.43	4.64
TiO_2	14.24	14.19	12.84	14.53	14.21	13.54
FeO	14.68	10.50	12.76	10.85	14.48	12.26
MnO	0.14	0.06	0.11	0.08	0.17	0.19
MgO	13.79	16.57	15.22	16.10	14.90	17.83
CaO	0.19	0.22	0.14	0.12	0.15	0.06
Na_2O	0.71	0.57	0.73	0.59	0.63	0.56
K_2O	9.19	8.84	8.88	8.46	8.62	9.28
Cr2O3	0.01	0.00	0.00	0.00	0.00	0.02
F	1.96	1.72	1.57	1.54	2.27	1.93
Cl	0.03	0.09	0.04	0.09	0.03	0.08
	97.65	96.28	95.99	95.11	97.65	99.37
-O=F,Cl	0.83	0.74	0.67	0.67	0.96	0.83
Total	96.82	95.54	95.32	94.44	96.69	98.54
	Numbers of ions on the basis of 22O					
Si	5.4392	5.3248	5.4843	5.2958	5.3502	5.5143
Al	2.4498	2.4290	2.2285	2.5183	2.4374	2.2569
Ti	0.5973	0.7483	0.7155	0.7455	0.5944	0.4938
Mg	3.0011	3.5881	3.3416	3.5299	3.2330	3.7604
Fe^{2+}	1.7919	1.2753	1.5713	1.3343	1.7622	1.4498
Mn	0.0173	0.0074	0.0137	0.0100	0.0210	0.0226
Na	0.2009	0.1605	0.2084	0.1682	0.1778	0.1534
Ca	0.0297	0.0342	0.0221	0.0189	0.0234	0.0095
K	1.7113	1.6378	1.6681	1.5870	1.6003	1.6750
F	0.9047	0.7900	0.7311	0.7162	1.0447	0.8638
Cl	0.0074	0.0222	0.0100	0.0224	0.0074	0.0202
Total	16.1508	16.0176	15.9947	15.9465	16.2518	16.2197

1: Spears Ranch Dike. Petrographic group: analcime-bearing.

2: Petrographic group: minette.

3: Spears Ranch Dike. Petrographic group: analcime-bearing.

4: Petrographic group: basaltic with significant biotite.

5: Pyroxene porphyry dike. Petrographic group: basaltic.

6: Petrographic group; basaltic with significant biotite.

Low analytical totals are the result of reporting wt% as water-free.

Analytical methods are reported in Appendix B.

Uncertainties based on replicate analyses of standard reference materials are reported in Appendix E.

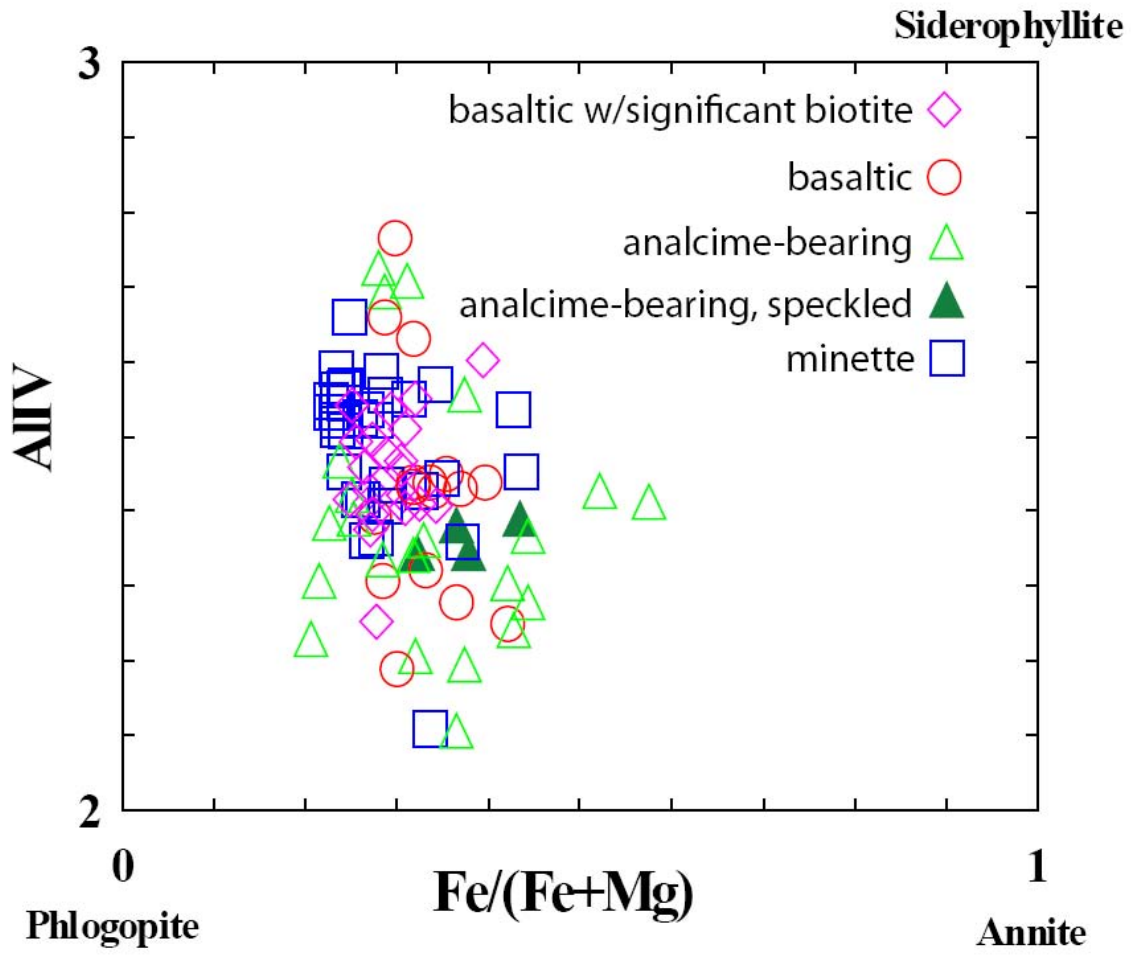

Figure 39. Mica classification diagram. Analcime-bearing dikes include both speckled and non-speckled dikes. AlIV = Al^{4+}.

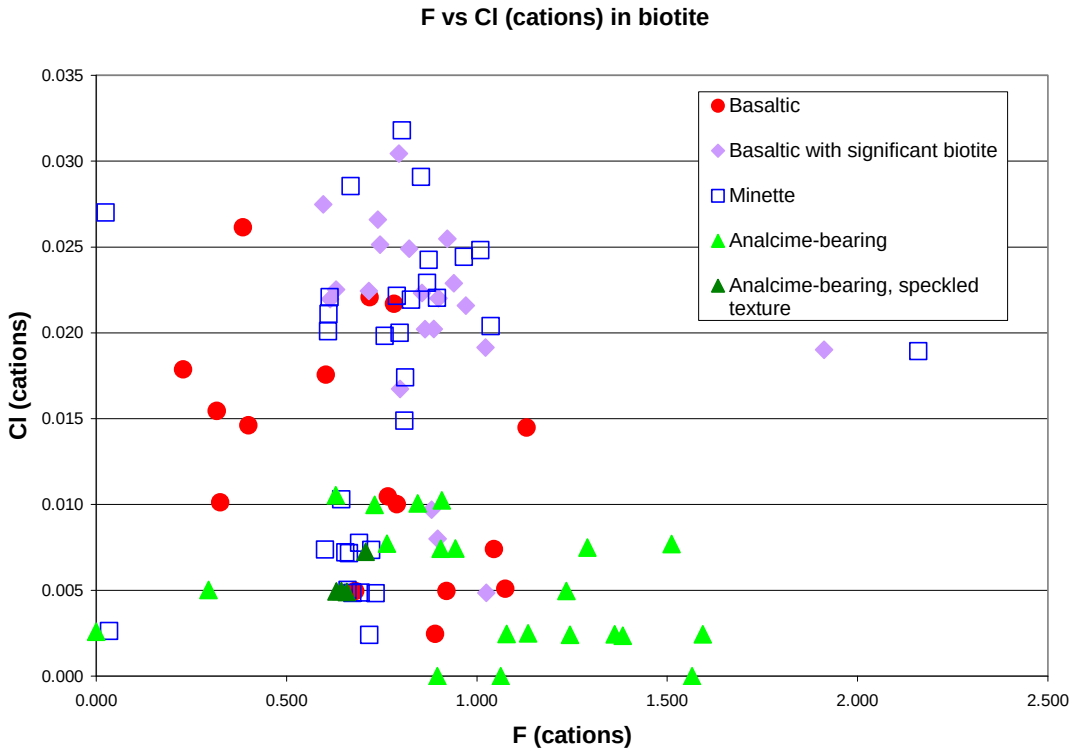

Figure 40. Plot of F vs. Cl cations in biotite.

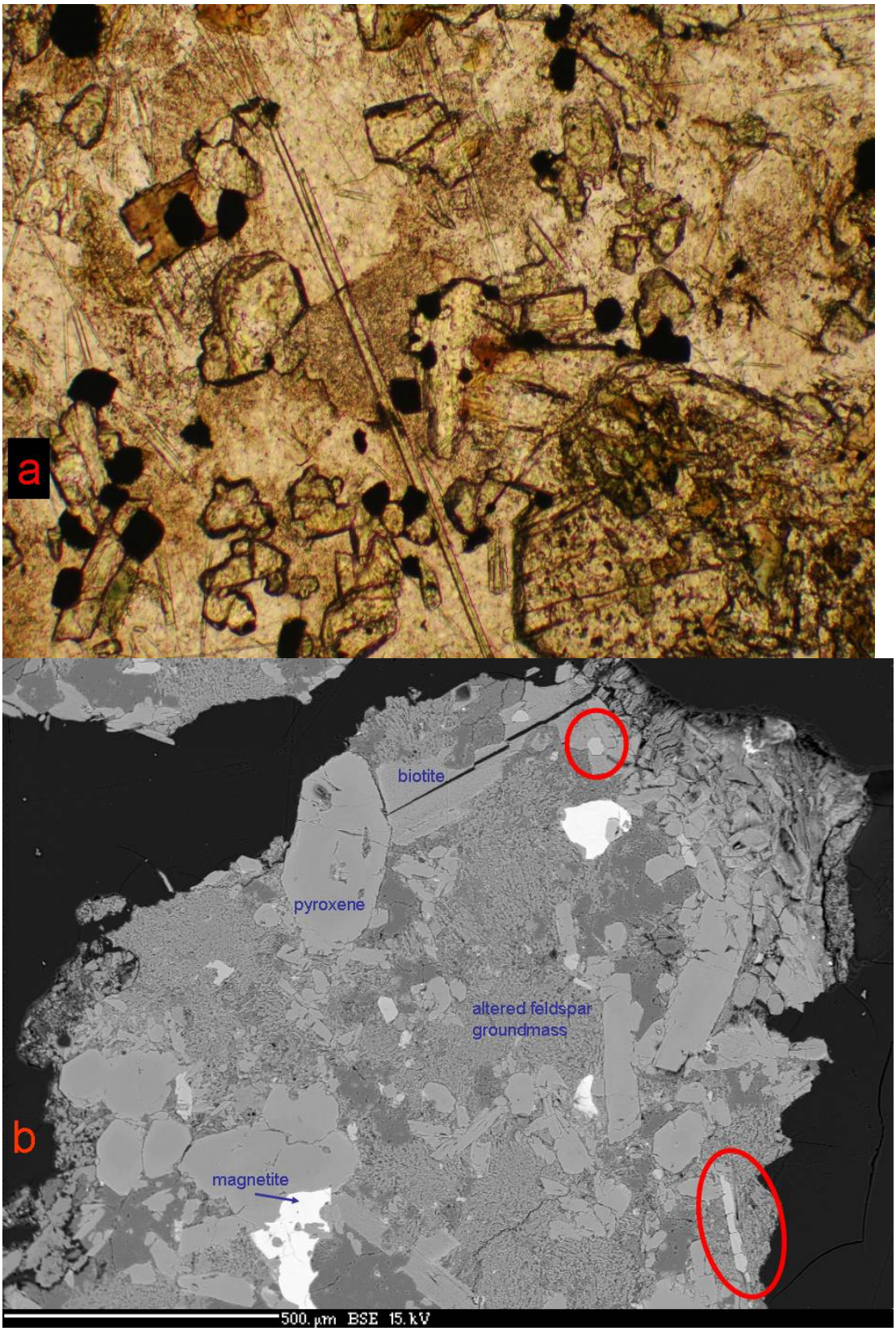

Figure 41. Electron backscatter images of apatite. a) Large apatite rod in sample RDS-203D. Field of view is 0.9 mm wide. b) Apatite crystals in sample RDS-3.

Table 6: Electron microprobe analyses of apatite. Values reported as wt%.

	1 RDS-5-32	2 RDS-5-33	3 RDS-009-12	4 RDS-009-14
SiO_2	0.77	1.08	1.09	1.61
FeO	0.41	0.34	0.27	0.24
MnO	0.03	0.03	0.02	0.06
CaO	52.62	52.99	52.67	52.86
SrO	0.52	0.49	0.36	0.29
P_2O_5	38.75	37.75	38.63	36.82
F	5.29	4.92	2.58	3.01
Cl	0.04	0.05	0.24	0.24
SO_2	0.18	0.18	0.85	1.13
	98.61	97.83	96.71	96.26
-O=F,Cl	2.24	2.08	1.14	1.32
Total	96.37	95.75	95.57	94.94
Numbers of ions on the basis of 26O				
P	5.732	5.678	5.918	5.756
Fe^{2+}	0.060	0.051	0.041	0.037
Mn	0.004	0.005	0.003	0.009
Ca	9.851	10.087	10.211	10.457
Sr	0.053	0.050	0.038	0.031
F	2.923	2.764	1.476	1.758
Cl	0.012	0.015	0.074	0.075
Total	18.635	18.650	17.761	18.123

1: Petrographic group: analcime-bearing.

2: Petrographic group: analcime-bearing.

3: Petrographic group: minette.

4: Petrographic group: minette.

Analytical methods are reported in Appendix B.
Uncertainties based on replicate analyses of standard reference materials are reported in Appendix E.

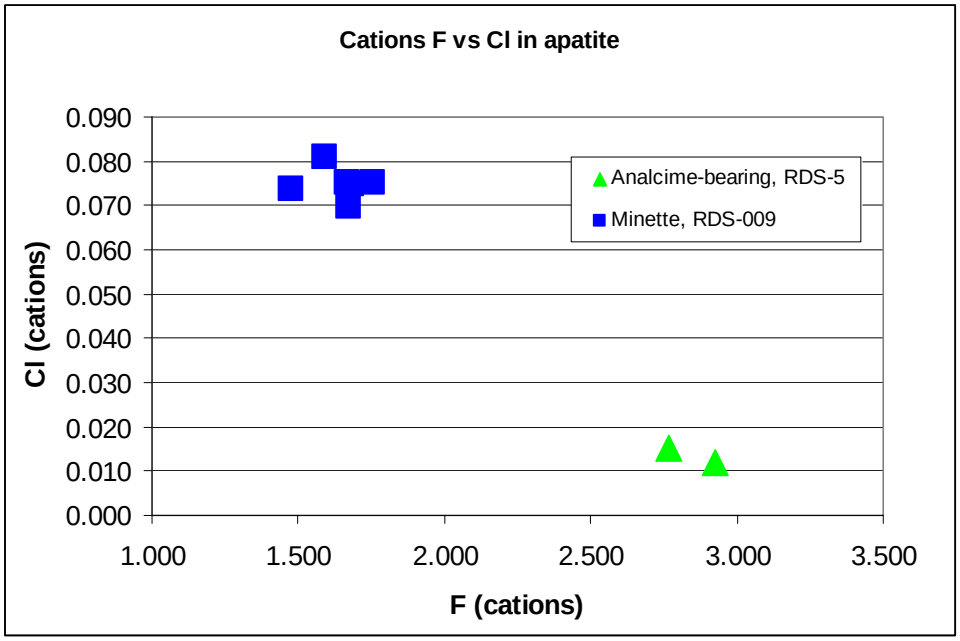

Figure 42. Plot of cations F vs. Cl for apatite crystals in RDS-5 and RDS-009.

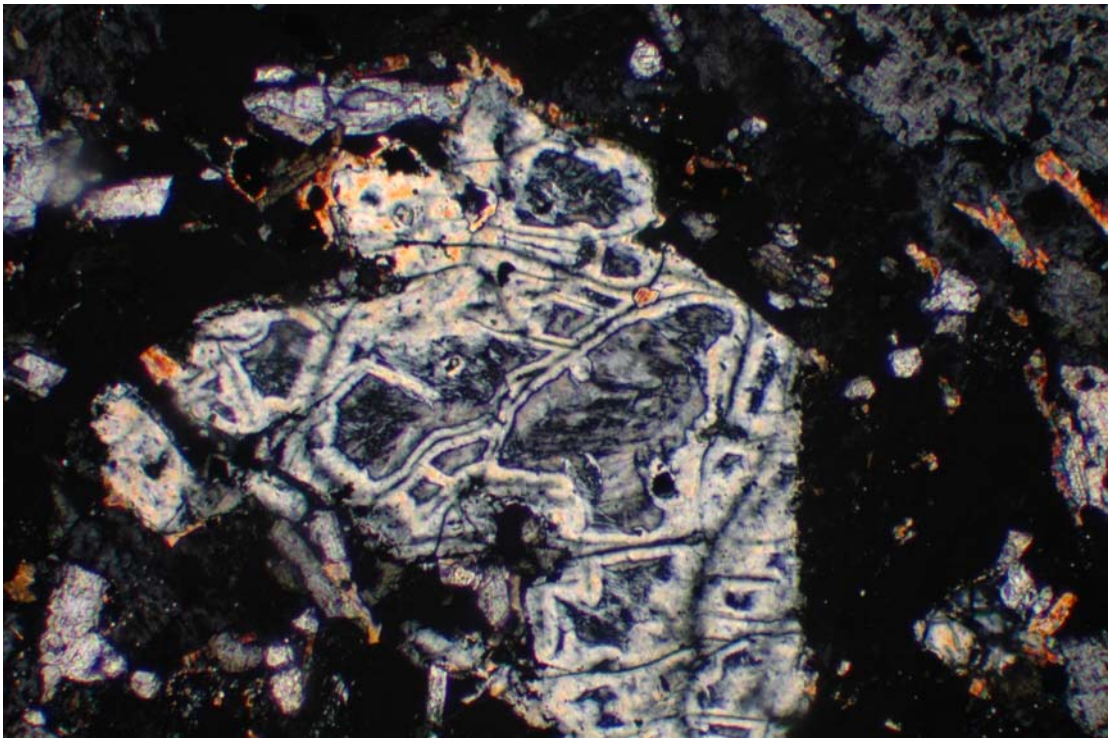

Figure 43. Olivine crystal replaced by serpentine in analcime-bearing sample RDS-2. Field of view is 1.8 mm.

analyzed with the electron microprobe in the analcime-bearing Spears Ranch Dike. RDS-10 (Fig. 44) contains both a small, fresh crystal and a larger, altered crystal. Table 7 contains electron microprobe analyses of olivine. The average composition of the three analyses is $Fo_{75.0}Fa_{25.0}$.

3.7 Magnetite

Magnetite is a common minor accessory mineral in most of the dikes. It is often euhedral and constitutes up to 5% of some samples. Crystals as large as 0.25 mm and 0.5 mm were observed in thin section and electron backscatter images, respectively.

Representative electron microprobe analyses of magnetite are shown in Table 8. Most magnetite is altered or contains exsolution lamellae (Fig. 45) observed in the electron backscatter images. Many mineral chemistry totals are low (most are ~92-97%, uncorrected) and structure formula ion calculations totals are low (less than 24) because of exsolution. Some of the analyses are similar to analyses of ulvöspinel (~19% TiO_2, ~4% Al_2O_3), the presence of which also indicates exsolution (Deer et al., 1992). Cr-spinel is also present. Some also contain high amounts of SiO_2 (up to 11.05 wt%) which suggests alteration.

3.8 Carbonate

The abundance of carbonate was noted early in the field study of these dikes. As reported in Chapter 2, many dikes fizz vigorously in contact with HCl. In thin section and electron microprobe, carbonate was observed as vesicle fillings, finely disseminated material in groundmass, and as a replacement of pyroxene and possibly olivine.

The amount and location of carbonate varied among the dikes but there are patterns between dike petrography and location of carbonate. Minettes contain finely

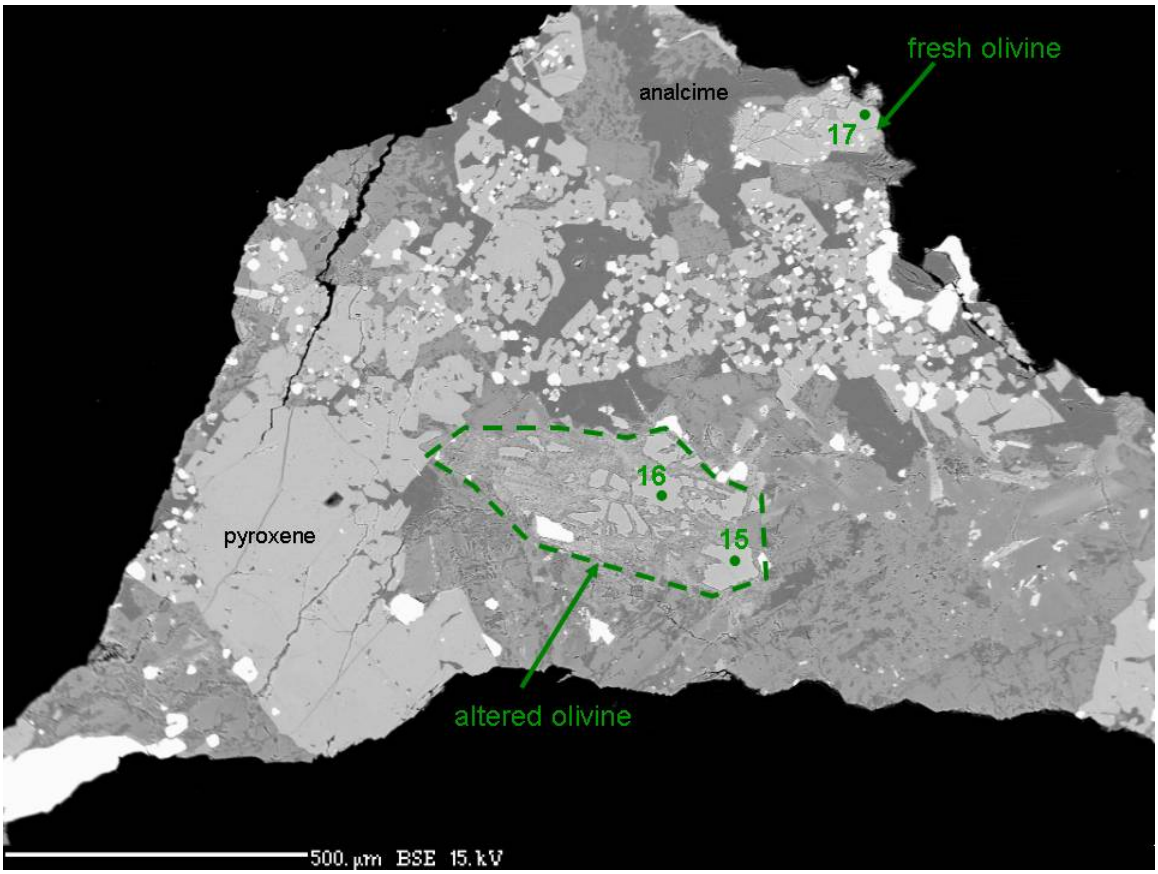

Figure 44. Rare olivine in RDS-10. Numbered points refer to data found in Appendix C.

Table 7: Electron microprobe analyses of olivine. Values reported in wt%.

	1 RDS-10-15	2 RDS-10-16	3 RDS-10-17
SiO_2	38.66	38.79	38.88
FeO	23.43	22.7	23.33
MnO	0.32	0.35	0.38
MgO	38.71	39.07	39.10
CaO	0.29	0.29	0.31
Total	101.4	101.19	102
Numbers of ions on the basis of 4O			
Si	0.996	0.998	0.996
Mg	1.487	1.499	1.493
Fe2+	0.505	0.489	0.500
Mn	0.007	0.008	0.008
Ca	0.008	0.008	0.009
Total	3.004	3.002	3.004
End-member percentages			
Fo	74.7	75.4	74.9
Fa	25.3	24.6	25.1

All three samples are from the analcime-bearing Spears Ranch Dike.

Analytical methods are reported in Appendix B.

Uncertainties based on replicate analyses of standard reference materials are reported in Appendix E.

Table 8: Representative electron microprobe analyses of magnetite (spinel).

	1 RDS-1-2	2 RDS-2-32	3 RDS-7-6	4 RDS-15B-01	5 RDS-027-01
SiO_2	0.31	0.11	0.17	0	0.13
TiO_2	10.89	12.83	10.88	2.55	9.07
Al_2O_3	3.07	3.63	2.21	9.3	5.37
Cr_2O_3	0.03	0	0.03	26.18	0.25
Fe_2O_3	45.36	38.40	45.84	29.94	45.54
FeO	38.15	41.46	41.55	24.90	35.10
MnO	0.61	0.61	0.13	0.59	0.54
MgO	2.17	0.48	0.12	6.15	2.89
CaO	0.22	0.19	0.22	0.41	0.17
Total	100.81	97.72	101.15	100.02	99.06
Numbers of ions on the basis of 32O					
Si	0.090	0.032	0.049	0.000	0.038
Al	1.053	1.245	0.758	3.189	1.842
Cr	0.007	0.000	0.007	6.024	0.058
Fe^{3+}	9.934	8.410	10.039	6.557	9.973
Ti	2.384	2.808	2.382	0.558	1.985
Mg	0.942	0.208	0.052	2.668	1.254
Fe^{2+}	9.285	10.091	10.112	6.060	8.543
Mn	0.150	0.150	0.032	0.145	0.133
Ca	0.069	0.059	0.069	0.128	0.053
Total	23.913	23.004	23.500	25.329	23.878

Analytical methods are reported in Appendix B.

Uncertainties based on replicate analyses of standard reference materials are reported in Appendix E.

1: Petrographic group: basaltic.

2: Spears Ranch Dike. Petrographic group: analcime-bearing.

3: Petrographic group: basaltic with significant biotite.

4: Petrographic group: basaltic.

5: Petrographic group: basaltic.

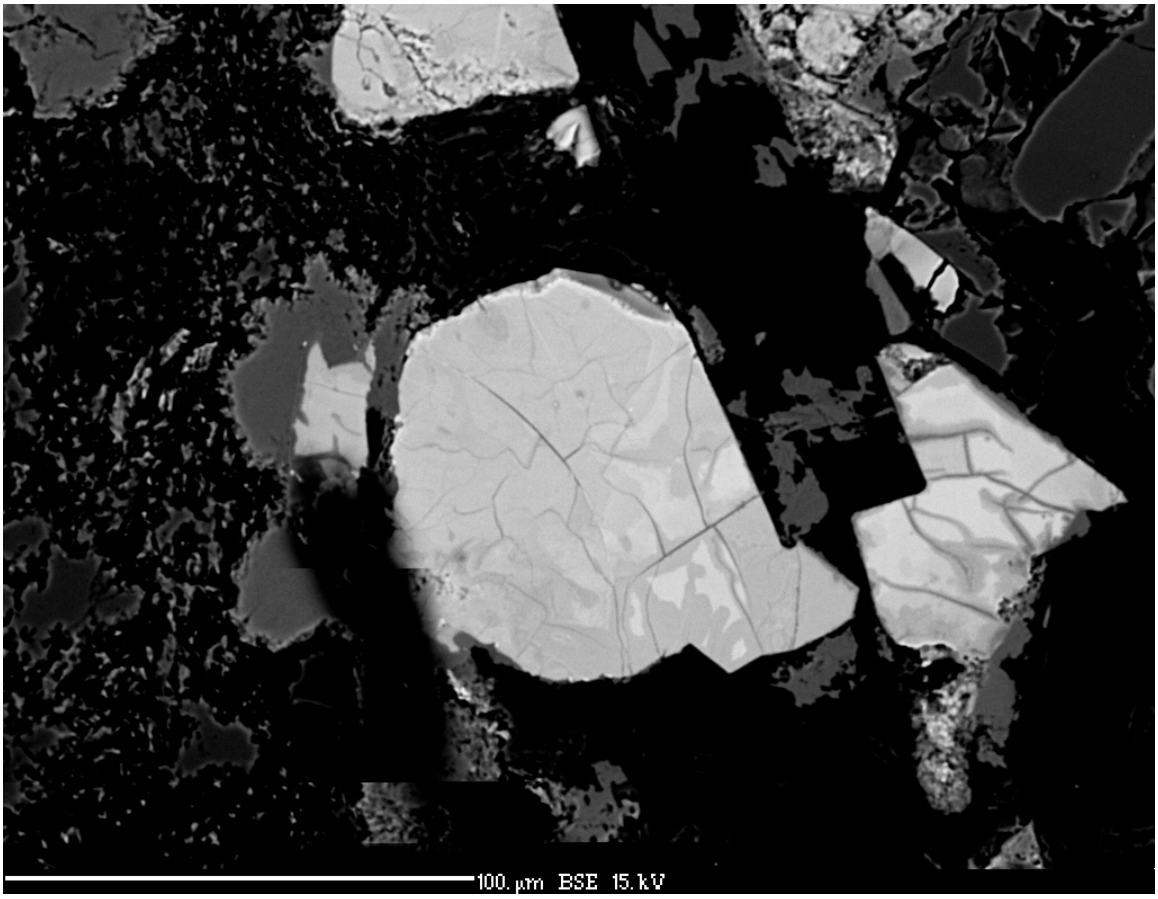

Figure 45. Magnetite in sample RDS-11 showing exsolution and alteration textures.

disseminated carbonate which likely contributes to the mottled texture of the groundmass noted in section 3.1.3. They also contain a few calcite pseudomorphs of pyroxene and possibly olivine. Carbonate is rarely observed in analcime-bearing dikes. Basaltic dikes contain finely disseminated carbonate but most commonly contain carbonate as a replacement of pyroxene. Three dikes were sampled from their core to their chilled margin (RDS-15, 16, and 202). Thin sections of these samples (Appendix C) show fresh clinopyroxene in the core of the dikes and pyroxenes that are partially to completely replaced by carbonate at the dike margins.

Most of the carbonate analyzed by electron microprobe is calcite. Some data points contain higher amounts of MgO and are compositionally ankerite. All ankerite points are from one sample, RDS-15B. Representative electron microprobe analyses of carbonate are shown in Table 9. The backscatter image (Figure 46) shows carbonate as a pseudomorph after pyroxene, with ankerite along the rims and fractures of the former pyroxene crystal.

3.8.1 Carbon isotopes

The carbon and oxygen isotope composition of carbonate was performed on powdered samples of several dikes from the Riley area to determine if the carbonate is magmatic, meteoric, or affected by local sedimentary carbonate. Three samples from the Riley Travertine and Madera Limestone north of the Riley field area and a sample of a carbonate-metasomatized biotite-rich basalt dike from the Oscura Mountains in south-central New Mexico were also analyzed for comparison.

All dikes plot between $\delta^{13}C$ = -3 and -9‰ and $\delta^{18}O$ = 12.5-16‰ (Table 10, Fig. 47). It is agreed (e.g. Grard et al., 2005; Hansen, 2006;) that typical basalts release CO_2

Table 9: Representative electron microprobe analyses of carbonate. Values reported in wt%.

	1 RDS-013B-14	2 RDS-4-01	3 RDS-13-03	4 RDS-15B-26
MgO	0.2	0.23	0.27	13.39
FeO	0.26	0.32	0.25	7.56
MnO	0.69	0.15	0.48	0.76
CaO	52.76	54.53	54.29	32.46
*CO_2	42.03	42.92	43.24	45.00
SiO_2	0.18	0.41	0.11	0.21
Total	96.12	98.56	98.64	99.38
	Numbers of ions on the basis of 6O			
Mg	0.010	0.012	0.014	0.649
Fe^{2+}	0.008	0.009	0.007	0.206
Mn	0.020	0.004	0.014	0.021
Ca	1.967	1.988	1.969	1.131
C	1.997	1.994	1.998	1.997
Total	4.003	4.006	4.002	4.003

1: Petrographic group: basaltic.

2: Petrographic group: basaltic.

3: Petrographic group: Basaltic with significant biotite.

4: Petrographic group: basaltic.

*CO_2 calculated by dividing measured oxide wt% by the ratio of atomic weights of the oxide over the respective carbonate.

For example: $CaO_{measured\ wt\%}/(CaO/CaCO3)_{atomic\ wt}$

Values were calculated for all oxides except SiO_2 and summed. Analytical total wt% was subtracted from this sum, and the result is the value of CO2.

Analytical methods are reported in Appendix B.

Uncertainties based on replicate analyses of standard reference materials are reported in Appendix E.

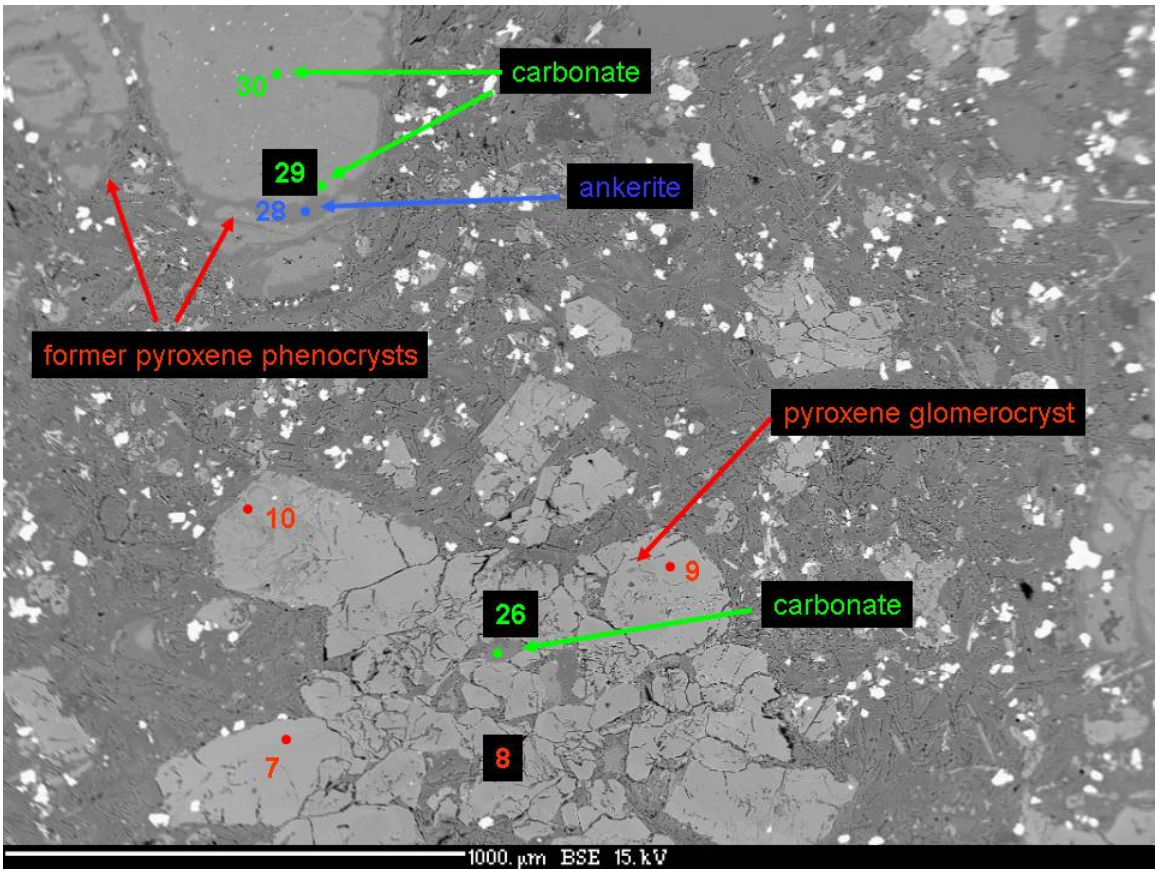

Figure 46. Backscatter image of sample RDS-15B showing a fresh pyroxene glomerocrysts (with minor carbonate in center) and two pyroxene crystals replaced by carbonate. The carbonate is mostly calcite with ankerite along rims and fractures of the replaced pyroxene. Numbered points refer to data in Appendix D.

Table 10: Carbon and oxygen isotopes for dikes and sedimentary units

Dikes at Riley

	$\delta^{13}C$	$\delta^{18}O$	dike classification
RDS-1	-8.9	14.1	basaltic
RDS-3	-4.1	13.2	minette
RDS-3 (dup)	-4.9	12.7	minette
RDS-4	-4.0	13.9	basaltic
RDS-5	-3.3	12.8	analcime-bearing
RDS-15B	-7.9	14.7	basaltic
RDS-009	-4.6	13.1	minette
RDS-013	-6.1	15.4	analcime-bearing, speckled
MDS-12	-9.0	14.6	analcime-bearing, speckled
MDS-16	-8.5	13.8	basaltic
MDS-16 (dup)	-8.7	13.4	basaltic
MDS-20C	-9.1	14.7	basaltic
MDS-20W	-8.8	14.6	basaltic

Dike in the Oscura Mtns.

	$\delta^{13}C$	$\delta^{18}O$
MDS-44	-3.21	15.97
MDS-44 (dup)	-3.35	15.31

Sedimentary units Riley Travertine (RT) and Madera Limestone (ML)

	$\delta^{13}C$	$\delta^{18}O$
RT-1	4.09	23.20
RD-1 (dup)	4.10	22.73
RT-2	4.66	22.55
ML-1	3.65	26.47

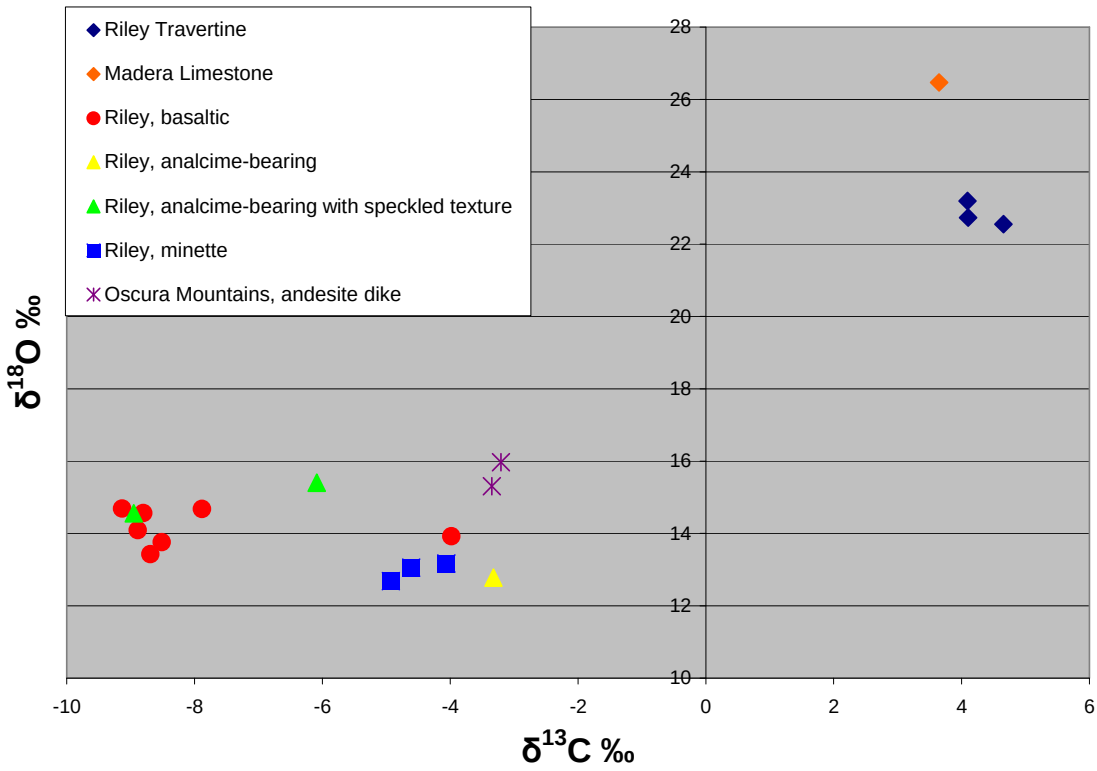

Figure 47. Plot of $\delta^{13}C$ vs. $\delta^{18}O$ for dikes and sedimentary carbonate.

with $\delta^{13}C \approx -5‰$. This is also accepted as a common upper mantle composition (Deines, 2002; Coltice et al., 2004). Values of $\delta^{13}C$ can vary greatly; many flood basalts and some mantle xenoliths have $\delta^{13}C = \sim -25‰$ (Deines, 2002; Hansen, 2006). The carbonate within the Riley dikes must be magmatic because the C isotopic composition of the dikes is ~-5‰, and samples Riley Travertine and Madera Limestone have much higher $\delta^{13}C$ values than the dikes.

3.9 Epidote, chlorite, zeolites, and clay

Alteration minerals are common in the dikes. The secondary mineral assemblage, which includes previously described carbonate and serpentine, suggests deuteric alteration. The abundance of epidote and chlorite in some dikes gives them a green color in the field as noted in Chapter 2.

Epidote, chlorite, and clay are often seen in thin section. Zeolites are occasionally observed. Epidote and chlorite occasionally replace pyroxene. Zeolites mostly appear to fill voids and occasionally form fibrous rosettes (Figure 48). Clay is commonly observed replacing mica and is rarely seen replacing feldspar.

3.10 Xenocrysts and xenoliths in thin section

Quartz is the most common xenocryst seen in thin section (Fig. 49). Fluorite was observed in one thin section, intimately associated with xenolithic calcite (Fig. 50). Other thin sections contain sanidine (RDS-16B, RDS-204).

3.10.1 Xenoliths in the speckled dike RDS-013A

The speckled dike (RDS-013A) contains a few small (1-6 mm) rounded sanidine-biotite-pyroxene xenoliths intermixed with or grading into near-isotropic material (Fig. 51). A sharp compositional and textural boundary occurs between the coarser-grained

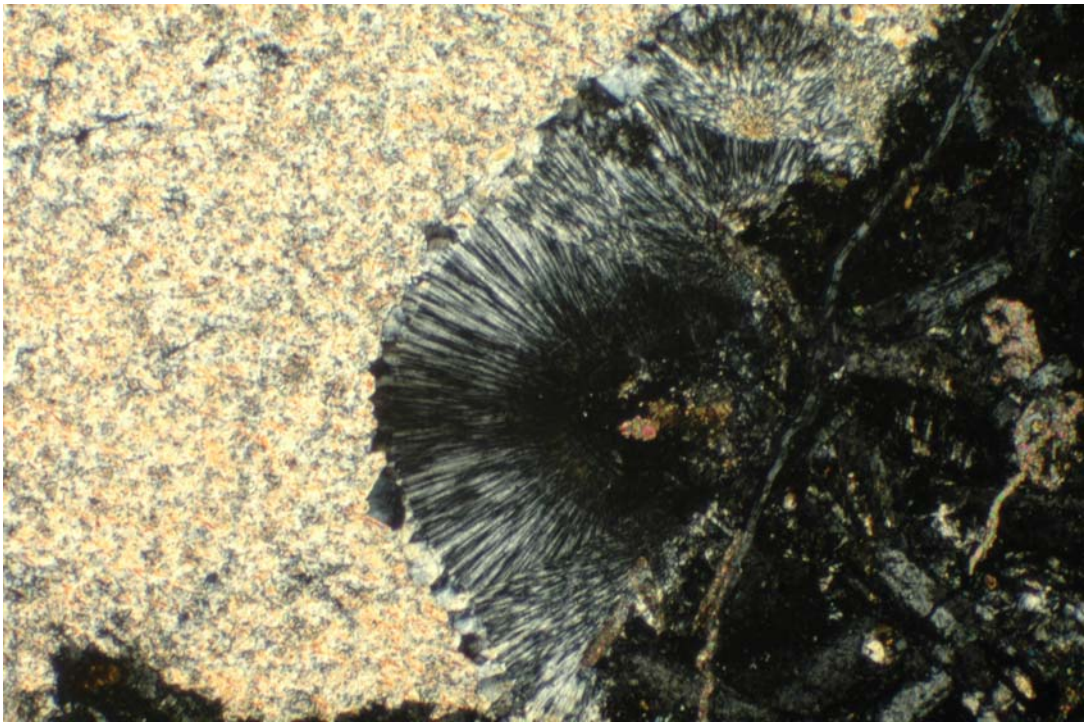

Figure 48. Fibrous zeolites form a rosette in sample RDS-6. Field of view is 1.8 mm wide.

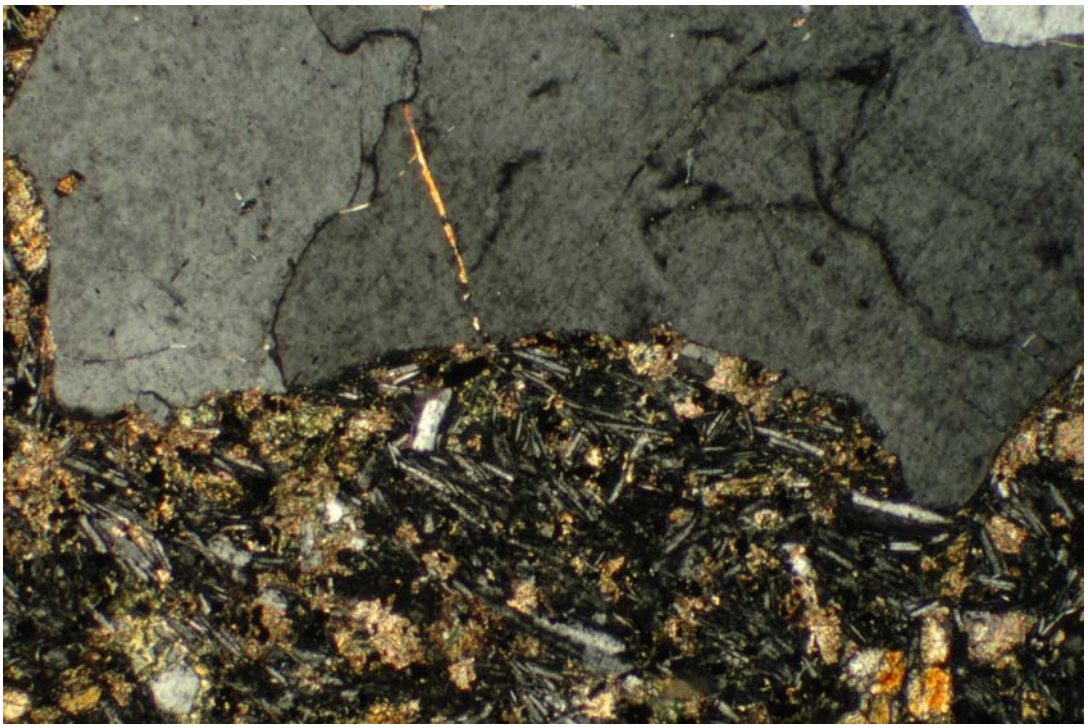

Figure 49. Embayed quartz xenocryst in basaltic sample RDS-027. Field of view is 1.8 mm.

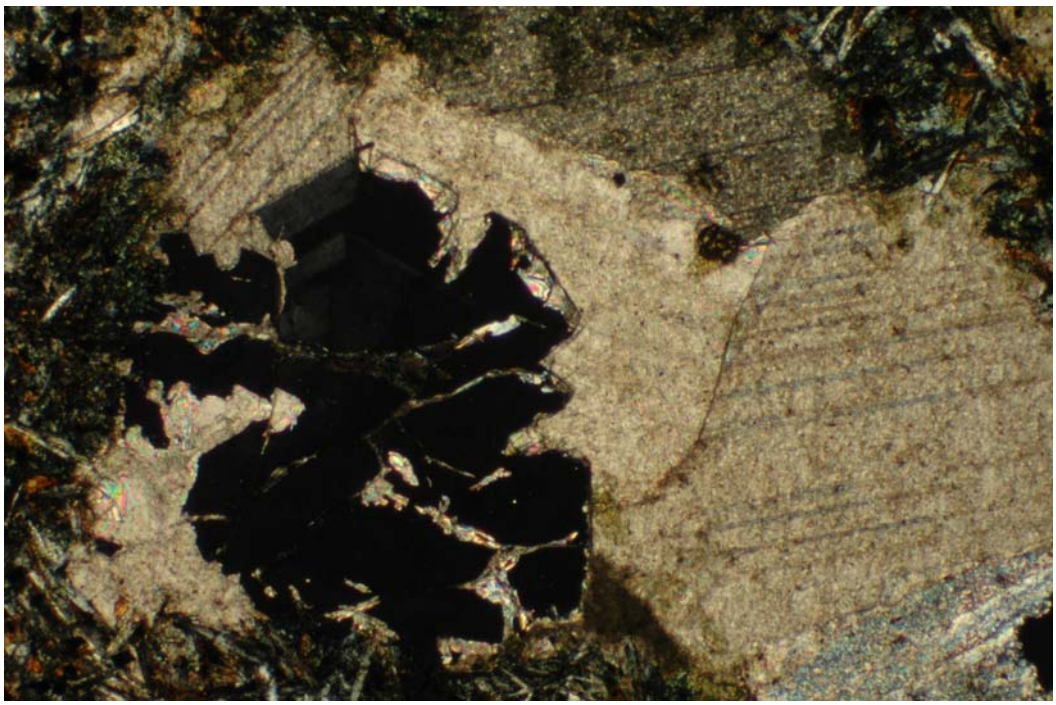

Figure 50. Fluorite (isotropic) surrounded by calcite in sample RDS-189B. Field of view is 1.8 mm wide.

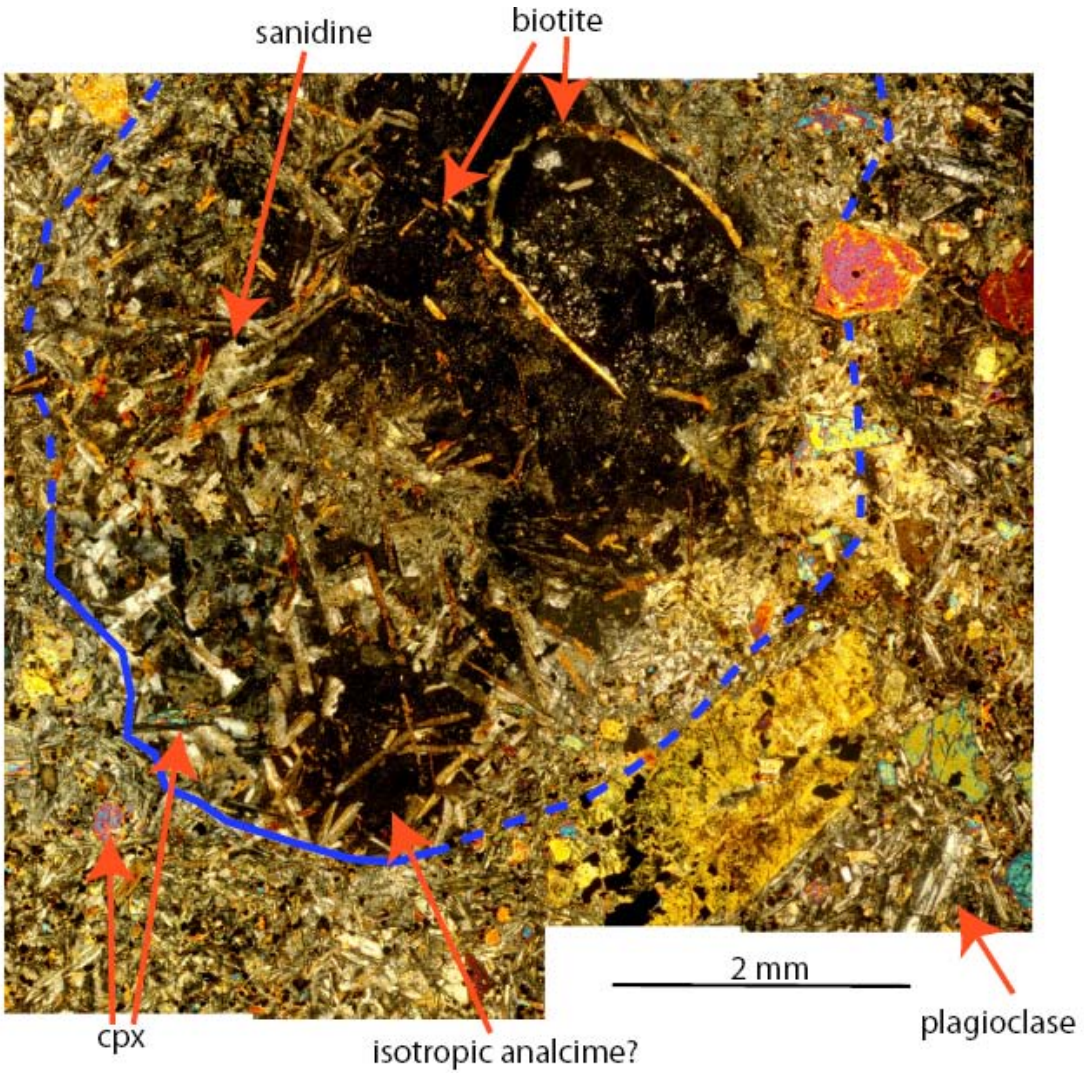

Figure 51. Partially assimilated xenolith in speckled dike sample RDS-013A. The xenolith consists of sanidine, biotite, clinopyroxene, and isotropic material that is probably analcime. The xenolith is coarser-grained than the plagioclase-clinopyroxene groundmass of the dike.

sanidine-rich xenolith and the finer-grained plagioclase-clinopyroxene groundmass of the dike. Embayments into the dike groundmass in Figure 51 suggest partial melting and mixing of the xenolith with the dike magma. The partially melted and assimilated sanidine-biotite-pyroxene xenolith contains uniformly disseminated cryptocrystalline white spots (spherulites?) within the nearly isotropic material. This material differs from the uniformly isotropic analcime observed in other analcime-bearing samples such as those from the Spears Ranch Dike.

The melting and assimilation of analcime-bearing xenoliths within basaltic magma observed in thin section of sample RDS-013A was not observed in electron backscatter images. Na_2O-rich masses observed within the plagioclase-rich groundmass of the sample in the electron microprobe have been interpreted here as analcime, but the presence of analcime may be the result of xenolith assimilation rather than representing composition of the dike magma. The observed textural differences are the result of the different scales of thin sections (~0.5-2 mm) and electron backscatter images (commonly 100-500 μm). If the analcime in speckled texture dikes is caused solely by assimilation of analcime-bearing xenoliths, then mixing of the xenoliths and host magma may be more complete than thin section observations reveal. Electron backscatter images reveal pervasive analcime, but the analyzed portion of sample may be a thorough mixture of melted xenolith and host magma rather than be representative of the host rock itself.

4. GEOCHEMISTRY

Major and trace element analyses of 7 samples (with prefix RDS) were made by x-ray fluorescence (XRF) and Inductively Coupled Plasma mass spectrometry (ICP-MS) at Washington State University GeoAnalytical Laboratory. XRF analyses of eight samples made at New Mexico Bureau of Geology and Mineral Resources from ongoing study of the Riley dikes by R.M. Chamberlin (pers. commun.) are included. Dikes are grouped according to petrography and mineral chemistry as described in Chapter 3. Geochemical analyses of the Riley dikes are shown in Table 11.

4.1 Major and Minor Elements

Using the total alkali-silica classification (Le Maitre, 2002), samples from the Riley dike swarm are mainly shoshonite and potassic trachybasalt (Fig. 52). Two samples plot outside those fields; one is basalt and one is basaltic andesite. All samples have $K_2O > Na_2O-2$ (Le Maitre, 2002) and are potassic according to the IUGS classification. Minette and analcime-bearing samples tend to have higher alkali contents than basaltic samples. Three Spears Ranch Dike samples plot similarly in shoshonite field but one sample, MDS-32, is potassic trachybasalt. This variation within one dike may be a result of sampling location across the width of the dike (margin vs. core), accidental sampling of an autolith, or natural variation along the strike of the dike. Duplicate samples of two dikes, the pyroxene porphyry dike and an analcime-bearing speckled dike, are compositionally similar.

Table 11. Geochemical analyses of Riley dikes listed in order of decreasing wt% MgO.

	RDS-211	MDS-32**	RDS-009	RDS-5	MDS-12	MDS-15**	RDS-130**	MDS-31	MDS-11	MDS-14	02-77-11-1**	RDS-013A	RDS-19	RDS-191	MDS-16
SiO2 (wt%)	48.04	48.91	48.06	46.88	51.50	50.55	50.63	51.39	52.10	54.37	54.64	51.63	51.99	54.38	52.48
TiO2	1.11	1.15	1.13	1.27	1.15	1.28	1.60	1.26	1.24	1.21	1.22	1.18	1.26	1.22	1.25
Al2O3	12.61	12.58	12.62	13.47	15.09	13.70	15.00	14.69	14.69	15.32	15.37	14.95	14.75	15.22	15.61
FeO	8.71	9.19	8.66	9.33	8.03	8.90	10.29	8.67	8.18	8.54	8.60	8.15	7.98	8.61	8.10
MnO	0.17	0.14	0.15	0.17	0.15	0.16	0.17	0.10	0.15	0.14	0.15	0.16	0.15	0.15	0.24
MgO	11.16	11.05	11.00	10.39	9.13	8.86	8.72	8.68	8.51	8.23	8.18	7.50	6.89	5.61	4.39
CaO	11.98	10.27	11.56	11.62	7.70	10.26	8.59	6.95	6.97	5.74	5.32	8.93	8.56	8.12	12.95
Na2O	3.29	2.70	2.82	3.94	4.01	3.12	3.06	3.03	4.64	3.15	3.14	3.11	3.25	3.07	3.02
K2O	2.25	3.40	3.27	2.07	2.69	2.51	1.47	4.63	2.92	2.85	2.93	3.84	4.57	3.17	1.60
P2O5	0.69	0.61	0.72	0.85	0.55	0.67	0.48	0.60	0.60	0.47	0.47	0.56	0.61	0.47	0.37
Total	100.00	100.00	100.00	100.00	100.00	100.00	100.00	100.00	100.00	100.00	100.00	100.00	100.00	100.00	100.00
LOI	3.90	2.87	5.50	5.55	3.32	1.06	1.95	1.52	1.91	1.44	0.30	3.07	2.13	2.85	10.32
An. Total	94.80	96.36	93.58	93.35	96.09	98.34	97.13	98.04	97.67	98.18	99.14	96.31	96.13	95.94	89.14
mg#	56	55	56	53	53	50	46	50	51	49	49	48	46	39	35
Sc* (ppm)	34	-	34	33	-	-	26	-	-	-	-	29	26	27	-
V	220	216	219	250	204	250	230	188	200	210	224	212	204	212	181
Cr	519	516	477	444	252	571	382	241	324	164	181	320	231	156	432
Ni	169	153	152	147	85	189	188	83	108	54	54	108	90	56	191
Cu	104	93	100	102	80	90	64	80	84	90	94	84	79	91	57
Zn	88	83	89	90	88	88	100	86	75	83	91	82	89	87	71
Ga	12	15	13	16	19	18	19	18	18	19	20	16	18	18	19
As	-	2	-	-	0	1	-	0	7	2	1	-	-	-	0
Rb*	77	61	93	52	154	84	27	175	150	117	116	139	175	114	23
Sr*	940	867	643	1037	907	1137	703	872	962	820	827	999	980	809	672
Y*	46	38	45	46	39	31	29	40	35	39	39	36	39	38	23
Zr*	309	265	301	313	333	258	205	319	350	333	336	329	315	316	174
Nb*	6	8	6	6	9	6	11	12	11	10	10	13	11	12	6
Mo	-	2	-	-	1	0	-	2	1	1	1	-	-	-	0
Cs	6	-	6	13	-	-	1	-	-	-	-	10	10	2	-
Ba*	618	985	601	698	1007	1188	842	1085	1030	1014	975	873	915	892	883
La*	54.76	-	54.20	64.23	-	-	37.84	-	-	-	-	55.96	53.21	50.97	-
Ce*	120.79	-	119.30	141.79	-	-	78.00	-	-	-	-	116.54	112.35	106.61	-
Pr	17.92	-	17.87	20.93	-	-	9.71	-	-	-	-	15.09	14.87	13.39	-
Nd*	77.15	-	78.01	89.36	-	-	39.35	-	-	-	-	59.71	61.28	51.17	-
Sm	18.86	-	19.01	21.43	-	-	8.24	-	-	-	-	12.69	13.32	10.72	-
Eu	5.11	-	5.16	5.65	-	-	2.35	-	-	-	-	3.19	3.48	2.60	-
Gd	16.59	-	16.79	18.10	-	-	7.17	-	-	-	-	10.67	11.49	9.24	-
Tb	2.19	-	2.19	2.31	-	-	1.08	-	-	-	-	1.48	1.59	1.37	-
Dy	10.75	-	10.76	11.07	-	-	6.13	-	-	-	-	7.72	8.45	7.72	-
Ho	1.76	-	1.75	1.79	-	-	1.17	-	-	-	-	1.41	1.51	1.48	-
Er	4.16	-	4.03	4.06	-	-	3.05	-	-	-	-	3.47	3.76	3.98	-
Tm	0.52	-	0.51	0.52	-	-	0.42	-	-	-	-	0.48	0.51	0.56	-
Yb	2.96	-	2.91	2.93	-	-	2.54	-	-	-	-	2.88	3.00	3.42	-
Lu	0.44	-	0.44	0.44	-	-	0.39	-	-	-	-	0.44	0.45	0.53	-
Hf	7.87	-	7.79	7.96	-	-	5.21	-	-	-	-	8.22	8.11	8.30	-
Ta	0.60	-	0.30	0.40	-	-	0.70	-	-	-	-	0.90	0.80	1.30	-
Pb*	8	13	7	7	15	13	10	15	16	19	17	15	13	16	12
Th*	8	6	6	7	13	4	5	8	14	17	16	14	9	15	5
U	3	5	2	3	4	3	1	6	5	6	6	4	3	4	2

*Averaged XRF and ICP-MS values for samples with the prefix "RDS".
**Averaged values from duplicate analyses. RDS-130 and MDS-15: averaged major and trace elements. MDS-32: averaged trace elements. 02-77-11-1: averaged major elements.
Total Fe reported as FeO. Complete analyses are in Appendix F and precision given in Appendix G.

LOI: loss on ignition
An. Total: Analytical total, uncorrected
mg# = 100*MgO/(MgO+FeO)

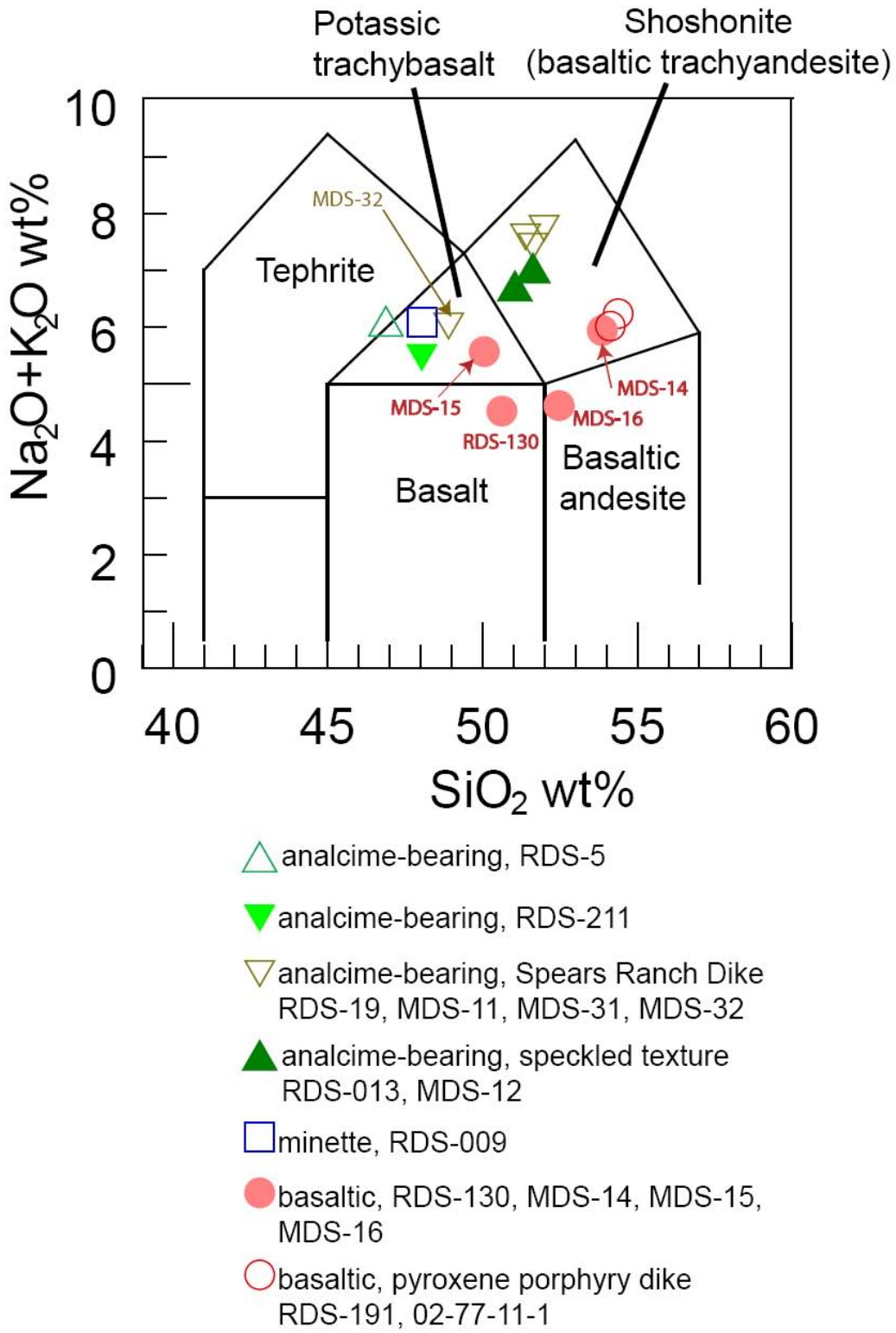

Figure 52. Total alkali vs. silica diagram of samples from Riley. Potassic trachybasalt and shoshonite fields are so named because for all samples wt% $K_2O > Na_2O - 2$. From Le Maitre (2002).

Major element oxides are plotted versus MgO in Figure 53. MgO and P_2O_5 are positively correlated. MgO is negatively correlated to SiO_2 and Al_2O_3. Values of TiO_2, FeO, and Na_2O do not vary with MgO content. MgO vs. CaO shows a crude positive correlation with some scatter, and MgO vs. K_2O shows significant scatter. Duplicate samples of the pyroxene porphyry dike and speckled-textured analcime-bearing samples are compositionally similar.

4.2 Trace Elements

Samples were analyzed at two different labs: New Mexico Institute of Mining and Technology and Washington State University. No interlaboratory duplicate analyses were performed, but analyses of 3 samples of the Spears Ranch Dike (MDS-11, MDS-31, MDS-32) were performed at New Mexico Tech and one analysis (RDS-19) was performed at Washington State. A spiderdiagram with data symbolized by lab (Fig. 54) shows that there is no obvious variation between the labs and that it is therefore valid to compare analyses performed at these two labs.

Trace elements normalized to pyrolite mantle of McDonough and Sun (1995) are shown in Figure 55. All the dikes share a similar pattern, although the mobile elements Cs, Rb, and U show significant scatter. All the dikes share prominent negative Nb, Ta, and Ti anomalies. The dikes also share less prominent negative P and Zr anomalies.

Analcime-bearing dikes tend to have higher values for pyrolite normalized elements than the basaltic dikes. The minette dike has low concentrations of Ba through Ta and Pb, Sr, and Ti, and higher concentrations of other trace elements. The minette dike and the analcime-bearing dikes RDS-5 and RDS-211 have negative Pb anomalies while all other samples (basaltic and analcime-bearing) have positive Pb anomalies. As

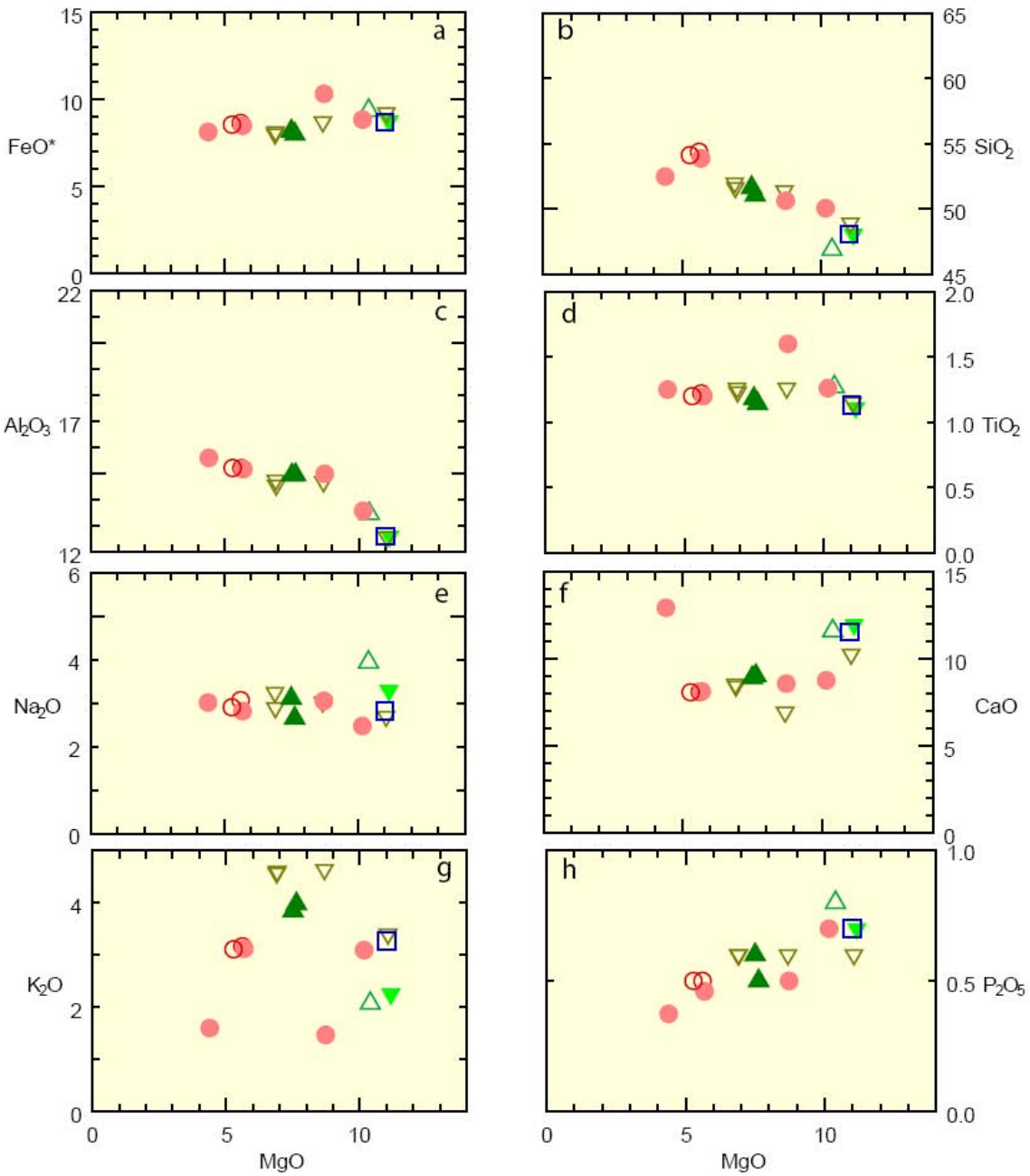

Figure 53. MgO vs. major oxide variation diagrams of Riley dikes. Symbols and colors are the same as in Figure 52.

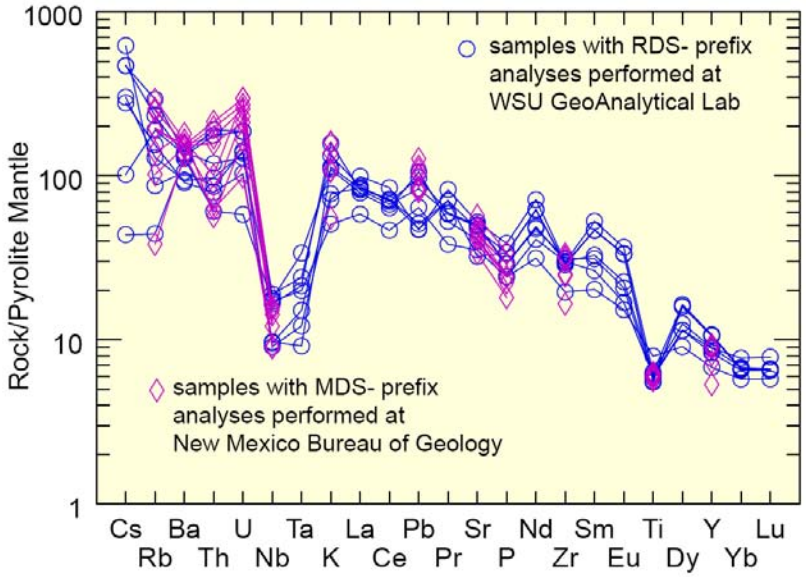

Figure 54. Spiderdiagram comparing samples with RDS- prefix which were analyzed at Washington State University, and MDS- prefix samples (including sample 02-77-11-1) analyzed at New Mexico Institute of Mining and Technology. No interlaboratory duplicates were performed but there is no obvious variation of analyses between the labs.

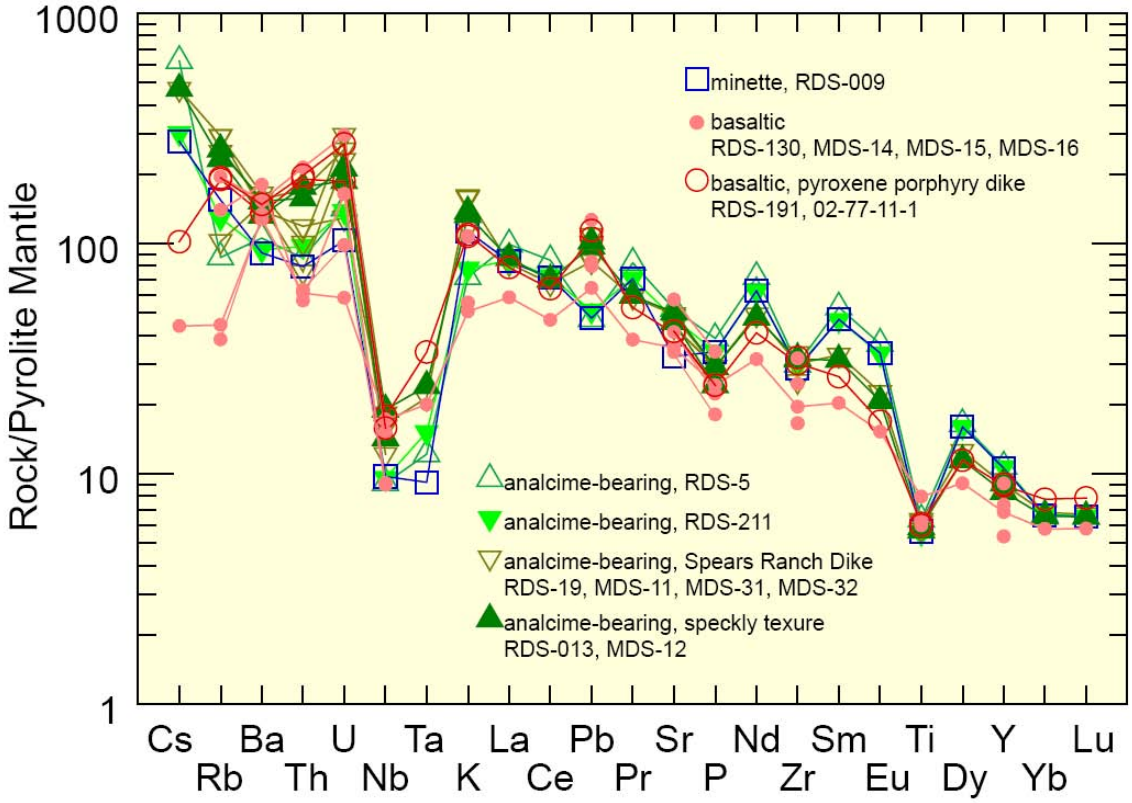

Figure 55. Riley dike samples normalized to pyrolite mantle of McDonough and Sun (1995).

with the major element oxides, duplicate samples of the pyroxene porphyry dike and the speckled analcime-bearing have similar trace element compositions.

4.3 Summary of geochemical analyses

All four dike types (minette, basaltic, analcime-bearing, and analcime-bearing speckled texture) are geochemically similar. All samples are potassic and 13 of 15 samples (8 of 10 dikes) are potassic trachybasalt or shoshonite. Multiple samples of the same dike contain similar concentrations of major element oxides and trace elements. The exception is sample MDS-32, which has lower concentrations of alkalis and SiO_2 than the other three samples of the Spears Ranch Dike. All samples have prominent negative Nb, Ta, and Ti anomalies on a pyrolite-normalized spiderdiagram.

5. ^{40}AR/^{39}AR GEOCHRONOLOGY

Dikes were dated using the ^{40}Ar/^{39}Ar method to test the hypothesis that the dike source migrated westward with the caldera eruptions of the Socorro-Magdalena caldera cluster. If true, and if dikes were emplaced in a simple radial pattern, dike trends should shift from NNW to NNE.

5.1 Methods

Crushed and sieved samples were hand-picked to remove alteration material and phenocrysts from groundmass and to collect biotite mineral separates. Samples were then placed in machined Al discs for irradiation. Irradiated samples were placed in copper packets and step-heated in a furnace to release Ar into the MAP-250-50 mass spectrometer at the New Mexico Geochronology Research Lab. One biotite separate was also analyzed by the single crystal CO_2 laser fusion method. Detailed sample preparation and methods of analyses are described in Appendix B. Data tables are in Appendix H.

Age spectra and isochrons were constructed for all step-heated samples and an age probability diagram (ideogram) was constructed for the sample analyzed by single-crystal laser fusion. For each age spectrum, an integrated age is calculated using all spectrum steps. Plateau ages are calculated using two or more contiguous and concordant (at 2σ) steps that comprise 50% or more of released ^{39}Ar. Isochrons are technically inverse isochrons (Turner, 1971, Roddick et al., 1980) that present ^{39}Ar/^{40}Ar vs. ^{36}Ar/^{40}Ar. Y-axis intercepts are reported as the ratio ^{40}Ar/^{36}Ar, which should

equal the atmospheric value of 295.5 if no significant extraneous ^{40}Ar is present. Values greater than atmosphere are interpreted as representing an excess trapped argon component.

Weighted mean ages and errorchron ages are presented in place of plateau ages and isochron ages, respectively, when the MSWD for the isochrons and plateaus are outside the acceptable range defined by Mahon (1996). Some preferred ages have high MSWD values resulting from some contamination of alteration, argon loss, ^{39}Ar recoil, or excess argon. Concordance among integrated, weighted mean age (or plateau), and isochron ages indicates accuracy of the ages.

5.2 Results

Analytical results are presented and discussed in the following sections for three dike types established in previous chapters: basaltic (separated into fresher and highly altered samples); analcime-bearing; and minette.

5.2.1 Basaltic groundmass concentrate samples

Three of five dated fresh to slightly altered basaltic groundmass samples yield reasonably good spectra (MSWD = 1.71-4.25, n = 6-7; Fig. 56). Two of the three samples (RDS-1, MDS-14) yield errorchrons with MSWD values slightly higher than the acceptable range of Mahon (1996). The other two of five samples yield discordant spectra and errorchrons with unreasonably high MSWD values.

The three groundmass samples that yield good spectra have concordant integrated, weighted mean (or plateau), and errorchron ages. Sample MDS-16 yields a flat spectrum with a plateau age of 28.33±0.15 Ma and an MSWD of 1.72. Samples RDS-1 and MDS-14 yield slightly less ideal spectra, with weighted mean ages of

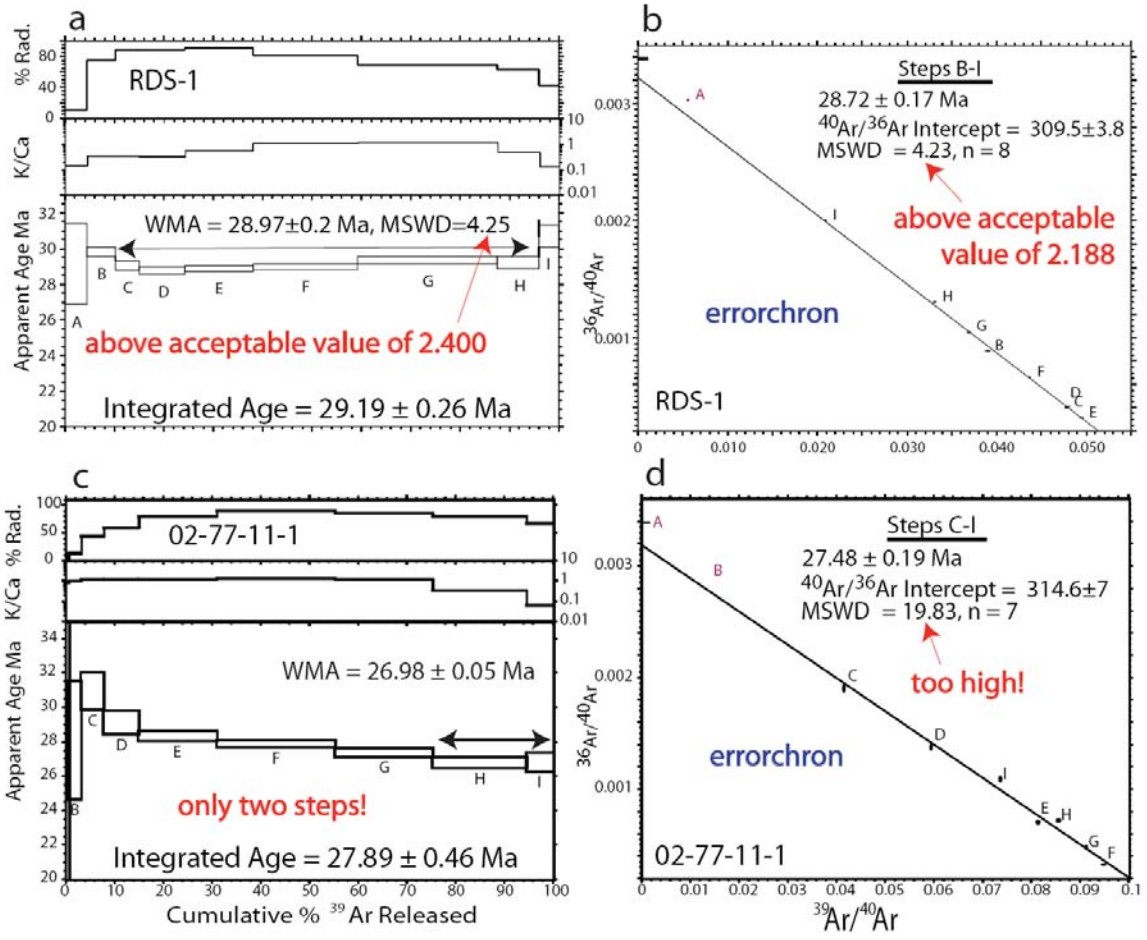

Figure 56. Age spectra and isochron plots for basaltic groundmass concentrate samples.

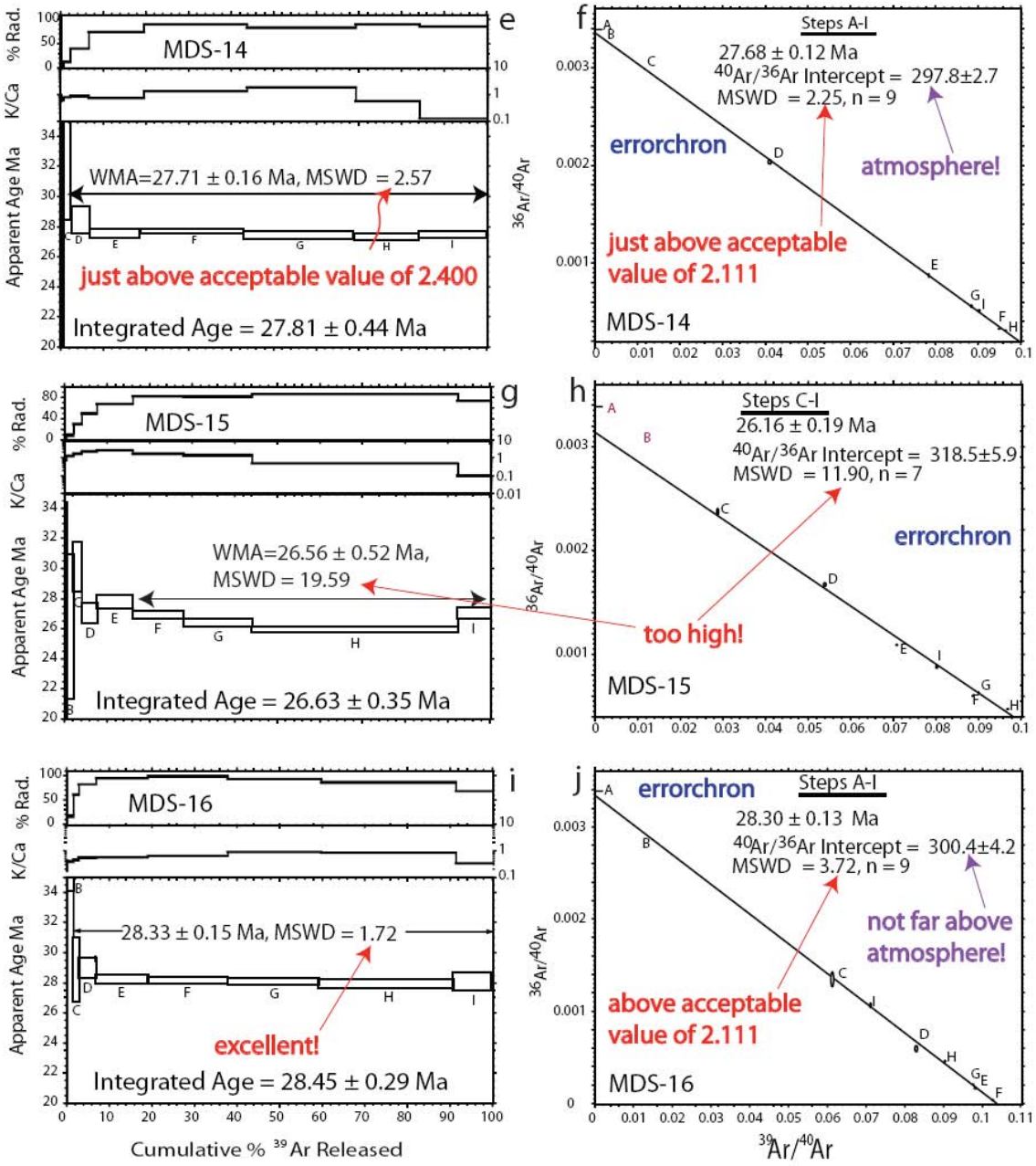

Figure 56. continued.

29.0±0.2 Ma and 27.70±0.15 Ma and MSWD values of 4.25 and 2.57, respectively. The errorchron ages of RDS-1, MDS-14, and MDS-16 are 28.72±0.17 Ma, 27.68±0.12 Ma, and 28.30±0.13 Ma, respectively. The respective MSWD values of the errorchrons are slightly higher than acceptable according to Mahon (1996). The errorchron intercept of RDS-1 is above atmosphere, the intercept of MDS-16 is slightly higher than atmosphere, and the intercept of MDS-14 is atmospheric.

The two fresher basaltic groundmass samples with less concordant spectra yield integrated and errorchron ages that are mutually concordant. The weighted mean age of steps F-I of MDS-15 is 26.56±0.52 Ma, with a high MSWD value of 19.59. Sample 02-77-11-1 yields the least concordant spectrum of the five fresher basaltic groundmass samples. A weighted mean age of 02-77-11-1 is reported for only two steps, H-I, as 26.98±0.05 Ma with an MSWD of 0.04. MDS-15 and 02-77-11-1 most clearly display a K/Ca pattern typical of basalts, characterized by higher values in early steps and lower values in later steps.

5.2.2 Heavily altered basaltic groundmass concentrate samples

The two dated groundmass samples, RDS-4 and RDS-6, are heavily altered (Chapter 3, Appendix C) and have similar highly disturbed saddle-shaped spectra (Fig. 57) commonly seen in the presence of excess Ar (McDougall and Harrison, 1999).

Both heavily altered samples have low radiogenic yields. Step A for both samples has low $^{40}Ar^*$ (~10%) and is the step that contains the most ^{39}Ar released (>30%). The low yield results in great (~5 Ma) uncertainties in the ages of both A steps. Radiogenic yields for all steps of RDS-6 are never greater than ~46, but $^{40}Ar^*$ reaches as high as 76 for one step of RDS-4.

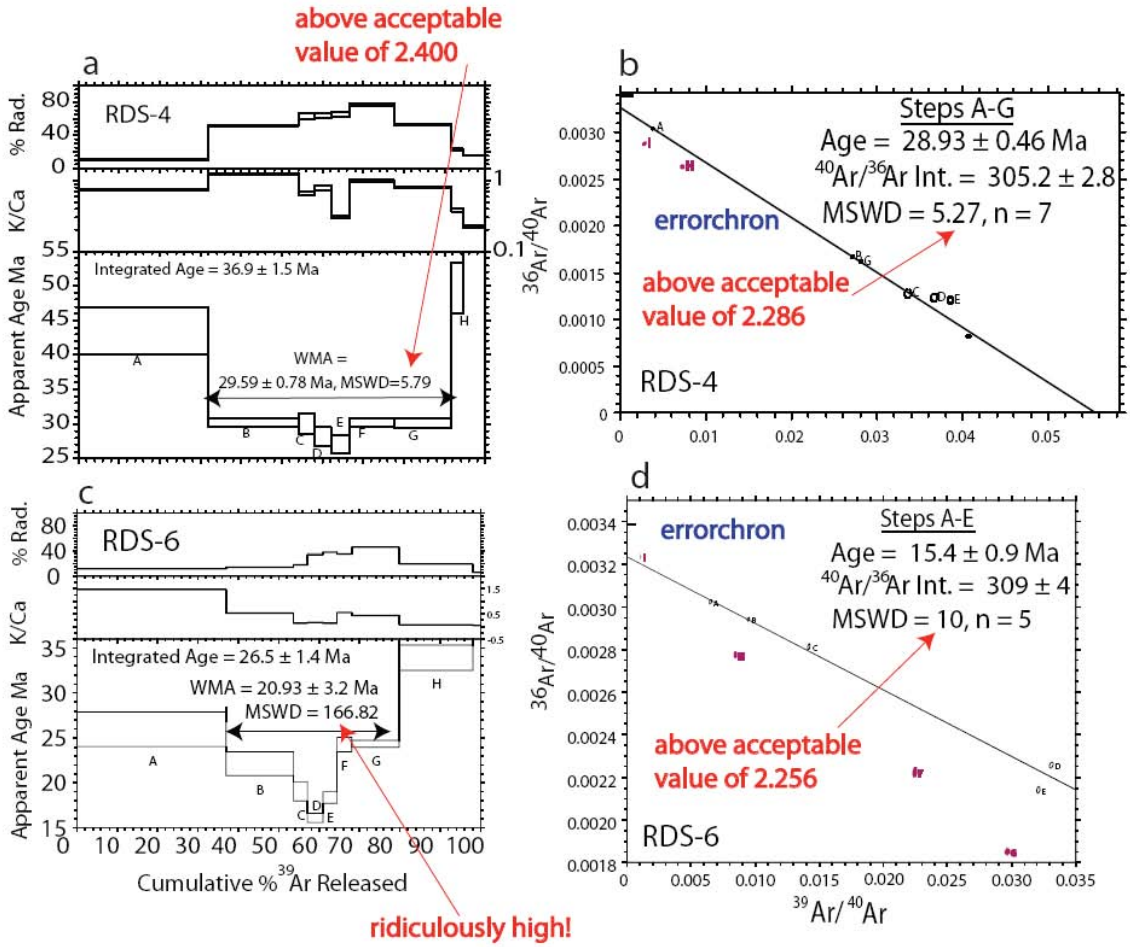

Figure 57. Age spectra and isochron plots for altered basaltic groundmass concentrate samples.

The combination of older age and higher K/Ca of step A vs. younger ages and lower K/Ca values for middle steps might suggest recoil. Step A of RDS-6 has the highest K/Ca value. The older ages of steps F-I do not fit this suggestion because of low K/Ca values. Recoil might affect RDS-4 but only three of the middle, younger steps have lower K/Ca values than step A. As in RDS-6, the higher temperature steps have lower K/Ca values.

The steps of RDS-6 form an isochron but the concordance is probably fortuitous. An isochron using steps A-D of RDS-6 has an MSWD of 0.13, an intercept of 311.2±1.3, and an age of 14.3±0.3 Ma. The MSWD is acceptable according to Mahon (1996). The intercept is higher than atmosphere suggesting excess ^{40}Ar or ^{39}Ar recoil (Singer and Pringle, 1996). A line forced through steps A-E (Fig. 57d) also has a high intercept (309±4) and an age much younger than local calderas (15.4±0.9 Ma). Steps A-E has an unacceptable MSWD of 10.

The steps of RDS-4 do not form a linear array. A line forced through steps A-G (Fig. 57b) has an MSWD of 5.27, nearly double the acceptable value. The $^{40}Ar/^{39}Ar$ intercept is above atmosphere (305.2±2.8). This errorchron is believed to best represent the age of RDS-4 (28.93±0.46) because it is concordant with the weighted mean age of spectrum steps B-G but has a slightly lower MSWD.

5.2.3 Analcime-bearing groundmass concentrate samples

The spectra of all five analcime-bearing samples are highly disturbed (Figs. 58 and 59). Four of the samples are from the Spears Ranch Dike. None of the hump-shaped spectra have plateaus. Steps A and some B steps are significantly younger than the following steps and probably represent Ar loss, but the integrated age is accurate because

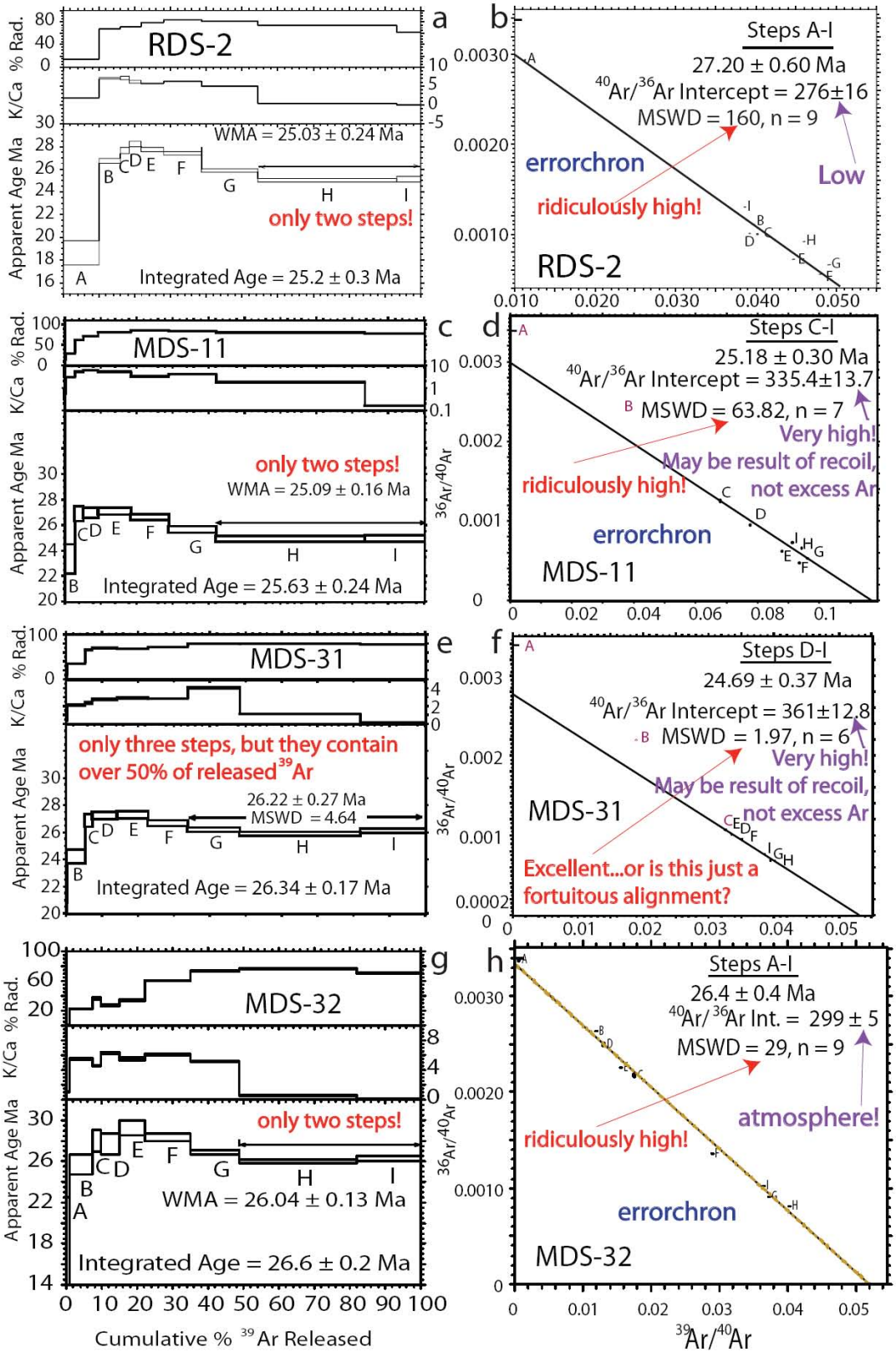

Figure 58. Age spectra and isochron diagrams of samples from the analcime-bearing Spears Ranch Dike.

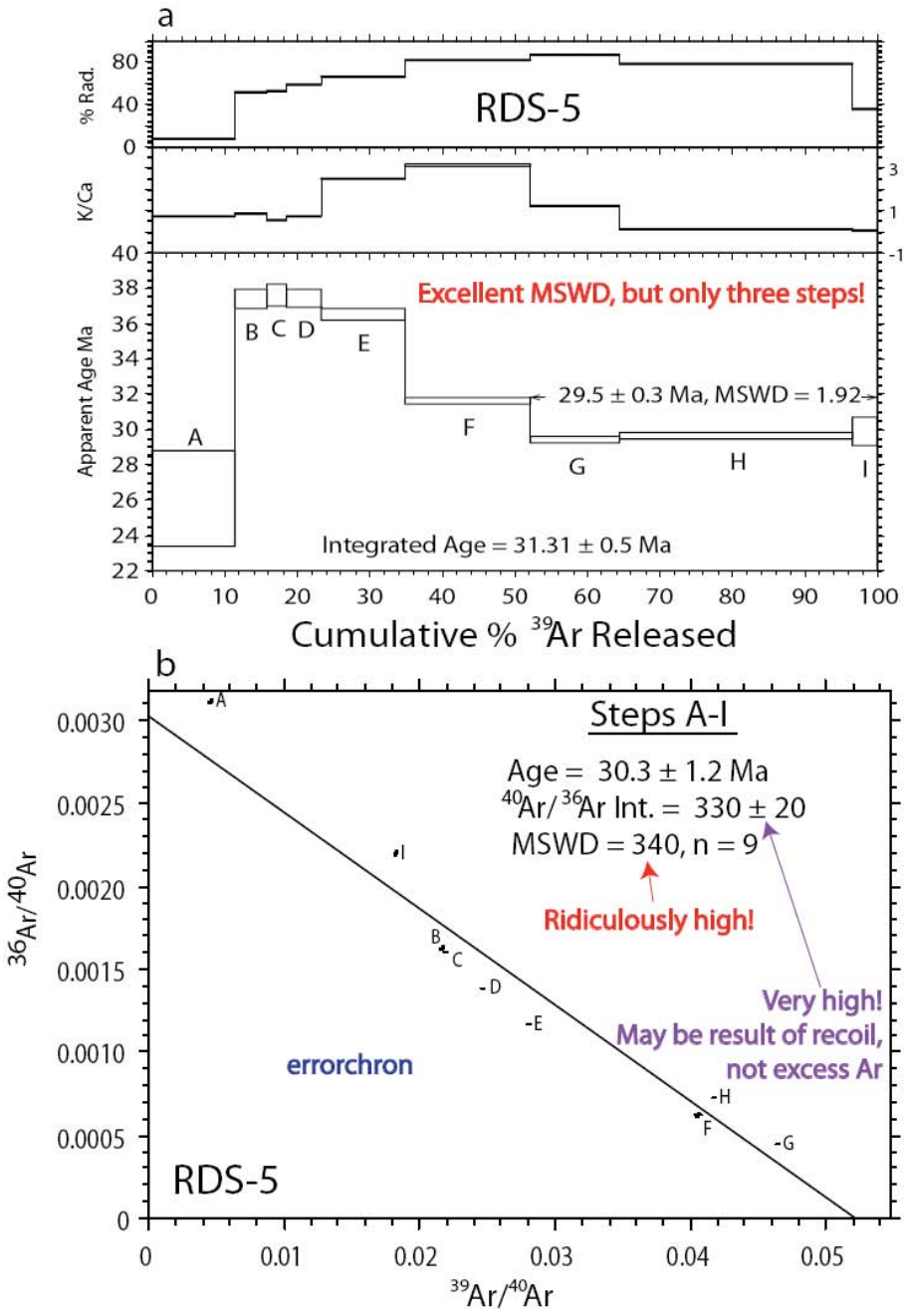

Figure 59. Age spectrum and isochron diagram for analcime-bearing sample RDS-5.

very little gas was released in steps A and B. The middle steps of all spectra are significantly older than the later steps. The last two to three steps of each spectrum contain the most released ^{39}Ar and appear to form plateaus. For example, steps H-I of MDS-11 contain ~62% of released ^{39}Ar. Because of the compositional complexity of the samples discussed below, the integrated age is the preferred age of analcime-bearing samples.

Early steps of the four Spears Ranch Dike samples have higher K/Ca values than later steps, a pattern typical of basalts. This K/Ca pattern and the age spectrum patterns are indicative of recoil because $^{39}Ar_K$ is a proxy for the amount of ^{39}K (and therefore amount of K) in each step. Recoil of ^{39}Ar from fine-grained groundmass K-feldspar into pyroxene likely caused the middle steps to appear much older than the later steps similar to the example of Huneke and Smith (1976).

The early and later steps of RDS-5 have lower K/Ca than the middle steps. The K/Ca pattern of RDS-5 is similar to that of MDS-31, which both has one middle step with a higher K/Ca than all other steps.

Of the analcime-bearing samples, only the data of MDS-31 form a well-defined linear array on an isochron line, but this may be a fortuitous alignment. Steps D-I form a line with an age of 24.69±0.37 Ma and an MSWD of 1.97. The intercept, however, is much greater than atmosphere at 360.8±12.8. MDS-31 may exhibit a phenomenon described by Singer and Pringle (1996) whereby ^{39}Ar recoil alters the position of data on the isochron plot, changing the intercept value (in this case, increasing the value). If ^{39}Ar recoiled from low degassing temperature K-rich phases into high degassing temperature K-poor phases, earlier steps may be adjusted to the left (lower $^{39}Ar/^{40}Ar$ values) and later

steps adjusted to the right (higher $^{39}Ar/^{40}Ar$ values) resulting in an increased trapped argon component value ($^{40}Ar/^{36}Ar > 295.5$).

The isochron plots of MDS-32, MDS-11, RDS-5, and RDS-2 are highly scattered. The plot of RDS-5 appears to contain two lines: one formed by steps A and G-I and another line formed by steps B-F. The intercept of the first line is atmospheric, 294±2, but is unacceptable because it contains non-contiguous steps. The second line, steps B-F, has an ideal MSWD of 1.5 but has a high intercept of 315±7 and is much older than expected for these dikes, and much older than all other samples, at 35.3±0.6 Ma. Because only one analcime-bearing sample is isochronous (which may be fortuitous) and all are greatly affected by recoil of ^{39}Ar, the integrated ages are the preferred ages for these samples.

The integrated ages of three of four samples of the Spears Ranch Dike are concordant within 2σ (Fig. 60). All four spectra are similarly shaped. The discordant sample, MDS-31, is slightly older. A possible explanation for the older age of MDS-31 is ^{39}Ar recoil out of the sample instead of recoil within the sample. This would cause the middle steps to be older but not cause later steps to be younger, resulting in an overall older age for the sample. MDS-31 and MDS-32 were irradiated in the same package so variation in irradiation lab or method is unlikely to explain the discrepancy. The average age of the three concordant samples, RDS-2, MDS-11, and MDS-32 is the accepted age of the Spears Ranch Dike (Fig. 61).

Recoil is likely the cause of the disturbed spectrum of sample RDS-5. Steps of the spectrum vary in age by ~10 Ma, much greater than the ~1-3 Ma variation among steps of the Spears Ranch Dike samples (ignoring A steps).

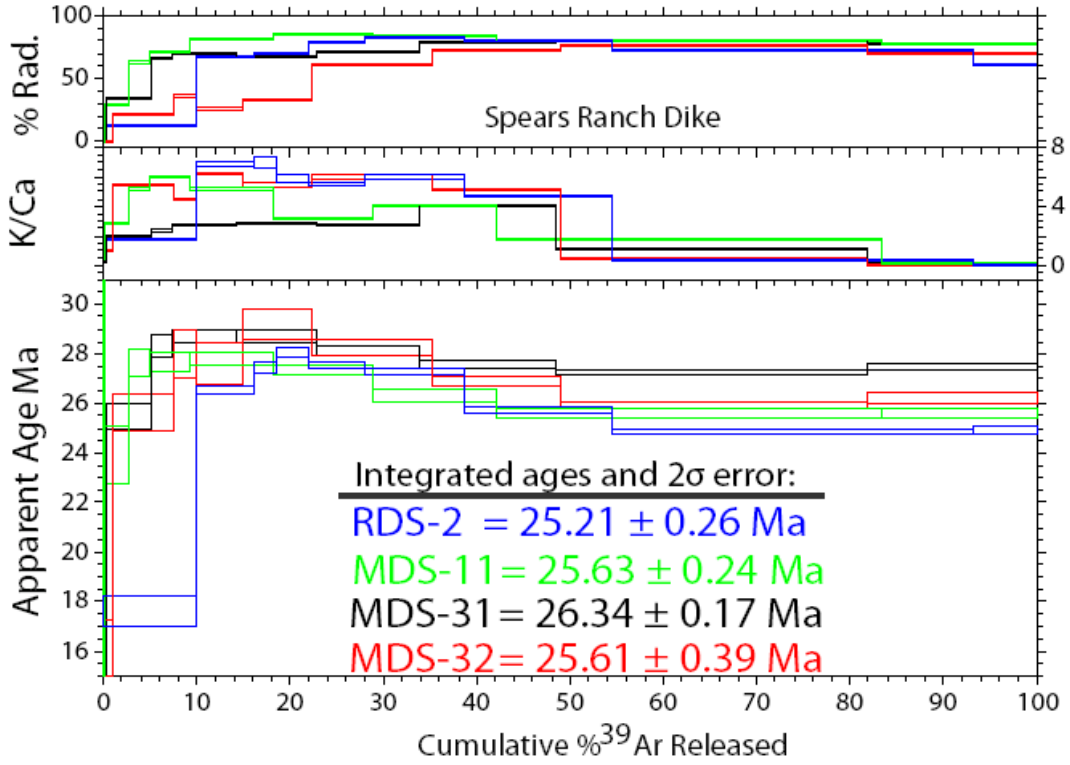

Figure 60. Comparison of age spectra of samples of the Spears Ranch Dike.

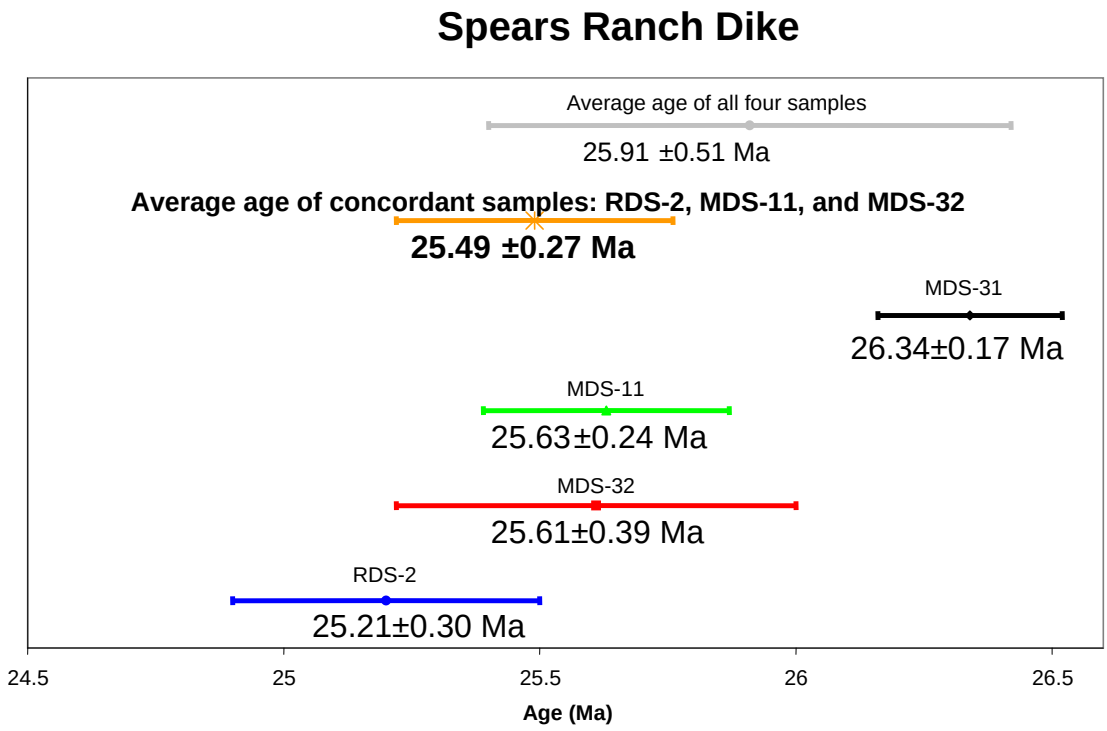

Figure 61. Comparison of integrated ages of samples from the Spears Ranch Dike. The integrated age of MDS-31 is much older than the other three samples. The average age calculated using all four samples has an error nearly double that of the average age of the three concordant samples. The average age of the three concordant samples is the preferred age of the Spears Ranch Dike.

5.2.4 Minette samples

Biotite separates from two minette samples, RDS-3 and RDS-106, were analyzed by bulk furnace step-heat. One biotite sample, RDS-3, was also analyzed by single crystal laser fusion. Age spectra and isochrons are shown in Figure 62 and an age probability diagram of RDS-3 is shown in Figure 63.

Both minette samples yield spectra with significant scatter. Both samples have several steps with radiogenic yields above 90%. The age spectrum of RDS-3 visually appears to have a plateau; a plateau incorporating steps C-L and 98.4% of released gas has an age of 28.67±0.23 but an extremely high MSWD of 25.11. This plateau age is concordant with the integrated age of 28.48±0.14 Ma. RDS-106 has no plateau. Step A is very young (12 Ma) but the rest of the spectrum shows a stair-step pattern of older to younger ages between ~55-16 Ma. The integrated age of 35.01±0.15 Ma of RDS-106 but it is much older than expected for the dikes.

Variations in the K/Ca patterns are typical of biotite. Calculated K_2O of 9.71% for sample RDS-3 is concordant with measured electron microprobe values of biotite from the same sample (Chapter 3, Appendix C). Calculated K_2O of 4.20% for RDS-106 is low for biotite and suggests that this mineral separate experienced K_2O loss or contained significant contamination of groundmass or pyroxene.

Data for neither sample form linear arrays on isochron plots. Steps C-L of RDS-3 form an errorchron of age 28.64±0.09 Ma with an atmospheric intercept (298.5±3.1) and an MSWD of 27.68. The isochron age is concordant with both the integrated and plateau ages reported above.

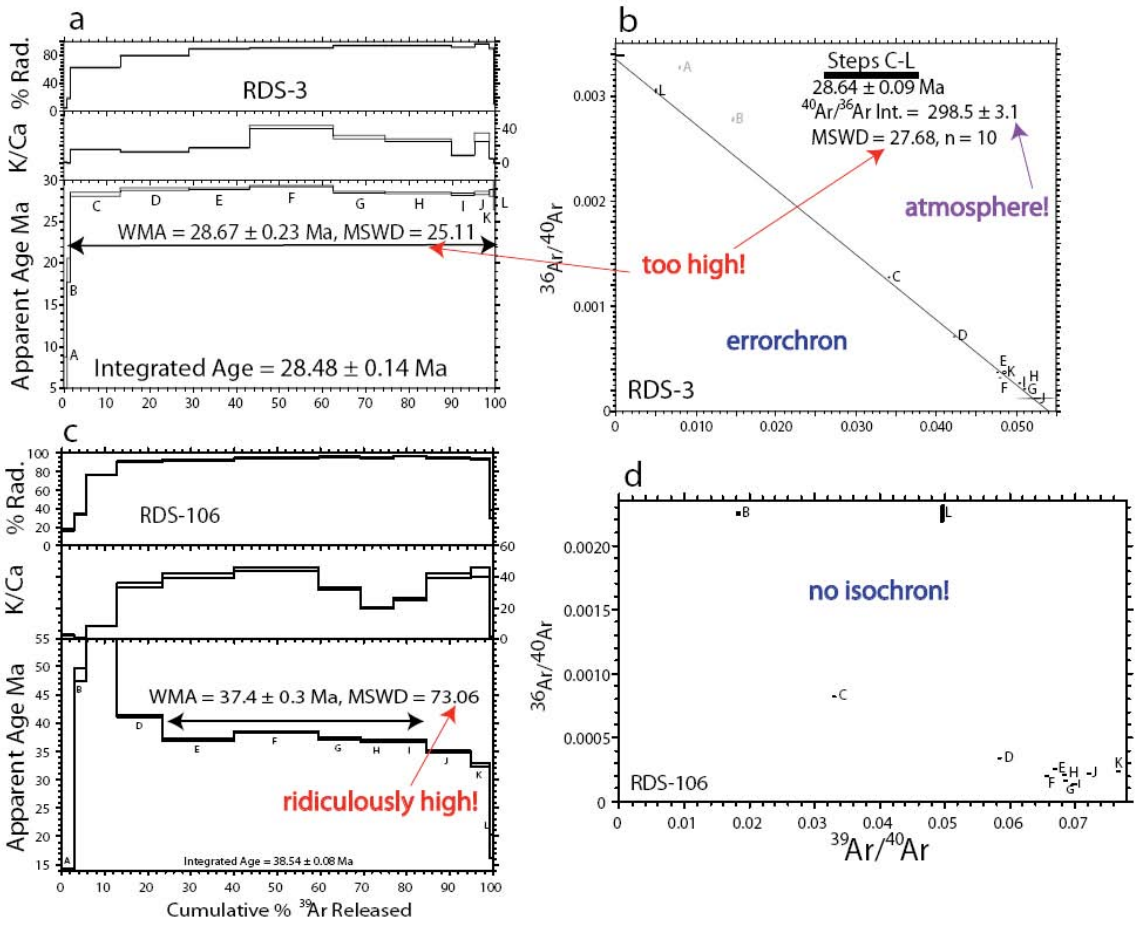

Figure 62. Age spectra and isochrons of biotite from samples RDS-3 and RDS-106.

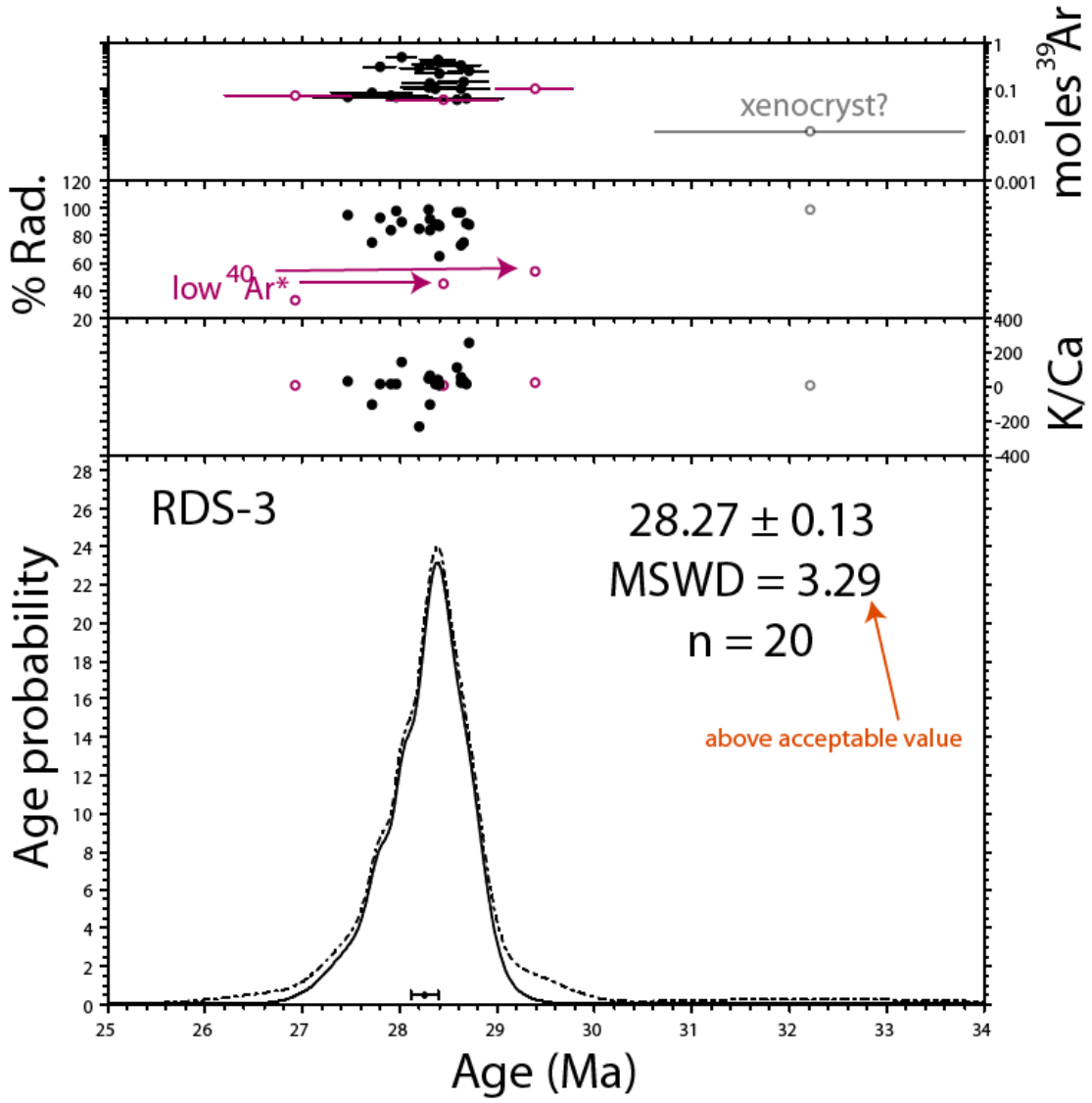

Figure 63. Age probability diagram of biotite from sample RDS-3.

The integrated, plateau, and isochron ages of RDS-3 are concordant suggesting that they represent an accurate intrusion age of the RDS-3 minette dike. The age-probability diagram of single crystal analyses from RDS-3 gives an age of 28.27±0.13 Ma. The MSWD of 3.29 is not ideal for n = 20. One point was removed from the age calculation because it is older than the other crystals and has a larger error (32.1±1.5 Ma). It is likely xenocrystic. Three other points were removed from the age calculation because of low radiogenic yield. The single crystal method is useful for removal of xenocrysts which cause increases in apparent ages, therefore the age obtained by single crystal laser fusion is the preferred age of RDS-3.

5.3 Relative $^{40}Ar/^{39}Ar$ ages vs. field relationships

Relative ages of dikes should match relative ages in the field! The dike of sample RDS-1 is cross-cut by the dike of sample MDS-15 and their $^{40}Ar/^{39}Ar$ ages agree with this relationship: RDS-1 is ~2 m.y. older than MDS-15. However, the field relationship between the dikes of samples RDS-3 and RDS-4 is not resolvable using $^{40}Ar/^{39}Ar$ ages. Sample RDS-3 is taken from a dike that cuts across the dike of sample RDS-4 but their $^{40}Ar/^{39}Ar$ ages are the same within 2σ error: 28.16±0.58 Ma and 28.93±0.46 Ma, respectively. They were emplaced close in time. An unclear field relationship exists between the dikes of samples MDS-15 and MDS-16. MDS-16 appears to be an offshoot of MDS-15 but is ~1 Ma older than MDS-15. This suggests that MDS-16 is an older dike that is not exposed south of its intersection with MDS-15.

5.4 Discussion of quality of analyses

The accepted ages of the dated dikes listed in Table 12 accurately represent intrusion ages of the dikes. The ages are accurate, but imprecise. The ages of dikes near Riley have 1-2% uncertainty.

It is apparent that the samples in this experienced different Ar loss, ^{39}Ar recoil, or trapped different excess Ar components. Spectra shapes are similar within groups of the same dike type suggesting ages of samples can be compared within their group, but even samples from the same dike experienced varying degrees of different processes. Study of the Spears Ranch Dike demonstrates that ages of a single dike are reproducible but there are outliers. The Spears Ranch Dike samples share similar spectra shapes and K/Ca and ^{40}Ar* yield patterns, but one sample has a different apparent age. As suggested in section 5.2.3, sample MDS-31 may have experienced different recoil patterns than the other samples, possibly recoil of ^{39}Ar out of the sample instead of within the sample. RDS-5 also likely experienced recoil out of the sample because the age variation between spectrum steps is much greater than the other analcime-bearing samples, ~10 Ma.

Why samples from the same dike experienced varying degrees of different processes is unknown. Samples within each dike type probably experienced similar processes because of mineralogy and amount and location of K. For groundmass concentrate, most analcime-bearing samples contain the largest amounts of K_2O, 2.25-4.88 wt%. As discussed in Chapter 3, analcime-bearing samples contain groundmass K-feldspar as well as the K-poor phases pyroxene and analcime. Pyroxene phenocrysts were removed by hand-picking the crushed sample, but groundmass analcime was part of

the analyzed concentrate. The large age discrepancies between middle and late spectra steps likely represent recoil from very fine-grained K-feldspar into analcime.

It is unlikely that the dikes contain significant argon inherited from xenoliths. Age determinations using groundmass concentrate and a sanidine separate of a xenocrystic sanidine-bearing dike from the Pie Town subswarm of the MRDS (Appendix I) are concordant. This concordance indicates that the age of the xenocrystic sanidine has been reset, i.e., their $^{40}Ar/^{39}Ar$ age represents that intrusion age of the dike. If the dikes near Riley had an intrusion temperature of ~1200°C (typical for basalts), then the ages of xenocrysts represent the dike intrusion ages.

Highly altered samples RDS-4 and RDS-6 contain the lowest amounts of K_2O of groundmass samples (0.24 and 1.71 wt%, respectively). Because of alteration, they likely experienced Ar loss, and K remaining in alteration clays likely contributed to recoil.

Recoil within biotite that has partially altered to chlorite is often the cause of disturbed data of biotite separates. Biotite from sample RDS-3 contains 9.71 wt% K_2O which is comparable to electron microprobe analyses of biotite indicating little or no chlorite is present. Biotite from sample RDS-106 contains only 4.20 wt% K_2O, suggesting the analyzed sample was partially altered to chlorite or unclean.

5.5 Summary of intrusion ages

Integrated ages are preferred for several samples (Table 12) because of recoil. One of two plateau ages, an isochron age, and a weighted mean age have high MSWD, but they are believed to be accurate because they are concordant with the other ages of their respective samples. Three of four samples from the analcime-bearing Spears Ranch

Table 12. Summary of preferred $^{40}Ar/^{39}Ar$ ages

Sample	Material	Analysis	n	MSWD	Preferred Age (Ma)	2σ	Age source
Basaltic samples							
RDS-1	GC	furnace step-heat	8		29.19	0.26	integrated
MDS-14	GC	furnace step-heat	9	2.57	27.71	0.16	plateau
MDS-15	GC	furnace step-heat	9		26.63	0.35	integrated
MDS-16	GC	furnace step-heat	7	1.72	28.33	0.15	plateau
Pyroxene porphyry dike							
02-77-11-1	GC	furnace step-heat	9		27.89	0.46	integrated
Highly altered basaltic samples							
RD5-4	GC	furnace step-heat	7	5.27	28.93	0.46	isochron
RDS-6	GC	furnace step-heat					disturbed data
Analcime-bearing samples							
RDS-5	GC	furnace step-heat	9				rejected data
Spears Ranch Dike samples							
RDS-2	GC	furnace step-heat	9		25.21	0.30	integrated
MDS-11	GC	furnace step-heat	9		25.63	0.24	integrated
MDS-31	GC	furnace step-heat	6		26.34	0.17	integrated
MDS-32	GC	furnace step-heat	9		25.61	0.39	integrated
Preferred age of Spears Ranch Dike							
Average age of RDS-2, MDS-11, MDS-32			3	0.65	25.49	0.27	
Minette samples							
RDS-3	Biotite	CO_2 Laser Fusion	23	3.29	28.27	0.13	weighted mean
RDS-106	Biotite	furnace step-heat	12				disturbed data

Dike are concordant. All four samples experienced significant ^{39}Ar recoil apparent in their highly disturbed spectra and therefore the integrated ages are chosen as preferred ages. The average of the three concordant samples is the preferred age of the Spears Ranch Dike. Sample RDS-5 is also from an analcime-bearing dike and it has the oldest apparent age of the dated dikes. Age variation between steps is ~10 Ma, much greater than the other analcime-bearing samples, indicating RDS-5 is extremely affected by recoil. The apparent age of RDS-5 (31.31±0.5 Ma) may be much older than the actual emplacement age of the dike.

The complex Ar compositions of samples and the age discrepancy among samples from the Spears Ranch dike suggest that using the $^{40}Ar/^{39}Ar$ age of one sample from a single dike of the Riley swarm as the absolute age of the dike may be inappropriate. Multiple samples that yield reproducible $^{40}Ar/^{39}Ar$ ages of individual dikes must be used for confidence of accurate age determinations.

6. SYNTHESIS AND DISCUSSION

A few questions about the dikes near Riley were posed in the Introduction to this thesis: Is there a pattern in trend versus age? Do dike trends correlate with chemistry or petrography? Is there a correlation between dike ages and ignimbrite eruptions? What is the dike magma source and did the source migrate westward with caldera activity? These questions can be answered using a combination of the field observations, geochemistry, petrography, and geochronology presented in previous chapters.

6.1 Answers to questions from the Introduction

The range of timing of emplacement of the dikes near Riley has been established as being within the same age range of the ignimbrite eruptions of the Socorro-Magdalena caldera cluster, ~29-25 Ma. If the dike source migrated westward with caldera activity NNW-trending dikes should be older and cut by NNE-trending dikes. Cross-cutting relationships presented in Chapter 2 do not fit this hypothesis. NNE-trending dikes do cut NNW-trending dikes, but the opposite cross-cutting relationship is also present. $^{40}Ar/^{39}Ar$ age relationships also do not support this hypothesis, as the two *youngest* dated dikes trend NNW, rather than NNE, and the *older* dated dikes trend NNE (Fig. 64). Only two NNW-trending dikes were analyzed by the $^{40}Ar/^{39}Ar$ method and age determinations of more dike samples will reveal if this pattern of younger NNW-trending dikes and older NNE-trending dikes is real or just a result of the small sample set.

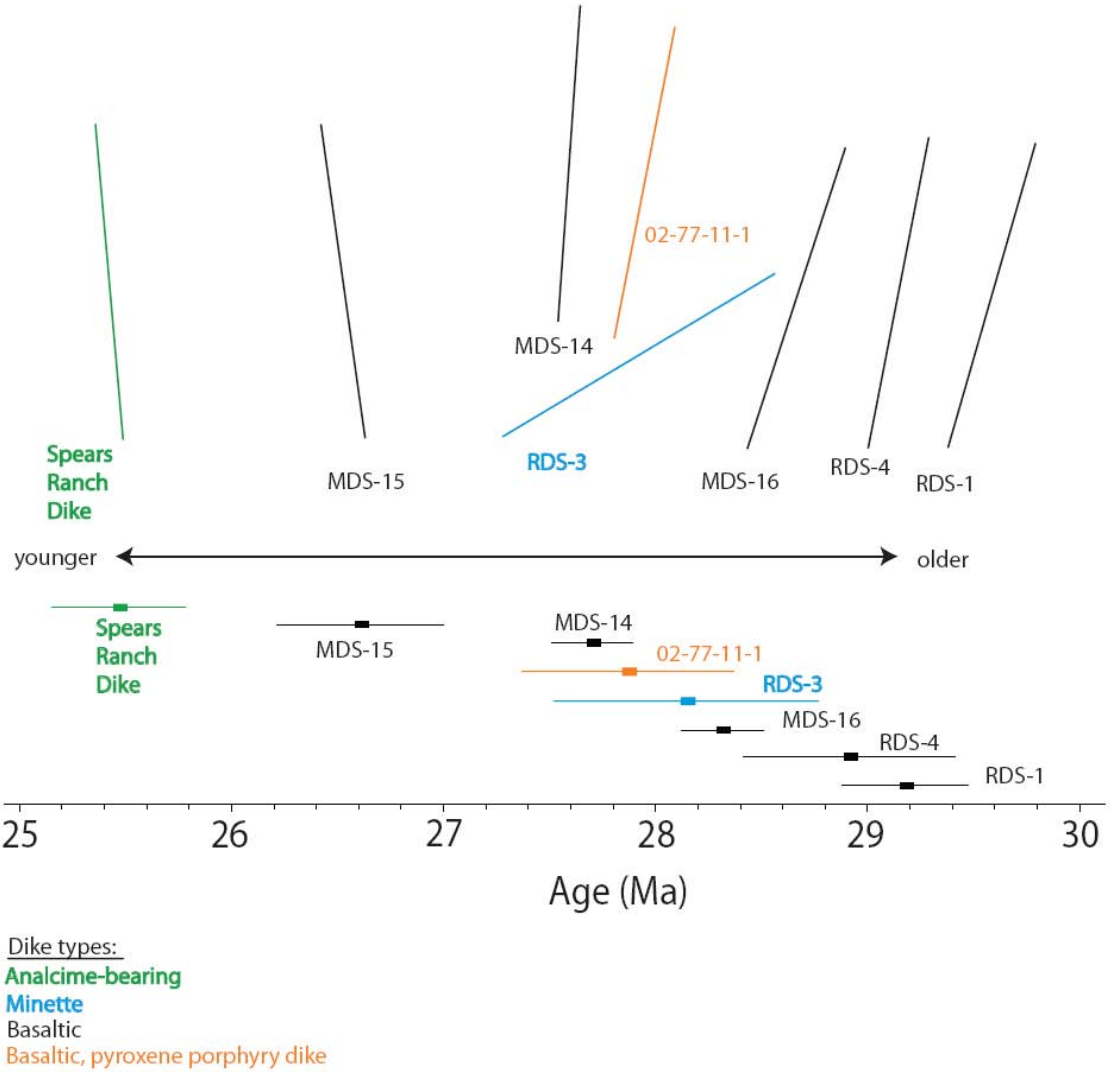

Figure 64. Schematic drawing of dikes oriented to measured azimuth and in order from youngest to oldest.

The timing of dike emplacement is coeval with ignimbrite eruptions but the mechanical relationship between the dikes and ignimbrite eruptions is poorly understood. Emplacement of dikes may relieve pressure within magma chambers. The ground surface above magma bodies often experiences uplift prior to caldera eruptions to relieve pressure due to growth of the magma chamber (Lipman, 1997). The volume of ground surface tumescence may be less than the volume of basalt injected into a magma chamber which may result in a pressure increase within the chamber (Snyder, 2000), and magma may escape the high-pressure chamber through diking events.

Six of 8 dikes were emplaced within a ~2 m.y. period during which 4 of 6 ignimbrites were erupted. Figure 65 shows the ages of dikes and the six largest local ignimbrites with 2σ error. Two dikes, the MDS-15 basaltic dike and the Spears Ranch Dike, are younger than the 2 m.y. period of caldera activity and dike emplacement, but both are older than the youngest local ignimbrite, the Turkey Springs Tuff.

Seven of 8 dikes appear to radiate northward from three calderas of the SMCC (Fig. 66). These three calderas, Sawmill Canyon, Hardy Ridge, and Mt. Withington, are three of the calderas nearest to Riley. The eruptions of the La Jencia, Lemitar, and South Canyon Tuffs, respectively, formed these three calderas within the ~2 m.y. period during which most of the dikes were emplaced. In Figure 66, the trends of 7 of 8 dated dikes intersect these three calderas. The coeval ages of 6 of 8 dikes and the 3 calderas and intersection of 7 of 8 dike trends with the 3 calderas indicates that the dike magma source is located under the 3 associated calderas and that the dikes were emplaced in response to pressure changes within the chamber(s) before or during the eruption of the ignimbrites. The emplacement of the two younger dikes, the MDS-15 basaltic dike and the Spears

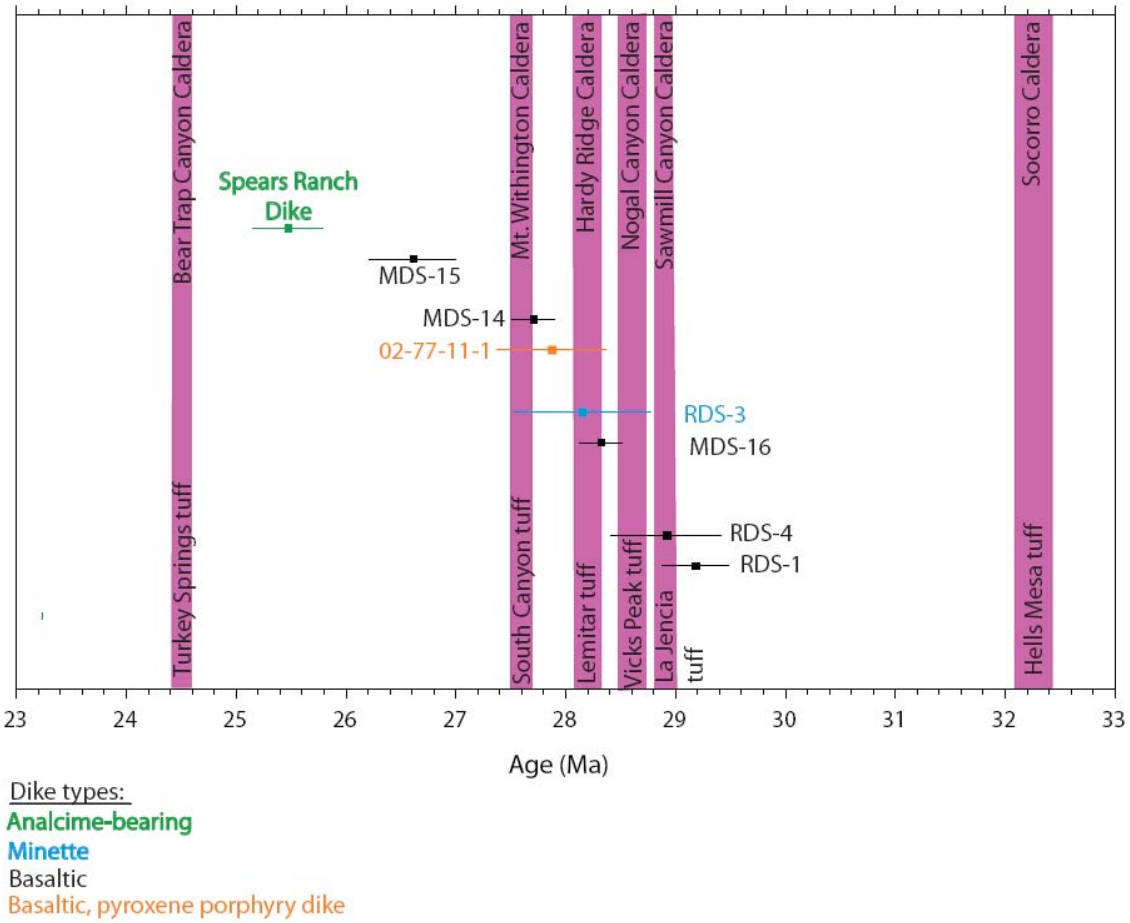

Figure 65. $^{40}Ar/^{39}Ar$ ages of dikes near Riley and the 6 largest local ignimbrites with 2σ error.

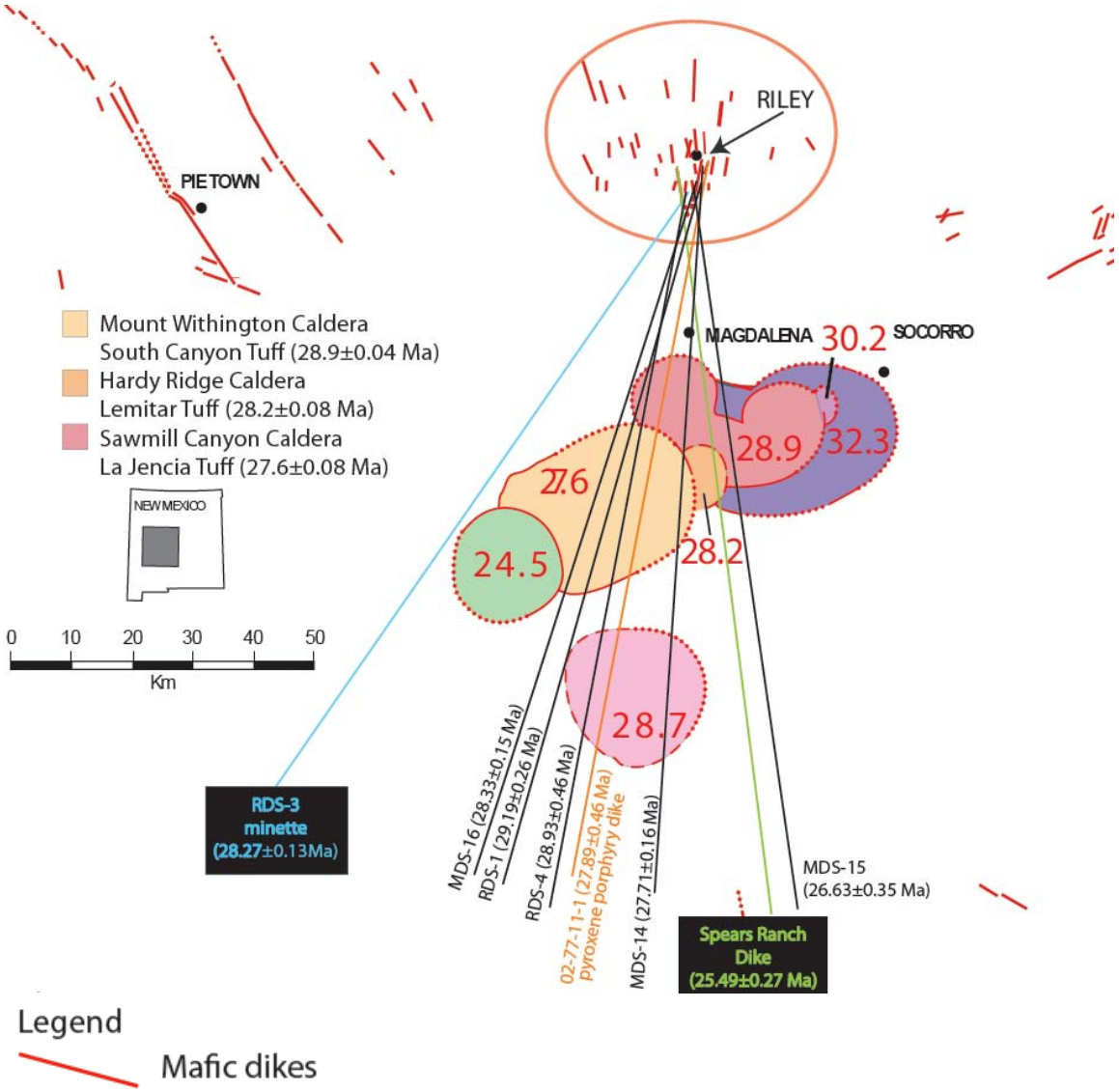

Figure 66. The Socorro-Magdalena caldera cluster (SMCC) and dikes near Riley extrapolated southward using their measured azimuth. Seven of 8 dikes appear to extend northward from the Mt. Withington, Hardy Ridge, and Sawmill Canyon calderas. Some also appear to radiate from Nogal Canyon caldera which is the farthest local caldera from Riley. Red numbers represent ages of the calderas (reported without error).

Ranch Dike, may be the result of pressure increases within a magma chamber that did not result in an ignimbrite eruption.

The dikes are drawn in Figure 66 using the azimuth measured at the outcrops near Riley which may only accurately represent the exposed dike rock instead of the entire length of the dikes. The RDS-3 minette dike has the most extreme azimuth (035) where it crops out near Riley, and it does not intersect any caldera. Three of the dikes also intersect the outline of the Nogal Canyon caldera, the caldera farthest from Riley. The dike source is probably located under calderas nearer to Riley.

There is no apparent correlation among dike trends, chemistry, and petrography. All types of dikes trend NNW and NNE and in-between. Minette dikes, however, often have the most extreme azimuths. As previously mentioned, a minette dike in the southwest quarter of the map area (samples RDS-3 and RDS-098 are from this dike) trends 035. Segments of minettes in the northwest quarter of the map area trend as westerly as 330-340.

The dike magma source is discussed in section 6.4.2. The following sections address questions about naming the dikes, the presence of carbonate, and the geochemical relationships of the dikes to other magmas.

6.2 Nomenclature

The dikes near Riley may be termed “lamprophyric” for several reasons related to their field geometry, mineralogy, and geochemistry according to Rock (1991). Lamprophyre dikes tend to be “serpentinous,” have changing widths along strike, and are segmented. The dikes near Riley show these characteristics, but irregularities in shape of

the exposures at Riley may be the result of the exposures being at or near the tops of the dikes (Fig. 16).

Abundant hydrous and CO_2-rich minerals such as biotite, analcime, and carbonate characterize lamprophyres (Rock, 1991). Lamprophyres are known to contain primary analcime, usually as matrix, and carbonate, commonly in groundmass and as a replacement of minerals such as pyroxene. High-Ti clinopyroxene is characteristic and most pyroxenes in lamprophyres straddle the diopside-augite boundary of the pyroxene quadrilateral (Fig. 36).

Minettes are a common lamprophyre and the existence of minettes in the Riley dike swarm was recognized before any petrographic or geochemical analysis revealed the presence of common lamprophyre phases such as primary analcime. The presence of minettes suggests that the other dikes may also be lamprophyres or at least lamprophyric.

Rock (1991) states that lamprophyres usually have negative Ta, Nb, and Ti anomalies. These are anomalies shared by the dikes near Riley, but as discussed in the following sections, these anomalies are shared by other magmas in the Mogollon-Datil volcanic field. Negative Ta, Nb, and Ti anomalies are probably indicative of the magma source rather than an identifying characteristic of lamprophyres.

The petrographic groups and mineral assemblages of the dikes (Appendix C) are the best terms to use to reference the Riley dikes. These names supply the most detail about the mineralogy and alteration of the dikes. The geochemical names of the dikes assigned by the total-alkali silica diagram also provide information about the composition of the dikes. The fields “potassic trachybasalt” and “shoshonite” indicate the potassic nature of the dikes. The problem with calling the dikes near Riley lamprophyres or

lamprophyric is that those terms imply little or nothing about the mineralogy, geochemistry, magma source or the evolution of the magma system. The term "lamprophyre" is too broad for use with the Riley dikes.

6.3 Origin of the carbonate

The origin of the carbonate in the dikes has three possible sources: meteoric fluids carrying carbonate from local limestones, assimilation of wallrock by the dike magma, and magmatic CO_2. A source of meteoric fluids is unlikely because the C and O isotope results presented in Chapter 3 show that all the dikes have isotope values significantly different than local sedimentary carbonate. The isotope compositions of the dikes indicate that the source of the carbonate is different than the source of the sedimentary carbonate, therefore the carbonate in the dikes cannot be explained by assimilation of wallrock. Assimilation of wallrock by the dike magma is also unlikely because the dike magma would need to have incorporated a significant amount of limestone wallrock. Only two samples containing carbonate xenoliths were observed in thin section, suggesting some of the carbonate could be from wallrock. If the majority of the carbonate resulted from assimilation, one would expect more than two samples to contain carbonate xenoliths.

The carbonate is probably magmatic. The dikes are relatively primitive (MgO ≈ 4-11%) suggesting a mantle magma source, which is also discussed in section 6.4.2. Mantle magmas contain CO_2 (Wilson, 1989) and the isotopic composition of the Riley dikes is similar to that of the mantle and typical basalts ($\delta^{13}C \approx -5‰$). The CO_2 did not escape the magma before the dikes solidified which resulted in CO_2 metasomatism of the dikes. During CO_2 metasomatism carbonate formed pseudomorphs after pyroxene.

Most of the basaltic and minette dikes experienced CO_2 metasomatism (Appendix C). One basaltic dike that contains little to no carbonate is the dike bordered by a large baked wallrock aureole (Chapter 2). The large baked wallrock aureole suggests this dike may have fed a lava flow. The lack of carbonate also fits with this being a feeder dike because surface venting would allow the basaltic magma to degas.

Analcime-bearing dikes (including speckled texture) also contain little to no carbonate. One unconfirmed occurrence of extrusive leucite- or analcime-bearing rocks in the local La Jara Peak basaltic andesite lavas (Canales and Sanders, 2006) suggests that analcime-bearing dikes may have reached the Oligocene land surface. However, analcime-bearing dikes lack significant metamorphic aureoles suggesting magma flow through the dike fracture was short-lived and probably never vented. Analcime-bearing dikes may have been fed by degassed portions of the magma chamber that fed the dikes. The analcime-bearing Spears Ranch Dike is the youngest of all dated dikes, and it seems possible that the gas-rich magmas escaped the chamber first (as basaltic and minette dikes), leaving gas-poor magma which fed analcime-bearing dikes.

Leucite is common in K-rich basic rocks (Deer et al., 1992). There is little difference between the geochemistry of analcime- (after leucite) bearing dikes and basaltic dikes, although analcime-bearing dikes tend to have higher alkali contents than basaltic dikes with equivalent SiO_2 (Fig. 52), and clinopyroxene in analcime-bearing dikes contain higher Ca than in other dikes. The lack of CO_2 pressure in some magmas may have caused the formation of the analcime-bearing dikes' primary mineral assemblage (leucite, clinopyroxene, biotite, ±olivine, ±plagioclase(?).

6.4 Geochemical comparison with other magmas

6.4.1 Magdalena Radial Dike Swarm

The Riley dikes are a subswarm of the Magdalena Radial dike swarm (MRDS). Samples from the Pie Town and Elephant Butte subswarms and four samples from a large dike near La Joya, east of Riley, are included in this discussion. Most dikes in the MRDS plot in three fields of the total alkali-silica diagram: potassic trachybasalt, shoshonite, and trachyandesite (Fig. 67). All of the samples are potassic (wt% Na_2O -2 < K_2O) except for two Elephant Butte samples which fall into the andesite and trachyandesite fields. Pie Town dikes fall in what *appears* to be an evolution trend line, but $^{40}Ar/^{39}Ar$ age determinations demonstrate that this is not the case (R.M. Chamberlin, pers. commun.). The Riley dikes tend to have lower SiO_2 than other MRDS dikes.

Trace elements of the MRDS samples normalized to pyrolite mantle of McDonough and Sun (1995) all share similar trends (Fig. 68). Only Riley samples with the RDS prefix were analyzed for Ta, but the other MRDS samples share negative Nb and Ti anomalies with the Riley samples. At least one sample from the Elephant Butte area has significantly lower amounts of some elements including Rb, K, and Y, than other dikes.

6.4.2 Mogollon-Datil Volcanic Field

The geochemistry of the Riley dikes is similar to that of other magmas of the Mogollon-Datil volcanic field (MDVF). The Riley dikes and the MRDS are at the northern margin of the MDVF. Davis and Hawkesworth (1993, 1995) compiled whole rock geochemistry data from lavas in a portion of the northern MDVF. The total alkali-silica diagram (Fig. 69) shows a differentiation trend in the samples from 20-30 Ma.

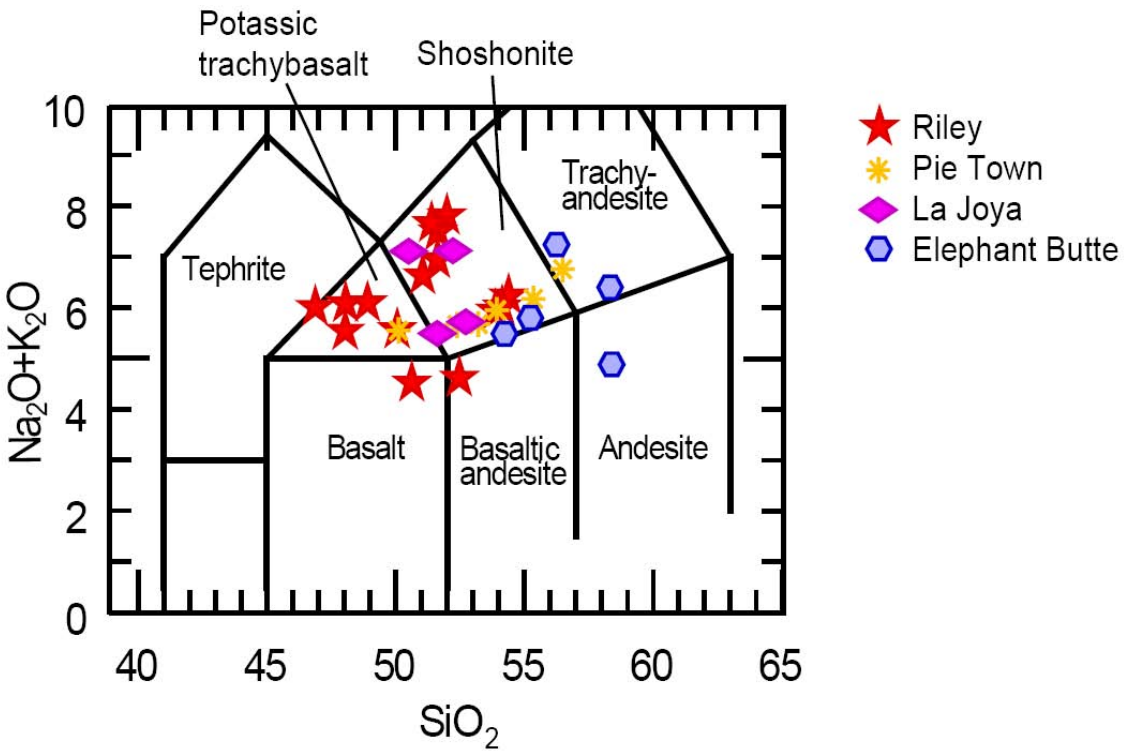

Figure 67. Total alkali-silica diagram of dikes in the Magdalena Radial Dike Swarm. Chemical data for dikes outside the Riley area from R.M. Chamberlin (pers. commun.).

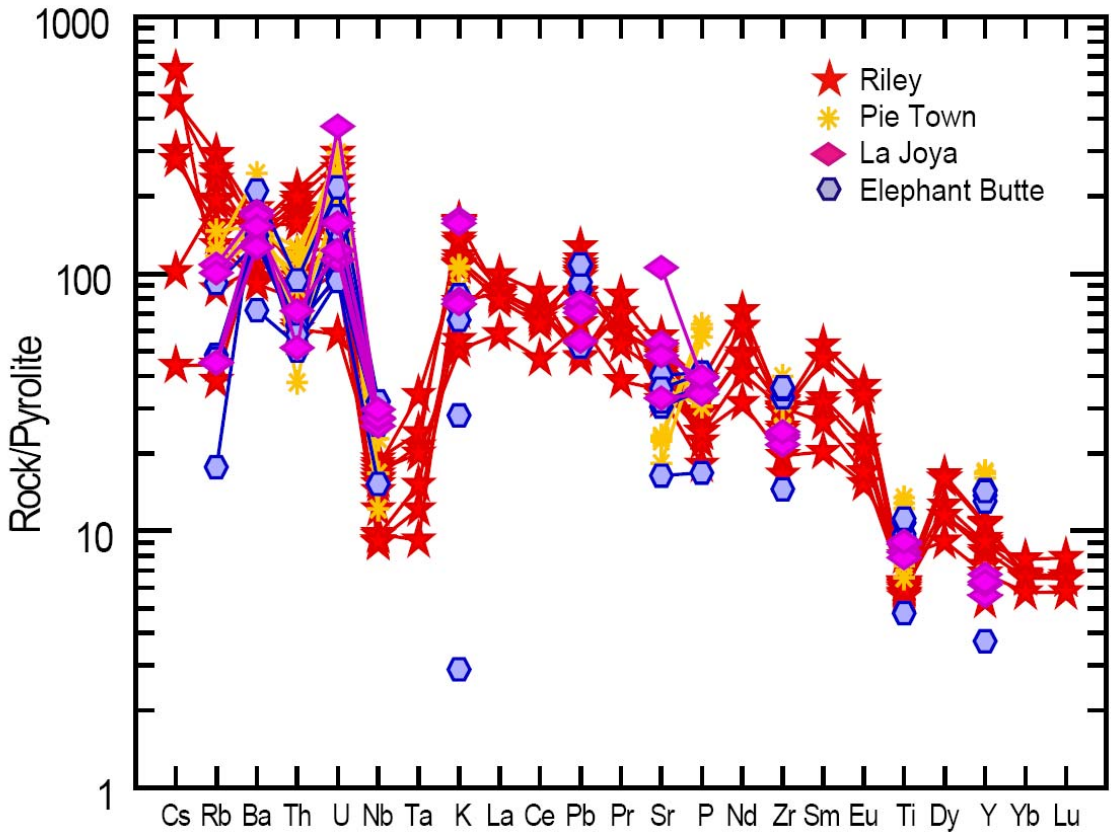

Figure 68. Trace elements from three subswarms and the La Joya dike of the Magdalena Radial Dike Swarm normalized to pyrolite mantle of McDonough and Sun (1995). Chemical data for dikes outside the Riley area from R.M. Chamberlin (pers. commun.).

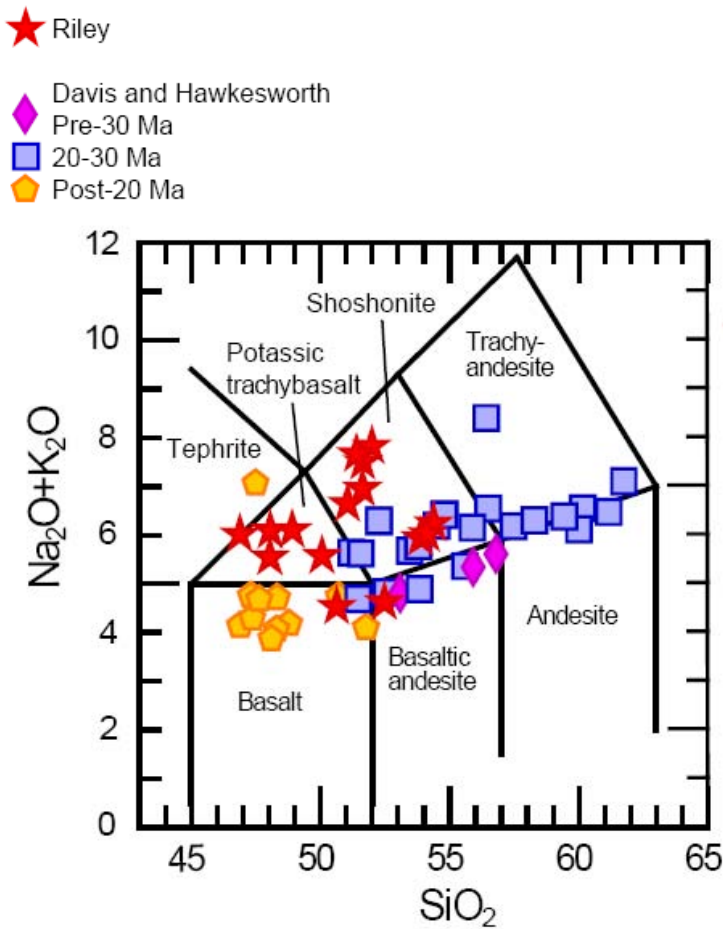

Figure 69. Total alkali-silica diagram of dikes near Riley and samples of lavas from Davis and Hawkesworth (1993, 1995).

Only seven of 38 samples from Davis and Hawkesworth are not potassic. Five of these are from post-20 Ma, implying the younger magmas have a different source than the older magmas or the younger source is contaminated.

Figure 70 shows Riley dike and other MDVF mafic geochemistry data normalized to pyrolite mantle (McDonough and Sun, 1995). Riley dike samples plot most similarly to 20-30 m.y. old MDVF magmas (Fig. 70b). The Riley samples also share a similar trend to the pre-30 Ma samples but this similarity is less apparent because there are only three pre-30 Ma samples. The post-20 Ma samples are noticeably missing the negative Nb, Ta, and Ti anomalies that are prominent characteristics of the other age groups.

Davis and Hawkesworth believe that the Mogollon-Datil volcanics are the result of partial melting of a lithospheric mantle source due to extension. The pre-30 Ma to 20 Ma lavas have a minor asthenospheric component that is greater in younger lavas. The post-20 Ma lavas have a significant asthenosphere component. The negative Nb and Ta anomalies are characteristic of source regions within the lithospheric mantle and did not arise from crustal contamination because an "unrealistically high" (Davis and Hawkesworth, 1995) amount of contaminant would be necessary. Trends of increasing asthenospheric component in magmas are noted in other studies of the western U.S. (e.g. Fitton et al, 1991, Kempton et al., 1991).

The argument of a lithospheric mantle source for the MDVF is supported by Sr isotopes and trace element ratios (Davis and Hawkesworth, 1993, 1995). Davis and Hawkesworth use the ratios Ba/Nb and Th/Ta to demonstrate the trends that indicate the amount of asthenospheric component increases from older to younger rocks. Older lavas have higher LILE/HFSE ratios than younger lavas. Ratios of samples from Davis and

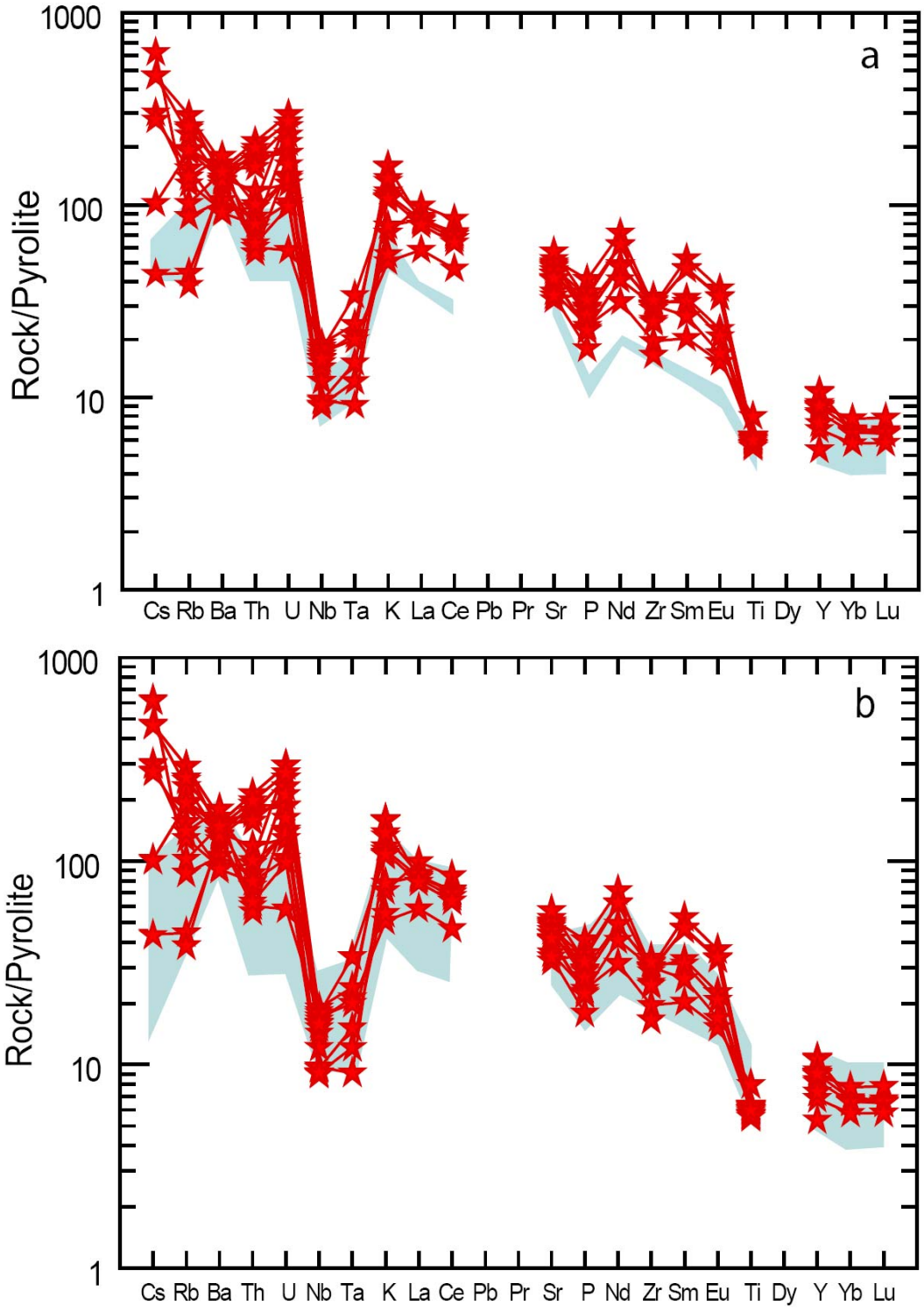

Figure 70. Spiderdiagrams of dikes near Riley (red stars) and lavas from three age groups (shaded blue) of Davis and Hawkesworth (1993 and 1995). a) pre-30 Ma, b) 30-20 Ma, c) post-20 Ma.

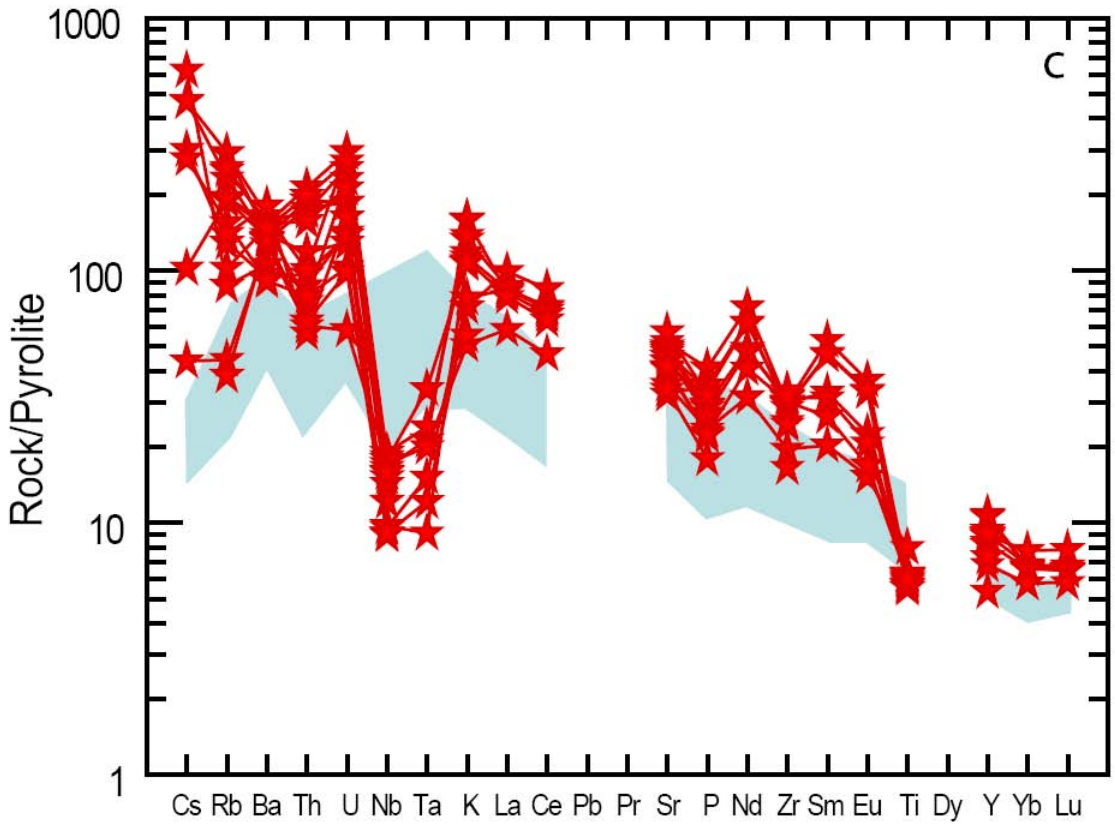

Figure 70. continued

Hawkesworth and from Riley are shown in Figure 71. Riley dikes with the MDS prefix were not analyzed for Ta and some of the MDVF lavas have values of Ta = 0. These samples are plotted at Th/Ta = 0 to show their Ba/Nb values. The Riley dikes have ratios similar to and much higher than pre-30 Ma and 30-20 Ma lavas. As stated above, Davis and Hawkesworth (1995) argue that the negative Nb and Ta anomalies arose from subduction-modified lithospheric mantle. The slightly lower Nb anomalies and much lower Ta anomalies in the Riley dikes resulted either from a smaller asthenospheric component than Davis and Hawkesworth's samples or from a combination of a subduction-modified or "fertile" lithospheric source and significant crustal contamination.

Tertiary ignimbrites of the western U.S. consist of mixtures of lithospheric mantle and crust (e.g. Johnson, 1993; Perry et al., 1993; Farmer et al., 2008). Oligocene ignimbrites, including those of the Mogollon-Datil volcanic field, contain more crustal contamination than younger ignimbrites (Perry et al., 1993). Though the dikes at Riley were fed by magma deeper in the Mogollon-Datil magmatic system, they may share a similar crustal component with the ignimbrite calderas they surround.

The source of the Riley dikes as partial melt of subduction-modified lithospheric mantle with little or no asthenospheric component and possible crustal contamination is inferred from similar trace element spiderdiagrams, significant negative Nb, Ta, and Ti anomalies, and similar LILE/HFSE ratios to other pre-30 Ma to 20 Ma MDVF lavas. Farmer et al. (2008) suggest conductive heating of subduction-modified lithospheric mantle (by heat from sub-lithospheric mantle) generated the mafic magmas that fueled

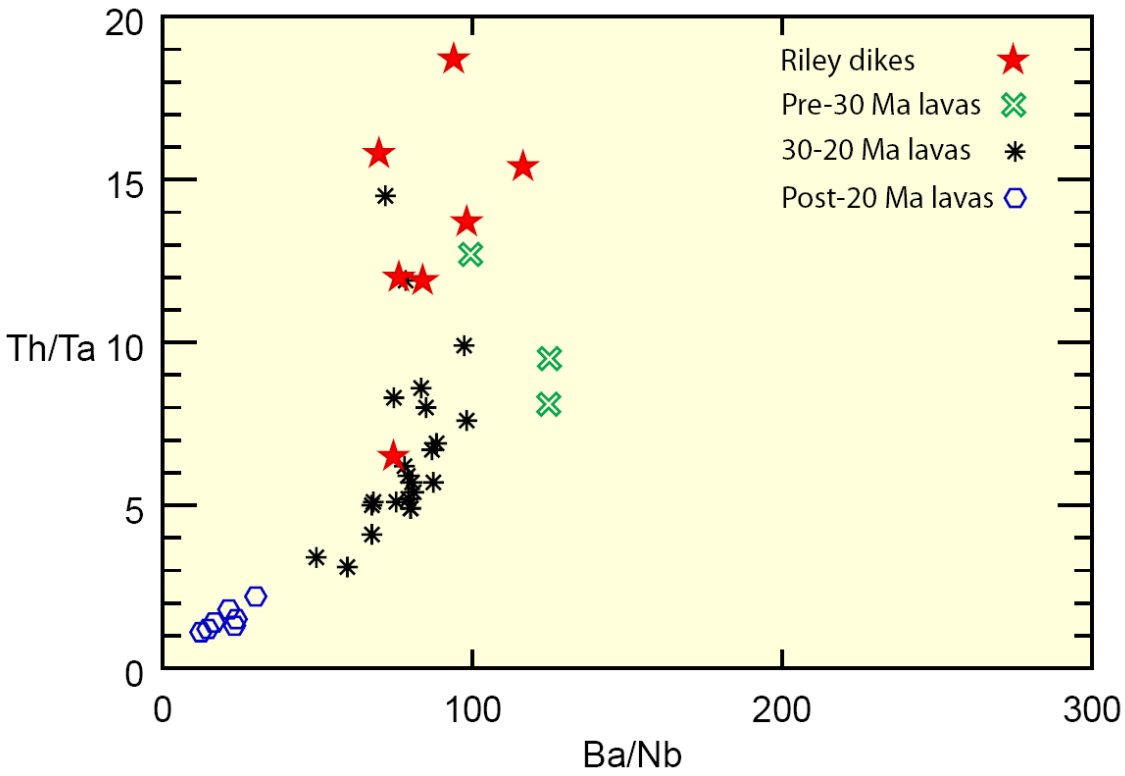

Figure 71. LILE/HFSE ratios for Riley dikes and Mogollon-Datil volcanic field lavas of Davis and Hawkesworth (1993, 1995).

ignimbrite eruptions in the western U.S. These mafic magmas fueled the ignimbrite calderas the Riley dikes surround and were parental to magmas that fed the Riley dikes.

6.5 Synthesis and summary

The dikes near Riley were emplaced between ~29-25 Ma. The dikes appear to radiate northward from three of the six local calderas that were formed by ignimbrite eruptions between ~32-24 Ma. The age vs. trend relationship of the dikes (the two youngest dated dikes trend NNW and the older 6 dated dikes trend NNE) is the opposite of the simple radial pattern of emplacement from a deep westward-migrating source under the local calderas.

The dikes are relatively primitive; they contain high MgO (~4-11%) and low SiO_2 (48-55%). The dikes are also potassic (wt% Na_2O -2 < K_2O). The potassic, more primitive magma formed minette dikes (with biotite clots), feldspathoidal dikes (analcime after leucite), and basaltic dikes. CO_2 metasomatism of many minette and basaltic dikes by magmatic CO_2 resulted in the presence of carbonate pseudomorphs after pyroxene and olivine(?) and finely disseminated carbonate in some dikes. As yet, there are no documented Oligocene extrusive equivalents to the minette and analcime-bearing magmas in the Socorro-Magdalena region.

The trace element geochemistry of the dikes is similar to that of magmas of similar age within the MDVF. The dikes and other magmas erupted between 30-20 Ma share higher LILE/HFSE than younger MDVF magmas in addition to significant negative Nb and Ta anomalies when normalized to pyrolite mantle (McDonough and Sun, 1995). These negative anomalies are characteristic of the subduction-modified lithospheric mantle source of the dikes and other MDVF lavas of similar age.

REFERENCES

Aldrich, M.J., Jr., Chapin, C.E., Laughlin, A.W., 1986. Stress history and tectonic development of the Rio Grande Rift, New Mexico, Special section on the Rio Grande Rift. J. Geophys. Res. 91: 6199-6211.

Ancochea, E., Brändle, J.L., Huertas, M.J., Hernán, F., Herrera, R., 2008. Dike-swarms, key to the reconstruction of major volcanic edifices: The basic dikes of La Gomera (Canary Islands). J. of Volcanol. Geotherm. Res. 173: 207-216.

Baldridge, W.S., Perry, F.V., Vaniman, D.T., Nealey, L.D., Laughlin, A.W., Kyle, P., Bartov, Y., Steinitz, G., Gladney, E.S., 1989. Magmatism associated with lithospheric extension: Middle to late Cenozoic magmatism of the southeastern Colorado Plateau and central Rio Grande rift, New Mexico and Arizona: In: C.E. Chapin, J. Zidek (Editors), Field Excursions to Volcanic Terranes in the Western United States, Volume I: Southern Rocky Mountain region, New Mexico Bureau of Mines and Mineral Resources Memoir 46. New Mexico Bureau of Geology and Mineral Resources, Socorro, NM, pp. 187-230.

Baldridge, W.S., Perry, F.V., Vaniman, D.T., Nealey, L.D., Leavy, B.D., Laughlin, A.W., Kyle, P.R., Bartov, Y., Steinitz, G., Gladney, E.S., 1991. Middle to late Cenozoic magmatism of the southeastern Colorado Plateau and central Rio Grande Rift (New Mexico and Arizona, U.S.A.); a model for continental rifting. Tectonophysics 197 (2-4): 327-354.

Bobrow, D.J., Kyle, P.R., 1983. Miocene rhyolitic volcanism in the Socorro area of New Mexico. In: C.E. Chapin (Editor), New Mexico Geol. Soc. Guidebook 34: Socorro Region II. New Mexico Geol. Soc., Socorro, NM, pp. 211-217.

Canales, D., Sanders, R., 2006. A new zeolite occurrence in the Bear Mountains, Socorro County, New Mexico. New Mexico Geology 28 (4): 112-113.

Cather, S.M., 1990. Stress and volcanism in the northern Mogollon-Datil volcanic field, New Mexico: effects of the post-Laramide tectonic transition. Geol. Soc. Am. Bull. 102 (11): 1447-1458.

Cather, S.M., Chamberlin, R.M, Chapin, C.E., McIntosh, W.C., 1994. Stratigraphic consequences of episodic extension in the Lemitar Mountains, central Rio Grande rift. In: G.R. Keller, S.M. Cather (Editors), Basins of the Rio Grande rift—structure, stratigraphy, and tectonic setting. Geol. Soc. Am. Special Paper 291, pp. 157-170.

Chamberlin, R.M., 1981. Uranium potential of the Datil Mountains-Pietown area, Catron County, New Mexico. New Mexico Bureau of Mines and Mineral Resources Open-File Report 138, 51 pp.

Chamberlin, R.M., 1983. Cenozoic domino-style crustal extension in the Lemitar Mountains, New Mexico; a summary. In: C.E. Chapin (Editor), New Mexico Geol. Soc. Guidebook 34: Socorro Region II. New Mexico Geol. Soc., Socorro, NM, pp. 111-118.

Chamberlin, R.M., Chapin, C.E., McIntosh, W.C., 2002. Westward migrating ignimbrite calderas and a large radiating mafic dike swarm of Oligocene age, central Rio Grande Rift, New Mexico: surface expression of an upper mantle diaper?, Geological Society of America poster, WWW page http://geoinfo.nmt.edu/staff/chamberlin/mrds/Chamberlin_2002_GSA_poster.pdf

Chamberlin, R.M., McIntosh, W.C., Chapin, C.E., 2003. Oligocene calderas, mafic lavas and radiating mafic dikes of the Socorro-Magdalena magmatic system, Rio Grande rift, New Mexico: surface expression of a miniplume?, Plume IV: Beyond the Plume Hypothesis poster, WWW page http://www.mantleplumes.org/Penrose/PenPDFAbstracts/Chamberlin_Richard_abs.pdf

Chamberlin, R.M., McIntosh, W.C., Dimeo, M.I., Geochronology of Oligocene mafic dikes within the southeastern Colorado Plateau: implications to regional stress fields of the early Rio Grande rift, Geological Society of America Annual Meeting. Abstracts with Programs 39 (6): 496.

Chamberlin, R.M., Osburn, G.R., 1986. Tectonic Framework, character, and evolution of upper crustal extensional domains in the Socorro area of the Rio Grande Rift, New Mexico. Arizona Geological Society Digest 26: 464.

Chapin, C.E., 1989. Volcanism along the Socorro accommodation zone, Rio Grande rift, New Mexico; In: C.E. Chapin, J. Zidek (Editors), Field excursions to volcanic terranes in the western United States Volume I: Southern Rocky Mountain Region. New Mexico Bureau of Mines and Mineral Resources, pp. 46-57.

Chapin, C.E., Cather, S.M., 1994. Tectonic setting of the axial basins of the northern and central Rio Grande rift. In: G.R. Keller, S.M. Cather (Editors), Basins of the Rio Grande rift—structure, stratigraphy, and tectonic setting. Geol. Soc. Am. Special Paper 291, pp. 5-21.

Chapin, C.E., McIntosh, W.C., Chamberlin, R.M., 2004. The late Eocene-Oligocene peak of Cenozoic volcanism in southwestern New Mexico. In: G.H. Mack, K.A. Giles (Editors), The Geology of New Mexico: A Geologic History. New Mexico Geological Society, Socorro, NM, pp. 271-293.

Chapin, C.E., Seager, W.R., 1975. Evolution of the Rio Grande Rift in the Socorro and Las Cruces areas. In: W.R. Seager, R.E. Clemons, J.F. Callender (Editors), New Mexico Geol. Soc. Guidebook 26: Las Cruces Country. New Mexico Geol. Soc., Socorro, NM, pp. 297-321.

Coltice, N., Simon, L., Lecuyer, C., 2004. Carbon isotope cycle and mantle structure. Geophys. Res. Lett. 31 (5): 1-5.

Davis, J.M., Hawkesworth, C.J., 1993. The petrogenesis of 30-20 ma basic and intermediate volcanics from the Mogollon-Datil volcanic field, New Mexico, USA. Contrib. Mineral. Petrol. 115 (2): 165-183.

Davis, J.M., Hawkesworth, C.J., 1995. Geochemical and tectonic transitions in the evolution of the Mogollon-Datil volcanic field, New Mexico, U.S.A. Chem. Geol. 119 (1-4): 31-53.

Deer, W.A., Howie, R.A., Zussman, J., 1992. An Introduction to the Rock-Forming Minerals, second ed. Pearson Education Ltd., England, pp. 696.

Dimeo, M.I., 2006. Petrography and geometry of Oligocene mafic dikes near Riley, New Mexico: indications of northward dike propagation into the southeastern margin of the Colorado Plateau. New Mexico Geology 28 (2): 59.

Dimeo, M.I., Chamberlin, R.M., 2006. Oligocene mafic dikes within the southeastern Colorado Plateau: evidence of northward propagation away from a coeval caldera cluster and implications to regional stress fields of the early Rio Grande Rift. Am. Geophys. Union 2006 Fall Meeting, 87, Abstract V23D-0665.

Deines, P., 2002. The carbon isotope geochemistry of mantle xenoliths. Earth-Sci. Rev. 58 (3-4): 247-278.

Ernst, R.E., Buchan, K.L., 2001. The use of mafic dike swarms in identifying and locating mantle plumes. In: R.E. Ernst, K.L. Buchan (Editors), Mantle Plumes: Their Identification Through Time. Geol. Soc. Am. Special Paper 352, pp. 247-265.

Farmer, G.L., Bailley, T., Elkins-Tanton, L.T., 2008. Mantle source volumes and the origin of the mid-Tertiary ignimbrite flare-up in the southern Rocky Mountains, western US. Lithos 102 (1-2): 279-294.

Fitton, J.G., James, D., Leeman, W.P., 1991. Basic magmatism associated with late Cenozoic extension in the Western United States: Compositional variations in space and time. J. Geophys. Res. 96: 13696-13711.

Grard, A., Francois, L.M., Dessert, C., Dupré, B., Goddéris, Y., 2005. Basaltic volcanism and mass extinction at the Permo-Triassic boundary: environmental impact and modeling of the global carbon cycle. Earth Planet. Sci. Lett. 234: 207-221.

Hansen, H.J., 2006. Stable isotopes of carbon from basaltic rocks and their possible relations to atmospheric isotope excursions. Lithos 92 (1-2): 105-116.

Huneke, J.C., Smith, S.P., 1976. The realities of recoil: ^{39}Ar recoil out of small grains and anomalous patterns in ^{39}Ar-^{40}Ar dating, Geochim. Chosmochim. Acta Suppl. 7 (Proceedings of the Seventh Lunar Science Conference): 2345-2362.

Johnson, C.M., 1993. Mesozoic and Cenozoic contributions to crustal growth in the Southwestern United States. Earth Planet. Sci. Lett. 118 (1-4): 75-89.

Kempton, P.D., Fitton, J.G., Hawkesworth, C.J., Ormerod, D.S., 1991. Isotopic and trace element constraints on the composition and evolution of the lithosphere beneath the wouthwestern United States. J. Geophys. Res. 96 (B8): 13713-13735.

Laughlin, A.W., Aldrich, M.J., Vaniman, D.T., 1983. Tectonic implications of mid-Tertiary dikes in west-central New Mexico. Geology 11: 45-48.

Le Maitre, R.W., 2002. Igneous rocks: a classification and glossary of terms: recommendations of the International Union of Geological Sciences, Subcomission on the Systematics of Igneous Rocks. Cambridge University Press, Cambridge, U.K., 236 pp.

Lipman, P.W., 1997. Subsidence of ash-flow calderas: relation to caldera size and magma-chamber geometry. Bull. Volcanol. 59: 198-218.

Luth, R.W., Bowerman, M., 2004. Microtextural and powder-diffraction study of the analcime phenocrysts in volcanic rocks of the Crowsnest Formation, southern Alberta, Canada. Can. Min. 42(3): 897-903.

Mahon, K.I., 1996. The new “York” regression: Application of an improved statistical method to geochemistry. Inter. Geol. Rev. 38: 293-303.

Massingill, G.L., 1979. Geology of Riley-Puertecito area, southeastern margin of Colorado Plateau, Socorro County, New Mexico. Ph.D. dissertation, University of Texas, El Paso.

McDonough, W.F., Sun, S.S., 1995. Chemical evolution of the mantle. Chem. Geol. 120 (3-4): 223-253.

McDougall, I., Harrison, T.M., 1999. Geochronology and Thermochronology by the $^{40}Ar/^{39}Ar$ Method, second ed. Oxford University Press, New York, 269 pp.

McIntosh, W.C., Chapin, C.E., Ratté, J.C., Sutter, J.F., 1992. Time-stratigraphic framework for the Eocene-Oligocene Mogollon-Datil volcanic field, southwest New Mexico. Geol. Soc. Am. Bull. 104: 851-871.

Morgan, W.J., 1971. Convection plumes in the lower mantle. Nature 230: 42-43.

Morimoto, M., 1988. Nomenclature of pyroxenes. Min. Mag. 52: 535-550.

Perry, F.V., DePaolo, D.J., Badlridge, W.S., 1993. Neodymium isotopic evidence for decreasing crustal contributions to Cenozoic ignimbrites of the Western United States: implications for the thermal evolution of the Cordilleran crust. Geol. Soc. Am. Bull. 105(7): 872-882.

Prelevic, D., Foley, S.F., Cvetkovic, V., Romer, R.L., 2004. The analcime problem and its impact on the geochemistry of ultrapotassic rocks from Serbia. Min. Mag. 68(4): 633-648.

Putnis, C.V., Geisler, T., Schmid-Beurmann, P., Stephan, T., Giampaolo, C., 2007. An experimental study of the replacement of leucite by analcime. Am. Min. 92: 19-26.

Rock, N.M.S., 1991. Lamprophyres. Blackie and Son Ltd, Glasgow, pp. 285.

Roddick, J.C., Cliff, R.A., Rex, D.C., 1980. The evolution of excess argon in alpine biotites—A ^{40}Ar-^{39}Ar analysis. Earth Planet. Sci. Lett. 48: 185-208.

Roux, J., Hamilton, D.L., 1976. Primary igneous analcite—an experimental study. J. Petrology 17(2): 244-257.

Sigurdsson, H., 1987. Dyke injection in Iceland: a review. In: H.C. Halls, W.F. Fahrig (Editors), Mafic Dyke Swarms. Geological Association of Canada Special Paper 34, Ontario, pp. 55-64.

Singer, B.S., Pringle, M.S., 1996. Age and duration of the Matuyama-Brunhes geomagnetic polarity reversal from $^{40}Ar/^{39}Ar$ incremental heating analyses of lavas. Earth Planet. Sci. Lett. 139: 47-61.

Snyder, D., 2000. Thermal effects of the intrusion of basaltic magma into a more silicic magma chamber and implications for eruption triggering. Earth Planet. Sci. Lett. 175: 257-273.

Steiger, R.H., Jäger, E., 1977. Subcommission on geochronology: Convention on the use of decay constants in geo- and cosmochronology. Earth Planet. Sci. Lett. 36: 359-362.

Taylor, S.R., 1982. Planetary science: A lunar perspective. Lunar and Planetary Institute, Houston, pp. 502.

Tonking, W.H., 1957. Geology of the Puertecito Quadrangle, Socorro County, New Mexico. New Mexico Bureau of Mines and Mineral Resources, Socorro, NM.

Turner, G., 1971. ^{40}Ar-^{39}Ar ages from the lunar maria. Earth Planet. Sci. Lett. 11: 169-191.

Wilson, D., Aster, R., West, M., Ni, J., Grand, S., Gao, W., Baldridge, W.S., Semken, S., 2005. Lithospheric structure of the Rio Grande Rift. Nature 433: 851-855.

Wilson, M., 1989. Igneous Petrogenesis: a global tectonic approach. Unwin Hyman, London, pp. 466.

Winchester, D.E., 1920. Geology of Alamosa Creek Valley, Socorro County, New Mexico, with special reference to the occurrence of oil and gas. U.S. Geol. Survey Bull. 716-A: 1-15.

Woodward, L.A., Callender, J.F., Gries, J., Seager, W.R., Chapin, C.E., Zilinski, R.E., Shaffer, W.L., 1975. Tectonic map of the Rio Grande region from New Mexico-Colorado border to Presidio, Texas. In: W.R. Seager, R.E. Clemons, J.F. Callender (Editors), New Mexico Geol. Soc. Guidebook 26: Las Cruces Country. New Mexico Geol. Soc., Socorro, NM, pp. 239.

APPENDIX A: SAMPLE LIST

Sample	UTM zone	easting	northing	± error (m)	Thin Section	Electron Microprobe	$^{40}Ar/^{39}Ar$ Geochronology	XRF and ICP-MS	C and O isotopes
Basaltic samples									
RDS-1	13S	0294694	3800467		x	x	x		x
RDS-4	13S	0292561	3799167		x	x	x		x
RDS-6	13S	0298967	3804145		x	x	x		
RDS-8	13S	0294808	3805983		x	x			
RDS-9	13S	0292125	3801064						
RDS-14	13S	0292493	3799156						
RDS-15A	13S	0295072	3800748		x	x			
RDS-15B	13S	0295072	3800748		x	x			x
RDS-15C	13S	0295072	3800748		x	x			
"Pyroxene porphyry dike"									
RDS-16A	13S	0295125	3800712		x	x			
RDS-16B	13S	0295125	3800712		x	x			
RDS-16C	13S	0295125	3800712		x	x			
RDS-191	13S	0295135	3800641	4	x			x	
RDS-199	13S	0295108	3800437	4	x				
RDS-202A	13S	0295122	3800530	4	x				
RDS-202B	13S	0295122	3800530	4	x				
02-77-11-1	13S	0295463	38029879				x	XRF	
RDS-18	13S	0292474	3799768		x				
RDS-005	13S	0292574	3799857	5	x				
RDS-011	13S	0292886	3800054	3					
RDS-013B	13S	0292857	3799934	4		x			
RDS-013C	13S	0292857	3799934	4					
RDS-027	13S	0292805	3799666	4	x	x			
RDS-031	13S	0293017	3800068	5	x				
RDS-031B	13S	0293017	3800068	5					
RDS-188	13S	0294827	3800561	4	x				
RDS-189A	13S	0294886	3800564	4					
RDS-189B	13S	0294886	3800564	4	x				
RDS-190	13S	0295022	3800625	4	x				
RDS-198	13S	0295212	3800489	4	x				
RDS-204	13S	0292757	3799652	5	x				
RDS-207	13S	0292898	3799794	4	x				
RDS-213	13S	0299224	3803964	5	x				
RDS-214	13S	0299203	3803932	4	x				
RDS-215	13S	0299083	3803898	4	x				
RDS-217	13S	0299050	3804167	5	x				
Feeder(?) dike									
RDS-11	13S	0292585	3800356		x	x			
RDS-12	13S	0292634	3800945		x				
RDS-17	13S	0292508	3800006		x	x			
RDS-17WR	13S	0292508	3800006						
RDS-130	13S	0292643	3801033	5	x	x		x	
MDS-14	13S	0295462	3803102				x	XRF	
MDS-15	13S	0294701	3800414				x	XRF	
MDS-16	13S	0294748	3800338				x	XRF	
Analcime-bearing samples									
RDS-5	13S	0296550	3803063		x	x	x	x	x
RDS-211	13S	0292751	3799304	8	x			x	

APPENDIX A: SAMPLE LIST

Sample	UTM zone	easting	northing	± error (m)	Thin Section	Electron Microprobe	$^{40}Ar/^{39}Ar$ Geochronology	XRF and ICP-MS	C and O isotopes
Spears Ranch Dike									
RDS-2	13S	0292421	3799256		x	x	x		
RDS-10	13S	0292200	3800200			x			
RDS-19	13S	0292392	3799646		x			x	
RDS-203A	13S	0292632	3799842	5	x				
RDS-203B	13S	0292632	3799842	5	x				
RDS-203C	13S	0292632	3799842	5	x				
RDS-203D	13S	0292632	3799842	5	x				
RDS-203E	13S	0292632	3799842	5					
MDS-11	13S	0292060	3801378				x	XRF	
MDS-31	13S	0292038	3801512				x	XRF	
MDS-32	13S	0291954	3802198				x	XRF	
Analcime-bearing, speckled texture									
RDS-013A	13S	0292857	3799934	4	x	x		x	x
MDS-12	13S	0292878	3801533					XRF	
Minette samples									
RDS-3	13S	0292503	3799167		x	x	x		x
RDS-098X	13S	0292631	3799295	6	x				
RDS-009	13S	0292767	3800053	5	x	x		x	x
RDS-102	13S	0292876	3799527	6		x			
RDS-106	13S	0292739	3799305	6		x	x		
Basaltic samples with significant biotite									
RDS-7	13S	0295229	3805175		x	x			
RDS-13	13S	0293361	3801395		x				
RDS-159	13S	0294137	3801551	4	x				
RDS-206	13S	0292950	3799846	5	x				
RDS-209	13S	0292889	3799594	5	x				
RDS-212	13S	0299512	3804155	7	x				
Other samples									
RDS-A-1	13S	0290260	3802217		x				
RDS-283	13S	0275856	3796976		x		x	x	
RDS-284	13S	0275759	3797921						
MDS-26	12S	0741572	3824661			x	x		

APPENDIX B: ANALYTICAL METHODS

A.B.1 Petrography

Thin section billets were cut using rock saws of the Earth and Environmental Science Department at New Mexico Institute of Technology. Billets were sent to Quality Thin Sections in Arizona where samples were mounted on glass slides and cover slips were applied. Petrographical analyses were conducted on a microscope at the New Mexico Bureau of Geology and Mineral Resources.

A.B.2 Electron microprobe analyses

Samples were crushed using a hammer or a jaw crusher to obtain grains up to several mm in size. Samples RDS-15A, RDS-15B, RDS-15C, RDS-16A, RDS-16B, and RDS-16C were placed in single-hole discs and all other sample grains were placed in 9-hole discs. Epoxy filled the holes and the discs were cured in an oven at 80° overnight. Cured discs were polished using 15, 6, and 1μm diamond powders and carbon-coated.

Samples were analyzed on the New Mexico Bureau of Geology and Mineral Resources CAMECA SX-100 electron microprobe with a 15 kV acceleration voltage and 20 nA beam current. Backscatter electron images were collected of textures and phases of interest and quantitative analyses were obtained for major phases. The beam sizes for quantitative points varied between 1-25 μm depending on material analyzed.

A.B.3 Carbon and oxygen isotopes

Several mg of each powdered dike sample and 0.2 mg of standards and sedimentary carbonate samples were weighed and placed in glass vials. Each sample was flushed with helium for 2.5 minutes, phosphoric acid for 16 hours at 45°C, and analyzed

on a Thermo-Finnigan Delta^{Plus} XP mass spectrometer at New Mexico Institute of Mining and Technology.

A.B.4 XRF and ICP-MS

Samples with the prefix "RDS" were crushed using a jaw crusher and powdered in a tungsten carbide TEMA mill. Powdered samples were placed in glass vials and analyses were conducted by staff at the Washington State University GeoAnalytical Lab.

A.B.5 $^{40}Ar/^{39}Ar$ geochronology

Samples were crushed in a jaw crusher and disc grinder and sieved to desired grain sizes for picking. Groundmass concentrate samples were hand picked to remove clay and phenocrysts. Biotite, sanidine, and hornblende crystals were separated using a Frantz magnetic separator and by hand picking techniques. Sanidine was also separated using heavy liquid, in which the crystals float near the surface of a liquid with a higher density than sanidine. Groundmass concentrate samples were then washed in 5% HCl in an ultrasonic bath for ~5 minutes and rinsed in deionized water. Mineral separates were washed in deionized water in an ultrasonic bath for ~5 minutes. Samples were dried in an oven for ~1 hour and placed in machined Al discs for irradiation.

Groundmass concentrate samples were step-heated in a Mo double-vacuum furnace. Biotite and hornblende were step-heated in a furnace and one biotite sample was also analyzed by the single-crystal method of fusion with a Synrad 50W CO_2 laser. Sanidine was analyzed by single crystal laser fusion and in bulk by laser step-heating. Extracted argon gas was analyzed on a MAP-215-50 mass spectrometer at the New Mexico Geochronology Research Laboratory. Technical notes including J-values and correction factors for each irradiation package are in Appendix H.

APPENDIX C: PETROGRAPHY

Basaltic dikes

RDS-	Notes	Phenocrysts	Groundmass	Alteration	Textures/xenoliths	Other
1		ol(?)	pl, mag, ol/cpx(?)	ol(?)-->carbonate+mag cpx(?)-->carbonate+chlorite		CO_2 autometasomatized
4		ol(?)	cpx, ol(?), pl, mag	ol(?)-->carbonate+mag+chlorite cpx-->carbonate		CO_2 autometasomatized
6	north of map area	ol(?)	cpx, pl, mag, bt	ol(?)-->chlorite+serpentine	trachytic (aligned microlites)	
8	north of map area	ol(?), cpx	pl, bt, mag, cpx	ol(?)-->carbonate+mag+chlorite		partially CO_2 autometasomatized
15A	dike core	ol(?) pl, cpx	pl, cpx, mag, bt, Kspar	ol(?)-->carbonate+mag+serpentine	fresh cpx	partially CO_2 autometasomatized plagioclase
15B	between core and margin		same as RDS-15A		quartz xenocryst	
15C	dike margin		same as RDS-15A	ol(?)--> carbonate+mag cpx-->carbonate	slightly altered cpx	
18		cpx, ol(?)	pl, ol(?), cpx, mag	ol(?)-->carbonate+serpentine+mag	amygdaloidal calcite	
005		ol(?(	pl, ol(?), cpx, mag	ol(?)--> serpentine+mag	quartz xenocrysts	
188		ol(?)	pl, cpx, ol(?), mag, bt	ol(?)--> carbonate+chlorite+quartz		CO_2 autometasomatized
189B		ol(?)	pl, cpx, ol(?), Kspar, bt	ol(?)-->serpentine+mag+chlorite cpx--> carbonate	carbonate+fluorite	CO_2 autometasomatized
190		ol(?), pl, cpx(?)	pl, cpx(?), ol(?), mag, bt	ol(?)-->carbonate+mag+chlorite cpx--> carbonate+chlorite	quartz xenocryst	CO_2 autometasomatized
198		cpx	pl, cpx(?), ol(?), mag, bt	cpx(?)-->carbonate+chlorite+mag ol(?)-->carbonate+serpentine		CO_2 autometasomatized
013B	different dike than 013A	cpx	pl, cpx(?), mag	cpx(?)-->carbonate+chlorite		CO_2 autometasomatized
013C	same dike as 013B	same as RDS-013B				
027		ol(?)	pl, cpx, ol(?), mag, bt	ol(?)--> serpentine+mag	quartz xenocrysts	CO_2 autometasomatized
031		ol(?), cpx	pl, cpx(?), ol(?), mag, bt	cpx--> carbonate+chlorite		partially CO_2 autometasomatized
031B		same as RDS-031B				
204		ol(?)	cpx, Kspar(?), mag, hb(?), bt	ol(?)--> chlorite+carbonate+mag+serpentine	quartz+pl+sanidine xenolith	
207		cpx(?)	pl, cpx(?), mag	cpx--> carbonate+chlorite	quartz xenocrysts	CO_2 autometasomatized

APPENDIX C: PETROGRAPHY

RDS-	Notes	Phenocrysts	Groundmass	Alteration	Textures/xenoliths	Other
Basaltic dikes (continued)						
213	north of map area	cpx(?)	pl, cpx(?), mag, bt		cpx(?)--> carbonate	CO_2 autometasomatized
214	north of map area	pl, cpx, ol(?)	pl, cpx(?), mag, Kspar(?), hb(?)	cpx--> carbonate+chlorite ol(?)--> serpentine+carboante		partially CO_2 autometasomatized
215	north of map area	cpx/ol (?)	pl, ol(?), cpx(?), mag, bt	cpx--> chlorite+carbonate		partially CO_2 autometasomatized
217	north of map area	cpx/ol (?)	pl, cpx, mag	ol(?)--> chlorite+serpentine pl--> sercite		
Feeder(?) dike						
11			pl, ol(?), cpx, mag	ol(?)-->serpentine+chlorite	subophitic	
12		ol	pl, cpx, mag		aligned microlites	
17			pl, ol(?), cpx, mag	ol(?)--> serpentine+carbonate+ chalcedony		
130		ol	pl, cpx, mag	ol--> serpentine+mag+chlorite		
"Pyroxene porphyry dike"						
16A	dike core	cpx, pl	pl, cpx, ol(?), mag, Kspar(?)	ol(?)--> carbonate+qtz+mag	porphyritic	pyroxene/ plagioclase porphyry
16B	between core and margin		same as RDS-16A		marble/sanidinite xenolith	
16C	dike margin		same as RDS-16A	ol(?)--> carbonate+qtz+mag cpx--->carbonate+chlorite+mag		autometasomatized pyroxene/ plagioclase porphyry
191		cpx, pl, ol(?)	pl, cpx, mag	ol(?)--> chlorite + mag		
199		cpx, pl	pl, mag, cpx	cpx--> chlorite+carbonate	gabbro xenolith	
202A		cpx, pl, ol(?)	pl, cpx, mag, ol(?)	ol(?)--> serpentine+carbonate	quartz/pl xenoliths	CO_2 autometasomatized
202B		cpx, pl	same as RDS-202A		quartz/feldspar xenolith	

APPENDIX C: PETROGRAPHY

RDS-	Notes	Phenocrysts	Groundmass	Alteration	Textures/xenoliths	Other
Analcime-bearing dikes						
5		cpx, ol	cpx, analcime, bt, mag, Kspar(?)	ol(?)--> serpentine		analcime after leucite (?)
211		cpx, ol(?)	analcime, Kspar(?), cpx, bt, mag	ol(?)--> serpentine+mag		analcime after leucite (?)
Spears Ranch Dike						
2		ol, cpx, leucite (4 xls)	cpx, Kspar, analcime, bt, mag	leucite--> analcime+Kspar+muscovite	quartz xenocrysts	
19		cpx, ol	cpx, analcime, mag, bt, pl, Kspar(?)			
203A	east margin	cpx, ol(?)	cpx, mag, Kspar(?), analcime(?)	ol(?)--> carbonate+quartz+mag cpx--> carbonate+chlorite		CO_2 autometasomatized
203B	between west margin and core	cpx, ol(?)	cpx, analcime, mag, bt, Kspar(?)	ol(?)-->serpentine		
203C	between west margin and core	same as RDS-203B				
203D	core	same as RDS-203B			cpx/pl gabbro xenolith	
Analcime-bearing, speckled-texture dike						
013A		cpx, ol(?), pl	pl, cpx, mag, bt, Kspar(?)	ol(?)--> serpentine	partially assimilated plag+anl/leucite xenoliths?	pyroxene/ plagioclase porphyry
Minette dikes						
3		mag, bt	mag, bt, Kspar, cpx/ol(?)	cpx/ol(?)--> carbonate+chlorite	quartz xenocrysts	CO_2 autometasomatized
098	same dike as RDS-3	cpx/ol (?)	Kspar, bt, cpx(?), mag	ol(?)--> hematite(?) cpx(?)--> carbonate+chlorite		CO_2 autometasomatized
098X	contains large xenolith	matrix same as RDS-098			coarse quartzite xenolith	

APPENDIX C: PETROGRAPHY

RDS-	Notes	Phenocrysts	Groundmass	Alteration	Textures/xenoliths	Other
Minette dikes (continued)						
102		ol(?)	Kspar, cpx(?), bt, mag, quartz(?)	ol(?)--> carbonate+chlorite+mag	quartzite xenolith	CO_2 autometasomatized
106		ol(?)	Kspar(?), cpx(?), mag, bt	ol(?)--> carbonate+serpentine groundmass cpx--> carbonate		CO_2 autometasomatized
009		cpx, ol(?)	Kspar, cpx, bt, glass?	ol(?)--> serpentine+mag		
Basaltic dikes with significant biotite						
7	north of map area	cpx, ol(?)	pl, bt, mag, cpx/ol(?)	ol(?)--> carbonate+serpentine		partially CO_2 autometasomatized
13		ol(?)	Kspar, bt, cpx(?), mag	ol(?)--> carbonate+mag+ quartz(?)	quartz xenocrysts	CO_2 autometasomatized
159		ol(?), cpx	pl, cpx(?), ol(?), mag, bt	carbonate+mag+serpentine cpx(?)--> chlorite+carbonate		CO_2 autometasomatized
206			bt, feldspar, cpx, mag	cpx(?)--> carbonate+mag		CO_2 autometasomatized
209	same dike as RDS-206?	cpx/ol (?)	bt, feldspar(?), cpx(?), ol(?), mag	cpx/ol(?)--> caronate+chlorite+mag		CO_2 autometasomatized
212	north of map area	cpx/ol (?)	cpx(?), ol(?), bt	cpx/ol(?)--> carbonate+serpentine		CO_2 autometasomatized
Other						
A1	Andesite at Fall Spring	pl, cpx, ol(?), hb(?)	pl, ol(?), cpx, hb(?)	ol(?)--> hematite(?)+serpentine		plagioclase/ pyroxene porphyry
A2	Andesite at Fall Spring	same as RDS-A1			patches of carbonate in groundmass	
283	Hornblende porphyry dike west of Riley	hb, cpx, bt, pl	pl, Kspar(?), hb, cpx, bt, mag		quartz xenocrysts	hornblende andesite porphyry

APPENDIX D.1: ELECTRON MICROPROBE ANALYSES OF FELDSPAR

	RDS-1-15 B	RDS-1-23 B	RDS-1-22 B	RDS-1-31 B	RDS-1-29 B	RDS-1-16 B	RDS-1-20 B	RDS-1-32 B
SiO_2	51.7	52.21	52.88	53.6	52.19	53.92	54.62	57.34
Al_2O_3	30.33	30.34	30.07	30.01	30.2	29.02	29.41	27.54
FeO	1.14	0.98	1	0.99	1.26	0.91	0.96	0.75
CaO	12.78	12.46	12.01	11.77	12.65	10.95	10.59	8.44
Na_2O	4.06	4.2	4.42	4.55	4.14	5.03	5.09	6.54
K_2O	0.26	0.3	0.3	0.31	0.32	0.39	0.42	0.66
BaO	0.02	0.08	0.04	0.06	0.01	0.12	0.2	0.2
SrO	0.22	0.24	0.28	0.29	0.26	0.31	0.28	0.26
Total	100.51	100.78	101.01	101.58	101.03	100.64	101.56	101.73
Numbers of ions on the basis of 32O								
Si	9.405	9.458	9.546	9.610	9.449	9.749	9.774	10.192
Al	6.503	6.477	6.397	6.341	6.444	6.184	6.202	5.769
Fe^{2+}	0.173	0.148	0.151	0.148	0.191	0.138	0.144	0.111
Ba	0.001	0.006	0.003	0.004	0.001	0.009	0.014	0.014
Ca	2.491	2.418	2.323	2.261	2.454	2.121	2.030	1.607
Na	1.432	1.475	1.547	1.581	1.453	1.763	1.766	2.254
K	0.060	0.069	0.069	0.071	0.074	0.090	0.096	0.150
Sr	0.023	0.025	0.029	0.030	0.027	0.032	0.029	0.027
Total	20.089	20.076	20.064	20.046	20.092	20.086	20.055	20.125
Or	1.5	1.7	1.8	1.8	1.9	2.3	2.5	3.7
Ab	36.0	37.2	39.3	40.4	36.5	44.4	45.4	56.2
An	62.5	61.0	59.0	57.8	61.6	53.4	52.2	40.1

	RDS-1-33 B	RDS-2-01b A-SRD	RDS-2-22 A-SRD	RDS-2-27 A-SRD	RDS-2-19 A-SRD	RDS-2-25 A-SRD	RDS-2-20 A-SRD	RDS-3-09 M
SiO_2	57.67	65.47	65.4	65.2	63.93	64.77	63.96	64.03
Al_2O_3	26.92	20.33	19.01	18.81	19.36	19.16	19.2	21.24
FeO	0.71	0.24	0.41	0.31	0.28	0.36	0.52	1.1
CaO	7.98	0.65	0.07	0.04	0.31	0.1	0.08	1.96
Na_2O	6.51	4.92	1.82	1.42	0.86	0.92	0.36	5.47
K_2O	0.7	9.79	14.4	15.01	15.56	15.59	16.4	7.44
BaO	0.23	0	0	0.02	0	0.02	0	0.25
SrO	0.28	0.09	0.03	0.03	0.05	0.04	0.01	0.34
Total	101.01	101.49	101.14	100.86	100.36	100.97	100.51	101.82
Numbers of ions on the basis of 32O								
Si	10.305	11.715	11.905	11.927	11.795	11.865	11.817	11.449
Al	5.669	4.287	4.078	4.055	4.210	4.136	4.181	4.476
Fe^{2+}	0.106	0.036	0.062	0.047	0.043	0.055	0.080	0.164
Ba	0.016	0.000	0.000	0.001	0.000	0.001	0.000	0.018
Ca	1.528	0.125	0.014	0.008	0.061	0.020	0.016	0.375
Na	2.255	1.707	0.642	0.504	0.308	0.327	0.129	1.896
K	0.160	2.234	3.344	3.503	3.662	3.643	3.865	1.697
Sr	0.029	0.009	0.003	0.003	0.005	0.004	0.001	0.035
Total	20.068	20.113	20.049	20.048	20.085	20.052	20.089	20.110
Or	4.0	55.0	83.6	87.3	90.8	91.3	96.4	42.8
Ab	57.2	42.0	16.1	12.5	7.6	8.2	3.2	47.8
An	38.7	3.1	0.3	0.2	1.5	0.5	0.4	9.5

A: analcime-bearing
A-SRD: analcime-bearing, Spears Ranch Dike
AS: analcime-bearing, speckled texture
B: basaltic
B-bt: basaltic with significant biotite
BPP: basaltic, pyroxene porphyry dike
BF: basaltic, feeder(?) dike
M: minette

APPENDIX D.1: ELECTRON MICROPROBE ANALYSES OF FELDSPAR

	RDS-3-12 M	RDS-3-08 M	RDS-3-20b M	RDS-3-11 M	RDS-3-24b M	RDS-3-20 M	RDS-3-19 M	RDS-3-18 M
SiO_2	63.37	63.55	63.48	63.18	62.73	63.44	62.83	64.07
Al_2O_3	21	21.27	21.09	20.88	21.01	21.45	21.35	20.87
FeO	1.14	1.11	0.83	1.34	0.77	0.76	1	0.91
CaO	1.99	2.03	1.84	2.11	1.79	1.9	1.71	1.68
Na_2O	5.28	5.21	5.11	5.01	4.59	4.38	4.09	4.1
K_2O	7.84	7.91	7.93	8.16	8.67	8.82	9.15	9.59
BaO	0.18	0.23	0.14	0.14	0.23	0.35	0.51	0.25
SrO	0.32	0.38	0.24	0.32	0.42	0.46	0.6	0.32
Total	101.12	101.69	100.67	101.14	100.21	101.58	101.25	101.79
Numbers of ions on the basis of 32O								
Si	11.436	11.411	11.469	11.425	11.440	11.421	11.397	11.520
Al	4.466	4.501	4.491	4.450	4.515	4.551	4.564	4.422
Fe^{2+}	0.172	0.167	0.125	0.203	0.117	0.114	0.152	0.137
Ba	0.013	0.016	0.010	0.010	0.016	0.025	0.036	0.018
Ca	0.385	0.391	0.356	0.409	0.350	0.366	0.332	0.324
Na	1.847	1.814	1.790	1.756	1.623	1.529	1.438	1.429
K	1.805	1.812	1.828	1.882	2.017	2.025	2.117	2.200
Sr	0.033	0.040	0.025	0.034	0.044	0.048	0.063	0.033
Total	20.157	20.151	20.094	20.169	20.123	20.080	20.099	20.083
Or	44.7	45.1	46.0	46.5	50.6	51.7	54.5	55.7
Ab	45.8	45.2	45.0	43.4	40.7	39.0	37.0	36.2
An	9.5	9.7	9.0	10.1	8.8	9.3	8.5	8.2

	RDS-4-11 B	RDS-5-40 A-SRD	RDS-5-28 A-SRD	RDS-5-41 A-SRD	RDS-5-30 A-SRD	RDS-5-33b A-SRD	RDS-5-32b A-SRD	RDS-5-42 A-SRD
SiO_2	69.24	59.76	62.57	61.33	64.17	62.05	63.7	65.13
Al_2O_3	20.49	21.34	19.96	20.84	19.83	20.65	19.62	19.13
FeO	0.25	0.77	0.48	0.44	0.52	0.34	0.25	0.36
CaO	0.13	0.32	0.16	0.29	0.35	0.48	0.14	0.11
Na_2O	11.37	3.63	3.63	2.79	2.6	2.47	1.58	1.36
K_2O	0.06	8.88	10.28	10.9	12.55	12.27	14.39	15.07
BaO	0	0.86	0.5	0.56	0.13	0.61	0.45	0.02
SrO	0.05	4.05	2.13	2.82	0.67	1.44	0.61	0.02
Total	101.59	99.61	99.71	99.96	100.81	100.3	100.75	101.2
Numbers of ions on the basis of 32O								
Si	11.903	11.242	11.607	11.431	11.723	11.498	11.736	11.879
Al	4.151	4.731	4.364	4.578	4.269	4.509	4.260	4.112
Fe^{2+}	0.036	0.121	0.074	0.069	0.079	0.053	0.039	0.055
Ba	0.000	0.063	0.036	0.041	0.009	0.044	0.032	0.001
Ca	0.024	0.064	0.032	0.058	0.068	0.095	0.028	0.021
Na	3.790	1.324	1.305	1.008	0.921	0.887	0.564	0.481
K	0.013	2.131	2.433	2.591	2.924	2.900	3.382	3.506
Sr	0.005	0.442	0.229	0.305	0.071	0.155	0.065	0.002
Total	19.922	20.119	20.080	20.080	20.065	20.141	20.107	20.058
Or	0.3	60.5	64.5	70.9	74.7	74.7	85.1	87.5
Ab	99.0	37.6	34.6	27.6	23.5	22.9	14.2	12.0
An	0.6	1.8	0.8	1.6	1.8	2.5	0.7	0.5

A: analcime-bearing
A-SRD: analcime-bearing, Spears Ranch Dike
AS: analcime-bearing, speckled texture
B: basaltic
B-bt: basaltic with significant biotite
BPP: basaltic, pyroxene porphyry dike
BF: basaltic, feeder(?) dike
M: minette

APPENDIX D.1: ELECTRON MICROPROBE ANALYSES OF FELDSPAR

	RDS-5-39 A-SRD	RDS-6-14 B	RDS-6-02 B	RDS-6-12 B	RDS-6-15 B	RDS-6-05 B	RDS-6-03 B	RDS-7-42 B-bt
SiO_2	60.86	68.57	68.23	68.45	68.25	67.77	67.85	49.64
Al_2O_3	21.04	20.9	20.82	20.65	20.62	20.81	20.86	32.23
FeO	0.87	0.32	0.16	0.14	0.14	0.14	0.23	0.93
CaO	0.04	0.44	0.51	0.35	0.47	0.46	0.47	14.16
Na_2O	0.72	11.71	11.55	11.67	11.49	11.47	11.48	2.94
K_2O	14.42	0.03	0.05	0.06	0.05	0.11	0.2	0.4
BaO	0.03	0	0.03	0.04	0.03	0.03	0.03	0.05
SrO	0.02	0.26	0.26	0.22	0.29	0.23	0.28	0.3
Total	98	102.24	101.61	101.58	101.33	101.02	101.4	100.65
Numbers of ions on the basis of 32O								
Si	11.483	11.775	11.781	11.815	11.810	11.769	11.755	9.051
Al	4.678	4.230	4.236	4.201	4.205	4.259	4.259	6.926
Fe^{2+}	0.137	0.046	0.023	0.020	0.020	0.020	0.033	0.142
Ba	0.002	0.000	0.002	0.003	0.002	0.002	0.002	0.004
Ca	0.008	0.081	0.094	0.065	0.087	0.086	0.087	2.766
Na	0.263	3.898	3.866	3.905	3.855	3.862	3.856	1.039
K	3.471	0.007	0.011	0.013	0.011	0.024	0.044	0.093
Sr	0.002	0.026	0.026	0.022	0.029	0.023	0.028	0.032
Total	20.045	20.063	20.040	20.044	20.020	20.045	20.065	20.052
Or	92.7	0.2	0.3	0.3	0.3	0.6	1.1	2.4
Ab	7.0	97.8	97.3	98.0	97.5	97.2	96.7	26.7
An	0.2	2.0	2.4	1.6	2.2	2.2	2.2	71.0

	RDS-7-17 B-bt	RDS-7-24 B-bt	RDS-7-28 B-bt	RDS-7-35 B-bt	RDS-7-39 B-bt	RDS-7-41 B-bt	RDS-7-31 B-bt	RDS-7-22 B-bt
SiO_2	50.93	51.07	51.26	51.37	50.78	51.89	52.98	53.61
Al_2O_3	31.34	31.41	31.07	31.32	31.38	30.68	30.09	29.63
FeO	0.83	0.78	0.79	0.94	0.86	0.78	0.8	0.6
CaO	13.21	13.28	12.85	13.07	13.21	12.6	11.63	11.12
Na_2O	3.55	3.5	3.76	3.67	3.51	3.93	4.38	4.7
K_2O	0.46	0.46	0.5	0.5	0.51	0.59	0.65	0.76
BaO	0.04	0.09	0.01	0.15	0.1	0.15	0.12	0.2
SrO	0.35	0.39	0.43	0.41	0.41	0.42	0.4	0.43
Total	100.73	100.97	100.67	101.42	100.76	101.04	101.04	101.04
Numbers of ions on the basis of 32O								
Si	9.257	9.260	9.315	9.284	9.238	9.400	9.566	9.671
Al	6.713	6.712	6.654	6.671	6.727	6.550	6.403	6.299
Fe^{2+}	0.126	0.118	0.120	0.142	0.131	0.118	0.121	0.091
Ba	0.003	0.006	0.001	0.011	0.007	0.011	0.008	0.014
Ca	2.572	2.580	2.502	2.531	2.574	2.445	2.250	2.149
Na	1.251	1.230	1.325	1.286	1.238	1.380	1.533	1.644
K	0.107	0.106	0.116	0.115	0.118	0.136	0.150	0.175
Sr	0.037	0.041	0.045	0.043	0.043	0.044	0.042	0.045
Total	20.065	20.053	20.078	20.082	20.077	20.084	20.073	20.088
Or	2.7	2.7	2.9	2.9	3.0	3.4	3.8	4.4
Ab	31.8	31.4	33.6	32.7	31.5	34.8	39.0	41.4
An	65.5	65.9	63.5	64.4	65.5	61.7	57.2	54.2

A: analcime-bearing
A-SRD: analcime-bearing, Spears Ranch Dike
AS: analcime-bearing, speckled texture
B: basaltic
B-bt: basaltic with significant biotite
BPP: basaltic, pyroxene porphyry dike
BF: basaltic, feeder(?) dike
M: minette

APPENDIX D.1: ELECTRON MICROPROBE ANALYSES OF FELDSPAR

	RDS-7-26 B-bt	RDS-7-37b B-bt	RDS-7-38 B-bt	RDS-7-21 B-bt	RDS-7-32b B-bt	RDS-7-37 B-bt	RDS-7-33b B-bt	RDS-7-23 B-bt
SiO_2	65.31	65.5	63.89	65.02	63.94	64.45	64.52	64.22
Al_2O_3	20.18	19.8	21.07	19.95	20.75	20.07	20.14	20.47
FeO	0.5	0.46	0.41	0.51	0.49	0.41	0.53	0.42
CaO	0.81	0.44	1.63	0.69	1.09	0.81	0.74	0.85
Na_2O	5.42	4.75	3.95	4.25	3.59	3.7	3.74	3.47
K_2O	8.7	10.11	10.07	10.58	10.91	11.05	11.12	11.07
BaO	0	0.02	0.18	0.1	0.58	0.44	0.39	0.96
SrO	0.01	0.03	0.08	0.03	0.18	0.08	0.08	0.19
Total	100.93	101.11	101.28	101.12	101.52	101.01	101.25	101.65
Numbers of ions on the basis of 32O								
Si	11.716	11.780	11.519	11.729	11.566	11.689	11.678	11.624
Al	4.266	4.196	4.477	4.241	4.423	4.290	4.296	4.366
Fe^{2+}	0.075	0.069	0.062	0.077	0.074	0.062	0.080	0.064
Ba	0.000	0.001	0.013	0.007	0.041	0.031	0.028	0.068
Ca	0.156	0.085	0.315	0.133	0.211	0.157	0.143	0.165
Na	1.885	1.656	1.381	1.486	1.259	1.301	1.312	1.218
K	1.991	2.319	2.316	2.434	2.517	2.556	2.567	2.556
Sr	0.001	0.003	0.008	0.003	0.019	0.008	0.008	0.020
Total	20.089	20.110	20.091	20.111	20.111	20.095	20.114	20.080
Or	49.4	57.1	57.7	60.0	63.1	63.7	63.8	64.9
Ab	46.8	40.8	34.4	36.7	31.6	32.4	32.6	30.9
An	3.9	2.1	7.8	3.3	5.3	3.9	3.6	4.2

	RDS-7-25b B-bt	RDS-7-24b B-bt	RDS-8-12 B	RDS-8-36 B	RDS-8-20b B	RDS-8-23b B	RDS-8-18 B	RDS-8-20 B
SiO_2	64.67	62.97	51.22	51.6	53.67	52.2	52.94	52
Al_2O_3	19.81	20.29	31.18	30.79	30	30.73	30.42	30.45
FeO	0.5	0.41	1.26	0.89	0.95	0.93	1.22	0.85
CaO	0.48	0.72	13.01	12.44	11.04	12.18	11.76	11.96
Na_2O	3.73	3.32	3.6	3.94	4.7	4.16	4.58	4.15
K_2O	11.41	10.94	0.28	0.3	0.34	0.33	0.36	0.36
BaO	0.01	1.87	0.16	0.15	0.24	0.08	0.14	0.13
SrO	0.04	0.24	0.42	0.49	0.44	0.51	0.44	0.43
Total	100.64	100.77	101.12	100.59	101.39	101.1	101.85	100.33
Numbers of ions on the basis of 32O								
Si	11.744	11.581	9.285	9.379	9.642	9.431	9.504	9.460
Al	4.240	4.398	6.661	6.595	6.352	6.543	6.436	6.528
Fe^{2+}	0.076	0.063	0.191	0.135	0.143	0.140	0.183	0.129
Ba	0.001	0.135	0.011	0.011	0.017	0.006	0.010	0.009
Ca	0.093	0.142	2.527	2.422	2.125	2.358	2.262	2.331
Na	1.313	1.184	1.265	1.388	1.637	1.457	1.594	1.464
K	2.643	2.567	0.065	0.070	0.078	0.076	0.082	0.084
Sr	0.004	0.026	0.044	0.052	0.046	0.053	0.046	0.045
Total	20.114	20.095	20.049	20.052	20.039	20.064	20.117	20.050
Or	65.3	65.9	1.7	1.8	2.0	2.0	2.1	2.2
Ab	32.4	30.4	32.8	35.8	42.6	37.5	40.5	37.7
An	2.3	3.6	65.5	62.4	55.3	60.6	57.4	60.1

A: analcime-bearing
A-SRD: analcime-bearing, Spears Ranch Dike
AS: analcime-bearing, speckled texture
B: basaltic
B-bt: basaltic with significant biotite
BPP: basaltic, pyroxene porphyry dike
BF: basaltic, feeder(?) dike
M: minette

APPENDIX D.1: ELECTRON MICROPROBE ANALYSES OF FELDSPAR

	RDS-8-34 B	RDS-8-22b B	RDS-8-22 B	RDS-8-11 B	RDS-8-17 B	RDS-8-33 B	RDS-8-27b B	RDS-8-26 B
SiO_2	52.88	54.03	53.9	53.43	54.53	55.68	52.94	56.42
Al_2O_3	30.2	29.73	29.85	29.87	29.2	28.32	27.1	27.94
FeO	0.94	0.75	0.69	0.73	0.74	0.73	0.95	0.68
CaO	11.63	10.92	10.7	11.03	10.29	9.27	8.5	8.68
Na_2O	4.53	4.93	5.09	4.83	5.32	5.57	5.11	5.99
K_2O	0.37	0.38	0.43	0.45	0.46	0.57	0.52	0.63
BaO	0.2	0.14	0.12	0.22	0.2	0	0.27	0.29
SrO	0.54	0.44	0.53	0.51	0.52	0.42	0.42	0.54
Total	101.31	101.33	101.31	101.08	101.27	100.9	95.82	101.18
Numbers of ions on the basis of 32O								
Si	9.538	9.698	9.681	9.636	9.795	10.012	10.005	10.101
Al	6.420	6.289	6.318	6.348	6.181	6.001	6.036	5.895
Fe^{2+}	0.142	0.113	0.104	0.110	0.111	0.110	0.150	0.102
Ba	0.014	0.010	0.008	0.016	0.014	0.000	0.020	0.020
Ca	2.247	2.100	2.059	2.131	1.980	1.786	1.721	1.665
Na	1.584	1.716	1.772	1.689	1.853	1.942	1.872	2.079
K	0.085	0.087	0.099	0.104	0.105	0.131	0.125	0.144
Sr	0.056	0.046	0.055	0.053	0.054	0.044	0.046	0.056
Total	20.087	20.058	20.096	20.086	20.094	20.024	19.976	20.063
Or	2.2	2.2	2.5	2.6	2.7	3.4	3.4	3.7
Ab	40.4	44.0	45.1	43.0	47.0	50.3	50.3	53.5
An	57.4	53.8	52.4	54.3	50.3	46.3	46.3	42.8

	RDS-8-28 B	RDS-8-23 B	RDS-8-25b B	RDS-10-31 A-SRD	RDS-10-28 A-SRD	RDS-10-19 A-SRD	RDS-10-27 A-SRD	RDS-10-30 A-SRD
SiO_2	60.48	61.06	65.09	50.85	51.61	51.16	50.65	52.08
Al_2O_3	25.43	24.66	21.37	31.47	30.73	30.88	31.29	30.3
FeO	0.61	0.66	0.74	0.83	0.93	0.64	0.71	0.75
CaO	5.82	5.09	2.05	13.22	12.51	12.48	13	11.83
Na_2O	7.56	7.74	8.38	3.62	4.03	3.93	3.44	4.19
K_2O	1.17	1.56	3.05	0.28	0.35	0.4	0.43	0.46
BaO	0.42	0.75	0.07	0.05	0.09	0.07	0.1	0.1
SrO	0.36	0.29	0.03	0.35	0.41	0.46	0.41	0.37
Total	101.85	101.81	100.78	100.68	100.65	100.02	100.03	100.08
Numbers of ions on the basis of 32O								
Si	10.686	10.814	11.515	9.240	9.377	9.346	9.261	9.489
Al	5.295	5.147	4.455	6.739	6.580	6.648	6.742	6.506
Fe^{2+}	0.090	0.098	0.109	0.126	0.141	0.098	0.109	0.114
Ba	0.029	0.052	0.005	0.004	0.006	0.005	0.007	0.007
Ca	1.102	0.966	0.389	2.574	2.435	2.442	2.546	2.309
Na	2.590	2.658	2.874	1.275	1.420	1.392	1.219	1.480
K	0.264	0.352	0.688	0.065	0.081	0.093	0.100	0.107
Sr	0.037	0.030	0.003	0.037	0.043	0.049	0.043	0.039
Total	20.093	20.117	20.039	20.060	20.083	20.073	20.028	20.052
Or	6.7	8.9	17.4	1.7	2.1	2.4	2.6	2.7
Ab	65.5	66.8	72.7	32.6	36.1	35.4	31.5	38.0
An	27.9	24.3	9.8	65.8	61.9	62.2	65.9	59.3

A: analcime-bearing
A-SRD: analcime-bearing, Spears Ranch Dike
AS: analcime-bearing, speckled texture
B: basaltic
B-bt: basaltic with significant biotite
BPP: basaltic, pyroxene porphyry dike
BF: basaltic, feeder(?) dike
M: minette

APPENDIX D.1: ELECTRON MICROPROBE ANALYSES OF FELDSPAR

	RDS-10-20 A-SRD	RDS-10-22 A-SRD	RDS-10-21 A-SRD	RDS-10-23 A-SRD	RDS-10-29 A-SRD	RDS-11-27 BF	RDS-11-20 BF	RDS-11-22 BF
SiO_2	53.15	64.67	62.39	65.87	65.14	68.55	68.54	68.71
Al_2O_3	29.75	20.71	20.67	19.8	20.01	20.84	20.85	20.84
FeO	0.9	0.34	0.35	0.32	0.33	0.97	0.14	0.31
CaO	11.27	1.28	1	0.52	0.75	0.53	0.45	0.36
Na_2O	4.45	5.44	4.8	5.48	5.08	11.65	11.76	11.86
K_2O	0.6	8.18	8.16	9.01	9.27	0.02	0.04	0.04
BaO	0.11	0.21	1.7	0	0.11	0.04	0	0.03
SrO	0.32	0.09	0.29	0.04	0.11	0.19	0.16	0.21
Total	100.55	100.92	99.37	101.06	100.79	102.79	101.94	102.37
Numbers of ions on the basis of 32O								
Si	9.629	11.611	11.515	11.799	11.732	11.746	11.788	11.786
Al	6.351	4.382	4.496	4.180	4.247	4.208	4.226	4.213
Fe^{2+}	0.136	0.051	0.054	0.048	0.050	0.139	0.020	0.044
Ba	0.008	0.015	0.123	0.000	0.008	0.003	0.000	0.002
Ca	2.187	0.246	0.198	0.100	0.145	0.097	0.083	0.066
Na	1.563	1.894	1.718	1.903	1.774	3.870	3.921	3.944
K	0.139	1.873	1.921	2.059	2.130	0.004	0.009	0.009
Sr	0.034	0.009	0.031	0.004	0.011	0.019	0.016	0.021
Total	20.047	20.081	20.056	20.092	20.096	20.087	20.064	20.084
Or	3.6	46.7	50.1	50.7	52.6	0.1	0.2	0.2
Ab	40.2	47.2	44.8	46.9	43.8	97.4	97.7	98.1
An	56.2	6.1	5.2	2.5	3.6	2.4	2.1	1.6

	RDS-11-21 BF	RDS-11-23 BF	RDS-11-24 BF	RDS-11-25 BF	RDS-11-26 BF	RDS-13-17 B-bt	RDS-13-23 B-bt	RDS-13-19 B-bt
SiO_2	68.19	69.2	68.52	68.87	68.82	62.46	63.6	62.51
Al_2O_3	21	20.68	20.99	20.9	20.62	20.33	19.99	20.92
FeO	0.13	0.42	0.1	0.14	0.95	1.02	1.21	1
CaO	0.7	0.31	0.5	0.47	0.19	1.94	1.32	1.94
Na_2O	11.43	11.72	11.67	11.62	11.88	4.62	4.88	4.25
K_2O	0.05	0.05	0.06	0.06	0.06	8.29	8.6	8.59
BaO	0.02	0.04	0.01	0.05	0	0.08	0.04	0.19
SrO	0.22	0.17	0.13	0.2	0.13	0.23	0.06	0.44
Total	101.73	102.59	102	102.29	102.65	98.97	99.69	99.83
Numbers of ions on the basis of 32O								
Si	11.756	11.832	11.776	11.801	11.794	11.505	11.615	11.441
Al	4.267	4.167	4.251	4.221	4.165	4.413	4.302	4.512
Fe^{2+}	0.019	0.060	0.014	0.020	0.136	0.157	0.185	0.153
Ba	0.001	0.003	0.001	0.003	0.000	0.006	0.003	0.014
Ca	0.129	0.057	0.092	0.086	0.035	0.383	0.258	0.380
Na	3.820	3.885	3.888	3.860	3.947	1.650	1.728	1.508
K	0.011	0.011	0.013	0.013	0.013	1.948	2.003	2.005
Sr	0.022	0.017	0.013	0.020	0.013	0.025	0.006	0.047
Total	20.026	20.032	20.049	20.025	20.103	20.087	20.100	20.060
Or	0.3	0.3	0.3	0.3	0.3	48.9	50.2	51.5
Ab	96.5	98.3	97.4	97.5	98.8	41.4	43.3	38.7
An	3.3	1.4	2.3	2.2	0.9	9.6	6.5	9.8

A: analcime-bearing
A-SRD: analcime-bearing, Spears Ranch Dike
AS: analcime-bearing, speckled texture
B: basaltic
B-bt: basaltic with significant biotite
BPP: basaltic, pyroxene porphyry dike
BF: basaltic, feeder(?) dike
M: minette

APPENDIX D.1: ELECTRON MICROPROBE ANALYSES OF FELDSPAR

	RDS-15A-10 B	RDS-15A-20 B	RDS-15A-17 B	RDS-15A-07 B	RDS-15A-09 B	RDS-15A-12 B	RDS-15A-26 B	RDS-15A-15 B
SiO_2	50.87	50.56	51.22	51.89	51.89	52.08	52.72	53.61
Al_2O_3	30.38	30.53	30.34	29.93	29.76	29.16	29.05	28.34
FeO	0.78	0.95	0.9	0.92	0.9	1	1	0.92
CaO	13.37	13.49	13.07	12.6	12.55	12.32	11.73	11.06
Na_2O	3.67	3.68	3.72	4.12	4.12	4.26	4.53	5.03
K_2O	0.14	0.14	0.19	0.21	0.21	0.22	0.28	0.32
BaO	0.01	0.03	0.02	0.06	0.05	0.03	0.04	0.13
SrO	0.41	0.49	0.48	0.44	0.52	0.51	0.43	0.46
Total	99.63	99.87	99.95	100.16	100.01	99.59	99.79	99.87
Numbers of ions on the basis of 32O								
Si	9.339	9.283	9.374	9.469	9.487	9.560	9.639	9.784
Al	6.573	6.606	6.544	6.436	6.412	6.308	6.259	6.096
Fe^{2+}	0.120	0.146	0.138	0.140	0.138	0.153	0.153	0.140
Ba	0.001	0.002	0.001	0.004	0.004	0.002	0.003	0.009
Ca	2.630	2.653	2.563	2.463	2.458	2.423	2.298	2.163
Na	1.306	1.310	1.320	1.458	1.460	1.516	1.606	1.780
K	0.033	0.033	0.044	0.049	0.049	0.052	0.065	0.074
Sr	0.044	0.052	0.051	0.047	0.055	0.054	0.046	0.049
Total	20.044	20.085	20.036	20.066	20.062	20.069	20.067	20.095
Or	0.8	0.8	1.1	1.2	1.2	1.3	1.6	1.9
Ab	32.9	32.8	33.6	36.7	36.8	38.0	40.5	44.3
An	66.3	66.4	65.3	62.1	62.0	60.7	57.9	53.8

	RDS-15A-56 B	RDS-15A-50 B	RDS-15A-51 B	RDS-15A-58 B	RDS-15A-11 B	RDS-15A-14 B	RDS-15A-08 B	RDS-15A-13 B
SiO_2	51.24	51.29	51.08	52	59.92	63.9	66.69	66.59
Al_2O_3	30.01	30.01	30.26	29.65	24.5	21.06	19.3	19.38
FeO	0.88	0.8	0.82	0.8	0.82	0.72	0.81	0.65
CaO	13.14	13.31	13.5	12.7	5.99	2.51	0.65	0.69
Na_2O	3.65	3.67	3.57	4.01	7.49	7.72	7.78	7.32
K_2O	0.37	0.4	0.4	0.51	1	4.1	5.97	6.34
BaO	0.05	0.06	0.12	0.04	0.45	0.33	0.08	0.11
SrO	0.27	0.26	0.33	0.34	0.39	0.12	0.02	0
Total	99.61	99.79	100.08	100.04	100.56	100.47	101.29	101.07
Numbers of ions on the basis of 32O								
Si	9.408	9.403	9.353	9.502	10.739	11.448	11.839	11.845
Al	6.493	6.484	6.530	6.385	5.175	4.446	4.038	4.062
Fe^{2+}	0.135	0.123	0.126	0.122	0.123	0.108	0.120	0.097
Ba	0.004	0.004	0.009	0.003	0.032	0.023	0.006	0.008
Ca	2.585	2.614	2.648	2.486	1.150	0.482	0.124	0.131
Na	1.299	1.304	1.267	1.421	2.602	2.681	2.678	2.524
K	0.087	0.094	0.093	0.119	0.229	0.937	1.352	1.438
Sr	0.029	0.028	0.035	0.036	0.041	0.012	0.002	0.000
Total	20.039	20.054	20.062	20.075	20.089	20.138	20.157	20.106
Or	2.2	2.3	2.3	3.0	5.7	22.9	32.6	35.1
Ab	32.7	32.5	31.6	35.3	65.4	65.4	64.5	61.7
An	65.1	65.2	66.1	61.8	28.9	11.7	3.0	3.2

A: analcime-bearing
A-SRD: analcime-bearing, Spears Ranch Dike
AS: analcime-bearing, speckled texture
B: basaltic
B-bt: basaltic with significant biotite
BPP: basaltic, pyroxene porphyry dike
BF: basaltic, feeder(?) dike
M: minette

APPENDIX D.1: ELECTRON MICROPROBE ANALYSES OF FELDSPAR

	RDS-15A-27 B	RDS-15A-59 B	RDS-15B-14 B	RDS-15B-19 B	RDS-15B-12 B	RDS-15B-16 B	RDS-15B-18 B	RDS-15B-21 B
SiO_2	66.55	66.2	51.17	52.24	52.34	52.86	53.24	54.79
Al_2O_3	19.28	18.84	30.47	29.55	29.25	28.71	28.83	28.05
FeO	0.8	0.35	0.81	0.97	1.06	0.95	1.08	0.85
CaO	0.62	0.41	13.54	12.47	12.34	11.61	11.77	10.88
Na_2O	7.3	4.18	3.71	4.26	4.37	4.64	4.35	4.81
K_2O	6.47	10.62	0.17	0.25	0.27	0.29	0.29	0.3
BaO	0.07	0	0.01	0.07	0.05	0.08	0.09	0.04
SrO	0	0.03	0.41	0.49	0.44	0.42	0.48	0.47
Total	101.1	100.63	100.29	100.29	100.12	99.55	100.12	100.19
Numbers of ions on the basis of 32O								
Si	11.848	11.950	9.339	9.526	9.561	9.685	9.698	9.924
Al	4.045	4.008	6.554	6.350	6.297	6.199	6.189	5.987
Fe^{2+}	0.119	0.053	0.124	0.148	0.162	0.146	0.165	0.129
Ba	0.005	0.000	0.001	0.005	0.004	0.006	0.006	0.003
Ca	0.118	0.079	2.647	2.436	2.415	2.279	2.297	2.111
Na	2.520	1.463	1.313	1.506	1.548	1.648	1.536	1.689
K	1.469	2.445	0.040	0.058	0.063	0.068	0.067	0.069
Sr	0.000	0.003	0.043	0.052	0.047	0.045	0.051	0.049
Total	20.124	20.001	20.060	20.081	20.096	20.074	20.009	19.962
Or	35.8	61.3	1.0	1.5	1.6	1.7	1.7	1.8
Ab	61.3	36.7	32.8	37.6	38.4	41.3	39.4	43.6
An	2.9	2.0	66.2	60.9	60.0	57.0	58.9	54.6

	RDS-15B-27 B	RDS-15B-20 B	RDS-15B-22 B	RDS-15B-15 B	RDS-15B-13 B	RDS-15B-25 B	RDS-15C-16 B	RDS-15C-18 B
SiO_2	53.46	54.24	61.33	61.91	65.3	67.62	49.77	50.33
Al_2O_3	28.69	28.28	23.75	22.8	19.83	18.45	30.74	30.45
FeO	1.05	0.95	0.57	0.68	0.77	1.05	0.82	0.77
CaO	11.45	10.96	5.36	4.29	0.86	0.23	14.11	13.51
Na_2O	4.75	5.01	7.84	7.42	7.62	7.64	3.3	3.55
K_2O	0.3	0.33	1.34	2.66	5.64	6.16	0.14	0.14
BaO	0.11	0.1	0.47	0.27	0.42	0.04	0.05	0.04
SrO	0.45	0.48	0.41	0.25	0.05	0.03	0.4	0.39
Total	100.27	100.33	101.07	100.28	100.5	101.23	99.35	99.16
Numbers of ions on the basis of 32O								
Si	9.727	9.840	10.919	11.103	11.713	11.998	9.194	9.289
Al	6.152	6.046	4.983	4.819	4.192	3.858	6.692	6.623
Fe^{2+}	0.160	0.144	0.085	0.102	0.115	0.156	0.127	0.119
Ba	0.008	0.007	0.033	0.019	0.030	0.003	0.004	0.003
Ca	2.232	2.130	1.022	0.824	0.165	0.044	2.793	2.671
Na	1.675	1.762	2.706	2.580	2.650	2.628	1.182	1.270
K	0.070	0.076	0.304	0.609	1.290	1.394	0.033	0.033
Sr	0.047	0.050	0.042	0.026	0.005	0.003	0.043	0.042
Total	20.070	20.056	20.095	20.082	20.161	20.084	20.067	20.051
Or	1.8	1.9	7.5	15.2	31.4	34.3	0.8	0.8
Ab	42.1	44.4	67.1	64.3	64.5	64.6	29.5	32.0
An	56.1	53.7	25.4	20.5	4.0	1.1	69.7	67.2

A: analcime-bearing
A-SRD: analcime-bearing, Spears Ranch Dike
AS: analcime-bearing, speckled texture
B: basaltic
B-bt: basaltic with significant biotite
BPP: basaltic, pyroxene porphyry dike
BF: basaltic, feeder(?) dike
M: minette

APPENDIX D.1: ELECTRON MICROPROBE ANALYSES OF FELDSPAR

	RDS-15C-14 B	RDS-15C-15 B	RDS-15C-19 B	RDS-15C-17 B	RDS-15C-22 B	RDS-15C-25 B	RDS-15C-20 B	RDS-15C-24 B
SiO_2	50.48	51.07	51.28	50.73	51.82	52.66	52.61	52.67
Al_2O_3	30.5	29.45	29.79	29.4	29.38	28.71	28.84	28.64
FeO	0.74	0.9	0.84	1.08	1.04	1.16	1.1	1.06
CaO	13.56	12.65	12.73	12.58	12.37	11.68	11.61	11.16
Na_2O	3.57	3.98	3.99	3.94	4.15	4.67	4.64	4.77
K_2O	0.17	0.21	0.21	0.23	0.23	0.3	0.33	0.33
BaO	0	0.07	0.08	0.07	0.04	0.09	0	0.08
SrO	0.4	0.46	0.5	0.5	0.49	0.48	0.46	0.49
Total	99.42	98.8	99.43	98.52	99.52	99.75	99.61	99.21
Numbers of ions on the basis of 32O								
Si	9.293	9.458	9.437	9.433	9.521	9.652	9.646	9.689
Al	6.617	6.428	6.461	6.443	6.362	6.202	6.232	6.209
Fe^{2+}	0.114	0.139	0.129	0.168	0.160	0.178	0.169	0.163
Ba	0.000	0.005	0.006	0.005	0.003	0.006	0.000	0.006
Ca	2.674	2.510	2.510	2.506	2.435	2.294	2.280	2.199
Na	1.274	1.429	1.424	1.420	1.478	1.659	1.649	1.701
K	0.040	0.050	0.049	0.055	0.054	0.070	0.077	0.077
Sr	0.043	0.049	0.053	0.054	0.052	0.051	0.049	0.052
Total	20.055	20.068	20.069	20.083	20.064	20.112	20.102	20.096
Or	1.0	1.2	1.2	1.4	1.4	1.7	1.9	1.9
Ab	31.9	35.8	35.7	35.7	37.3	41.2	41.2	42.8
An	67.1	62.9	63.0	63.0	61.4	57.0	56.9	55.3

	RDS-15C-21 B	RDS-15C-26 B	RDS-16A-11 BPP	RDS-16A-13 BPP	RDS-16A-34 BPP	RDS-16A-47 BPP	RDS-16A-15 BPP	RDS-16A-45 BPP
SiO_2	66.1	66.28	50.42	53.38	51.79	50.77	51.52	51.88
Al_2O_3	19.65	18.43	31.11	28.89	29.93	30.6	30.22	30.09
FeO	0.87	1.01	0.78	0.94	0.92	0.92	0.73	0.85
CaO	0.91	0.34	14.04	11.65	13.03	13.7	13.35	12.87
Na_2O	7.92	6.62	3.21	4.6	3.83	3.34	3.68	3.82
K_2O	5.09	7.03	0.33	0.37	0.4	0.41	0.44	0.45
BaO	0.17	0	0.01	0.04	0.05	0.06	0.07	0.04
SrO	0.02	0	0.29	0.27	0.29	0.29	0.25	0.29
Total	100.72	99.71	100.2	100.14	100.25	100.1	100.26	100.28
Numbers of ions on the basis of 32O								
Si	11.775	11.966	9.218	9.707	9.450	9.296	9.400	9.453
Al	4.125	3.921	6.703	6.192	6.436	6.603	6.498	6.461
Fe^{2+}	0.130	0.152	0.119	0.143	0.140	0.141	0.111	0.130
Ba	0.012	0.000	0.001	0.003	0.004	0.004	0.005	0.003
Ca	0.174	0.066	2.750	2.270	2.547	2.687	2.609	2.512
Na	2.735	2.317	1.138	1.622	1.355	1.186	1.302	1.349
K	1.157	1.619	0.077	0.086	0.093	0.096	0.102	0.105
Sr	0.002	0.000	0.031	0.028	0.031	0.031	0.026	0.031
Total	20.109	20.041	20.037	20.051	20.056	20.043	20.054	20.043
Or	28.4	40.5	1.9	2.2	2.3	2.4	2.6	2.6
Ab	67.3	57.9	28.7	40.8	33.9	29.9	32.4	34.0
An	4.3	1.6	69.4	57.1	63.8	67.7	65.0	63.3

A: analcime-bearing
A-SRD: analcime-bearing, Spears Ranch Dike
AS: analcime-bearing, speckled texture
B: basaltic
B-bt: basaltic with significant biotite
BPP: basaltic, pyroxene porphyry dike
BF: basaltic, feeder(?) dike
M: minette

APPENDIX D.1: ELECTRON MICROPROBE ANALYSES OF FELDSPAR

	RDS-16A-46 BPP	RDS-16A-35 BPP	RDS-16A-55 BPP	RDS-16A-50 BPP	RDS-16A-29 BPP	RDS-16A-48 BPP	RDS-16A-49 BPP	RDS-16A-14 BPP
SiO_2	52.78	53.78	54.62	53.98	53.15	52.23	52.89	54.52
Al_2O_3	29.32	28.88	28.09	28.11	28.85	29.43	28.7	28.29
FeO	0.87	0.81	1.08	1.07	0.99	0.79	1.03	0.74
CaO	12.34	11.38	10.6	11.31	11.88	12.33	11.5	10.96
Na_2O	4.16	4.94	5.14	4.75	4.42	4.07	4.61	4.77
K_2O	0.45	0.47	0.52	0.54	0.55	0.55	0.61	0.8
BaO	0.07	0.15	0.11	0.07	0.1	0.04	0.03	0.1
SrO	0.31	0.28	0.28	0.2	0.3	0.29	0.3	0.26
Total	100.29	100.68	100.44	100.04	100.25	99.73	99.67	100.43
Numbers of ions on the basis of 32O								
Si	9.604	9.734	9.893	9.828	9.680	9.560	9.686	9.872
Al	6.287	6.161	5.996	6.032	6.192	6.348	6.194	6.037
Fe^{2+}	0.132	0.123	0.164	0.163	0.151	0.121	0.158	0.112
Ba	0.005	0.011	0.008	0.005	0.007	0.003	0.002	0.007
Ca	2.406	2.207	2.057	2.206	2.318	2.418	2.256	2.126
Na	1.467	1.734	1.805	1.677	1.561	1.444	1.637	1.674
K	0.104	0.109	0.120	0.125	0.128	0.128	0.142	0.185
Sr	0.033	0.029	0.029	0.021	0.032	0.031	0.032	0.027
Total	20.039	20.106	20.072	20.057	20.068	20.053	20.107	20.040
Or	2.6	2.7	3.0	3.1	3.2	3.2	3.5	4.6
Ab	36.9	42.8	45.3	41.8	39.0	36.2	40.6	42.0
An	60.5	54.5	51.7	55.0	57.9	60.6	55.9	53.3

	RDS-16B-35 BPP	RDS-16B-09 BPP	RDS-16B-21 BPP	RDS-16B-08 BPP	RDS-16B-36 BPP	RDS-16B-22 BPP	RDS-16B-27 BPP	RDS-16B-34 BPP
SiO_2	51.01	51.21	51.17	50.85	51.55	52.06	65.36	66.39
Al_2O_3	30.13	30.09	30.04	29.79	29.73	29.27	19.37	19.03
FeO	0.87	0.77	0.81	0.74	0.89	0.84	0.5	0.32
CaO	13.25	13.18	13.14	12.96	12.8	12.6	1.02	0.58
Na_2O	3.57	3.64	3.7	3.71	3.9	3.95	5.6	5.7
K_2O	0.35	0.39	0.4	0.44	0.46	0.54	8.13	8.57
BaO	0	0.09	0.06	0.09	0.06	0.03	0.03	0.05
SrO	0.27	0.32	0.3	0.33	0.29	0.35	0.04	0.01
Total	99.46	99.68	99.62	98.92	99.68	99.65	100.05	100.64
Numbers of ions on the basis of 32O								
Si	9.379	9.398	9.398	9.408	9.460	9.549	11.808	11.913
Al	6.529	6.508	6.502	6.495	6.430	6.327	4.124	4.024
Fe^{2+}	0.134	0.118	0.124	0.114	0.137	0.129	0.076	0.048
Ba	0.000	0.006	0.004	0.007	0.004	0.002	0.002	0.004
Ca	2.610	2.591	2.585	2.569	2.516	2.476	0.197	0.112
Na	1.273	1.295	1.317	1.331	1.387	1.405	1.961	1.983
K	0.082	0.091	0.094	0.104	0.108	0.126	1.874	1.962
Sr	0.029	0.034	0.032	0.035	0.031	0.037	0.004	0.001
Total	20.034	20.042	20.057	20.062	20.073	20.052	20.047	20.047
Or	2.1	2.3	2.3	2.6	2.7	3.2	46.5	48.4
Ab	32.1	32.6	33.0	33.2	34.6	35.1	48.6	48.9
An	65.8	65.1	64.7	64.2	62.7	61.8	4.9	2.7

A: analcime-bearing
A-SRD: analcime-bearing, Spears Ranch Dike
AS: analcime-bearing, speckled texture
B: basaltic
B-bt: basaltic with significant biotite
BPP: basaltic, pyroxene porphyry dike
BF: basaltic, feeder(?) dike
M: minette

APPENDIX D.1: ELECTRON MICROPROBE ANALYSES OF FELDSPAR

	RDS-16B-25 BPP	RDS-16B-26 BPP	RDS-16B-23 BPP	RDS-16C-26 BPP	RDS-16C-19 BPP	RDS-16C-21 BPP	RDS-16C-23 BPP	RDS-16C-24 BPP
SiO_2	65.86	63.49	64.54	51	51.36	52.43	52.32	51.48
Al_2O_3	19.21	19.87	19.53	30.31	29.84	29.14	29.2	29.85
FeO	0.51	0.51	0.36	0.77	0.76	0.88	0.8	0.77
CaO	0.7	0.55	0.76	13.55	13.02	12.19	12.5	12.98
Na_2O	5.52	4.8	4.92	3.54	3.74	4.17	4.01	3.66
K_2O	8.82	8.46	9.18	0.37	0.46	0.51	0.52	0.52
BaO	0.03	2.99	0.96	0.08	0.08	0.04	0.03	0.02
SrO	0.02	0.21	0.19	0.26	0.28	0.29	0.28	0.25
Total	100.67	100.88	100.45	99.88	99.53	99.65	99.67	99.54
Numbers of ions on the basis of 32O								
Si	11.850	11.645	11.746	9.348	9.436	9.603	9.583	9.451
Al	4.073	4.295	4.189	6.547	6.461	6.290	6.303	6.458
Fe^{2+}	0.077	0.078	0.055	0.118	0.117	0.135	0.123	0.118
Ba	0.002	0.215	0.068	0.006	0.006	0.003	0.002	0.001
Ca	0.135	0.108	0.148	2.661	2.563	2.392	2.453	2.553
Na	1.925	1.707	1.736	1.258	1.332	1.481	1.424	1.303
K	2.024	1.979	2.131	0.087	0.108	0.119	0.121	0.122
Sr	0.002	0.022	0.020	0.028	0.030	0.031	0.030	0.027
Total	20.089	20.050	20.093	20.051	20.053	20.052	20.038	20.032
Or	49.6	52.2	53.1	2.2	2.7	3.0	3.0	3.1
Ab	47.1	45.0	43.2	31.4	33.3	37.1	35.6	32.8
An	3.3	2.8	3.7	66.4	64.0	59.9	61.3	64.2

	RDS-16C-25 BPP	RDS-16C-20 BPP	RDS-16C-22 BPP	RDS-16C-28 BPP	RDS-16C-27 BPP	RDS-17-06 BF	RDS-17-29 BF	RDS-17-05 BF
SiO_2	52.5	52.65	65.4	64.45	63.56	50.03	51.04	50.57
Al_2O_3	29.25	28.63	19.08	19.45	19.73	31.95	31.31	31.4
FeO	0.86	0.8	0.34	0.32	0.32	0.87	0.77	0.83
CaO	12.35	11.82	0.65	1.16	0.83	13.81	13.61	13.53
Na_2O	4.1	4.31	5.42	4.7	4.58	3.27	3.53	3.46
K_2O	0.55	0.57	8.98	9.43	9.1	0.15	0.17	0.18
BaO	0.15	0.1	0.05	0.53	1.82	0.02	0.03	0
SrO	0.33	0.33	0.02	0.06	0.26	0.21	0.25	0.17
Total	100.09	99.22	99.93	100.1	100.19	100.31	100.73	100.14
Numbers of ions on the basis of 32O								
Si	9.587	9.682	11.856	11.744	11.672	9.125	9.262	9.226
Al	6.295	6.205	4.076	4.177	4.270	6.867	6.696	6.751
Fe^{2+}	0.131	0.123	0.052	0.049	0.049	0.133	0.117	0.127
Ba	0.011	0.007	0.004	0.038	0.131	0.001	0.002	0.000
Ca	2.416	2.329	0.126	0.226	0.163	2.698	2.646	2.644
Na	1.452	1.537	1.905	1.660	1.631	1.156	1.242	1.224
K	0.128	0.134	2.077	2.192	2.132	0.035	0.039	0.042
Sr	0.035	0.035	0.002	0.006	0.028	0.022	0.026	0.018
Total	20.055	20.051	20.097	20.093	20.075	20.037	20.031	20.032
Or	3.2	3.3	50.6	53.7	54.3	0.9	1.0	1.1
Ab	36.3	38.4	46.4	40.7	41.5	29.7	31.6	31.3
An	60.5	58.2	3.1	5.6	4.2	69.4	67.4	67.6

A: analcime-bearing
A-SRD: analcime-bearing, Spears Ranch Dike
AS: analcime-bearing, speckled texture
B: basaltic
B-bt: basaltic with significant biotite
BPP: basaltic, pyroxene porphyry dike
BF: basaltic, feeder(?) dike
M: minette

APPENDIX D.1: ELECTRON MICROPROBE ANALYSES OF FELDSPAR

	RDS-17-13 BF	RDS-17-14 BF	RDS-17-16 BF	RDS-17-22 BF	RDS-17-21 BF	RDS-17-27 BF	RDS-17-01 BF	RDS-013A-09 AS
SiO_2	50.64	50.5	51.08	51.83	54.47	53.49	65.49	51.42
Al_2O_3	31.39	31.65	31.13	30.44	28.33	29.76	20.28	31.28
FeO	0.92	0.82	1	0.95	1.12	0.84	0.67	0.82
CaO	13.46	13.62	13.13	12.38	11.16	11.6	1.41	12.66
Na_2O	3.54	3.46	3.63	4	4.4	4.56	7.35	3.68
K_2O	0.2	0.2	0.2	0.21	0.25	0.42	4.81	0.51
BaO	0.02	0.03	0	0.01	0.05	0.03	0.44	0.09
SrO	0.24	0.28	0.26	0.27	0.22	0.21	0	0.3
Total	100.41	100.56	100.45	100.09	100	100.91	100.45	100.77
Numbers of ions on the basis of 32O								
Si	9.225	9.188	9.293	9.440	9.876	9.641	11.690	9.323
Al	6.739	6.786	6.674	6.534	6.054	6.321	4.266	6.684
Fe^{2+}	0.140	0.125	0.152	0.145	0.170	0.127	0.100	0.124
Ba	0.001	0.002	0.000	0.001	0.004	0.002	0.031	0.006
Ca	2.627	2.655	2.559	2.416	2.168	2.240	0.270	2.459
Na	1.250	1.220	1.280	1.412	1.547	1.593	2.544	1.294
K	0.046	0.046	0.046	0.049	0.058	0.097	1.095	0.118
Sr	0.025	0.030	0.027	0.029	0.023	0.022	0.000	0.032
Total	20.054	20.052	20.033	20.024	19.899	20.043	19.996	20.040
Or	1.2	1.2	1.2	1.3	1.5	2.5	28.0	3.0
Ab	31.9	31.1	32.9	36.4	41.0	40.5	65.1	33.4
An	67.0	67.7	65.9	62.3	57.5	57.0	6.9	63.5

	RDS-013A-17 AS	RDS-013A-15 AS	RDS-013A-10 AS	RDS-013A-14 AS	RDS-013A-16 AS	RDS-013A-11 AS	RDS-013A-12 AS	RDS-013A-13 AS
SiO_2	51.44	51.67	64.78	65.13	65.24	63.91	65.26	65.96
Al_2O_3	31.39	31.04	20.9	20.61	20.25	20.78	20.2	20
FeO	0.95	0.84	0.25	0.23	0.28	0.32	0.35	0.34
CaO	12.64	12.46	1.31	0.97	0.64	0.68	0.72	0.57
Na_2O	3.48	3.51	4.57	4.36	4.24	3.93	4.13	4.14
K_2O	0.62	0.75	9.66	10.38	10.52	10.11	10.86	11.1
BaO	0.08	0.08	0.03	0	0.32	1.66	0.05	0.02
SrO	0.26	0.29	0.04	0.05	0.18	0.24	0.03	0.01
Total	100.86	100.65	101.54	101.73	101.68	101.62	101.61	102.13
Numbers of ions on the basis of 32O								
Si	9.318	9.376	11.597	11.656	11.712	11.581	11.715	11.774
Al	6.701	6.638	4.410	4.347	4.284	4.438	4.273	4.207
Fe^{2+}	0.144	0.127	0.037	0.034	0.042	0.048	0.053	0.051
Ba	0.006	0.006	0.002	0.000	0.023	0.118	0.004	0.001
Ca	2.453	2.422	0.251	0.186	0.123	0.132	0.138	0.109
Na	1.222	1.235	1.586	1.513	1.476	1.381	1.437	1.433
K	0.143	0.174	2.206	2.370	2.409	2.337	2.487	2.527
Sr	0.027	0.031	0.004	0.005	0.019	0.025	0.003	0.001
Total	20.014	20.009	20.094	20.111	20.088	20.059	20.110	20.103
Or	3.8	4.5	54.6	58.2	60.1	60.7	61.2	62.1
Ab	32.0	32.2	39.2	37.2	36.8	35.9	35.4	35.2
An	64.2	63.2	6.2	4.6	3.1	3.4	3.4	2.7

A: analcime-bearing
A-SRD: analcime-bearing, Spears Ranch Dike
AS: analcime-bearing, speckled texture
B: basaltic
B-bt: basaltic with significant biotite
BPP: basaltic, pyroxene porphyry dike
BF: basaltic, feeder(?) dike
M: minette

APPENDIX D.1: ELECTRON MICROPROBE ANALYSES OF FELDSPAR

	RDS-013B-18 B	RDS-013B-19 B	RDS-013B-16 B	RDS-013B-17 B	RDS-013B-22 B	RDS-013B-15 B	RDS-013B-20 B
SiO_2	50.71	52.02	51.95	52.13	51.87	52.56	52.62
Al_2O_3	32.36	30.88	31.05	31.27	31.41	30.88	30.7
FeO	0.91	0.97	1.09	1.06	0.99	0.79	0.85
CaO	13.82	12.45	12.53	12.65	12.62	12.07	12.15
Na_2O	3.15	3.81	3.83	3.86	3.74	4.06	4.04
K_2O	0.2	0.27	0.29	0.29	0.28	0.31	0.31
BaO	0.02	0.05	0.09	0.07	0.08	0.08	0.08
SrO	0.21	0.23	0.26	0.26	0.24	0.29	0.22
Total	101.37	100.67	101.09	101.6	101.23	101.04	100.97
Numbers of ions on the basis of 32O							
Si	9.142	9.416	9.381	9.367	9.347	9.469	9.486
Al	6.875	6.587	6.608	6.622	6.670	6.556	6.522
Fe^{2+}	0.137	0.147	0.165	0.159	0.149	0.119	0.128
Ba	0.001	0.004	0.006	0.005	0.006	0.006	0.006
Ca	2.669	2.414	2.424	2.435	2.436	2.329	2.347
Na	1.101	1.337	1.341	1.345	1.307	1.418	1.412
K	0.046	0.062	0.067	0.066	0.064	0.071	0.071
Sr	0.022	0.024	0.027	0.027	0.025	0.030	0.023
Total	19.994	19.991	20.019	20.027	20.004	19.998	19.995
Or	1.2	1.6	1.7	1.7	1.7	1.9	1.9
Ab	28.8	35.1	35.0	35.0	34.3	37.1	36.9
An	69.9	63.3	63.3	63.3	64.0	61.0	61.3

	RDS-027-19 B	RDS-027-16 B	RDS-027-17 B	RDS-027-20 B	RDS-027-27 B	RDS-027-18 B	RDS-027-25 B
SiO_2	51.51	51.71	51.65	51.54	51.22	51.93	52.95
Al_2O_3	31.33	31.33	31.05	31.19	31.22	31.43	30.45
FeO	0.93	0.86	0.99	0.95	0.98	0.94	1.02
CaO	13.26	13.07	12.95	12.96	12.93	13.03	12.01
Na_2O	3.64	3.84	3.81	3.71	3.82	3.7	4.33
K_2O	0.23	0.25	0.26	0.27	0.27	0.29	0.34
BaO	0.05	0.03	0.09	0	0.06	0.09	0.1
SrO	0.3	0.25	0.26	0.29	0.24	0.24	0.26
Total	101.24	101.34	101.06	100.9	100.74	101.65	101.47
Numbers of ions on the basis of 32O							
Si	9.299	9.319	9.341	9.327	9.295	9.330	9.516
Al	6.666	6.654	6.618	6.652	6.677	6.655	6.449
Fe^{2+}	0.140	0.130	0.150	0.144	0.149	0.141	0.153
Ba	0.004	0.002	0.006	0.000	0.004	0.006	0.007
Ca	2.565	2.523	2.509	2.513	2.514	2.508	2.312
Na	1.274	1.342	1.336	1.302	1.344	1.289	1.509
K	0.053	0.057	0.060	0.062	0.062	0.066	0.078
Sr	0.031	0.026	0.027	0.030	0.025	0.025	0.027
Total	20.032	20.053	20.048	20.029	20.070	20.020	20.052
Or	1.4	1.5	1.5	1.6	1.6	1.7	2.0
Ab	32.7	34.2	34.2	33.6	34.3	33.4	38.7
An	65.9	64.3	64.3	64.8	64.1	64.9	59.3

A: analcime-bearing
A-SRD: analcime-bearing, Spears Ranch Dike
AS: analcime-bearing, speckled texture
B: basaltic
B-bt: basaltic with significant biotite
BPP: basaltic, pyroxene porphyry dike
BF: basaltic, feeder(?) dike
M: minette

APPENDIX D.1: ELECTRON MICROPROBE ANALYSES OF FELDSPAR

	RDS-102-25 M	RDS-102-22 M	RDS-102-33 M	RDS-102-34 M	RDS-102-24 M	RDS-102-21 M	RDS-102-19 M	RDS-102-23 M
SiO_2	65	64.86	65.12	68.41	65.83	65.51	65.16	63.52
Al_2O_3	20.38	20.62	20.33	19.43	19.77	19.81	20.21	20.27
FeO	0.58	0.56	0.43	0.65	0.45	0.44	0.43	0.77
CaO	1.39	1.41	1.03	0.3	0.61	0.58	0.83	1.01
Na_2O	5.07	4.4	4.47	4.65	4.33	4.08	3.67	3.45
K_2O	8.71	9.89	9.87	9.47	10.59	11.08	11.23	10.93
BaO	0.04	0.07	0	0	0	0.09	0.08	1.01
SrO	0.04	0.03	0.07	0	0.04	0.03	0.11	0.3
Total	101.21	101.82	101.32	102.91	101.63	101.62	101.72	101.27
Numbers of ions on the basis of 32O								
Si	11.652	11.610	11.687	11.990	11.794	11.770	11.707	11.583
Al	4.305	4.350	4.300	4.013	4.174	4.195	4.279	4.356
Fe^{2+}	0.087	0.084	0.065	0.095	0.067	0.066	0.065	0.117
Ba	0.003	0.005	0.000	0.000	0.000	0.006	0.006	0.072
Ca	0.267	0.270	0.198	0.056	0.117	0.112	0.160	0.197
Na	1.762	1.527	1.555	1.580	1.504	1.421	1.278	1.220
K	1.992	2.258	2.259	2.117	2.420	2.539	2.574	2.542
Sr	0.004	0.003	0.007	0.000	0.004	0.003	0.011	0.032
Total	20.072	20.107	20.071	19.852	20.081	20.113	20.079	20.120
Or	49.5	55.7	56.3	56.4	59.9	62.4	64.2	64.2
Ab	43.8	37.7	38.8	42.1	37.2	34.9	31.9	30.8
An	6.6	6.7	4.9	1.5	2.9	2.7	4.0	5.0

	RDS-102-31 M	RDS-106-16 M	RDS-106-24 M	RDS-106-29 M	RDS-106-26 M	RDS-106-30 M	RDS-106-25 M	RDS-106-27 M
SiO_2	64.31	52.06	60.05	64.98	66.04	64.92	66.61	66.37
Al_2O_3	19.84	30.09	24.73	20.56	20.16	19.52	19.84	19.54
FeO	0.54	1.05	0.69	1.02	0.53	0.81	0.61	0.63
CaO	0.48	12.24	5.59	1.54	0.77	0.67	0.61	0.38
Na_2O	3.02	4.23	7.41	7.84	7.67	7.19	7.33	6.58
K_2O	11.87	0.29	1.21	4.46	5.3	5.43	6.22	7.38
BaO	0.68	0	0.27	0.1	0.15	0.09	0.02	0.03
SrO	0.24	0.3	0.33	0.01	0.09	0.07	0	0.01
Total	100.98	100.26	100.28	100.52	100.71	98.7	101.24	100.92
Numbers of ions on the basis of 32O								
Si	11.722	9.478	10.757	11.597	11.746	11.787	11.807	11.844
Al	4.262	6.456	5.221	4.324	4.226	4.177	4.144	4.109
Fe^{2+}	0.082	0.160	0.103	0.152	0.079	0.123	0.090	0.094
Ba	0.049	0.000	0.019	0.007	0.010	0.006	0.001	0.002
Ca	0.094	2.387	1.073	0.294	0.147	0.130	0.116	0.073
Na	1.067	1.493	2.573	2.713	2.645	2.531	2.519	2.276
K	2.760	0.067	0.276	1.015	1.202	1.258	1.406	1.680
Sr	0.025	0.032	0.034	0.001	0.009	0.007	0.000	0.001
Total	20.061	20.074	20.057	20.105	20.065	20.019	20.084	20.080
Or	70.4	1.7	7.0	25.2	30.1	32.1	34.8	41.7
Ab	27.2	37.8	65.6	67.4	66.2	64.6	62.3	56.5
An	2.4	60.5	27.3	7.3	3.7	3.3	2.9	1.8

A: analcime-bearing
A-SRD: analcime-bearing, Spears Ranch Dike
AS: analcime-bearing, speckled texture
B: basaltic
B-bt: basaltic with significant biotite
BPP: basaltic, pyroxene porphyry dike
BF: basaltic, feeder(?) dike
M: minette

APPENDIX D.1: ELECTRON MICROPROBE ANALYSES OF FELDSPAR

	RDS-130-24 BF	RDS-130-32 BF	RDS-130-29 BF	RDS-130-25 BF	RDS-130-26 BF	RDS-130-23 BF	RDS-130-27 BF	RDS-130-31 BF
SiO_2	52.28	51.69	53.54	53.8	53.35	53.28	54.02	53.61
Al_2O_3	30.56	29.38	29.87	29.77	29.34	29.46	29.54	28.11
FeO	1.27	1.25	1.2	1.25	1.51	1.25	1.17	1.27
CaO	12.33	12.74	11.68	11.57	11.07	11.44	11.15	11.19
Na_2O	4.03	3.82	4.65	4.74	4.64	4.75	4.87	4.71
K_2O	0.29	0.3	0.35	0.4	0.38	0.41	0.42	0.42
BaO	0.11	0.06	0.1	0.07	0.07	0.09	0.09	0.03
SrO	0.23	0.28	0.15	0.21	0.21	0.21	0.14	0.19
Total	101.08	99.51	101.54	101.8	100.58	100.9	101.4	99.52
Numbers of ions on the basis of 32O								
Si	9.445	9.501	9.611	9.636	9.668	9.635	9.696	9.808
Al	6.507	6.364	6.319	6.284	6.266	6.278	6.248	6.061
Fe^{2+}	0.192	0.192	0.180	0.187	0.229	0.189	0.176	0.194
Ba	0.008	0.004	0.007	0.005	0.005	0.006	0.006	0.002
Ca	2.387	2.509	2.246	2.220	2.149	2.216	2.144	2.193
Na	1.412	1.361	1.618	1.646	1.630	1.665	1.695	1.671
K	0.067	0.070	0.080	0.091	0.088	0.095	0.096	0.098
Sr	0.024	0.030	0.016	0.022	0.022	0.022	0.015	0.020
Total	20.041	20.032	20.078	20.091	20.058	20.106	20.075	20.046
Or	1.7	1.8	2.0	2.3	2.3	2.4	2.4	2.5
Ab	36.5	34.5	41.0	41.6	42.2	41.9	43.1	42.2
An	61.7	63.7	56.9	56.1	55.6	55.7	54.5	55.4

	RDS-130-28 BF	RDS-130-30 BF	RDS-130-33 BF	RDS-159-08 B-bt	RDS-159-03 B-bt	RDS-159-04 B-bt	RDS-159-010 B-bt	RDS-159-07 B-bt
SiO_2	55.44	58.39	64.98	60.863	65.444	65.2827	63.3036	64.554
Al_2O_3	28.5	25.59	21.58	24.4836	19.5106	19.7359	20.715	19.9724
FeO	1.32	0.72	0.46	0.5035	0.6915	0.5419	0.4744	0.4776
CaO	9.9	7.7	2.1	5.0048	0.3115	0.5988	0.8896	0.7664
Na_2O	5.38	6.61	7.46	6.6305	5.2826	5.015	4.0965	4.1067
K_2O	0.54	0.88	4.47	2.8539	9.3856	9.5757	9.6245	10.6706
BaO	0.11	0.22	0.21	0.228	0	0.0567	1.7562	0.0326
SrO	0.21	0.26	0.06	0.209	0.0107	0.0098	0.4241	0.0332
Total	101.42	100.37	101.31	100.7764	100.6364	100.8166	101.2839	100.6136
Numbers of ions on the basis of 32O								
Si	9.928	10.493	11.492	10.866	11.805	11.766	11.535	11.707
Al	6.015	5.419	4.498	5.151	4.148	4.192	4.448	4.269
Fe^{2+}	0.198	0.108	0.068	0.075	0.104	0.082	0.072	0.072
Ba	0.008	0.015	0.015	0.016	0.000	0.004	0.125	0.002
Ca	1.899	1.482	0.398	0.957	0.060	0.116	0.174	0.149
Na	1.868	2.303	2.558	2.295	1.847	1.752	1.447	1.444
K	0.123	0.202	1.008	0.650	2.160	2.202	2.237	2.468
Sr	0.022	0.027	0.006	0.022	0.001	0.001	0.045	0.003
Total	20.060	20.050	20.042	20.031	20.125	20.115	20.083	20.115
Or	3.2	5.1	25.4	16.7	53.1	54.1	58.0	60.8
Ab	48.0	57.8	64.5	58.8	45.4	43.1	37.5	35.6
An	48.8	37.2	10.0	24.5	1.5	2.8	4.5	3.7

A: analcime-bearing
A-SRD: analcime-bearing, Spears Ranch Dike
AS: analcime-bearing, speckled texture
B: basaltic
B-bt: basaltic with significant biotite
BPP: basaltic, pyroxene porphyry dike
BF: basaltic, feeder(?) dike
M: minette

APPENDIX D.1: ELECTRON MICROPROBE ANALYSES OF FELDSPAR

	MDS-26-01 S-PT	MDS-26-019 S-PT	MDS-26-021 S-PT	MDS-26-024 S-PT	MDS-26-026 S-PT	MDS-26-028 S-PT	MDS-26-029 S-PT	MDS-26-030 S-PT
SiO_2	56.1908	65.4208	59.8307	62.2454	65.097	61.2956	65.923	60.7514
Al_2O_3	26.9826	20.3652	24.9608	24.0093	21.6822	24.9025	20.8477	25.3869
FeO	0.1791	0.3108	0.2139	0.2157	0.3072	0.2135	0.3203	0.2152
CaO	8.1245	0.8897	5.7238	4.6175	3.1495	5.6766	1.2616	6.1213
Na_2O	6.5444	6.8779	7.6985	8.3197	7.3021	7.6168	7.5418	7.616
K_2O	0.4243	6.4295	0.768	1.0002	2.5989	0.9323	5.1112	0.7334
BaO	0.0591	0.0499	0.0785	0.1459	0.1735	0.0698	0.3833	0.0305
SrO	0.1743	0.0205	0.1672	0.1474	0.0454	0.2019	0.0144	0.1689
Total	98.6791	100.3642	99.4414	100.7012	100.3559	100.909	101.4033	101.0237
Numbers of ions based on 32O								
Si	10.236	11.705	10.745	11.010	11.510	10.837	11.652	10.736
Al	5.792	4.294	5.283	5.005	4.518	5.189	4.343	5.287
Fe^{2+}	0.027	0.046	0.032	0.032	0.045	0.032	0.047	0.032
Ba	0.004	0.003	0.006	0.010	0.012	0.005	0.027	0.002
Ca	1.585	0.171	1.101	0.875	0.597	1.075	0.239	1.159
Na	2.311	2.386	2.680	2.853	2.503	2.611	2.584	2.609
K	0.099	1.467	0.176	0.226	0.586	0.210	1.152	0.165
Sr	0.018	0.002	0.017	0.015	0.005	0.021	0.001	0.017
Total	20.073	20.075	20.041	20.026	19.776	19.979	20.045	20.008
Or	2.5	36.5	4.4	5.7	15.9	5.4	29.0	4.2
Ab	57.8	59.3	67.7	72.2	67.9	67.0	65.0	66.3
An	39.7	4.2	27.8	22.1	16.2	27.6	6.0	29.5

	MDS-26-031 S-PT	MDS-26-033 S-PT	MDS-26-037 S-PT
SiO_2	65.6969	63.7121	63.3698
Al_2O_3	20.8307	23.0239	23.1079
FeO	0.3406	0.1993	0.1578
CaO	1.6405	3.758	3.5992
Na_2O	7.2323	8.5384	8.7765
K_2O	4.7011	1.3181	1.063
BaO	1.2318	0.0257	0.0427
SrO	0.027	0.0664	0.0845
Total	101.701	100.6419	100.2014
Numbers of ions based on 32O			
Si	11.630	11.234	11.214
Al	4.346	4.784	4.819
Fe^{2+}	0.050	0.029	0.023
Ba	0.085	0.002	0.003
Ca	0.311	0.710	0.682
Na	2.482	2.919	3.011
K	1.062	0.296	0.240
Sr	0.003	0.007	0.009
Total	19.969	19.981	20.002
Or	27.5	7.6	6.1
Ab	64.4	74.4	76.6
An	8.1	18.1	17.3

S-PT: Sanidine-bearing dike near Pie Town

APPENDIX D.2: ELECTRON MICROPROBE ANALYSES OF ANALCIME

	RDS-2-18	RDS-2-21	RDS-2-23	RDS-2-24	RDS-5-22	RDS-5-27	RDS-5-29
	A-SRD	A-SRD	A-SRD	A-SRD	A	A	A
SiO_2	56.06	53.68	60.42	55.32	60.53	58.71	60.77
Al_2O_3	27.31	27.25	24.74	27.57	26.07	25.74	25.76
FeO	0.15	0.18	0.51	0.16	0.60	0.77	0.70
CaO	1.89	1.27	0.23	2.40	0.16	0.23	0.14
Na_2O	10.90	11.70	11.73	11.25	9.85	12.13	10.49
K_2O	0.23	0.03	0.08	0.06	0.14	0.12	0.09
BaO	0.03	0.00	0.00	0.02	0.00	0.00	0.00
SrO	0.14	0.07	0.03	0.13	0.01	0.04	0.03
Total	93.42	88.36	95.50	93.82	94.70	95.48	95.96
	Numbers of ions on the basis of 96O						
Si	31.0617	30.6009	32.8317	30.6933	32.7455	32.0880	32.7678
Al	17.8330	18.3071	15.8432	18.0272	16.6208	16.5794	16.3694
Fe^{2+}	0.0695	0.0858	0.2317	0.0742	0.2714	0.3519	0.3156
Ca	1.1219	0.7756	0.1339	1.4266	0.0927	0.1347	0.0809
Na	11.7087	12.9305	12.3572	12.1010	10.3306	12.8529	10.9658
K	0.1626	0.0218	0.0555	0.0425	0.0966	0.0837	0.0619
Total	61.9574	62.7217	61.4531	62.3648	60.1577	62.0905	60.5614

	RDS-5-34	RDS-5-35	RDS-5-36	RDS-5-37	RDS-5-38	RDS-5-25b	RDS-5-26b
	A	A	A	A	A	A	A
SiO_2	60.62	59.85	59.37	60.50	60.75	61.43	60.55
Al_2O_3	25.44	25.95	25.91	25.69	26.01	26.10	26.29
FeO	0.49	0.32	0.54	0.61	0.49	0.59	0.52
CaO	0.12	0.10	0.15	0.11	0.09	0.14	0.13
Na_2O	10.83	11.15	11.78	9.61	9.31	8.77	8.95
K_2O	0.07	0.08	0.11	0.07	0.08	0.10	0.09
BaO	0.02	0.03	0.00	0.04	0.01	0.00	0.03
SrO	0.02	0.03	0.04	0.00	0.00	0.02	0.00
Total	95.20	95.04	95.82	93.24	93.48	94.28	93.14
	Numbers of ions on the basis of 96O						
Si	32.8244	32.4964	32.2656	32.9249	32.9378	33.0924	32.8627
Al	16.2341	16.6050	16.5947	16.4764	16.6195	16.5698	16.8155
Fe^{2+}	0.2219	0.1453	0.2454	0.2776	0.2222	0.2658	0.2360
Ca	0.0696	0.0582	0.0873	0.0641	0.0523	0.0808	0.0756
Na	11.3689	11.7369	12.4116	10.1391	9.7860	9.1592	9.4172
K	0.0483	0.0554	0.0763	0.0486	0.0553	0.0687	0.0623
Total	60.7672	61.0972	61.6809	59.9308	59.6731	59.2366	59.4693

A: analcime-bearing

A-SRD: analcime-bearing, Spears Ranch Dike

AS: analcime-bearing, speckled texture

APPENDIX D.2: ELECTRON MICROPROBE ANALYSES OF ANALCIME

	RDS-5-27b A	RDS-5-28b A	RDS-5-29b A	RDS-5-30b A	RDS-10-18 A-SRD	RDS-10-24 A-SRD	RDS-10-25 A-SRD
SiO_2	60.47	61.05	61.22	60.83	58.10	57.95	57.60
Al_2O_3	25.84	26.15	26.08	26.20	23.34	23.09	22.93
FeO	0.61	0.59	0.65	0.70	0.38	0.52	0.45
CaO	0.09	0.12	0.09	0.14	0.21	0.10	0.15
Na_2O	8.80	8.73	8.74	7.96	12.27	12.71	12.58
K_2O	0.09	0.09	0.09	0.08	0.51	0.37	0.43
BaO	0.00	0.00	0.00	0.00	0.03	0.03	0.00
SrO	0.00	0.02	0.03	0.00	0.04	0.01	0.00
Total	91.82	93.48	93.78	91.82	89.76	89.58	88.26
	Numbers of ions on the basis of 96O						
Si	33.0187	33.0245	33.0710	33.0902	32.7668	32.7602	32.7699
Al	16.6281	16.6706	16.6032	16.7963	15.5127	15.3832	15.3740
Fe^{2+}	0.2785	0.2669	0.2936	0.3184	0.1792	0.2458	0.2141
Ca	0.0526	0.0695	0.0521	0.0816	0.1269	0.0606	0.0914
Na	9.3156	9.1553	9.1532	8.3947	13.4156	13.9299	13.8753
K	0.0627	0.0621	0.0620	0.0555	0.3669	0.2668	0.3121
Total	59.3563	59.2489	59.2351	58.7367	62.3681	62.6465	62.6368

	RDS-10-26 A-SRD	RDS-013A-18 AS	RDS-013A-19 AS	RDS-013A-20 AS	RDS-013A-21 AS	RDS-013A-22 AS
SiO_2	57.89	59.08	53.88	54.31	58.59	55.07
Al_2O_3	23.15	24.61	28.59	28.22	23.91	27.07
FeO	0.44	0.16	0.18	0.07	0.11	0.01
CaO	0.20	0.64	2.76	0.53	0.10	1.52
Na_2O	12.34	13.13	10.56	12.39	13.25	11.91
K_2O	0.44	0.09	0.27	0.15	0.10	0.20
BaO	0.01	0.00	0.05	0.05	0.00	0.01
SrO	0.00	0.03	0.23	0.07	0.00	0.06
Total	88.96	95.46	93.02	91.58	92.14	91.66
	Numbers of ions on the basis of 96O					
Si	32.7818	32.3599	30.1048	30.4474	32.5965	30.8619
Al	15.4494	15.8858	18.8257	18.6448	15.6768	17.8783
Fe^{2+}	0.2083	0.0733	0.0841	0.0328	0.0512	0.0047
Ca	0.1213	0.3756	1.6521	0.3183	0.0596	0.9126
Na	13.5473	13.9425	11.4388	13.4664	14.2913	12.9398
K	0.3178	0.0629	0.1924	0.1073	0.0710	0.1430
Total	62.4260	62.6999	62.2980	63.0170	62.7463	62.7403

A: analcime-bearing

A-SRD: analcime-bearing, Spears Ranch Dike

AS: analcime-bearing, speckled texture

APPENDIX D.3: ELECTRON MICROPROBE ANALYSES OF PYROXENE

	RDS-2-04 A-SRD	RDS-2-06 A-SRD	RDS-2-08 A-SRD	RDS-2-31 A-SRD	RDS-2-02 A-SRD	RDS-2-03 A-SRD	RDS-2-30 A-SRD	RDS-2-07 A-SRD
SiO_2	47.53	48.18	48.08	48.2	51.29	52.88	52.59	52.76
TiO_2	1.66	1.43	1.34	1.48	0.96	0.55	0.54	0.46
Al_2O_3	6.14	5.72	5.56	5.42	3.01	2.36	2.2	2.22
FeO	8.54	8.25	8.17	8.28	6.68	5.68	5.4	5.47
MnO	0.14	0.14	0.15	0.1	0.11	0.14	0.09	0.12
MgO	12.84	13.13	13.3	13.42	15	16.59	16.25	16.66
CaO	23.06	23.15	23.05	22.67	23.05	22.65	22.89	22.67
Na_2O	0.37	0.38	0.33	0.36	0.26	0.26	0.26	0.29
Total	100.28	100.38	99.98	99.93	100.36	101.11	100.22	100.65
Numbers of ions on the basis of 6O								
Si	1.784	1.802	1.805	1.809	1.896	1.924	1.930	1.928
Al	0.272	0.252	0.246	0.240	0.131	0.101	0.095	0.096
Ti	0.047	0.040	0.038	0.042	0.027	0.015	0.015	0.013
Mg	0.718	0.732	0.744	0.751	0.827	0.900	0.889	0.907
Fe^{2+}	0.268	0.258	0.256	0.260	0.206	0.173	0.166	0.167
Mn	0.004	0.004	0.005	0.003	0.003	0.004	0.003	0.004
Ca	0.927	0.928	0.927	0.912	0.913	0.883	0.900	0.887
Na	0.027	0.028	0.024	0.026	0.019	0.018	0.019	0.021
Total	4.047	4.045	4.046	4.042	4.021	4.019	4.017	4.022
Atomic percentages								
Mg	37.5	38.1	38.5	39.0	42.4	45.9	45.4	46.2
Fe+Mn	14.2	13.7	13.5	13.7	10.8	9.0	8.6	8.7
Ca	48.3	48.3	48.0	47.3	46.8	45.0	46.0	45.1
mg#	72.5	73.6	74.0	74.1	79.7	83.6	84.1	84.2

	RDS-2-01 A-SRD	RDS-2-09 A-SRD	RDS-5-12 A	RDS-5-11b A	RDS-5-13b A	RDS-5-21 A	RDS-5-14 A	RDS-5-07b A
SiO_2	52.7	52.8	43.33	45.92	45	46.61	45.95	46.46
TiO_2	0.46	0.55	2.39	1.82	2.26	1.69	2.1	1.88
Al_2O_3	2.1	2.34	8.73	6.8	7.7	6.99	7.41	6.95
FeO	5.26	4.38	9.4	8.53	8.07	8.16	7.86	7.73
MnO	0.14	0.09	0.12	0.1	0.15	0.1	0.13	0.16
MgO	16.59	16.51	11.16	12.14	11.76	12.53	12.2	12.56
CaO	22.85	23.44	23.45	22.88	22.9	23.22	23.09	22.15
Na_2O	0.25	0.28	0.31	0.31	0.41	0.35	0.38	0.39
Total	100.35	100.39	98.89	98.5	98.25	99.65	99.12	98.28
Numbers of ions on the basis of 6O								
Si	1.931	1.928	1.670	1.758	1.727	1.760	1.743	1.770
Al	0.091	0.101	0.396	0.307	0.348	0.311	0.331	0.312
Ti	0.013	0.015	0.069	0.052	0.065	0.048	0.060	0.054
Mg	0.906	0.899	0.641	0.693	0.673	0.705	0.690	0.713
Fe^{2+}	0.161	0.134	0.303	0.273	0.259	0.258	0.249	0.246
Mn	0.004	0.003	0.004	0.003	0.005	0.003	0.004	0.005
Ca	0.897	0.917	0.968	0.938	0.941	0.939	0.939	0.904
Na	0.018	0.020	0.023	0.023	0.031	0.026	0.028	0.029
Total	4.020	4.016	4.074	4.048	4.049	4.050	4.045	4.034
Atomic percentages								
Mg	46.0	46.0	33.5	36.3	35.8	37.0	36.7	38.2
Fe+Mn	8.4	7.0	16.0	14.5	14.0	13.7	13.5	13.5
Ca	45.6	47.0	50.5	49.2	50.1	49.3	49.9	48.4
mg#	84.6	86.8	67.6	71.5	71.8	73.0	73.1	73.9

A: analcime-bearing
A-SRD: analcime-bearing, Spears Ranch Dike
AS: analcime-bearing, speckled texture
B: basaltic
B-bt: basaltic with significant biotite
BPP: basaltic, pyroxene porphyry dike
BF: basaltic, feeder(?) dike
M: minette
mg# = Mg/(Mg+Fe+Mn)

APPENDIX D.3: ELECTRON MICROPROBE ANALYSES OF PYROXENE

	RDS-5-13 A	RDS-5-14b A	RDS-5-09b A	RDS-5-20 A	RDS-5-08b A	RDS-5-11 A	RDS-5-12b A	RDS-5-10b A
SiO_2	48.73	48.74	49.2	49.96	49.31	50.01	50.85	51.77
TiO_2	1.42	1.19	1.17	1.06	1.1	1.02	0.73	0.66
Al_2O_3	5.05	4.39	4.25	3.8	4.08	4.23	2.5	2.48
FeO	6.99	6.82	6.65	6.77	6.49	5.73	5.21	5.03
MnO	0.18	0.24	0.16	0.1	0.1	0.09	0.11	0.11
MgO	13.52	13.41	13.81	14.58	14.24	15.02	15.37	15.61
CaO	23.56	22.16	22.91	23.83	22.8	23.97	23.1	22.95
Na_2O	0.34	0.41	0.37	0.18	0.19	0.18	0.16	0.18
Total	99.79	97.36	98.52	100.28	98.31	100.25	98.03	98.79
Numbers of ions on the basis of 6O								
Si	1.825	1.862	1.858	1.857	1.863	1.851	1.913	1.926
Al	0.223	0.198	0.189	0.166	0.182	0.184	0.111	0.109
Ti	0.040	0.034	0.033	0.030	0.031	0.028	0.021	0.018
Mg	0.755	0.764	0.778	0.808	0.802	0.829	0.862	0.866
Fe^{2+}	0.219	0.218	0.210	0.210	0.205	0.177	0.164	0.157
Mn	0.006	0.008	0.005	0.003	0.003	0.003	0.004	0.003
Ca	0.945	0.907	0.927	0.949	0.923	0.950	0.931	0.915
Na	0.025	0.030	0.027	0.013	0.014	0.013	0.012	0.013
Total	4.036	4.020	4.027	4.037	4.022	4.035	4.017	4.007
Atomic percentages								
Mg	39.2	40.3	40.5	41.0	41.5	42.3	44.0	44.6
Fe+Mn	11.7	11.9	11.2	10.8	10.8	9.2	8.5	8.2
Ca	49.1	47.8	48.3	48.2	47.7	48.5	47.5	47.1
mg#	77.1	77.2	78.3	79.1	79.4	82.1	83.7	84.4

	RDS-5-01 A	RDS-6-28 B	RDS-6-26 B	RDS-6-23 B	RDS-6-25 B	RDS-6-19 B	RDS-6-22 B	RDS-6-27 B
SiO_2	50.81	45.83	44.25	47.29	48.33	47.74	50	50.8
TiO_2	0.69	1.92	1.72	1.62	1.26	1.58	0.94	0.82
Al_2O_3	3.53	7.66	6.93	6.51	6.3	5.54	3.84	3.19
FeO	4.54	9.17	8.23	8.15	7.97	7.61	7.59	7.01
MnO	0.06	0.13	0.16	0.13	0.12	0.17	0.17	0.21
MgO	15.16	12.56	13.09	13.39	13.6	14.15	15.01	15.7
CaO	24.27	22.3	22.3	22.48	22.6	22.34	22.34	21.93
Na_2O	0.23	0.34	0.39	0.36	0.38	0.44	0.27	0.27
Total	99.29	99.91	97.07	99.93	100.56	99.57	100.16	99.93
Numbers of ions on the basis of 6O								
Si	1.887	1.731	1.722	1.775	1.798	1.795	1.860	1.885
Al	0.154	0.341	0.318	0.288	0.276	0.245	0.168	0.140
Ti	0.019	0.055	0.050	0.046	0.035	0.045	0.026	0.023
Mg	0.839	0.707	0.760	0.749	0.754	0.793	0.833	0.869
Fe^{2+}	0.141	0.290	0.268	0.256	0.248	0.239	0.236	0.218
Mn	0.002	0.004	0.005	0.004	0.004	0.005	0.005	0.007
Ca	0.966	0.903	0.930	0.904	0.901	0.900	0.890	0.872
Na	0.017	0.025	0.029	0.026	0.027	0.032	0.019	0.019
Total	4.025	4.056	4.083	4.048	4.043	4.054	4.039	4.032
Atomic percentages								
Mg	43.1	37.2	38.7	39.2	39.6	40.9	42.4	44.2
Fe+Mn	7.3	15.4	13.9	13.6	13.2	12.6	12.3	11.4
Ca	49.6	47.4	47.4	47.2	47.2	46.4	45.3	44.4
mg#	85.5	70.7	73.6	74.2	75.0	76.4	77.5	79.5

A: analcime-bearing
A-SRD: analcime-bearing, Spears Ranch Dike
AS: analcime-bearing, speckled texture
B: basaltic
B-bt: basaltic with significant biotite
BPP: basaltic, pyroxene porphyry dike
BF: basaltic, feeder(?) dike
M: minette
mg# = Mg/(Mg+Fe+Mn)

APPENDIX D.3: ELECTRON MICROPROBE ANALYSES OF PYROXENE

	RDS-6-24 B	RDS-6-29 B	RDS-7-19b B-bt	RDS-7-16b B-bt	RDS-7-20b B-bt	RDS-7-29 B-bt	RDS-7-22b B-bt	RDS-7-17b B-bt
SiO_2	51.4	50.65	48.03	47.4	47.33	48.19	48.12	47.93
TiO_2	0.76	0.9	1.3	1.3	1.25	1.46	1.1	1.07
Al_2O_3	2.97	2.52	5.31	5.47	5.5	5.35	5.45	5.32
FeO	6.53	6.25	8.66	8.36	8.6	8.52	8.44	8.13
MnO	0.21	0.24	0.19	0.25	0.15	0.21	0.17	0.2
MgO	15.98	15.88	13.37	13.13	13.41	13.56	13.53	13.53
CaO	22.32	22.4	21.34	21.01	21.08	22.65	21.28	21.29
Na_2O	0.34	0.36	0.29	0.31	0.34	0.35	0.32	0.3
Total	100.51	99.2	98.49	97.23	97.66	100.29	98.41	97.77
Numbers of ions on the basis of 6O								
Si	1.893	1.893	1.825	1.823	1.815	1.805	1.827	1.830
Al	0.129	0.111	0.238	0.248	0.249	0.236	0.244	0.239
Ti	0.021	0.025	0.037	0.038	0.036	0.041	0.031	0.031
Mg	0.877	0.885	0.757	0.753	0.767	0.757	0.766	0.770
Fe^{2+}	0.201	0.195	0.275	0.269	0.276	0.267	0.268	0.260
Mn	0.007	0.008	0.006	0.008	0.005	0.007	0.005	0.006
Ca	0.881	0.897	0.869	0.866	0.866	0.909	0.866	0.871
Na	0.024	0.026	0.021	0.023	0.025	0.025	0.024	0.022
Total	4.033	4.039	4.029	4.027	4.038	4.048	4.031	4.030
Atomic percentages								
Mg	44.6	44.6	39.7	39.7	40.1	39.0	40.2	40.4
Fe+Mn	10.6	10.2	14.7	14.6	14.7	14.1	14.4	13.9
Ca	44.8	45.2	45.5	45.7	45.3	46.9	45.4	45.7
mg#	80.9	81.3	72.9	73.1	73.2	73.5	73.7	74.3

	RDS-7-30 B-bt	RDS-7-21b B-bt	RDS-7-13 B-bt	RDS-7-15b B-bt	RDS-7-14b B-bt	RDS-7-15 B-bt	RDS-8-10 B	RDS-8-29 B
SiO_2	48.97	51.24	51.03	50.31	49.09	52.61	47.45	48.55
TiO_2	1.17	0.64	0.79	0.77	0.66	0.5	1.67	1.21
Al_2O_3	4.83	2.82	3.65	3.89	3.19	2.45	6.15	5.52
FeO	8.63	7.43	6.69	6.61	6.04	5.75	8.53	7.94
MnO	0.19	0.21	0.15	0.08	0.13	0.09	0.11	0.17
MgO	14.51	15.41	15.21	14.98	15.14	16.27	13.23	13.75
CaO	22.03	20.75	23.34	20.99	20.9	23.01	23.04	22.98
Na_2O	0.31	0.24	0.28	0.3	0.26	0.28	0.37	0.4
Total	100.64	98.74	101.14	97.93	95.41	100.96	100.55	100.52
Numbers of ions on the basis of 6O								
Si	1.823	1.918	1.874	1.894	1.898	1.920	1.776	1.810
Al	0.212	0.124	0.158	0.173	0.145	0.105	0.271	0.242
Ti	0.033	0.018	0.022	0.022	0.019	0.014	0.047	0.034
Mg	0.805	0.860	0.833	0.841	0.873	0.885	0.738	0.764
Fe^{2+}	0.269	0.233	0.205	0.208	0.195	0.176	0.267	0.247
Mn	0.006	0.007	0.005	0.003	0.004	0.003	0.003	0.005
Ca	0.879	0.832	0.918	0.847	0.866	0.900	0.924	0.918
Na	0.022	0.017	0.020	0.022	0.019	0.020	0.027	0.029
Total	4.049	4.010	4.035	4.009	4.020	4.023	4.054	4.050
Atomic percentages								
Mg	41.1	44.5	42.5	44.3	45.0	45.1	38.2	39.5
Fe+Mn	14.0	12.4	10.7	11.1	10.3	9.1	14.0	13.1
Ca	44.9	43.1	46.8	44.6	44.7	45.8	47.8	47.4
mg#	74.6	78.2	79.9	80.0	81.4	83.2	73.2	75.1

A: analcime-bearing
A-SRD: analcime-bearing, Spears Ranch Dike
AS: analcime-bearing, speckled texture
B: basaltic
B-bt: basaltic with significant biotite
BPP: basaltic, pyroxene porphyry dike
BF: basaltic, feeder(?) dike
M: minette
mg# = Mg/(Mg+Fe+Mn)

APPENDIX D.3: ELECTRON MICROPROBE ANALYSES OF PYROXENE

	RDS-8-06b B	RDS-8-28b B	RDS-8-9 B	RDS-8-31 B	RDS-8-07b B	RDS-8-8 B	RDS-8-30 B	RDS-8-05b B
SiO_2	48.5	49.93	50.97	51.02	50.9	50.83	51.33	51.19
TiO_2	1.22	1.11	0.82	0.8	0.83	0.86	0.79	0.76
Al_2O_3	5.35	4.68	3.09	3.23	3.25	3.35	3.04	3.09
FeO	7.67	7.38	7.71	7.63	6.99	7.04	7.05	6.75
MnO	0.14	0.16	0.2	0.22	0.21	0.2	0.18	0.17
MgO	13.71	14.4	15.51	15.46	14.94	15.3	15.54	15.1
CaO	20.88	22.84	22.33	22.25	21.18	22.84	22.86	21.25
Na_2O	0.36	0.37	0.21	0.33	0.38	0.33	0.32	0.31
Total	97.83	100.87	100.84	100.94	98.68	100.75	101.11	98.62
Numbers of ions on the basis of 6O								
Si	1.842	1.845	1.882	1.881	1.907	1.876	1.887	1.915
Al	0.239	0.204	0.134	0.140	0.143	0.146	0.132	0.136
Ti	0.035	0.031	0.023	0.022	0.023	0.024	0.022	0.021
Mg	0.776	0.793	0.854	0.850	0.834	0.842	0.852	0.842
Fe^{2+}	0.244	0.228	0.238	0.235	0.219	0.217	0.217	0.211
Mn	0.005	0.005	0.006	0.007	0.007	0.006	0.006	0.005
Ca	0.850	0.904	0.883	0.879	0.850	0.903	0.900	0.852
Na	0.027	0.027	0.015	0.024	0.028	0.024	0.023	0.022
Total	4.017	4.036	4.036	4.038	4.012	4.039	4.037	4.006
Atomic percentages								
Mg	41.4	41.1	43.1	43.1	43.7	42.8	43.1	44.1
Fe+Mn	13.2	12.1	12.3	12.3	11.8	11.4	11.3	11.3
Ca	45.3	46.8	44.6	44.6	44.5	45.9	45.6	44.6
mg#	75.8	77.3	77.8	77.8	78.7	79.0	79.3	79.5

	RDS-8-16 B	RDS-8-09b B	RDS-10-08 A-SRD	RDS-10-09 A-SRD	RDS-10-10 A-SRD	RDS-10-12 A-SRD	RDS-10-11 A-SRD	RDS-10-14 A-SRD
SiO_2	51.72	51.75	51.86	52.03	52.41	48.94	47.57	47.14
TiO_2	0.69	0.68	0.31	0.4	0.36	1.56	2.16	2.05
Al_2O_3	2.72	2.84	2.33	2.32	2.11	5.27	7.03	6.94
FeO	6.68	6.51	8.83	8.42	8.32	8.06	7.7	7.63
MnO	0.17	0.16	0.23	0.21	0.24	0.12	0.08	0.11
MgO	15.66	15.33	13.5	14.24	14.1	13.71	13.06	13.67
CaO	22.73	20.98	22.82	22.75	22.87	22.56	22.49	22.49
Na_2O	0.29	0.29	0.56	0.54	0.52	0	0	0.38
Total	100.66	98.54	100.44	100.91	100.93	100.22	100.09	100.41
Numbers of ions on the basis of 6O								
Si	1.904	1.932	1.933	1.926	1.938	1.824	1.774	1.757
Al	0.118	0.125	0.102	0.101	0.092	0.231	0.309	0.305
Ti	0.019	0.019	0.009	0.011	0.010	0.044	0.061	0.057
Mg	0.859	0.853	0.750	0.786	0.777	0.762	0.726	0.760
Fe^{2+}	0.206	0.203	0.275	0.261	0.257	0.251	0.240	0.238
Mn	0.005	0.005	0.007	0.007	0.008	0.004	0.003	0.003
Ca	0.896	0.839	0.911	0.902	0.906	0.901	0.899	0.898
Na	0.021	0.021	0.040	0.039	0.037	0.000	0.000	0.027
Total	4.028	3.997	4.028	4.032	4.025	4.017	4.011	4.046
Atomic percentages								
Mg	43.7	44.9	38.6	40.2	39.9	39.7	38.9	40.0
Fe+Mn	10.7	11.0	14.5	13.7	13.6	13.3	13.0	12.7
Ca	45.6	44.1	46.9	46.1	46.5	47.0	48.1	47.3
mg#	80.3	80.4	72.6	74.6	74.6	74.9	75.0	75.9

A: analcime-bearing
A-SRD: analcime-bearing, Spears Ranch Dike
AS: analcime-bearing, speckled texture
B: basaltic
B-bt: basaltic with significant biotite
BPP: basaltic, pyroxene porphyry dike
BF: basaltic, feeder(?) dike
M: minette
mg# = Mg/(Mg+Fe+Mn)

APPENDIX D.3: ELECTRON MICROPROBE ANALYSES OF PYROXENE

	RDS-10-13 A-SRD	RDS-11-13 BF	RDS-11-14 BF	RDS-11-15 BF	RDS-11-16 BF	RDS-11-17 BF	RDS-11-18 BF	RDS-15A-25 B
SiO_2	49.15	49.42	51.02	50.61	50.38	52.61	52.67	46.09
TiO_2	1.48	1.58	1.27	1.33	1.33	0.72	0.79	2.24
Al_2O_3	4.74	3.97	2.91	3.17	3.64	1.76	1.84	7.59
FeO	7.71	9.53	9.09	9.1	8.97	8.97	9.05	9.34
MnO	0.09	0.23	0.29	0.25	0.22	0.32	0.28	0.13
MgO	13.85	14	14.46	14.48	14.54	15.66	15.82	13.02
CaO	22.74	20.58	20.65	20.87	20.91	20.12	19.92	21.95
Na_2O	0	0	0.36	0.35	1.75	0.28	0.31	0.5
Total	99.76	99.31	100.05	100.16	101.74	100.44	100.68	100.86
Numbers of ions on the basis of 6O								
Si	1.838	1.861	1.902	1.887	1.858	1.944	1.941	1.725
Al	0.209	0.176	0.128	0.139	0.158	0.077	0.080	0.335
Ti	0.042	0.045	0.036	0.037	0.037	0.020	0.022	0.063
Mg	0.772	0.786	0.804	0.805	0.800	0.863	0.869	0.727
Fe^{2+}	0.241	0.300	0.283	0.284	0.277	0.277	0.279	0.292
Mn	0.003	0.007	0.009	0.008	0.007	0.010	0.009	0.004
Ca	0.911	0.830	0.825	0.834	0.826	0.797	0.786	0.880
Na	0.000	0.000	0.026	0.025	0.125	0.020	0.022	0.036
Total	4.016	4.006	4.012	4.019	4.088	4.007	4.008	4.063
Atomic percentages								
Mg	40.1	40.9	41.8	41.7	41.9	44.3	44.7	38.2
Fe+Mn	12.7	16.0	15.2	15.1	14.8	14.8	14.8	15.6
Ca	47.3	43.2	42.9	43.2	43.3	40.9	40.5	46.2
mg#	76.0	71.9	73.3	73.4	73.8	75.0	75.1	71.0

	RDS-15A-44 B	RDS-15A-21 B	RDS-15A-30 B	RDS-15A-18 B	RDS-15A-29 B	RDS-15A-28 B	RDS-15A-52 B	RDS-15A-39 B
SiO_2	51.36	47.44	47.27	47.21	48.23	48.97	51.14	51.06
TiO_2	0.84	1.87	1.82	1.79	1.57	1.5	0.76	0.72
Al_2O_3	2.18	6.71	6.1	6.71	5.85	5.39	3.31	3.34
FeO	9.32	8.39	8.48	8.27	8.05	7.86	8.29	8.13
MnO	0.33	0.17	0.16	0.12	0.14	0.18	0.18	0.18
MgO	14.85	13.27	13.65	13.48	14.04	14.1	15.33	15.12
CaO	21.24	22.61	22.3	22.32	22.6	22.77	21.44	21.81
Na_2O	0.33	0.42	0.48	0.43	0.42	0.43	0.34	0.32
Total	100.45	100.88	100.26	100.33	100.9	101.2	100.79	100.68
Numbers of ions on the basis of 6O								
Si	1.913	1.767	1.773	1.766	1.791	1.811	1.888	1.888
Al	0.096	0.294	0.270	0.296	0.256	0.235	0.144	0.146
Ti	0.024	0.052	0.051	0.050	0.044	0.042	0.021	0.020
Mg	0.824	0.737	0.763	0.752	0.777	0.777	0.844	0.833
Fe^{2+}	0.290	0.261	0.266	0.259	0.250	0.243	0.256	0.251
Mn	0.010	0.005	0.005	0.004	0.004	0.006	0.006	0.006
Ca	0.847	0.902	0.896	0.894	0.899	0.902	0.848	0.864
Na	0.024	0.030	0.035	0.031	0.030	0.031	0.024	0.023
Total	4.028	4.049	4.059	4.052	4.052	4.046	4.031	4.031
Atomic percentages								
Mg	41.8	38.7	39.5	39.4	40.3	40.3	43.2	42.6
Fe+Mn	15.2	14.0	14.0	13.8	13.2	12.9	13.4	13.1
Ca	43.0	47.3	46.4	46.9	46.6	46.8	43.4	44.2
mg#	73.3	73.4	73.8	74.1	75.3	75.8	76.3	76.4

A: analcime-bearing
A-SRD: analcime-bearing, Spears Ranch Dike
AS: analcime-bearing, speckled texture
B: basaltic
B-bt: basaltic with significant biotite
BPP: basaltic, pyroxene porphyry dike
BF: basaltic, feeder(?) dike
M: minette
mg# = Mg/(Mg+Fe+Mn)

APPENDIX D.3: ELECTRON MICROPROBE ANALYSES OF PYROXENE

	RDS-15A-42 B	RDS-15A-23 B	RDS-15A-24 B	RDS-15A-22 B	RDS-15A-40 B	RDS-15A-19 B	RDS-15A-41 B	RDS-15A-37 B
SiO_2	50.71	48.76	48.55	51.48	52.25	52.25	51.75	52.54
TiO_2	0.65	1.47	1.37	0.84	0.48	0.68	0.45	0.39
Al_2O_3	4.67	5.28	5.49	3.23	3.12	2.59	3.55	2.82
FeO	8.59	7.1	6.6	6.64	6.91	6.79	6.49	6.36
MnO	0.26	0.1	0.11	0.15	0.16	0.15	0.15	0.17
MgO	16.4	14.3	14.42	15.68	16.62	16.53	16.89	16.83
CaO	18.39	22.67	22.52	22.94	20.56	21.58	20.04	20.87
Na_2O	0.43	0.38	0.39	0.35	0.36	0.27	0.38	0.36
Total	100.1	100.06	99.45	101.31	100.46	100.84	99.7	100.34
Numbers of ions on the basis of 6O								
Si	1.871	1.816	1.815	1.885	1.914	1.912	1.905	1.923
Al	0.203	0.232	0.242	0.139	0.135	0.112	0.154	0.122
Ti	0.018	0.041	0.039	0.023	0.013	0.019	0.012	0.011
Mg	0.902	0.794	0.804	0.856	0.908	0.902	0.927	0.918
Fe^{2+}	0.265	0.221	0.206	0.203	0.212	0.208	0.200	0.195
Mn	0.008	0.003	0.003	0.005	0.005	0.005	0.005	0.005
Ca	0.727	0.905	0.902	0.900	0.807	0.846	0.790	0.818
Na	0.031	0.027	0.028	0.025	0.026	0.019	0.027	0.026
Total	4.025	4.040	4.039	4.035	4.018	4.023	4.019	4.018
Atomic percentages								
Mg	47.4	41.3	42.0	43.6	47.0	46.0	48.2	47.4
Fe+Mn	14.4	11.7	11.0	10.6	11.2	10.8	10.6	10.3
Ca	38.2	47.0	47.1	45.8	41.8	43.2	41.1	42.3
mg#	76.8	78.0	79.3	80.5	80.7	80.9	81.9	82.1

	RDS-15A-43 B	RDS-15A-38 B	RDS-15B-24 B	RDS-15B-11 B	RDS-15B-23 B	RDS-15B-10 B	RDS-15B-07 B	RDS-15B-09 B
SiO_2	53.54	52.61	48.28	48.3	49.62	51.63	49.17	50.5
TiO_2	0.28	0.32	1.52	1.49	1.86	0.82	1.07	1.06
Al_2O_3	1.79	2.67	5.92	5.89	4.32	3.4	4.54	4.2
FeO	5.71	5.08	8.19	8.17	7.86	7.06	6.44	6.42
MnO	0.17	0.14	0.14	0.14	0.24	0.19	0.11	0.12
MgO	18.27	16.9	13.84	13.88	14.65	15.6	15.03	15.04
CaO	20.41	21.76	22.45	22.72	21.63	22.22	22.96	22.89
Na_2O	0.26	0.35	0.41	0.41	0.61	0.34	0.34	0.35
Total	100.43	99.83	100.75	101	100.79	101.26	99.66	100.58
Numbers of ions on the basis of 6O								
Si	1.948	1.929	1.795	1.793	1.837	1.889	1.835	1.861
Al	0.077	0.115	0.259	0.258	0.188	0.147	0.200	0.182
Ti	0.008	0.009	0.043	0.042	0.052	0.023	0.030	0.029
Mg	0.991	0.924	0.767	0.768	0.809	0.851	0.836	0.826
Fe^{2+}	0.174	0.156	0.255	0.254	0.243	0.216	0.201	0.198
Mn	0.005	0.004	0.004	0.004	0.008	0.006	0.003	0.004
Ca	0.795	0.855	0.894	0.904	0.858	0.871	0.918	0.904
Na	0.018	0.025	0.030	0.030	0.044	0.024	0.025	0.025
Total	4.016	4.017	4.047	4.051	4.039	4.027	4.048	4.030
Atomic percentages								
Mg	50.4	47.7	39.9	39.8	42.2	43.8	42.7	42.8
Fe+Mn	9.1	8.3	13.5	13.4	13.1	11.4	10.4	10.4
Ca	40.5	44.1	46.6	46.8	44.7	44.8	46.9	46.8
mg#	84.7	85.2	74.8	74.9	76.3	79.3	80.4	80.4

A: analcime-bearing
A-SRD: analcime-bearing, Spears Ranch Dike
AS: analcime-bearing, speckled texture
B: basaltic
B-bt: basaltic with significant biotite
BPP: basaltic, pyroxene porphyry dike
BF: basaltic, feeder(?) dike
M: minette
mg# = Mg/(Mg+Fe+Mn)

APPENDIX D.3: ELECTRON MICROPROBE ANALYSES OF PYROXENE

	RDS-15B-08 B	RDS-15C-09 B	RDS-15C-07 B	RDS-15C-11 B	RDS-15C-13 B	RDS-15C-12 B	RDS-15C-10 B	RDS-15C-30 B
SiO_2	51.94	45.92	48.17	48.95	48.03	51.07	51.36	52.42
TiO_2	0.62	1.83	1.47	1.29	1.52	0.78	0.66	0.59
Al_2O_3	3.64	6.53	5.84	4.15	4.99	3	2.61	2.18
FeO	5.46	8.38	7.82	8.08	7.87	7.07	6.24	5.61
MnO	0.12	0.13	0.13	0.21	0.13	0.16	0.11	0.18
MgO	16.38	13.23	13.87	14.82	14.27	16.15	16.2	16.5
CaO	21.8	22.31	22.5	21.43	21.9	21.66	22.42	22.46
Na_2O	0.49	0.45	0.41	0.48	0.51	0.32	0.26	0.26
Total	100.45	98.78	100.21	99.41	99.22	100.21	99.86	100.2
Numbers of ions on the basis of 6O								
Si	1.898	1.751	1.798	1.840	1.811	1.888	1.902	1.926
Al	0.157	0.294	0.257	0.184	0.222	0.131	0.114	0.094
Ti	0.017	0.052	0.041	0.036	0.043	0.022	0.018	0.016
Mg	0.893	0.752	0.772	0.830	0.802	0.890	0.894	0.904
Fe^{2+}	0.167	0.267	0.244	0.254	0.248	0.219	0.193	0.172
Mn	0.004	0.004	0.004	0.007	0.004	0.005	0.003	0.006
Ca	0.854	0.912	0.900	0.863	0.885	0.858	0.889	0.884
Na	0.035	0.033	0.030	0.035	0.037	0.023	0.019	0.019
Total	4.024	4.066	4.047	4.049	4.053	4.036	4.032	4.020
Atomic percentages								
Mg	46.6	38.9	40.2	42.5	41.4	45.1	45.2	46.0
Fe+Mn	8.9	14.0	12.9	13.3	13.0	11.3	9.9	9.1
Ca	44.5	47.1	46.9	44.2	45.6	43.5	44.9	45.0
mg#	84.0	73.5	75.7	76.1	76.1	79.9	82.0	83.5

	RDS-16A-08 BPP	RDS-16A-37 BPP	RDS-16A-36 BPP	RDS-16A-16 BPP	RDS-16A-40 BPP	RDS-16A-25 BPP	RDS-16A-26 BPP	RDS-16A-05 BPP
SiO_2	69.29	50.16	50.19	51.89	51.76	52.06	52.38	49.58
TiO_2	0.12	1.39	1.21	0.88	0.87	0.8	0.75	1.04
Al_2O_3	20.87	3.08	3.16	2.25	2.53	2.05	1.8	4.87
FeO	0.45	11.48	11.54	11.08	10.49	10.2	10.03	9.1
MnO	0.02	0.42	0.34	0.36	0.3	0.36	0.4	0.26
MgO	0	14.07	14.45	15.42	15.25	15.56	15.65	14.53
CaO	1.35	19.77	19.21	18.79	19.63	19.47	20.14	21.14
Na_2O	5.78	0.39	0.39	0.49	0.5	0.42	0.39	0.39
Total	97.88	100.76	100.49	101.16	101.33	100.92	101.54	100.91
Numbers of ions on the basis of 6O								
Si	2.271	1.877	1.879	1.919	1.910	1.925	1.927	1.838
Al	0.806	0.136	0.139	0.098	0.110	0.089	0.078	0.213
Ti	0.003	0.039	0.034	0.024	0.024	0.022	0.021	0.029
Mg	0.000	0.785	0.807	0.850	0.839	0.858	0.858	0.803
Fe^{2+}	0.012	0.359	0.361	0.343	0.324	0.315	0.309	0.282
Mn	0.001	0.013	0.011	0.011	0.009	0.011	0.012	0.008
Ca	0.047	0.793	0.771	0.744	0.776	0.771	0.794	0.840
Na	0.367	0.028	0.028	0.035	0.036	0.030	0.028	0.028
Total	3.507	4.030	4.031	4.025	4.028	4.023	4.027	4.041
Atomic percentages								
Mg	0.0	40.3	41.4	43.6	43.1	43.9	43.5	41.5
Fe+Mn	21.4	19.1	19.1	18.2	17.1	16.7	16.3	15.0
Ca	78.6	40.6	39.5	38.2	39.8	39.4	40.2	43.4
mg#	0.0	67.8	68.4	70.6	71.6	72.4	72.8	73.5

A: analcime-bearing
A-SRD: analcime-bearing, Spears Ranch Dike
AS: analcime-bearing, speckled texture
B: basaltic
B-bt: basaltic with significant biotite
BPP: basaltic, pyroxene porphyry dike
BF: basaltic, feeder(?) dike
M: minette
mg# = Mg/(Mg+Fe+Mn)

APPENDIX D.3: ELECTRON MICROPROBE ANALYSES OF PYROXENE

	RDS-16A-21 BPP	RDS-16A-23 BPP	RDS-16A-18 BPP	RDS-16A-44 BPP	RDS-16A-09 BPP	RDS-16A-41 BPP	RDS-16A-22 BPP	RDS-16A-43 BPP
SiO_2	52.1	49.85	49.94	52.1	49.78	50.23	49.92	50.46
TiO_2	0.64	1.02	0.95	0.75	0.98	0.87	1.06	0.85
Al_2O_3	2.18	4.78	4.74	2.03	4.41	4.4	5.49	3.65
FeO	9.23	8.89	8.72	9.58	8.49	8.7	8.64	8.37
MnO	0.38	0.23	0.24	0.31	0.21	0.18	0.24	0.22
MgO	15.3	14.49	14.24	15.73	14.59	15.13	15.36	15.01
CaO	20.52	21.21	21.48	19.92	21.7	20.69	19.94	21.42
Na_2O	0.45	0.38	0.41	0.39	0.36	0.36	0.44	0.32
Total	100.8	100.85	100.72	100.81	100.52	100.56	101.09	100.3
Numbers of ions on the basis of 6O								
Si	1.926	1.846	1.852	1.925	1.850	1.860	1.835	1.875
Al	0.095	0.209	0.207	0.088	0.193	0.192	0.238	0.160
Ti	0.018	0.028	0.026	0.021	0.027	0.024	0.029	0.024
Mg	0.843	0.800	0.787	0.867	0.808	0.835	0.842	0.831
Fe^{2+}	0.285	0.275	0.270	0.296	0.264	0.269	0.266	0.260
Mn	0.012	0.007	0.008	0.010	0.007	0.006	0.007	0.007
Ca	0.813	0.842	0.853	0.789	0.864	0.821	0.785	0.853
Na	0.032	0.027	0.029	0.028	0.026	0.026	0.031	0.023
Total	4.025	4.035	4.033	4.024	4.039	4.033	4.033	4.033
Atomic percentages								
Mg	43.2	41.6	41.0	44.2	41.6	43.3	44.3	42.6
Fe+Mn	15.2	14.7	14.5	15.6	13.9	14.2	14.4	13.7
Ca	41.6	43.7	44.5	40.2	44.5	42.5	41.3	43.7
mg#	73.9	73.9	73.9	73.9	74.9	75.2	75.5	75.7

	RDS-16A-27 BPP	RDS-16A-19 BPP	RDS-16A-20 BPP	RDS-16A-24 BPP	RDS-16A-33 BPP	RDS-16A-42 BPP	RDS-16A-06 BPP	RDS-16A-32 BPP
SiO_2	50.7	50.88	51.22	50.48	49.94	50.19	49.95	53.24
TiO_2	0.82	0.75	0.65	0.73	0.74	0.91	0.67	0.31
Al_2O_3	3.94	4.83	3.24	4.54	4.58	5.31	4.65	2.11
FeO	8.36	8.56	8.44	8.21	8.01	7.99	7.78	5.6
MnO	0.22	0.22	0.18	0.19	0.18	0.22	0.18	0.17
MgO	15.09	15.74	15.61	15.63	15.54	15.58	15.53	17.68
CaO	21.5	19.96	21.08	20.37	20.49	19.86	20.79	21.36
Na_2O	0.32	0.47	0.34	0.42	0.38	0.43	0.45	0.3
Total	100.95	101.41	100.76	100.57	99.86	100.49	100	100.77
Numbers of ions on the basis of 6O								
Si	1.871	1.861	1.891	1.862	1.856	1.848	1.854	1.936
Al	0.171	0.208	0.141	0.197	0.201	0.230	0.203	0.090
Ti	0.023	0.021	0.018	0.020	0.021	0.025	0.019	0.008
Mg	0.830	0.858	0.859	0.860	0.861	0.855	0.859	0.958
Fe^{2+}	0.258	0.262	0.261	0.253	0.249	0.246	0.241	0.170
Mn	0.007	0.007	0.006	0.006	0.006	0.007	0.006	0.005
Ca	0.850	0.782	0.834	0.805	0.816	0.784	0.827	0.832
Na	0.023	0.033	0.024	0.030	0.027	0.031	0.032	0.021
Total	4.032	4.031	4.033	4.034	4.036	4.027	4.042	4.021
Atomic percentages								
Mg	42.7	45.0	43.9	44.7	44.6	45.2	44.5	48.7
Fe+Mn	13.6	14.1	13.6	13.5	13.2	13.4	12.8	8.9
Ca	43.7	41.0	42.6	41.8	42.2	41.4	42.8	42.3
mg#	75.8	76.2	76.3	76.8	77.2	77.2	77.7	84.5

A: analcime-bearing
A-SRD: analcime-bearing, Spears Ranch Dike
AS: analcime-bearing, speckled texture
B: basaltic
B-bt: basaltic with significant biotite
BPP: basaltic, pyroxene porphyry dike
BF: basaltic, feeder(?) dike
M: minette
mg# = Mg/(Mg+Fe+Mn)

APPENDIX D.3: ELECTRON MICROPROBE ANALYSES OF PYROXENE

	RDS-16B-17 BPP	RDS-16B-18 BPP	RDS-16B-20 BPP	RDS-16B-15 BPP	RDS-16B-19 BPP	RDS-16B-28 BPP	RDS-16B-16 BPP	RDS-16C-09 BPP
SiO_2	50.22	51.22	51.56	49.43	51.53	50.54	52.29	51.92
TiO_2	1.09	0.87	0.78	1.14	0.76	0.86	0.34	0.39
Al_2O_3	2.99	2.25	1.98	3.75	2.06	3.56	3.11	1.9
FeO	10.53	10.57	10.37	9.06	8.82	8.39	5.92	10.28
MnO	0.33	0.32	0.34	0.24	0.35	0.23	0.14	0.39
MgO	14.78	15.03	15.09	14.48	15.35	14.92	16.83	13.49
CaO	19.77	19.38	19.77	21.42	21.14	21.84	21.27	21.05
Na_2O	0.37	0.43	0.4	0.34	0.29	0.32	0.36	0.7
Total	100.08	100.07	100.29	99.86	100.3	100.66	100.26	100.12
Numbers of ions on the basis of 6O								
Si	1.883	1.916	1.924	1.855	1.916	1.874	1.914	1.946
Al	0.132	0.099	0.087	0.166	0.090	0.156	0.134	0.084
Ti	0.031	0.024	0.022	0.032	0.021	0.024	0.009	0.011
Mg	0.826	0.838	0.839	0.810	0.851	0.825	0.919	0.754
Fe^{2+}	0.330	0.331	0.324	0.284	0.274	0.260	0.181	0.322
Mn	0.010	0.010	0.011	0.008	0.011	0.007	0.004	0.012
Ca	0.794	0.777	0.790	0.861	0.842	0.868	0.834	0.845
Na	0.027	0.031	0.029	0.025	0.021	0.023	0.026	0.051
Total	4.034	4.026	4.025	4.042	4.028	4.036	4.022	4.026
Atomic percentages								
Mg	42.1	42.9	42.7	41.3	43.0	42.1	47.4	39.0
Fe+Mn	17.4	17.4	17.0	14.9	14.4	13.6	9.6	17.3
Ca	40.5	39.7	40.2	43.9	42.6	44.3	43.0	43.7
mg#	70.8	71.1	71.5	73.5	74.9	75.5	83.2	69.3

	RDS-16C-08 BPP	RDS-16C-07 BPP	RDS-16C-11 BPP	RDS-16C-10 BPP	RDS-17-19 BF	RDS-17-26 BF	RDS-17-25 BF	RDS-17-23 BF
SiO_2	50.69	49.83	48.38	51.75	46.48	48.11	51.28	51.51
TiO_2	0.92	0.89	1	0.33	1.74	1.41	0.75	0.74
Al_2O_3	2.39	4.51	5.03	2.68	6.64	6.04	3.39	3.16
FeO	10.63	8.76	8.39	5.84	8.79	8.46	7.35	7.01
MnO	0.36	0.22	0.22	0.16	0.13	0.12	0.17	0.16
MgO	15.13	14.5	14.54	16.95	12.97	13.73	15.51	15.45
CaO	19.22	21.36	21.25	21.41	22.24	22.78	22.23	22.71
Na_2O	0.46	0.41	0.35	0.35	0.33	0.37	0.3	0.27
Total	99.8	100.48	99.16	99.47	99.32	101.02	100.98	101.01
Numbers of ions on the basis of 6O								
Si	1.904	1.853	1.824	1.913	1.762	1.788	1.885	1.892
Al	0.106	0.198	0.223	0.117	0.297	0.265	0.147	0.137
Ti	0.026	0.025	0.028	0.009	0.050	0.039	0.021	0.020
Mg	0.847	0.804	0.817	0.934	0.733	0.761	0.850	0.846
Fe^{2+}	0.334	0.272	0.265	0.181	0.279	0.263	0.226	0.215
Mn	0.011	0.007	0.007	0.005	0.004	0.004	0.005	0.005
Ca	0.773	0.851	0.858	0.848	0.903	0.907	0.876	0.894
Na	0.033	0.030	0.026	0.025	0.024	0.027	0.021	0.019
Total	4.034	4.038	4.049	4.032	4.052	4.053	4.031	4.029
Atomic percentages								
Mg	43.1	41.6	42.0	47.5	38.2	39.3	43.4	43.2
Fe+Mn	17.6	14.4	13.9	9.4	14.7	13.8	11.8	11.2
Ca	39.3	44.0	44.1	43.1	47.1	46.9	44.7	45.6
mg#	71.0	74.2	75.1	83.4	72.2	74.0	78.6	79.3

A: analcime-bearing
A-SRD: analcime-bearing, Spears Ranch Dike
AS: analcime-bearing, speckled texture
B: basaltic
B-bt: basaltic with significant biotite
BPP: basaltic, pyroxene porphyry dike
BF: basaltic, feeder(?) dike
M: minette
mg# = Mg/(Mg+Fe+Mn)

APPENDIX D.3: ELECTRON MICROPROBE ANALYSES OF PYROXENE

	RDS-17-24 BF	RDS-013A-05 AS	RDS-013A-08 AS	RDS-013A-03 AS	RDS-013A-06 AS	RDS-013A-02 AS	RDS-013A-40 AS
SiO_2	51.27	48.65	48.86	50.62	51.05	50.93	50.99
TiO_2	0.66	1.79	1.6	1.13	0.9	1.1	1.04
Al_2O_3	3.02	5.61	5.15	3.54	2.87	3.48	3.3
FeO	6.97	8.81	8.61	8.5	8.59	8.33	8.01
MnO	0.14	0.24	0.25	0.22	0.25	0.22	0.27
MgO	15.56	13.03	13.44	14.75	15.2	14.88	14.49
CaO	22.16	21.64	21.74	20.55	20.1	20.63	21.31
Na_2O	0.25	0.5	0.44	0.45	0.5	0.4	0.41
Total	100.03	100.27	100.09	99.76	99.46	99.97	99.82
Numbers of ions on the basis of 6O							
Si	1.899	1.818	1.828	1.887	1.907	1.892	1.899
Al	0.132	0.247	0.227	0.156	0.126	0.152	0.145
Ti	0.018	0.050	0.045	0.032	0.025	0.031	0.029
Mg	0.859	0.726	0.750	0.820	0.847	0.824	0.804
Fe^{2+}	0.216	0.275	0.269	0.265	0.268	0.259	0.249
Mn	0.004	0.008	0.008	0.007	0.008	0.007	0.009
Ca	0.879	0.866	0.871	0.821	0.804	0.821	0.850
Na	0.018	0.036	0.032	0.033	0.036	0.029	0.030
Total	4.026	4.026	4.030	4.020	4.022	4.015	4.015
Atomic percentages							
Mg	43.9	38.7	39.5	42.9	43.9	43.1	42.1
Fe+Mn	11.2	15.1	14.6	14.2	14.3	13.9	13.5
Ca	44.9	46.2	45.9	42.9	41.7	43.0	44.5
mg#	79.6	72.0	73.0	75.1	75.4	75.6	75.7

	RDS-013A-39 AS	RDS-013A-07 AS	RDS-013A-04 AS	RDS-013A-01 AS	RDS-013A-33 AS	RDS-027-10 B	RDS-027-13 B
SiO_2	50.91	49.53	50.08	51.69	50.48	51.84	51.42
TiO_2	0.91	1.12	1.03	0.68	0.88	0.71	0.72
Al_2O_3	3.19	5.95	5.66	3.32	5.32	2.83	3
FeO	7.66	6.4	6.38	6.68	5.24	8.55	8.33
MnO	0.22	0.13	0.15	0.21	0.13	0.26	0.21
MgO	14.6	14.27	14.58	15.64	14.95	15.97	15.53
CaO	21.45	21.79	21.98	21.2	21.93	20.44	21.1
Na_2O	0.37	0.4	0.39	0.32	0.35	0.24	0.24
Total	99.31	99.59	100.25	99.74	99.28	100.84	100.55
Numbers of ions on the basis of 6O							
Si	1.903	1.838	1.845	1.910	1.866	1.908	1.900
Al	0.141	0.260	0.246	0.145	0.232	0.123	0.131
Ti	0.026	0.031	0.029	0.019	0.024	0.020	0.020
Mg	0.814	0.789	0.801	0.862	0.824	0.876	0.856
Fe^{2+}	0.239	0.199	0.197	0.206	0.162	0.263	0.257
Mn	0.007	0.004	0.005	0.007	0.004	0.008	0.007
Ca	0.859	0.866	0.868	0.839	0.869	0.806	0.835
Na	0.027	0.029	0.028	0.023	0.025	0.017	0.017
Total	4.015	4.016	4.017	4.010	4.006	4.020	4.023
Atomic percentages							
Mg	42.4	42.5	42.8	45.0	44.3	44.9	43.8
Fe+Mn	12.8	10.9	10.8	11.1	8.9	13.9	13.5
Ca	44.8	46.6	46.4	43.9	46.7	41.3	42.7
mg#	76.8	79.6	79.9	80.2	83.2	76.4	76.4

A: analcime-bearing
A-SRD: analcime-bearing, Spears Ranch Dike
AS: analcime-bearing, speckled texture
B: basaltic
B-bt: basaltic with significant biotite
BPP: basaltic, pyroxene porphyry dike
BF: basaltic, feeder(?) dike
M: minette
mg# = Mg/(Mg+Fe+Mn)

APPENDIX D.3: ELECTRON MICROPROBE ANALYSES OF PYROXENE

	RDS-027-11 B	RDS-027-12 B	RDS-027-09 B	RDS-027-07 B	RDS-027-08 B	RDS-106-08 M	RDS-106-05 M	RDS-106-06 M
SiO_2	52	52.57	53.66	53.45	53.44	47.13	48.26	48.81
TiO_2	0.67	0.48	0.27	0.27	0.22	1.62	1.34	1.21
Al_2O_3	2.71	2.91	2.19	2.7	2.57	6.52	5.26	5.11
FeO	7.83	5.74	5.61	4.81	4.71	8.41	7.93	8.05
MnO	0.19	0.14	0.14	0.16	0.15	0.11	0.14	0.17
MgO	15.74	16.12	17.6	17.61	18.12	13.52	14	14.37
CaO	21.55	22.24	20.4	20.53	19.84	22.23	22.3	21.97
Na_2O	0.24	0.31	0.36	0.46	0.5	0	0.39	0.46
Total	100.93	100.51	100.23	99.99	99.55	99.54	99.62	100.15
Numbers of ions on the basis of 6O								
Si	1.911	1.922	1.953	1.944	1.948	1.775	1.813	1.822
Al	0.117	0.125	0.094	0.116	0.110	0.289	0.233	0.225
Ti	0.019	0.013	0.007	0.007	0.006	0.046	0.038	0.034
Mg	0.862	0.879	0.955	0.955	0.985	0.759	0.784	0.800
Fe^{2+}	0.241	0.176	0.171	0.146	0.144	0.265	0.249	0.251
Mn	0.006	0.004	0.004	0.005	0.005	0.004	0.004	0.005
Ca	0.848	0.871	0.795	0.800	0.775	0.897	0.897	0.878
Na	0.017	0.022	0.025	0.032	0.035	0.000	0.028	0.033
Total	4.021	4.013	4.005	4.006	4.008	4.035	4.047	4.049
Atomic percentages								
Mg	44.1	45.5	49.6	50.1	51.6	39.4	40.5	41.3
Fe+Mn	12.6	9.3	9.1	7.9	7.8	13.9	13.1	13.3
Ca	43.3	45.1	41.3	42.0	40.6	46.6	46.4	45.4
mg#	77.8	83.0	84.5	86.3	86.9	73.9	75.6	75.7

	RDS-106-07 M	RDS-106-04 M	RDS-106-14 M	RDS-130-02 BF	RDS-130-01 BF	RDS-130-07 BF	RDS-130-04 BF	RDS-130-12 BF
SiO_2	49.33	51.21	51.64	47.4	46.69	49.63	50.54	48.86
TiO_2	1.1	0.81	0.76	2.07	2.01	1.58	1.39	1.58
Al_2O_3	4.52	3.34	2.97	6.12	6.96	3.8	3.18	4.79
FeO	7.03	6.76	6.67	9.83	9.44	9.76	9.92	9.71
MnO	0.15	0.17	0.14	0.17	0.15	0.28	0.28	0.23
MgO	14.76	15.57	15.64	12.84	12.85	13.9	14.33	13.99
CaO	22.32	22.37	22.37	21.84	21.44	21.09	20.44	21.05
Na_2O	0	0.37	0.33	0.39	0.27	0.45	0.5	0
Total	99.21	100.6	100.52	100.66	99.81	100.49	100.58	100.21
Numbers of ions on the basis of 6O								
Si	1.847	1.886	1.901	1.777	1.761	1.855	1.883	1.829
Al	0.199	0.145	0.129	0.270	0.309	0.167	0.140	0.211
Ti	0.031	0.022	0.021	0.058	0.057	0.044	0.039	0.044
Mg	0.824	0.855	0.858	0.718	0.722	0.775	0.796	0.781
Fe^{2+}	0.220	0.208	0.205	0.308	0.298	0.305	0.309	0.304
Mn	0.005	0.005	0.004	0.005	0.005	0.009	0.009	0.007
Ca	0.895	0.883	0.882	0.877	0.866	0.845	0.816	0.844
Na	0.000	0.026	0.024	0.028	0.020	0.033	0.036	0.000
Total	4.022	4.032	4.025	4.043	4.038	4.033	4.027	4.021
Atomic percentages								
Mg	42.4	43.8	44.0	37.6	38.2	40.1	41.2	40.3
Fe+Mn	11.6	10.9	10.8	16.4	16.0	16.2	16.5	16.1
Ca	46.1	45.2	45.2	46.0	45.8	43.7	42.3	43.6
mg#	78.6	80.0	80.4	69.6	70.5	71.2	71.5	71.5

A: analcime-bearing
A-SRD: analcime-bearing, Spears Ranch Dike
AS: analcime-bearing, speckled texture
B: basaltic
B-bt: basaltic with significant biotite
BPP: basaltic, pyroxene porphyry dike
BF: basaltic, feeder(?) dike
M: minette
mg# = Mg/(Mg+Fe+Mn)

APPENDIX D.3: ELECTRON MICROPROBE ANALYSES OF PYROXENE

	RDS-130-05 BF	RDS-130-10 BF	RDS-130-09 BF	RDS-130-08 BF	RDS-130-03 BF	RDS-130-11 BF	RDS-130-06 BF
SiO_2	46.84	49.5	48.91	52.06	50.56	51.73	51.83
TiO_2	1.91	1.49	1.41	0.92	1.03	0.86	0.79
Al_2O_3	6.85	4.31	4.32	1.99	3.97	2.63	2.87
FeO	9.04	9.78	9.34	9.62	8.64	8.81	7.66
MnO	0.15	0.26	0.2	0.29	0.22	0.23	0.15
MgO	13.04	14.36	14.04	15.3	15.2	16.2	16.2
CaO	21.43	20.61	21.02	20.1	20.69	20.06	20.99
Na_2O	1.76	1.89	0.14	0.39	0.55	0.31	1.64
Total	101.02	102.2	99.38	100.67	100.86	100.83	102.13
Numbers of ions on the basis of 6O							
Si	1.752	1.827	1.844	1.928	1.867	1.905	1.888
Al	0.302	0.187	0.192	0.087	0.173	0.114	0.123
Ti	0.054	0.041	0.040	0.026	0.029	0.024	0.022
Mg	0.727	0.790	0.789	0.845	0.837	0.890	0.880
Fe^{2+}	0.283	0.302	0.294	0.298	0.267	0.271	0.233
Mn	0.005	0.008	0.006	0.009	0.007	0.007	0.005
Ca	0.859	0.815	0.849	0.797	0.819	0.792	0.819
Na	0.128	0.135	0.010	0.028	0.039	0.022	0.116
Total	4.108	4.106	4.025	4.017	4.037	4.025	4.086
Atomic percentages							
Mg	38.8	41.3	40.7	43.3	43.4	45.4	45.4
Fe+Mn	15.3	16.2	15.5	15.8	14.2	14.2	12.3
Ca	45.8	42.6	43.8	40.9	42.4	40.4	42.3
mg#	71.7	71.8	72.4	73.3	75.4	76.2	78.7

A: analcime-bearing
A-SRD: analcime-bearing, Spears Ranch Dike
AS: analcime-bearing, speckled texture
B: basaltic
B-bt: basaltic with significant biotite
BPP: basaltic, pyroxene porphyry dike
BF: basaltic, feeder(?) dike
M: minette
mg# = Mg/(Mg+Fe+Mn)

APPENDIX D.4: ELECTRON MICROPROBE ANALYSES OF BIOTITE

	RDS-2-15 A-SRD	RDS-2-16 A-SRD	RDS-2-17 A-SRD	RDS-2-33 A-SRD	RDS-2-03b A-SRD	RDS-2-06b A-SRD	RDS-2-07b A-SRD	RDS-3-13 M
SiO_2	35.63	35.46	37.26	37.70	36.99	35.69	35.25	36.66
TiO_2	13.98	14.07	14.24	14.36	13.59	13.35	13.36	14.19
Al_2O_3	5.07	5.20	5.44	4.26	5.05	5.16	4.53	6.85
FeO	16.58	16.52	14.68	14.45	17.40	16.60	21.90	10.50
MnO	0.20	0.22	0.14	0.18	0.25	0.22	0.34	0.06
MgO	12.46	11.70	13.79	14.08	12.22	12.83	9.11	16.57
CaO	0.12	1.16	0.19	0.16	0.11	0.14	0.15	0.22
Na_2O	0.66	0.59	0.71	0.73	0.49	0.62	0.46	0.57
K_2O	8.31	8.84	9.19	9.10	9.64	9.10	8.94	8.84
Cr2O3	0.01	0.00	0.01	0.02	0.03	0.01	0.01	0.00
F	1.59	1.90	1.96	2.04	1.80	6.57	1.28	1.72
Cl	0.03	0.04	0.03	0.03	0.04	0.05	0.04	0.09
	94.65	95.69	97.65	97.12	97.61	100.35	95.35	96.28
-O=F,Cl	0.68	0.81	0.83	0.87	0.77	2.78	0.55	0.74
Total	93.97	94.88	96.82	96.25	96.84	97.57	94.80	95.54
Numbers of ions on the basis of 22O								
Si	5.4128	5.3599	5.4392	5.5164	5.1346	5.4814	5.4911	5.3248
Al	2.5029	2.5063	2.4498	2.4763	2.2634	2.4483	2.3775	2.4290
Ti	0.5793	0.5912	0.5973	0.4688	0.5583	0.5298	0.5638	0.7483
Fe^{2+}	2.1062	2.0880	1.7919	1.7680	1.9970	2.8476	2.1599	1.2753
Mn	0.0257	0.0282	0.0173	0.0223	0.0268	0.0448	0.0314	0.0074
Mg	2.8219	2.6365	3.0011	3.0714	2.7517	2.1119	2.7044	3.5881
Ca	0.0195	0.1878	0.0297	0.0251	0.0216	0.0250	0.0175	0.0342
Na	0.1944	0.1729	0.2009	0.2071	0.1729	0.1387	0.1410	0.1605
K	1.6103	1.7044	1.7113	1.6985	1.6700	1.7733	1.8254	1.6378
F	0.7638	0.9081	0.9047	0.9439	2.9888	0.6294	0.8449	0.7900
Cl	0.0077	0.0102	0.0074	0.0074	0.0122	0.0105	0.0101	0.0222
Total	16.0446	16.1936	16.1508	16.2051	17.5973	16.0406	16.1670	16.0176

	RDS-3-14 M	RDS-3-16 M	RDS-3-17 M	RDS-3-22 M	RDS-3-23 M	RDS-3-28 M	RDS-3-37 M	RDS-3-41 M
SiO_2	33.36	35.81	36.63	35.99	33.76	34.05	37.79	34.94
TiO_2	12.85	7.04	14.33	14.05	13.42	14.22	15.58	13.84
Al_2O_3	6.16	13.72	7.17	7.12	7.43	7.56	6.25	6.81
FeO	13.40	16.47	11.49	10.19	12.05	15.45	11.88	13.51
MnO	0.18	10.70	0.11	0.10	0.12	0.20	0.14	0.19
MgO	12.72	0.08	15.90	16.56	13.88	11.63	12.86	14.07
CaO	3.36	0.53	0.10	0.12	0.13	0.35	2.21	0.53
Na_2O	0.53	0.16	0.61	0.59	0.49	0.55	0.70	0.57
K_2O	7.93	8.79	8.85	8.81	8.52	8.51	7.52	8.35
Cr2O3	0.00	0.02	0.00	0.00	0.00	0.05	0.01	0.01
F	1.73	1.30	1.96	1.75	1.24	1.38	1.76	1.83
Cl	0.11	0.08	0.09	0.07	0.08	0.11	0.13	0.09
	92.35	94.71	97.24	95.35	91.11	94.05	96.86	94.71
-O=F,Cl	0.75	0.57	0.85	0.75	0.54	0.61	0.77	0.79
Total	91.60	94.14	96.39	94.60	90.57	93.44	96.09	93.92
Numbers of ions on the basis of 22O								
Si	5.2043	5.3071	5.2913	5.2797	5.2539	5.2149	5.4523	5.2492
Al	2.3625	2.3963	2.4395	2.4290	2.4613	2.5666	2.6491	2.4504
Ti	0.7228	0.7847	0.7790	0.7856	0.8697	0.8708	0.6782	0.7695
Fe^{2+}	1.7480	1.3260	1.3879	1.2500	1.5681	1.9786	1.4332	1.6972
Mn	0.0238	0.0100	0.0135	0.0124	0.0158	0.0259	0.0171	0.0242
Mg	2.9583	3.6389	3.4241	3.6217	3.2203	2.6554	2.7661	3.1513
Ca	0.5616	0.0254	0.0155	0.0189	0.0217	0.0574	0.3416	0.0853
Na	0.1603	0.1523	0.1708	0.1678	0.1478	0.1633	0.1958	0.1660
K	1.5780	1.6617	1.6307	1.6486	1.6913	1.6625	1.3840	1.6002
F	0.8534	0.6092	0.8953	0.8118	0.6102	0.6683	0.8030	0.8693
Cl	0.0291	0.0201	0.0220	0.0174	0.0211	0.0286	0.0318	0.0229
Total	16.2021	15.9317	16.0694	16.0429	15.8811	15.8923	15.7522	16.0854

APPENDIX D.4: ELECTRON MICROPROBE ANALYSES OF BIOTITE

	RDS-3-08b M	RDS-3-14b M	RDS-3-17b M	RDS-5-09 A	RDS-5-10 A	RDS-5-15 A	RDS-5-16 A	RDS-5-23 A
SiO_2	33.30	34.87	37.94	36.00	35.95	35.84	36.09	35.74
TiO_2	13.61	13.50	16.61	3.73	16.57	16.11	16.26	15.94
Al_2O_3	7.02	6.89	5.86	16.08	4.06	3.79	4.24	4.02
FeO	15.87	11.17	9.88	18.34	10.30	13.31	10.35	12.58
MnO	0.26	0.12	0.05	9.57	0.16	0.23	0.14	0.21
MgO	11.52	15.55	14.41	0.15	17.26	15.27	17.11	15.13
CaO	0.10	0.14	0.12	0.48	0.14	0.02	0.14	0.06
Na_2O	0.59	0.56	0.60	0.09	0.54	0.51	0.54	0.55
K_2O	8.31	8.65	8.08	8.46	9.04	8.89	8.93	8.82
Cr2O3	0.00	0.02	0.03	0.00	0.01	0.00	0.02	0.03
F	0.05	2.18	4.89	1.94	2.32	2.67	2.35	2.43
Cl	0.10	0.08	0.08	0.00	0.00	0.02	0.01	0.01
	90.74	93.73	98.55	94.85	96.35	96.66	96.19	95.52
-O=F,Cl	0.04	0.94	2.08	0.82	0.98	1.13	0.99	1.03
Total	90.70	92.79	96.47	94.03	95.37	95.53	95.20	94.49
Numbers of ions on the basis of 22(			Numbers of ions on the basis of 22O					
Si	5.3077	5.2430	5.2993	5.2613	5.2072	5.2435	5.2347	5.2759
Al	2.5565	2.3922	2.7342	2.7696	2.8285	2.7777	2.7794	2.7731
Ti	0.8416	0.7792	0.6156	0.4100	0.4423	0.4170	0.4626	0.4463
Fe^{2+}	2.1151	1.4044	1.1539	1.1695	1.2475	1.6283	1.2553	1.5528
Mn	0.0351	0.0153	0.0059	0.0186	0.0196	0.0285	0.0172	0.0263
Mg	2.7374	3.4856	3.0006	3.9959	3.7271	3.3306	3.6998	3.3297
Ca	0.0171	0.0226	0.0180	0.0141	0.0217	0.0031	0.0218	0.0095
Na	0.1823	0.1632	0.1625	0.1360	0.1516	0.1447	0.1518	0.1574
K	1.6895	1.6590	1.4396	1.5772	1.6703	1.6591	1.6522	1.6608
F	0.0252	1.0365	2.1598	0.8965	1.0626	1.2352	1.0778	1.1343
Cl	0.0270	0.0204	0.0189	0.0000	0.0000	0.0050	0.0025	0.0025
Total	15.5345	16.2213	16.6084	16.2487	16.3785	16.4726	16.3552	16.3687

	RDS-5-24 A	RDS-5-25 A	RDS-5-26 A	RDS-5-15b A	RDS-5-16b A	RDS-5-17b A	RDS-5-21b A	RDS-5-22b A
SiO_2	36.92	36.64	38.51	34.75	35.37	34.32	34.98	37.30
TiO_2	16.59	16.33	16.87	15.76	15.85	3.55	14.94	15.30
Al_2O_3	3.77	2.32	1.58	3.93	3.31	15.68	1.69	1.20
FeO	11.73	9.20	9.29	11.35	11.88	15.67	15.54	10.66
MnO	0.20	0.15	0.13	0.20	0.21	12.67	0.31	0.18
MgO	16.48	18.89	19.99	16.45	16.65	0.24	14.62	19.24
CaO	0.19	0.06	0.05	0.09	0.08	0.44	0.25	0.08
Na_2O	0.58	0.55	0.58	0.54	0.57	0.04	0.41	0.59
K_2O	8.98	9.10	9.33	8.59	8.76	8.73	9.09	9.10
Cr2O3	0.00	0.00	0.00	0.00	0.00	0.01	0.01	0.00
F	2.76	2.99	3.15	0.00	2.77	3.31	3.16	3.51
Cl	0.01	0.01	0.01	0.01	0.03	0.00	0.03	0.01
	98.20	96.24	99.50	91.68	95.46	94.66	95.02	97.15
-O=F,Cl	1.16	1.26	1.33	0.00	1.17	1.39	1.34	1.48
Total	97.04	94.98	98.17	91.68	94.29	93.27	93.68	95.67
Numbers of ions on the basis of 22O								
Si	5.2657	5.2769	5.3468	5.3252	5.2119	5.1319	5.2909	5.3557
Al	2.7885	2.7717	2.7604	2.8462	2.7524	2.7631	2.6631	2.5890
Ti	0.4044	0.2513	0.1650	0.4530	0.3668	0.3993	0.1923	0.1296
Fe^{2+}	1.3989	1.1079	1.0785	1.4544	1.4638	1.5842	1.9655	1.2799
Mn	0.0242	0.0183	0.0153	0.0260	0.0262	0.0304	0.0397	0.0219
Mg	3.5041	4.0558	4.1377	3.7581	3.6576	3.4932	3.2967	4.1185
Ca	0.0290	0.0093	0.0074	0.0148	0.0126	0.0064	0.0405	0.0123
Na	0.1604	0.1536	0.1561	0.1604	0.1628	0.1276	0.1202	0.1642
K	1.6337	1.6718	1.6524	1.6791	1.6465	1.6651	1.7538	1.6667
F	1.2448	1.3617	1.3830	0.0000	1.2907	1.5651	1.5114	1.5936
Cl	0.0024	0.0024	0.0024	0.0026	0.0075	0.0000	0.0077	0.0024
Total	16.4562	16.6807	16.7049	15.7198	16.5989	16.7662	16.8818	16.9338

APPENDIX D.4: ELECTRON MICROPROBE ANALYSES OF BIOTITE

	RDS-7-7 B-bt	RDS-7-8 B-bt	RDS-7-12 B-bt	RDS-7-07b B-bt	RDS-7-08b B-bt	RDS-7-09b B-bt	RDS-7-10b B-bt	RDS-7-11b B-bt
SiO_2	37.20	38.37	37.58	37.80	38.16	36.49	38.49	38.78
TiO_2	14.74	14.87	14.73	14.09	14.37	13.69	14.92	3.93
Al_2O_3	5.68	4.86	4.99	4.55	4.51	4.65	4.00	14.45
FeO	12.78	11.44	13.13	11.47	11.35	12.49	10.96	10.81
MnO	0.16	0.15	0.19	0.17	0.14	0.20	0.11	0.14
MgO	16.43	17.90	16.89	17.16	17.09	15.68	18.00	18.38
CaO	0.08	0.11	0.08	0.11	0.15	0.05	0.08	0.06
Na_2O	0.62	0.65	0.63	0.68	0.66	0.62	0.67	0.66
K_2O	8.74	8.82	9.09	9.07	8.71	8.85	9.07	9.14
Cr2O3	0.02	0.00	0.01	0.00	0.00	0.03	0.04	0.03
F	1.35	1.79	1.64	1.97	4.31	1.88	2.17	2.29
Cl	0.09	0.07	0.11	0.09	0.08	0.08	0.09	0.08
	97.90	99.03	99.06	97.16	99.53	94.72	98.59	98.75
-O=F,Cl	0.59	0.77	0.72	0.85	1.83	0.81	0.93	0.98
Total	97.31	98.26	98.34	96.31	97.70	93.91	97.66	97.77
Numbers of ions on the basis of 22O								
Si	5.3564	5.4119	5.3614	5.4559	5.3530	5.4424	5.4458	5.4761
Al	2.5013	2.4717	2.4766	2.3967	2.3756	2.4063	2.4878	2.4047
Ti	0.6151	0.5156	0.5354	0.4939	0.4758	0.5216	0.4257	0.4174
Fe^{2+}	1.5387	1.3492	1.5664	1.3843	1.3313	1.5577	1.2967	1.2764
Mn	0.0195	0.0179	0.0230	0.0208	0.0166	0.0253	0.0132	0.0167
Mg	3.5269	3.7639	3.5923	3.6925	3.5740	3.4865	3.7968	3.8693
Ca	0.0123	0.0166	0.0122	0.0170	0.0225	0.0080	0.0121	0.0091
Na	0.1731	0.1777	0.1742	0.1903	0.1795	0.1793	0.1838	0.1807
K	1.6053	1.5868	1.6542	1.6699	1.5585	1.6837	1.6369	1.6463
F	0.6147	0.7983	0.7398	0.8991	1.9118	0.8867	0.9709	1.0225
Cl	0.0220	0.0167	0.0266	0.0220	0.0190	0.0202	0.0216	0.0191
Total	15.9853	16.1265	16.1623	16.2425	16.8178	16.2177	16.2912	16.3385

	RDS-7-12b B-bt	RDS-7-13b B-bt	RDS-8-13b B	RDS-8-14b B	RDS-8-15b B	RDS-8-16b B	RDS-8-26b B	RDS-10-33 A-SRD
SiO_2	36.72	35.85	35.87	32.38	5.30	35.56	35.70	37.24
TiO_2	14.00	13.61	16.14	15.10	0.68	16.09	13.33	12.84
Al_2O_3	5.92	4.74	3.59	6.67	2.49	5.01	6.39	6.46
FeO	13.84	13.21	12.54	14.91	3.55	13.96	15.80	12.76
MnO	0.16	0.18	0.24	0.28	1.66	0.24	0.29	0.11
MgO	14.89	15.37	16.58	18.00	0.02	19.51	15.42	15.22
CaO	0.09	0.12	0.87	0.21	0.24	0.10	0.07	0.14
Na_2O	0.62	0.60	1.55	0.20	0.03	0.57	0.45	0.73
K_2O	8.87	8.91	2.78	3.54	1.38	4.55	7.40	8.88
Cr2O3	0.00	0.02	0.00	0.00	0.00	0.01	0.06	0.00
F	1.85	1.98	0.48	0.66	0.39	0.88	0.69	1.57
Cl	0.09	0.09	0.07	0.06	0.03	0.06	0.04	0.04
	97.06	94.67	90.71	92.01	15.78	96.54	95.65	95.99
-O=F,Cl	0.80	0.85	0.22	0.29	0.17	0.38	0.30	0.67
Total	96.26	93.82	90.49	91.72	15.61	96.16	95.35	95.32
Numbers of ions on the basis of 22O								
Si	5.3728	5.3799	5.4012	4.9197	5.3055	5.1110	5.3292	5.4843
Al	2.4141	2.4070	2.8641	2.7038	2.4945	2.7254	2.3450	2.2285
Ti	0.6515	0.5350	0.4066	0.7622	0.6834	0.5416	0.7174	0.7155
Fe^{2+}	1.6933	1.6576	1.5789	1.8943	1.6577	1.6778	1.9722	1.5713
Mn	0.0198	0.0229	0.0306	0.0360	0.0235	0.0292	0.0367	0.0137
Mg	3.2480	3.4386	3.7219	4.0772	3.5557	4.1805	3.4316	3.3416
Ca	0.0141	0.0193	0.1403	0.0342	0.0298	0.0154	0.0112	0.0221
Na	0.1759	0.1746	0.4525	0.0589	0.2363	0.1588	0.1302	0.2084
K	1.6555	1.7056	0.5340	0.6861	1.3795	0.8342	1.4091	1.6681
F	0.8560	0.9396	0.2285	0.3171	0.3854	0.3999	0.3257	0.7311
Cl	0.0223	0.0229	0.0179	0.0155	0.0261	0.0146	0.0101	0.0100
Total	16.1234	16.3029	15.3766	15.5049	15.7775	15.6885	15.7184	15.9947

APPENDIX D.4: ELECTRON MICROPROBE ANALYSES OF BIOTITE

	RDS-10-34 A-SRD	RDS-13-09 B-bt	RDS-13-10 B-bt	RDS-13-11 B-bt	RDS-13-12 B-bt	RDS-13-13 B-bt	RDS-13-14 B-bt	RDS-13-26 B-bt
SiO_2	38.27	35.68	36.01	35.49	35.59	34.56	35.71	35.94
TiO_2	14.33	6.95	14.53	13.83	14.77	14.39	13.89	15.19
Al_2O_3	7.75	14.36	6.74	6.46	6.00	5.83	6.51	7.03
FeO	16.60	15.69	10.85	10.24	12.17	12.99	10.72	14.94
MnO	0.19	11.38	0.08	0.09	0.12	0.17	0.08	0.12
MgO	8.52	0.13	16.10	15.45	16.37	15.46	16.29	12.95
CaO	0.77	0.37	0.12	1.55	1.20	0.38	0.61	0.20
Na_2O	0.49	0.87	0.59	0.44	0.00	0.65	0.56	0.72
K_2O	9.37	8.36	8.46	8.36	7.08	7.46	8.51	7.84
Cr2O3	0.00	0.00	0.00	0.00	0.01	0.01	0.02	0.00
F	0.63	1.77	1.54	1.68	1.35	1.94	1.59	1.28
Cl	0.02	0.10	0.09	0.12	0.09	0.10	0.10	0.11
	96.95	95.67	95.11	93.72	94.75	93.95	94.59	96.34
-O=F,Cl	0.27	0.77	0.67	0.73	0.59	0.84	0.69	0.56
Total	96.68	94.90	94.44	92.99	94.16	93.11	93.90	95.78
Numbers of ions on the basis of 22O								
Si	5.6673	5.2428	5.2958	5.3116	5.2546	5.1960	5.2973	5.2982
Al	2.5009	2.4867	2.5183	2.4394	2.5699	2.5497	2.4283	2.6390
Ti	0.8632	0.7681	0.7455	0.7272	0.6663	0.6593	0.7263	0.7795
Fe^{2+}	2.0555	1.3982	1.3343	1.2815	1.5025	1.6331	1.3297	1.8416
Mn	0.0238	0.0162	0.0100	0.0114	0.0150	0.0216	0.0101	0.0150
Mg	1.8810	3.4370	3.5299	3.4473	3.6031	3.4652	3.6025	2.8460
Ca	0.1222	0.1370	0.0189	0.2485	0.1898	0.0612	0.0969	0.0316
Na	0.1407	0.1054	0.1682	0.1277	0.0000	0.1895	0.1610	0.2058
K	1.7700	1.5669	1.5870	1.5960	1.3334	1.4307	1.6103	1.4743
F	0.2950	0.8224	0.7162	0.7951	0.6303	0.9223	0.7458	0.5967
Cl	0.0050	0.0249	0.0224	0.0304	0.0225	0.0255	0.0251	0.0275
Total	15.3245	16.0056	15.9465	16.0161	15.7873	16.1539	16.0334	15.7550

	RDS-15A-31 B	RDS-15C-28 B	RDS-16B-10 BPP	RDS-16B-12 BPP	RDS-16B-13 BPP	RDS-16B-14 BPP	RDS-16B-29 BPP	RDS-16B-33 BPP
SiO_2	39.07	37.45	36.56	35.18	36.99	36.40	36.76	36.70
TiO_2	13.85	14.16	14.29	6.48	14.28	14.10	14.21	6.32
Al_2O_3	7.26	6.46	6.12	12.45	5.38	6.35	5.43	14.10
FeO	10.84	11.07	13.60	12.22	13.17	15.48	14.48	14.00
MnO	0.11	0.16	0.16	15.78	0.13	0.21	0.17	14.58
MgO	15.27	16.25	15.05	0.21	15.91	13.23	14.90	0.18
CaO	0.17	0.21	0.08	0.53	0.06	0.11	0.15	0.60
Na_2O	1.01	1.26	0.63	0.19	0.71	0.60	0.63	0.17
K_2O	8.18	7.48	8.85	8.70	8.78	8.42	8.62	8.48
Cr2O3	0.00	0.03	0.00	0.00	0.00	0.00	0.00	0.00
F	1.74	1.57	1.47	1.57	1.94	1.69	2.27	1.99
Cl	0.09	0.09	0.02	0.04	0.01	0.04	0.03	0.02
	97.60	96.19	96.83	93.36	97.37	96.63	97.65	97.13
-O=F,Cl	0.75	0.68	0.62	0.67	0.82	0.72	0.96	0.84
Total	96.85	95.51	96.21	92.69	96.55	95.91	96.69	96.29
Numbers of ions on the basis of 22O								
Si	5.5572	5.4189	5.3545	5.4317	5.3684	5.3782	5.3502	5.3690
Al	2.3216	2.4146	2.4665	2.2654	2.4424	2.4552	2.4374	2.4309
Ti	0.7767	0.7030	0.6742	0.7525	0.5873	0.7057	0.5944	0.6954
Fe^{2+}	1.2893	1.3394	1.6655	2.0373	1.5983	1.9125	1.7622	1.7835
Mn	0.0133	0.0196	0.0198	0.0275	0.0160	0.0263	0.0210	0.0223
Mg	3.2380	3.5054	3.2861	2.8128	3.4424	2.9142	3.2330	3.0533
Ca	0.0259	0.0326	0.0126	0.0314	0.0093	0.0174	0.0234	0.0266
Na	0.2785	0.3535	0.1789	0.1586	0.1998	0.1719	0.1778	0.1702
K	1.4841	1.3806	1.6534	1.7134	1.6254	1.5869	1.6003	1.5824
F	0.7826	0.7183	0.6808	0.7665	0.8903	0.7896	1.0447	0.9206
Cl	0.0217	0.0221	0.0050	0.0105	0.0025	0.0100	0.0074	0.0050
Total	15.7888	15.9080	15.9971	16.0076	16.1821	15.9678	16.2518	16.0593

APPENDIX D.4: ELECTRON MICROPROBE ANALYSES OF BIOTITE

	RDS-16C-29 BPP	RDS-16C-30 BPP	RDS-17-32 BF	RDS-009-07 M	RDS-009-18 M	RDS-009-19 M	RDS-009-20 M	RDS-009-21 M
SiO_2	37.91	36.39	37.23	36.71	37.79	36.26	37.98	36.93
TiO_2	14.31	13.02	12.74	15.19	15.40	4.10	15.64	15.10
Al_2O_3	5.06	4.46	6.31	4.51	4.23	14.64	4.36	4.53
FeO	14.36	13.34	12.03	10.32	10.00	18.00	10.66	10.26
MnO	0.11	0.18	0.14	0.13	0.13	9.84	0.20	0.13
MgO	15.62	15.11	15.80	18.21	18.95	0.10	18.55	18.03
CaO	0.10	0.07	0.21	0.13	0.07	0.45	0.12	0.09
Na_2O	0.70	0.62	0.87	0.50	0.52	0.11	0.54	0.48
K_2O	8.65	8.94	8.33	9.33	9.57	9.39	9.60	9.32
Cr2O3	0.03	0.04	0.00	0.00	0.00	0.03	0.00	0.01
F	2.51	2.26	1.29	1.58	1.60	1.41	1.49	1.31
Cl	0.06	0.02	0.07	0.03	0.01	0.02	0.03	0.03
	99.41	94.46	95.01	96.62	98.28	94.36	99.16	96.21
-O=F,Cl	1.07	0.96	0.56	0.67	0.68	0.60	0.63	0.56
Total	98.34	93.50	94.45	95.95	97.60	93.76	98.53	95.65
Numbers of ions on the basis of 22O								
Si	5.4004	5.4719	5.5087	5.3118	5.3599	5.3717	5.3541	5.3614
Al	2.4024	2.3073	2.2215	2.5903	2.5741	2.5560	2.5984	2.5835
Ti	0.5421	0.5044	0.7022	0.4908	0.4512	0.4568	0.4623	0.4946
Fe^{2+}	1.7105	1.6773	1.4884	1.2487	1.1860	1.2189	1.2566	1.2455
Mn	0.0133	0.0229	0.0175	0.0159	0.0156	0.0125	0.0239	0.0160
Mg	3.3172	3.3873	3.4853	3.9282	4.0070	3.9754	3.8985	3.9023
Ca	0.0153	0.0113	0.0333	0.0202	0.0106	0.0175	0.0181	0.0140
Na	0.1933	0.1807	0.2496	0.1403	0.1430	0.1292	0.1476	0.1351
K	1.5718	1.7148	1.5722	1.7221	1.7314	1.7744	1.7263	1.7259
F	1.1306	1.0746	0.6036	0.7229	0.7176	0.6605	0.6642	0.6014
Cl	0.0145	0.0051	0.0176	0.0074	0.0024	0.0050	0.0072	0.0074
Total	16.3114	16.3576	15.8998	16.1985	16.1990	16.1781	16.1571	16.0871

	RDS-009-22 M	RDS-009-23 M	RDS-009-24 M	RDS-009-25 M	RDS-009-27 M	RDS-009-28 M	RDS-013A-27 AS	RDS-013A-28 AS
SiO_2	35.34	37.03	38.04	34.04	37.59	37.66	37.23	37.06
TiO_2	13.78	4.59	4.30	15.05	15.40	15.23	14.06	6.30
Al_2O_3	4.24	15.47	15.37	4.38	4.17	4.37	5.91	13.77
FeO	9.68	18.41	18.79	10.40	10.26	10.01	14.64	13.86
MnO	0.13	9.94	9.90	0.12	0.13	0.09	0.24	15.10
MgO	17.09	0.11	0.16	17.60	18.62	18.59	14.35	0.20
CaO	0.14	0.50	0.52	0.57	0.11	0.09	0.08	0.61
Na_2O	0.43	0.06	0.05	0.41	0.53	0.56	0.69	0.16
K_2O	9.47	9.45	9.68	8.28	9.42	9.44	9.39	9.14
Cr2O3	0.00	0.00	0.00	0.00	0.01	0.00	0.00	0.00
F	1.43	1.53	1.46	1.34	1.63	1.49	1.37	1.39
Cl	0.03	0.02	0.03	0.04	0.02	0.02	0.02	0.02
	91.75	97.11	98.28	92.24	97.89	97.57	97.97	97.61
-O=F,Cl	0.61	0.65	0.62	0.57	0.69	0.63	0.58	0.59
Total	91.14	96.46	97.66	91.67	97.20	96.94	97.39	97.02
Numbers of ions on the basis of 22O								
Si	5.3994	5.3185	5.3919	5.1736	5.3575	5.3797	5.4253	5.4281
Al	2.4812	2.6185	2.5675	2.6957	2.5867	2.5639	2.4146	2.3769
Ti	0.4872	0.4958	0.4584	0.5007	0.4470	0.4695	0.6478	0.6940
Fe^{2+}	1.2367	1.1938	1.1734	1.3217	1.2228	1.1957	1.7839	1.8494
Mn	0.0168	0.0134	0.0192	0.0154	0.0157	0.0109	0.0296	0.0248
Mg	3.8927	3.9420	3.9706	3.9878	3.9564	3.9589	3.1175	3.0264
Ca	0.0229	0.0092	0.0076	0.0928	0.0168	0.0138	0.0125	0.0251
Na	0.1274	0.1392	0.1429	0.1208	0.1464	0.1551	0.1949	0.1732
K	1.8456	1.7313	1.7502	1.6052	1.7126	1.7201	1.7455	1.7076
F	0.6909	0.6949	0.6544	0.6440	0.7346	0.6730	0.6313	0.6438
Cl	0.0078	0.0049	0.0072	0.0103	0.0048	0.0048	0.0049	0.0050
Total	16.2086	16.1615	16.1433	16.1681	16.2013	16.1454	16.0079	15.9543

APPENDIX D.4: ELECTRON MICROPROBE ANALYSES OF BIOTITE

	RDS-013A-30 AS	RDS-013A-32 AS	RDS-102-08 M	RDS-102-09 M	RDS-102-10 M	RDS-102-11 M	RDS-102-12 M	RDS-102-13 M
SiO_2	38.32	37.46	37.18	37.69	37.44	36.51	35.91	36.28
TiO_2	14.09	14.21	15.07	4.22	14.82	14.54	15.13	14.79
Al_2O_3	6.03	6.00	4.75	14.80	3.64	4.59	6.52	4.59
FeO	13.17	17.65	11.23	18.57	11.17	11.43	11.17	11.81
MnO	0.18	0.26	0.12	10.18	0.12	0.12	0.11	0.13
MgO	15.53	12.87	17.28	0.08	17.91	16.73	15.98	16.48
CaO	0.12	0.07	0.13	0.00	0.09	0.21	0.10	0.07
Na_2O	0.72	0.71	0.49	0.11	0.56	0.49	0.56	0.52
K_2O	9.43	9.29	9.06	9.16	9.16	9.07	8.73	8.87
Cr2O3	0.00	0.02	0.01	0.00	0.01	0.00	0.01	0.00
F	1.57	1.44	1.34	1.82	2.12	2.18	1.64	1.71
Cl	0.03	0.02	0.09	0.09	0.10	0.10	0.08	0.08
	99.18	99.99	96.76	96.72	97.13	95.96	95.93	95.35
-O=F,Cl	0.67	0.61	0.58	0.79	0.92	0.94	0.71	0.74
Total	98.51	99.38	96.18	95.93	96.21	95.02	95.22	94.61
Numbers of ions on the basis of 22O								
Si	5.4642	5.4143	5.3818	5.4170	5.3971	5.3461	5.2490	5.3506
Al	2.3678	2.4204	2.5708	2.5068	2.5177	2.5091	2.6063	2.5706
Ti	0.6467	0.6522	0.5171	0.4562	0.3947	0.5055	0.7168	0.5091
Fe^{2+}	1.5703	2.1331	1.3593	1.2234	1.3464	1.3995	1.3653	1.4564
Mn	0.0217	0.0318	0.0147	0.0097	0.0147	0.0149	0.0136	0.0162
Mg	3.3014	2.7732	3.7290	3.9790	3.8490	3.6521	3.4823	3.6234
Ca	0.0183	0.0108	0.0202	0.0169	0.0139	0.0329	0.0157	0.0111
Na	0.1990	0.1989	0.1375	0.0000	0.1565	0.1391	0.1587	0.1487
K	1.7152	1.7128	1.6728	1.6793	1.6844	1.6941	1.6277	1.6687
F	0.7079	0.6581	0.6133	0.8271	0.9664	1.0094	0.7580	0.7975
Cl	0.0072	0.0049	0.0221	0.0219	0.0244	0.0248	0.0198	0.0200
Total	16.0199	16.0106	16.0386	16.1376	16.3652	16.3276	16.0132	16.1723

	RDS-102-14 M	RDS-102-15 M	RDS-106-01 M	RDS-159-02 B-bt	RDS-159-06 B-bt	RDS-159-09 B-bt	RDS-159-011 B-bt
SiO_2	36.17	38.07	37.58	38.98	36.61	36.89	36.76
TiO_2	14.86	3.06	12.03	13.54	14.12	14.77	14.91
Al_2O_3	5.77	14.89	0.05	4.64	5.02	5.27	4.97
FeO	12.71	18.74	17.41	12.26	12.85	12.83	10.62
MnO	0.14	10.74	0.12	0.19	0.18	0.21	0.09
MgO	15.61	0.12	19.34	17.83	16.24	16.11	17.70
CaO	0.03	0.42	1.53	0.06	0.73	0.10	0.04
Na_2O	0.56	0.05	0.13	0.56	0.65	0.66	0.66
K_2O	8.85	9.51	0.08	9.28	8.73	8.82	9.09
Cr2O3	0.03	0.01	0.00	0.02	0.00	0.00	0.02
F	1.75	1.93	0.07	1.93	1.95	1.93	2.25
Cl	0.06	0.10	0.01	0.08	0.03	0.04	0.02
	96.53	97.62	88.34	99.37	97.12	97.64	97.14
-O=F,Cl	0.75	0.84	0.03	0.83	0.83	0.82	0.95
Total	95.78	96.78	88.31	98.54	96.30	96.81	96.19
Numbers of ions on the basis of 22O							
Si	5.2928	5.4475	5.8252	5.5143	5.3360	5.3317	5.2938
Al	2.5626	2.5110	2.1976	2.2569	2.4259	2.5168	2.5297
Ti	0.6350	0.3293	0.0058	0.4938	0.5508	0.5731	0.5388
Fe^{2+}	1.5552	1.2851	2.2566	1.4498	1.5662	1.5511	1.2793
Mn	0.0174	0.0145	0.0158	0.0226	0.0223	0.0259	0.0116
Mg	3.4054	3.9977	4.4692	3.7604	3.5295	3.4719	3.8005
Ca	0.0047	0.0077	0.2541	0.0095	0.1140	0.0153	0.0066
Na	0.1589	0.1165	0.0391	0.1534	0.1834	0.1841	0.1855
K	1.6519	1.7358	0.0158	1.6750	1.6225	1.6269	1.6695
F	0.8098	0.8733	0.0343	0.8638	0.8969	0.8808	1.0250
Cl	0.0149	0.0243	0.0026	0.0202	0.0080	0.0097	0.0049
Total	16.1085	16.3426	15.1161	16.2197	16.2556	16.1874	16.3450

APPENDIX D.5: ELECTRON MICROPROBE ANALYSES OF APATITE

	RDS-5-32 A	RDS-5-33 A	RDS-009-12 M	RDS-009-13 M	RDS-009-14 M	RDS-009-15 M	RDS-009-16 M
SiO_2	0.77	1.08	1.09	1.43	1.61	1.18	0.99
FeO	0.41	0.34	0.27	0.35	0.24	0.30	0.26
MnO	0.03	0.03	0.02	0.00	0.06	0.02	0.00
CaO	52.62	52.99	52.67	52.60	52.86	52.54	52.93
SrO	0.52	0.49	0.36	0.29	0.29	0.27	0.42
P_2O_5	38.75	37.75	38.63	37.46	36.82	37.19	37.00
F	5.29	4.92	2.58	2.74	3.01	2.86	2.89
Cl	0.04	0.05	0.24	0.26	0.24	0.24	0.24
SO_2	0.18	0.18	0.85	1.05	1.13	0.89	0.83
	98.61	97.83	42.30	41.51	41.20	41.18	40.96
-O=F,Cl	2.24	2.08	1.14	1.21	1.32	1.26	1.27
Total	96.37	95.75	41.16	40.30	39.88	39.92	39.69
	Numbers of ions on the basis of 26O						
P	5.7323	5.6782	5.9181	5.8290	5.7558	5.8066	5.7726
Fe^{2+}	0.0599	0.0505	0.0409	0.0538	0.0371	0.0463	0.0401
Mn	0.0044	0.0045	0.0031	0.0000	0.0094	0.0031	0.0000
Ca	9.8508	10.0869	10.2114	10.3581	10.4573	10.3814	10.4505
Sr	0.0527	0.0505	0.0378	0.0309	0.0310	0.0289	0.0449
F	2.9230	2.7643	1.4764	1.5926	1.7576	1.6680	1.6842
Cl	0.0118	0.0151	0.0736	0.0810	0.0751	0.0750	0.0750
Total	18.6350	18.6500	17.7611	17.9453	18.1232	18.0093	18.0672

	RDS-009-17 M
SiO_2	1.54
FeO	0.44
MnO	0.01
CaO	53.08
SrO	0.29
P_2O_5	35.92
F	2.83
Cl	0.22
SO_2	0.98
	39.95
-O=F,Cl	1.24
Total	38.71
P	5.6919
Fe^{2+}	0.0689
Mn	0.0016
Ca	10.6444
Sr	0.0315
F	1.6751
Cl	0.0698
Total	18.1831

A: analcime-bearing

M: minette

APPENDIX D.6: ELECTRON MICROPROBE ANALYSES OF OLIVINE

	RDS-10-15 A-SRD	RDS-10-16 A-SRD	RDS-10-17 A-SRD
SiO_2	38.66	38.79	38.88
FeO	23.43	22.70	23.33
MnO	0.32	0.35	0.38
MgO	38.71	39.07	39.10
CaO	0.29	0.29	0.31
Total	101.40	101.19	102.00
Numbers of ions on the basis of 4O			
Si	0.996	0.998	0.996
Mg	1.487	1.499	1.493
Fe^{2+}	0.505	0.489	0.500
Mn	0.007	0.008	0.008
Ca	0.008	0.008	0.009
Total	3.004	3.002	3.004
End-member percentages			
Fo	74.7	75.4	74.9
Fa	25.3	24.6	25.1

A-SRD: analcime-bearing, Spears Ranch Dike

APPENDIX D.7: ELECTRON MICROPROBE ANALYSES OF MAGNETITE

	RDS-1-1 B	RDS-1-2 B	RDS-1-3 B	RDS-1-4 B	RDS-1-5 B	RDS-1-6 B	RDS-1-8 B	RDS-2-11 A-SRD
SiO_2	0.16	0.31	0.26	0.6	0.15	0.14	0.16	0.12
TiO_2	10.72	10.89	11.74	10.86	9.33	9.2	11.82	13.12
Al_2O_3	3.32	3.07	1.69	1.18	3.79	4.3	2.27	2.43
Cr_2O_3	0.04	0.03	0.07	0.06	0.36	0.02	0.02	0.07
Fe_2O_3	45.96	45.36	43.86	43.96	47.60	48.04	43.57	39.58
FeO	37.77	38.15	39.78	40.94	36.46	36.30	38.28	41.63
MnO	0.74	0.61	0.37	0.34	0.66	0.55	0.63	1.69
MgO	2.24	2.17	1.07	0.02	2.28	2.48	2.11	0
CaO	0.15	0.22	0.5	0.23	0.16	0.2	0.14	0.08
Total	101.11	100.81	99.33	98.18	100.79	101.23	98.99	98.73
Numbers of ions on the basis of 32O								
Si	0.047	0.090	0.076	0.175	0.044	0.041	0.047	0.035
Al	1.139	1.053	0.580	0.405	1.300	1.475	0.778	0.833
Cr	0.009	0.007	0.016	0.014	0.083	0.005	0.005	0.016
Fe^{3+}	10.066	9.934	9.605	9.627	10.424	10.520	9.541	8.669
Ti	2.347	2.384	2.570	2.377	2.042	2.014	2.587	2.872
Mg	0.972	0.942	0.464	0.009	0.989	1.076	0.916	0.000
Fe^{2+}	9.192	9.285	9.680	9.962	8.874	8.835	9.316	10.132
Mn	0.182	0.150	0.091	0.084	0.163	0.136	0.155	0.417
Ca	0.047	0.069	0.156	0.072	0.050	0.062	0.044	0.025
Total	24.000	23.913	23.237	22.724	23.967	24.163	23.388	22.998

	RDS-2-12 A-SRD	RDS-2-13 A-SRD	RDS-2-14 A-SRD	RDS-2-32 A-SRD	RDS-2-34 A-SRD	RDS-3-01 M	RDS-3-02 M	RDS-3-03 M
SiO_2	0.15	0.2	2.72	0.11	0.1	2.22	0.35	0.17
TiO_2	13.61	13.26	12.68	12.83	9.87	8.39	8.35	8.46
Al_2O_3	2.79	2.35	2.33	3.63	5.1	3.64	3.07	3.33
Cr_2O_3	0.05	0.03	0.03	0	0.41	0.25	0.08	0.04
Fe_2O_3	36.47	38.91	35.18	38.40	45.62	40.53	47.45	47.78
FeO	41.81	41.50	40.61	41.46	38.01	38.41	37.17	37.48
MnO	1.15	1.6	1.67	0.61	0.5	0.98	1.05	1.04
MgO	0.02	0.07	1.31	0.48	2.09	0.96	0.3	0.47
CaO	0.18	0.21	1.69	0.19	0.05	0.16	0.5	0.09
Total	96.23	98.13	98.23	97.72	101.75	95.54	98.32	98.86
Numbers of ions on the basis of 32O								
Si	0.044	0.058	0.792	0.032	0.029	0.646	0.102	0.049
Al	0.957	0.806	0.799	1.245	1.749	1.248	1.053	1.142
Cr	0.012	0.007	0.007	0.000	0.094	0.058	0.018	0.009
Fe^{3+}	7.987	8.521	7.705	8.410	9.990	8.876	10.392	10.463
Ti	2.979	2.903	2.776	2.808	2.161	1.837	1.828	1.852
Mg	0.009	0.030	0.568	0.208	0.907	0.417	0.130	0.204
Fe^{2+}	10.176	10.099	9.883	10.091	9.251	9.348	9.046	9.121
Mn	0.283	0.394	0.412	0.150	0.123	0.242	0.259	0.256
Ca	0.056	0.065	0.527	0.059	0.016	0.050	0.156	0.028
Total	22.502	22.884	23.469	23.004	24.320	22.720	22.984	23.125

A: analcime-bearing
A-SRD: analcime-bearing, Spears Ranch Dike
AS: analcime-bearing, speckled texture
BF: basaltic, feeder(?) dike
B: basaltic
B-bt: basaltic with significant biotite
BPP: basaltic, pyroxene porphyry dike
M: minette

APPENDIX D.7: ELECTRON MICROPROBE ANALYSES OF MAGNETITE

	RDS-3-04 M	RDS-3-05 M	RDS-3-06 M	RDS-3-01b M	RDS-3-02b M	RDS-3-03b M	RDS-3-04b M	RDS-4-05 B
SiO_2	0.17	0.33	0.18	0.18	0.16	1.05	1.11	1.15
TiO_2	7.69	8.38	8.17	8.19	8.04	7.91	5.41	5.07
Al_2O_3	3.07	2.63	3.15	2.86	3.02	2.51	2.92	0.68
Cr_2O_3	0.07	0.06	0.06	0	0.07	0.05	8.82	0
Fe_2O_3	48.93	47.09	47.81	47.69	47.58	45.82	36.61	55.41
FeO	35.90	37.28	36.17	36.05	35.34	37.45	32.42	36.22
MnO	1.01	0.87	1.09	1.12	1.18	1.02	1.37	0.48
MgO	0.8	0.28	0.7	0.76	1.01	0.26	0.53	0.02
CaO	0.08	0.21	0.29	0.08	0.06	0.16	0.26	0.42
Total	97.72	97.13	97.62	96.93	96.46	96.23	89.45	99.45
Numbers of ions on the basis of 32O								
Si	0.049	0.096	0.052	0.052	0.047	0.306	0.323	0.335
Al	1.053	0.902	1.080	0.981	1.036	0.861	1.001	0.233
Cr	0.016	0.014	0.014	0.000	0.016	0.012	2.029	0.000
Fe^{3+}	10.716	10.312	10.471	10.444	10.419	10.035	8.017	12.135
Ti	1.683	1.834	1.788	1.793	1.760	1.732	1.184	1.110
Mg	0.347	0.121	0.304	0.330	0.438	0.113	0.230	0.009
Fe^{2+}	8.737	9.073	8.802	8.772	8.601	9.114	7.890	8.815
Mn	0.249	0.214	0.269	0.276	0.291	0.251	0.338	0.118
Ca	0.025	0.065	0.090	0.025	0.019	0.050	0.081	0.131
Total	22.876	22.632	22.870	22.673	22.626	22.472	21.094	22.885

	RDS-4-06 B	RDS-4-07 B	RDS-4-08 B	RDS-4-09 B	RDS-5-01b A	RDS-5-02b A	RDS-5-03b A	RDS-5-04b A
SiO_2	2.16	1.43	0.89	0.47	7.28	6.35	5.42	2.73
TiO_2	2.25	2.99	7.88	11.25	6.76	4.36	4.21	5.86
Al_2O_3	0.3	0.44	0.98	1.94	2.54	4.3	1.3	4.31
Cr_2O_3	0.05	0.02	0.01	0.04	0.04	0.03	0.01	0.03
Fe_2O_3	57.32	57.68	48.30	42.38	34.64	40.58	44.45	43.50
FeO	34.29	34.08	38.14	39.36	41.53	36.98	38.40	35.63
MnO	0.13	0.29	0.26	1.06	0.31	1.11	0.29	0.91
MgO	0.04	0.04	0.03	0.11	2.68	3.37	1.29	1.51
CaO	0.58	0.49	0.21	0.93	0.27	0.17	0.36	0.35
Total	97.12	97.46	96.70	97.54	96.05	97.26	95.73	94.83
Numbers of ions on the basis of 32O								
Si	0.629	0.416	0.259	0.137	2.119	1.848	1.577	0.795
Al	0.103	0.151	0.336	0.665	0.871	1.475	0.446	1.478
Cr	0.012	0.005	0.002	0.009	0.009	0.007	0.002	0.007
Fe^{3+}	12.553	12.632	10.577	9.281	7.586	8.887	9.735	9.526
Ti	0.493	0.655	1.725	2.463	1.480	0.954	0.922	1.283
Mg	0.017	0.017	0.013	0.048	1.163	1.462	0.560	0.655
Fe^{2+}	8.345	8.293	9.283	9.578	10.107	9.000	9.346	8.671
Mn	0.032	0.071	0.064	0.261	0.076	0.274	0.071	0.224
Ca	0.181	0.153	0.065	0.290	0.084	0.053	0.112	0.109
Total	22.364	22.393	22.324	22.732	23.495	23.961	22.771	22.748

A: analcime-bearing
A-SRD: analcime-bearing, Spears Ranch Dike
AS: analcime-bearing, speckled texture
BF: basaltic, feeder(?) dike
B: basaltic
B-bt: basaltic with significant biotite
BPP: basaltic, pyroxene porphyry dike
M: minette

APPENDIX D.7: ELECTRON MICROPROBE ANALYSES OF MAGNETITE

	RDS-5-05b A	RDS-5-07b A	RDS-5-08b A	RDS-5-17b A	RDS-5-18b A	RDS-5-19b A	RDS-6-07 B	RDS-7-1 B-bt
SiO_2	1.47	0.92	11.05	0.94	0.14	1.96	0.15	0.6
TiO_2	9.32	8.14	9.22	10.19	9.53	8.54	7.25	11.52
Al_2O_3	3.49	3.42	4.87	3.9	6.1	3.79	1.41	2.37
Cr_2O_3	0.04	0.06	0.04	0.07	0.05	0.05	0.41	0.03
Fe_2O_3	41.31	45.55	21.94	42.27	41.93	42.76	51.20	42.79
FeO	37.63	37.19	47.98	38.23	35.50	38.41	36.47	41.97
MnO	1.23	0.99	0.57	0.99	0.86	0.95	0.94	0.31
MgO	1.22	0.8	4.24	1.65	2.34	1.33	0	0.3
CaO	0.23	0.12	0.17	0.16	0.1	0.19	0.16	0.22
Total	95.94	97.19	100.08	98.41	96.55	97.97	97.99	100.11
Numbers of ions on the basis of 32O								
Si	0.428	0.268	3.216	0.274	0.041	0.570	0.044	0.175
Al	1.197	1.173	1.670	1.337	2.092	1.300	0.484	0.813
Cr	0.009	0.014	0.009	0.016	0.012	0.012	0.094	0.007
Fe^{3+}	9.046	9.975	4.804	9.258	9.183	9.364	11.213	9.371
Ti	2.040	1.782	2.018	2.231	2.086	1.869	1.587	2.522
Mg	0.529	0.347	1.840	0.716	1.015	0.577	0.000	0.130
Fe^{2+}	9.158	9.052	11.677	9.304	8.639	9.347	8.875	10.213
Mn	0.303	0.244	0.140	0.244	0.212	0.234	0.232	0.076
Ca	0.072	0.037	0.053	0.050	0.031	0.059	0.050	0.069
Total	22.783	22.892	25.428	23.430	23.311	23.332	22.578	23.375

	RDS-7-2 B-bt	RDS-7-3 B-bt	RDS-7-4 B-bt	RDS-7-5 B-bt	RDS-7-6 B-bt	RDS-7-01b B-bt	RDS-7-02b B-bt	RDS-7-03b B-bt
SiO_2	0.14	0.28	0.11	0.18	0.17	0.15	0.79	0.13
TiO_2	10.01	10.54	10.37	9.45	10.88	9.32	9.52	9.13
Al_2O_3	2.36	2.44	2.78	3.77	2.21	3.33	4.89	4.14
Cr_2O_3	0.04	0.04	0.03	0.07	0.03	0.03	0	0.07
Fe_2O_3	47.55	45.30	46.62	46.59	45.84	45.30	41.27	45.07
FeO	40.23	41.08	38.98	38.15	41.55	37.52	37.50	36.79
MnO	0.29	0.26	0.85	0.81	0.13	0.59	0.69	0.8
MgO	0.46	0.18	0.98	1.04	0.12	0.78	1.51	1.11
CaO	0.06	0.07	0.22	0.2	0.22	0.28	0.11	0.3
Total	101.14	100.19	100.94	100.27	101.15	97.30	96.27	97.55
Numbers of ions on the basis of 32O								
Si	0.041	0.081	0.032	0.052	0.049	0.044	0.230	0.038
Al	0.809	0.837	0.953	1.293	0.758	1.142	1.677	1.420
Cr	0.009	0.009	0.007	0.016	0.007	0.007	0.000	0.016
Fe^{3+}	10.414	9.921	10.210	10.204	10.039	9.920	9.037	9.871
Ti	2.191	2.307	2.270	2.069	2.382	2.040	2.084	1.999
Mg	0.200	0.078	0.425	0.451	0.052	0.338	0.655	0.482
Fe^{2+}	9.791	9.997	9.486	9.285	10.112	9.131	9.126	8.954
Mn	0.071	0.064	0.210	0.200	0.032	0.145	0.170	0.197
Ca	0.019	0.022	0.069	0.062	0.069	0.087	0.034	0.094
Total	23.545	23.316	23.662	23.633	23.500	22.855	23.013	23.069

A: analcime-bearing
A-SRD: analcime-bearing, Spears Ranch Dike
AS: analcime-bearing, speckled texture
BF: basaltic, feeder(?) dike
B: basaltic
B-bt: basaltic with significant biotite
BPP: basaltic, pyroxene porphyry dike
M: minette

APPENDIX D.7: ELECTRON MICROPROBE ANALYSES OF MAGNETITE

	RDS-7-04b B-bt	RDS-7-05b B-bt	RDS-7-06b B-bt	RDS-8-1 B	RDS-8-2 B	RDS-8-3 B	RDS-8-4 B	RDS-8-5 B
SiO_2	0.48	0.65	0.14	0.13	0.84	0.13	0.14	0.07
TiO_2	10	9.35	9.61	7.9	8.02	8.12	9.37	8.25
Al_2O_3	3.52	4.59	3.09	0.54	0.85	1.47	0.73	0.73
Cr_2O_3	0.22	0.03	0.04	0.04	0.02	0.04	0.01	0.42
Fe_2O_3	42.38	42.38	45.35	53.89	50.50	51.97	50.70	53.32
FeO	37.13	38.34	37.59	37.14	38.95	37.47	38.05	37.24
MnO	0.86	0.65	0.77	1.55	0.55	1.22	1.87	1.46
MgO	1.34	0.87	0.83	0.11	0	0.07	0.13	0.09
CaO	0.31	0.11	0.29	0.21	0.2	0.41	0.27	0.65
Total	96.25	96.98	97.71	101.51	99.93	100.90	101.27	102.23
Numbers of ions on the basis of 32O								
Si	0.140	0.189	0.041	0.038	0.244	0.038	0.041	0.020
Al	1.207	1.574	1.060	0.185	0.291	0.504	0.250	0.250
Cr	0.051	0.007	0.009	0.009	0.005	0.009	0.002	0.097
Fe^{3+}	9.281	9.282	9.932	11.803	11.059	11.381	11.103	11.677
Ti	2.189	2.047	2.104	1.729	1.756	1.777	2.051	1.806
Mg	0.581	0.377	0.360	0.048	0.000	0.030	0.056	0.039
Fe^{2+}	9.037	9.331	9.149	9.038	9.480	9.119	9.260	9.063
Mn	0.212	0.160	0.190	0.382	0.136	0.301	0.461	0.360
Ca	0.097	0.034	0.090	0.065	0.062	0.128	0.084	0.203
Total	22.795	23.002	22.934	23.297	23.032	23.287	23.309	23.515

	RDS-8-6 B	RDS-8-01b B	RDS-8-02b B	RDS-8-03b B	RDS-8-04b B	RDS-11-03 BF	RDS-11-04 BF	RDS-11-05 BF
SiO_2	0.13	0.1	0.12	0.15	0.8	2.98	11	3.1
TiO_2	8.56	7.47	7.92	7.43	6.74	4.27	11.53	3.31
Al_2O_3	0.97	0.66	0.79	0.62	0.51	0.82	1.65	0.85
Cr_2O_3	0.01	0.03	0.04	0.16	0.01	2.08	1	1.7
Fe_2O_3	52.05	51.81	51.41	53.90	53.21	45.93	25.75	47.39
FeO	37.53	35.39	36.12	36.58	36.03	35.46	21.60	34.95
MnO	1.61	1.33	1.76	1.32	1.27	0.62	0.47	0.53
MgO	0.15	0.16	0.12	0.25	0.44	0.06	0	0.04
CaO	0.3	0.35	0.1	0.1	0.19	0.65	8.55	0.42
Total	101.31	97.30	98.38	100.51	99.20	92.87	81.55	92.29
Numbers of ions on the basis of 32O								
Si	0.038	0.029	0.035	0.044	0.233	0.867	3.201	0.902
Al	0.333	0.226	0.271	0.213	0.175	0.281	0.566	0.291
Cr	0.002	0.007	0.009	0.037	0.002	0.479	0.230	0.391
Fe^{3+}	11.399	11.347	11.259	11.804	11.653	10.058	5.639	10.379
Ti	1.874	1.635	1.734	1.626	1.475	0.935	2.524	0.725
Mg	0.065	0.069	0.052	0.108	0.191	0.026	0.000	0.017
Fe^{2+}	9.135	8.612	8.790	8.902	8.768	8.631	5.256	8.505
Mn	0.397	0.328	0.434	0.325	0.313	0.153	0.116	0.131
Ca	0.094	0.109	0.031	0.031	0.059	0.203	2.666	0.131
Total	23.335	22.363	22.615	23.091	22.870	21.632	20.199	21.472

A: analcime-bearing
A-SRD: analcime-bearing, Spears Ranch Dike
AS: analcime-bearing, speckled texture
BF: basaltic, feeder(?) dike
B: basaltic
B-bt: basaltic with significant biotite
BPP: basaltic, pyroxene porphyry dike
M: minette

APPENDIX D.7: ELECTRON MICROPROBE ANALYSES OF MAGNETITE

	RDS-11-07 BF	RDS-11-08 BF	RDS-13-01 B-bt	RDS-13-02 B-bt	RDS-13-05 B-bt	RDS-13-06 B-bt	RDS-15A-01 B
SiO_2	3	5.5	1.58	1.43	6.27	7.57	0.15
TiO_2	2.67	2.72	7.62	7.72	7.46	7.78	8.37
Al_2O_3	1.21	2.94	4.25	3.34	4.33	4.45	5.19
Cr_2O_3	0.49	0.02	0.03	0.07	0.02	0.05	0.08
Fe_2O_3	48.12	43.61	44.63	43.44	32.60	33.12	48.78
FeO	33.50	38.20	36.11	29.17	43.47	42.31	31.27
MnO	0.45	0.49	0.85	0.81	0.93	0.99	0.55
MgO	0.07	0.23	1.8	0.9	0.73	3.61	5.1
CaO	0.49	0.5	0.31	5.97	0.34	0.32	0.11
Total	90.00	94.21	97.18	92.85	96.15	100.20	99.60
Numbers of ions on the basis of 32O							
Si	0.873	1.601	0.460	0.416	1.825	2.203	0.044
Al	0.415	1.008	1.457	1.145	1.485	1.526	1.780
Cr	0.113	0.005	0.007	0.016	0.005	0.012	0.018
Fe^{3+}	10.538	9.550	9.774	9.514	7.140	7.252	10.682
Ti	0.584	0.595	1.668	1.690	1.633	1.703	1.832
Mg	0.030	0.100	0.781	0.391	0.317	1.566	2.213
Fe^{2+}	8.153	9.297	8.788	7.099	10.578	10.297	7.610
Mn	0.111	0.121	0.210	0.200	0.229	0.244	0.136
Ca	0.153	0.156	0.097	1.861	0.106	0.100	0.034
Total	20.970	22.432	23.241	22.332	23.317	24.903	24.349

	RDS-15A-02 B	RDS-15A-03 B	RDS-15A-04 B	RDS-15A-05 B	RDS-15A-06 B	RDS-15A-53 B	RDS-15A-54 B
SiO_2	0.4	0.2	0.14	0.16	0.15	0.14	0.25
TiO_2	9.66	13.86	12.18	7.3	8.29	14.44	13.83
Al_2O_3	1.62	1.08	0.89	5.33	4.96	2.27	1.7
Cr_2O_3	0	0	0.02	0.22	0.21	0.56	0.17
Fe_2O_3	46.79	38.75	42.33	50.82	48.98	36.31	38.54
FeO	37.16	43.06	41.31	30.59	32.60	43.33	43.41
MnO	0.68	0.24	0.22	0.4	0.52	0.39	0.43
MgO	1.48	0.05	0.02	5.04	4.3	0.39	0.08
CaO	0.03	0.17	0.28	0.2	0.09	0.07	0.08
Total	97.83	97.40	97.39	100.06	100.10	97.90	98.49
Numbers of ions on the basis of 32O							
Si	0.116	0.058	0.041	0.047	0.044	0.041	0.073
Al	0.556	0.370	0.305	1.828	1.701	0.778	0.583
Cr	0.000	0.000	0.005	0.051	0.048	0.129	0.039
Fe^{3+}	10.248	8.485	9.270	11.129	10.726	7.951	8.439
Ti	2.115	3.034	2.666	1.598	1.815	3.161	3.027
Mg	0.642	0.022	0.009	2.187	1.866	0.169	0.035
Fe^{2+}	9.045	10.479	10.054	7.445	7.933	10.546	10.566
Mn	0.168	0.059	0.054	0.099	0.128	0.096	0.106
Ca	0.009	0.053	0.087	0.062	0.028	0.022	0.025
Total	22.898	22.560	22.491	24.445	24.289	22.892	22.893

A: analcime-bearing
A-SRD: analcime-bearing, Spears Ranch Dike
AS: analcime-bearing, speckled texture
BF: basaltic, feeder(?) dike
B: basaltic
B-bt: basaltic with significant biotite
BPP: basaltic, pyroxene porphyry dike
M: minette

APPENDIX D.7: ELECTRON MICROPROBE ANALYSES OF MAGNETITE

	RDS-15B-01 B	RDS-15B-02 B	RDS-15B-03 B	RDS-15B-04 B	RDS-15B-05 B	RDS-15B-06 B	RDS-15C-01 B	RDS-15C-02 B
SiO_2	0	0.08	0.02	0	0.19	1.3	0.12	0.17
TiO_2	2.55	10.82	9.28	1.23	11.5	12.25	10.41	10.87
Al_2O_3	9.3	2.08	3.77	17.72	1.83	2.29	3.16	1.17
Cr_2O_3	26.18	5.19	5.76	36.57	0.02	0.08	0.08	0
Fe_2O_3	29.94	39.98	43.00	14.68	43.85	38.53	44.70	44.74
FeO	24.90	37.08	32.64	17.23	35.41	40.00	36.37	38.79
MnO	0.59	0.75	0.72	0.31	0.85	0.58	0.74	0.38
MgO	6.15	2.01	4.32	11.06	3	1.85	2.36	0.86
CaO	0.41	0.11	0.31	1.04	0.43	0.19	0.05	0.16
Total	100.02	98.11	99.83	99.84	97.08	97.07	97.99	97.14
Numbers of ions on the basis of 32O								
Si	0.000	0.023	0.006	0.000	0.055	0.378	0.035	0.049
Al	3.189	0.713	1.293	6.077	0.628	0.785	1.084	0.401
Cr	6.024	1.194	1.325	8.414	0.005	0.018	0.018	0.000
Fe^{3+}	6.557	8.756	9.418	3.215	9.603	8.437	9.789	9.798
Ti	0.558	2.369	2.031	0.269	2.517	2.682	2.279	2.379
Mg	2.668	0.872	1.874	4.799	1.302	0.803	1.024	0.373
Fe^{2+}	6.060	9.025	7.944	4.193	8.618	9.736	8.851	9.441
Mn	0.145	0.185	0.177	0.076	0.210	0.143	0.182	0.094
Ca	0.128	0.034	0.097	0.324	0.134	0.059	0.016	0.050
Total	25.329	23.171	24.166	27.368	23.071	23.041	23.278	22.585

	RDS-15C-03 B	RDS-15C-05 B	RDS-15C-33 B	RDS-16A-01 BPP	RDS-16A-02 BPP	RDS-16A-03 BPP	RDS-16A-04 BPP	RDS-16A-07 BPP
SiO_2	0.47	0.29	0	0.15	0.09	0.17	0.11	0.16
TiO_2	10.99	7.08	2.82	12.8	14.93	17.74	15.25	12.01
Al_2O_3	1.09	6.05	11.42	2.65	1.16	1.8	2	1.1
Cr_2O_3	0.02	0.27	27.94	0.62	0.28	0.02	0.42	0.05
Fe_2O_3	43.96	49.90	25.75	39.82	37.90	31.11	35.16	43.39
FeO	40.77	28.92	21.60	42.10	44.52	45.29	44.22	41.67
MnO	0.14	0.39	0.3	0.35	0.44	0.48	0.45	0.43
MgO	0.13	5.8	8.68	0.52	0.02	0.92	0.21	0
CaO	0.24	0.48	0.42	0.06	0.06	0.14	0.06	0.16
Total	97.80	99.18	98.93	99.07	99.40	97.67	97.88	98.97
Numbers of ions on the basis of 32O								
Si	0.137	0.084	0.000	0.044	0.026	0.049	0.032	0.047
Al	0.374	2.075	3.916	0.909	0.398	0.617	0.686	0.377
Cr	0.005	0.062	6.429	0.143	0.064	0.005	0.097	0.012
Fe^{3+}	9.626	10.927	5.639	8.720	8.300	6.812	7.700	9.502
Ti	2.406	1.550	0.617	2.802	3.268	3.883	3.338	2.629
Mg	0.056	2.517	3.766	0.226	0.009	0.399	0.091	0.000
Fe^{2+}	9.922	7.039	5.256	10.246	10.834	11.022	10.762	10.141
Mn	0.035	0.096	0.074	0.086	0.108	0.118	0.111	0.106
Ca	0.075	0.150	0.131	0.019	0.019	0.044	0.019	0.050
Total	22.634	24.499	25.829	23.194	23.026	22.950	22.836	22.863

A: analcime-bearing
A-SRD: analcime-bearing, Spears Ranch Dike
AS: analcime-bearing, speckled texture
BF: basaltic, feeder(?) dike
B: basaltic
B-bt: basaltic with significant biotite
BPP: basaltic, pyroxene porphyry dike
M: minette

APPENDIX D.7: ELECTRON MICROPROBE ANALYSES OF MAGNETITE

	RDS-16A-17 BPP	RDS-16A-38 BPP	RDS-16A-39 BPP	RDS-16A-54 BPP	RDS-16B-02 BPP	RDS-16B-03 BPP	RDS-16B-04 BPP	RDS-16B-05 BPP
SiO_2	0.52	0.17	2.83	0.23	0.14	0.13	0.12	0.16
TiO_2	9.55	13.08	25.84	11.32	11.88	13.01	13.87	13.9
Al_2O_3	1.07	1.33	2.31	4.59	0.86	1.14	1.65	1.33
Cr_2O_3	0.05	0.04	0.04	0.47	0.06	0.14	0.26	0.04
Fe_2O_3	46.96	40.94	9.30	42.96	43.99	41.20	38.38	38.59
FeO	39.45	42.69	54.27	38.18	41.63	42.49	43.08	42.99
MnO	0.34	0.5	0.71	0.4	0.49	0.56	0.59	0.54
MgO	0.15	0.03	1.95	2.87	0	0.01	0.01	0.01
CaO	0.21	0.05	0.49	0	0.01	0.04	0.08	0.12
Total	98.29	98.83	97.74	101.01	99.06	98.72	98.04	97.69
Numbers of ions on the basis of 32O								
Si	0.151	0.049	0.824	0.067	0.041	0.038	0.035	0.047
Al	0.367	0.456	0.792	1.574	0.295	0.391	0.566	0.456
Cr	0.012	0.009	0.009	0.108	0.014	0.032	0.060	0.009
Fe^{3+}	10.283	8.966	2.038	9.407	9.634	9.023	8.405	8.452
Ti	2.090	2.863	5.656	2.478	2.601	2.848	3.036	3.043
Mg	0.065	0.013	0.846	1.245	0.000	0.004	0.004	0.004
Fe^{2+}	9.600	10.389	13.207	9.291	10.130	10.340	10.483	10.463
Mn	0.084	0.123	0.175	0.099	0.121	0.138	0.145	0.133
Ca	0.065	0.016	0.153	0.000	0.003	0.012	0.025	0.037
Total	22.718	22.885	23.700	24.269	22.838	22.826	22.760	22.644

	RDS-16B-06 BPP	RDS-16B-07 BPP	RDS-16C-01 BPP	RDS-16C-03 BPP	RDS-16C-04 BPP	RDS-16C-05 BPP	RDS-16C-06 BPP	RDS-009-01 M
SiO_2	0.15	0.15	0.27	0.09	0.19	0.21	0.16	4.04
TiO_2	12.68	12.3	10.12	8.6	11.86	11.42	12.21	4.19
Al_2O_3	1.74	1.03	0.87	6.21	1.24	3.06	2.68	1.3
Cr_2O_3	0.05	0.03	0.05	0.14	0.07	0.59	0.61	0.03
Fe_2O_3	40.51	42.78	46.09	45.76	43.02	41.47	40.31	48.11
FeO	42.08	41.84	39.94	33.55	41.70	41.83	42.22	36.19
MnO	0.46	0.5	0.23	0.39	0.24	0.18	0.24	0.84
MgO	0.03	0	0.01	3.8	0.01	0	0.01	0.07
CaO	0.04	0.1	0.03	0	0.07	0.1	0.14	2.04
Total	97.74	98.74	97.61	98.53	98.40	98.87	98.59	96.81
Numbers of ions on the basis of 32O								
Si	0.044	0.044	0.079	0.026	0.055	0.061	0.047	1.176
Al	0.597	0.353	0.298	2.130	0.425	1.049	0.919	0.446
Cr	0.012	0.007	0.012	0.032	0.016	0.136	0.140	0.007
Fe^{3+}	8.872	9.370	10.094	10.021	9.421	9.083	8.829	10.537
Ti	2.776	2.692	2.215	1.883	2.596	2.500	2.673	0.917
Mg	0.013	0.000	0.004	1.649	0.004	0.000	0.004	0.030
Fe^{2+}	10.240	10.183	9.719	8.164	10.149	10.180	10.276	8.807
Mn	0.113	0.123	0.057	0.096	0.059	0.044	0.059	0.207
Ca	0.012	0.031	0.009	0.000	0.022	0.031	0.044	0.636
Total	22.678	22.803	22.487	24.000	22.748	23.085	22.991	22.763

A: analcime-bearing
A-SRD: analcime-bearing, Spears Ranch Dike
AS: analcime-bearing, speckled texture
BF: basaltic, feeder(?) dike
B: basaltic
B-bt: basaltic with significant biotite
BPP: basaltic, pyroxene porphyry dike
M: minette

APPENDIX D.7: ELECTRON MICROPROBE ANALYSES OF MAGNETITE

	RDS-009-02 M	RDS-009-03 M	RDS-009-04 M	RDS-009-05 M	RDS-009-06 M	RDS-009-34 M	RDS-013A-34 AS	RDS-013A-35 AS
SiO_2	1.11	2.44	0.12	2.09	0.11	0.13	0.08	0.1
TiO_2	5.03	3.73	6.69	2.14	6.98	7.23	13.14	11.59
Al_2O_3	2.21	1.68	4.98	1.39	5.29	5.61	1.74	3.95
Cr_2O_3	0.04	0	0.07	0.03	0.03	0	0.06	1.05
Fe_2O_3	51.45	51.99	52.36	56.01	51.42	50.17	41.84	41.22
FeO	34.53	35.20	34.58	33.74	32.75	32.40	41.29	39.85
MnO	0.86	0.79	1.1	0.64	1	0.88	2.56	1.5
MgO	0.36	0.05	2.05	0.08	3.29	3.64	0	0.77
CaO	0.3	0.81	0.06	0.4	0.05	0.05	0.02	0.14
Total	95.88	96.69	102.01	96.51	100.92	100.11	100.73	100.17
Numbers of ions on the basis of 32O								
Si	0.323	0.710	0.035	0.608	0.032	0.038	0.023	0.029
Al	0.758	0.576	1.708	0.477	1.814	1.924	0.597	1.355
Cr	0.009	0.000	0.016	0.007	0.007	0.000	0.014	0.242
Fe^{3+}	11.266	11.387	11.466	12.265	11.260	10.987	9.163	9.028
Ti	1.101	0.816	1.464	0.468	1.528	1.583	2.876	2.537
Mg	0.156	0.022	0.889	0.035	1.427	1.579	0.000	0.334
Fe^{2+}	8.403	8.565	8.415	8.210	7.971	7.885	10.049	9.697
Mn	0.212	0.195	0.271	0.158	0.246	0.217	0.631	0.370
Ca	0.094	0.253	0.019	0.125	0.016	0.016	0.006	0.044
Total	22.322	22.524	24.284	22.353	24.302	24.227	23.359	23.635

	RDS-013A-36 AS	RDS-013A-37 AS	RDS-013A-38 AS	RDS-013B-01 AS	RDS-013B-02 AS	RDS-013B-03 AS	RDS-013B-06 AS	RDS-027-01 B
SiO_2	0.11	0.11	0.61	1.74	9.24	0.97	0.87	0.13
TiO_2	13.4	12.77	12.68	4.14	8.97	6.95	8.92	9.07
Al_2O_3	1.29	2.33	1.85	0.25	3.36	0.69	0.87	5.37
Cr_2O_3	0.01	0.08	0.22	0.04	0.04	0.04	0.02	0.25
Fe_2O_3	40.61	40.81	40.52	56.69	24.45	51.91	47.58	45.54
FeO	41.14	40.40	40.90	36.31	41.07	37.67	38.18	35.10
MnO	2.34	2.7	2.49	0.47	0.83	0.74	1.39	0.54
MgO	0	0.02	0.2	0.08	5.15	0.02	0.1	2.89
CaO	0.04	0.08	0.1	0.3	0.42	0.18	0.31	0.17
Total	98.94	99.30	99.57	100.02	93.53	99.16	98.24	99.06
Numbers of ions on the basis of 32O								
Si	0.032	0.032	0.178	0.506	2.689	0.282	0.253	0.038
Al	0.442	0.799	0.634	0.086	1.152	0.237	0.298	1.842
Cr	0.002	0.018	0.051	0.009	0.009	0.009	0.005	0.058
Fe^{3+}	8.894	8.936	8.873	12.415	5.356	11.367	10.420	9.973
Ti	2.933	2.795	2.776	0.906	1.964	1.521	1.953	1.985
Mg	0.000	0.009	0.087	0.035	2.235	0.009	0.043	1.254
Fe^{2+}	10.011	9.833	9.954	8.836	9.994	9.166	9.291	8.543
Mn	0.577	0.666	0.614	0.116	0.205	0.182	0.343	0.133
Ca	0.012	0.025	0.031	0.094	0.131	0.056	0.097	0.053
Total	22.904	23.113	23.197	23.003	23.734	22.830	22.702	23.878

A: analcime-bearing
A-SRD: analcime-bearing, Spears Ranch Dike
AS: analcime-bearing, speckled texture
BF: basaltic, feeder(?) dike
B: basaltic
B-bt: basaltic with significant biotite
BPP: basaltic, pyroxene porphyry dike
M: minette

APPENDIX D.7: ELECTRON MICROPROBE ANALYSES OF MAGNETITE

	RDS-027-03 B	RDS-027-04 B	RDS-027-05 B	RDS-027-06 B	RDS-102-01 M	RDS-102-02 M	RDS-102-03 M	RDS-102-04 M
SiO_2	2.29	0.21	0.32	0.15	0.19	7.97	9.8	8.95
TiO_2	13.53	11.46	12.29	11.56	6.81	8.06	6.73	7.82
Al_2O_3	1.55	3.48	2.57	3.24	1.2	1.94	1.41	4.15
Cr_2O_3	0.04	0.04	0.03	0.15	0.03	1.27	0.17	0.81
Fe_2O_3	30.90	41.69	40.55	42.14	53.24	32.43	33.40	24.08
FeO	41.00	39.63	40.65	39.20	36.99	48.90	47.88	39.40
MnO	2.01	0.76	1.85	0.65	0.26	0.37	0.41	0.25
MgO	0.77	1.02	0.08	1.4	0.1	0.4	1.72	5.3
CaO	0.33	0.1	0.22	0.09	0.07	0.1	0.22	0.4
Total	92.42	98.40	98.55	98.58	98.88	101.44	101.74	91.16
Numbers of ions on the basis of 32O								
Si	0.666	0.061	0.093	0.044	0.055	2.320	2.852	2.605
Al	0.532	1.193	0.881	1.111	0.412	0.665	0.484	1.423
Cr	0.009	0.009	0.007	0.035	0.007	0.292	0.039	0.186
Fe^{3+}	6.766	9.131	8.880	9.229	11.659	7.101	7.314	5.274
Ti	2.962	2.509	2.690	2.530	1.491	1.764	1.473	1.712
Mg	0.334	0.443	0.035	0.607	0.043	0.174	0.746	2.300
Fe^{2+}	9.978	9.645	9.892	9.540	9.001	11.901	11.652	9.589
Mn	0.495	0.187	0.456	0.160	0.064	0.091	0.101	0.062
Ca	0.103	0.031	0.069	0.028	0.022	0.031	0.069	0.125
Total	21.845	23.210	23.002	23.284	22.754	24.340	24.730	23.275

	RDS-102-05 M	RDS-102-06 M	RDS-130-13 BF	RDS-130-14 BF	RDS-130-15 BF	RDS-130-16 BF	RDS-130-17 BF	RDS-130-19 BF
SiO_2	0.24	0.15	0.13	0.17	0.16	0.09	0.15	0.11
TiO_2	8.72	9.69	15.39	11.14	14.46	18.62	12.29	18.48
Al_2O_3	4.1	1.67	0.99	0.63	3.57	0.7	1.25	0.94
Cr_2O_3	2.23	0.56	0.2	0.02	0.25	0.04	0.13	0.25
Fe_2O_3	44.51	46.96	37.39	46.42	38.84	31.35	43.42	31.51
FeO	36.35	39.64	43.93	40.30	38.41	46.59	40.79	46.69
MnO	0.8	0.37	1.32	0.44	0.41	1.66	0.4	1.57
MgO	1.65	0.05	0.03	0.47	3.99	0	0.93	0.01
CaO	0.1	0.2	0.23	0.16	0.44	0.05	0.07	0.13
Total	98.70	99.30	99.61	99.75	100.53	99.10	99.43	99.69
Numbers of ions on the basis of 32O								
Si	0.070	0.044	0.038	0.049	0.047	0.026	0.044	0.032
Al	1.406	0.573	0.339	0.216	1.224	0.240	0.429	0.322
Cr	0.513	0.129	0.046	0.005	0.058	0.009	0.030	0.058
Fe^{3+}	9.747	10.285	8.188	10.166	8.505	6.866	9.508	6.900
Ti	1.909	2.121	3.369	2.439	3.165	4.076	2.690	4.045
Mg	0.716	0.022	0.013	0.204	1.731	0.000	0.404	0.004
Fe^{2+}	8.846	9.648	10.690	9.807	9.349	11.338	9.928	11.363
Mn	0.197	0.091	0.325	0.108	0.101	0.409	0.099	0.387
Ca	0.031	0.062	0.072	0.050	0.137	0.016	0.022	0.041
Total	23.436	22.974	23.081	23.045	24.317	22.980	23.152	23.152

A: analcime-bearing
A-SRD: analcime-bearing, Spears Ranch Dike
AS: analcime-bearing, speckled texture
BF: basaltic, feeder(?) dike
B: basaltic
B-bt: basaltic with significant biotite
BPP: basaltic, pyroxene porphyry dike
M: minette

APPENDIX C.8: ELECTRON MICROPROBE ANALYSES OF CARBONATE

	RDS-3-21 M	RDS-4-01 B	RDS-4-02 B	RDS-4-03 B	RDS-8-7 B	RDS-8-19 B	RDS-8-08b B	RDS-8-11b B
SiO_2	0.45	0.41	0.02	0.18	0.06	0.07	0.69	0.00
FeO	0.52	0.32	0.22	0.24	0.22	0.61	0.34	0.32
MnO	0.35	0.15	0.13	0.53	0.49	1.65	2.37	0.38
MgO	0.35	0.23	0.08	0.33	0.27	0.25	0.95	0.29
CaO	51.22	54.53	55.17	53.45	56.01	53.80	48.68	52.18
CO_2	40.68	42.92	43.55	42.55	44.62	43.83	40.05	41.63
Total	93.57	98.56	99.17	97.28	101.67	100.21	93.08	94.80
	Numbers of ions on the basis of 6O							
Mg	0.0187	0.0117	0.0040	0.0169	0.0132	0.0125	0.0514	0.0152
Fe^{2+}	0.0156	0.0091	0.0062	0.0069	0.0060	0.0170	0.0103	0.0094
Mn	0.0106	0.0043	0.0037	0.0154	0.0136	0.0467	0.0729	0.0113
Ca	1.9694	1.9879	1.9876	1.9679	1.9692	1.9256	1.8941	1.9663
C	1.9928	1.9935	1.9993	1.9964	1.9990	1.9991	1.9856	1.9989
Total	4.0072	4.0065	4.0007	4.0036	4.0010	4.0009	4.0144	4.0011

	RDS-13-03 B-bt	RDS-13-07 B-bt	RDS-13-08 B-bt	RDS-013B-11 B	RDS-013B-14 B	RDS-013B-21 B	RDS-15B-26 B	RDS-15B-28 B
SiO_2	0.11	0.08	0.05	0.23	0.18	0.34	0.21	0.17
FeO	0.25	0.22	0.33	0.21	0.26	0.35	7.56	7.80
MnO	0.48	0.37	0.36	0.85	0.69	0.77	0.76	0.74
MgO	0.27	0.15	0.13	0.20	0.20	0.28	13.39	13.81
CaO	54.29	54.57	54.50	52.57	52.76	51.24	32.46	32.12
CO_2	43.24	43.27	43.29	41.90	42.03	40.87	45.00	45.35
Total	98.64	98.66	98.66	95.96	96.12	93.85	99.38	99.99
	Numbers of ions on the basis of 6O							
Mg	0.0136	0.0076	0.0066	0.0104	0.0104	0.0149	0.6490	0.6643
Fe^{2+}	0.0071	0.0062	0.0093	0.0061	0.0076	0.0105	0.2055	0.2104
Mn	0.0138	0.0106	0.0103	0.0251	0.0203	0.0233	0.0209	0.0202
Ca	1.9689	1.9780	1.9753	1.9656	1.9674	1.9623	1.1306	1.1103
C	1.9983	1.9988	1.9993	1.9964	1.9972	1.9945	1.9970	1.9974
Total	4.0017	4.0012	4.0007	4.0036	4.0028	4.0055	4.0030	4.0026

	RDS-15B-29 B	RDS-15B-30 B	RDS-15C-32 B	RDS-16B-01 BPP	RDS-106-21 M
SiO_2	0.13	3.00	0.06	0.05	0.55
FeO	0.36	0.93	0.67	2.05	0.49
MnO	1.07	1.09	0.81	0.19	0.09
MgO	1.12	2.23	1.55	18.40	0.35
CaO	52.14	49.38	51.71	31.51	54.12
CO_2	42.95	39.41	43.17	46.17	42.66
Total	97.77	96.04	97.97	98.37	98.26
Numbers of ions on the basis of 6O					
Mg	0.0569	0.1205	0.0784	0.8703	0.0178
Fe^{2+}	0.0103	0.0282	0.0190	0.0544	0.0140
Mn	0.0309	0.0335	0.0233	0.0051	0.0026
Ca	1.9042	1.9177	1.8798	1.0710	1.9826
C	1.9989	1.9501	1.9998	1.9996	1.9915
Total	4.0011	4.0499	4.0002	4.0004	4.0085

B: basaltic
B-bt: basaltic with significant biotite
BPP: basaltic, pyroxene porphyry dike
M: minette

APPENDIX D.9: ELECTRON MICROPROBE ANALYSES OF HORNBLENDE

	RDS-283-01 HB	RDS-283-02 HB	RDS-283-03 HB	RDS-283-04 HB	RDS-283-05 HB	RDS-283-06 HB	RDS-283-07 HB
SiO_2	40.81	40.12	40.44	40.06	40.63	40.87	40.07
Al_2O_3	12.59	12.97	13.22	13.15	12.59	12.79	13.14
TiO_2	3.99	3.88	4.12	3.81	3.92	3.95	3.78
MgO	14.16	13.27	14.18	13.15	14.13	14.50	13.13
FeO	11.69	12.68	11.28	13.07	11.36	10.71	13.06
MnO	0.12	0.14	0.11	0.15	0.08	0.09	0.13
Na_2O	2.26	2.35	2.28	2.29	2.23	2.29	2.31
CaO	11.88	11.61	11.70	11.59	11.86	11.98	11.83
K_2O	1.45	1.34	1.51	1.33	1.51	1.49	1.34
F	0.34	0.33	0.33	0.34	0.23	0.32	0.38
Cl	0.00	0.01	0.00	0.02	0.01	0.01	0.04
	99.30	98.70	99.18	98.96	98.54	98.99	99.19
-O=F,Cl	0.15	0.14	0.14	0.15	0.10	0.14	0.17
Total	99.15	98.56	99.04	98.81	98.44	98.85	99.02
Numbers of ions on the basis of 23O							
Si	5.9690	5.9304	5.9111	5.9147	5.9812	5.9704	5.9056
Al	2.1696	2.2590	2.2773	2.2875	2.1841	2.2012	2.2825
Ti	0.4394	0.4311	0.4527	0.4232	0.4337	0.4341	0.4189
Mg	3.0871	2.9243	3.0901	2.8947	3.1013	3.1584	2.8851
Fe^{2+}	1.4301	1.5675	1.3792	1.6132	1.3982	1.3086	1.6091
Mn	0.0146	0.0179	0.0142	0.0191	0.0099	0.0106	0.0157
Na	0.6409	0.6743	0.6471	0.6542	0.6356	0.6486	0.6605
Ca	1.8618	1.8378	1.8323	1.8324	1.8703	1.8744	1.8679
K	0.2698	0.2520	0.2815	0.2513	0.2841	0.2775	0.2522
F	0.1588	0.1532	0.1533	0.1576	0.1068	0.1457	0.1772
Cl	0.0007	0.0022	0.0000	0.0042	0.0023	0.0027	0.0089
Total	16.0419	16.0498	16.0386	16.0520	16.0075	16.0322	16.0836

	RDS-283-08 HB	RDS-283-010 HB	RDS-283-011 HB	RDS-283-014 HB	RDS-283-015 HB	RDS-283-016 HB	RDS-283-017 HB
SiO_2	40.29	40.81	40.86	40.64	39.85	40.32	40.07
Al_2O_3	13.31	12.62	12.66	12.78	12.97	12.64	13.01
TiO_2	3.95	3.98	3.86	3.63	3.86	3.94	3.62
MgO	13.33	13.75	13.81	13.20	13.26	13.96	13.58
FeO	12.72	11.74	12.14	12.86	12.89	11.84	12.83
MnO	0.17	0.13	0.08	0.17	0.15	0.14	0.13
Na_2O	2.33	2.29	2.35	2.42	2.38	2.38	2.28
CaO	11.73	11.68	11.54	11.57	11.61	11.64	11.57
K_2O	1.32	1.42	1.37	1.26	1.37	1.33	1.40
F	0.38	0.30	0.29	0.23	0.32	0.33	0.24
Cl	0.02	0.01	0.00	0.02	0.02	0.01	0.01
	99.56	98.72	98.96	98.76	98.69	98.53	98.75
-O=F,Cl	0.16	0.13	0.12	0.10	0.14	0.14	0.10
Total	99.39	98.59	98.84	98.66	98.55	98.39	98.65
Numbers of ions on the basis of 23O							
Si	5.9029	5.9993	5.9977	5.9986	5.9034	5.9479	5.9248
Al	2.2975	2.1868	2.1901	2.2233	2.2647	2.1984	2.2663
Ti	0.4358	0.4400	0.4256	0.4026	0.4305	0.4375	0.4025
Mg	2.9110	3.0140	3.0220	2.9038	2.9284	3.0697	2.9935
Fe^{2+}	1.5578	1.4427	1.4898	1.5868	1.5971	1.4609	1.5861
Mn	0.0212	0.0157	0.0105	0.0214	0.0186	0.0174	0.0161
Na	0.6632	0.6517	0.6693	0.6939	0.6824	0.6800	0.6538
Ca	1.8414	1.8399	1.8152	1.8290	1.8428	1.8401	1.8330
K	0.2463	0.2666	0.2556	0.2367	0.2592	0.2508	0.2646
F	0.1750	0.1375	0.1366	0.1074	0.1485	0.1546	0.1142
Cl	0.0060	0.0016	0.0000	0.0054	0.0062	0.0017	0.0018
Total	16.0578	15.9959	16.0124	16.0088	16.0819	16.0590	16.0568

HB: hornblende porphyry dike west of the Riley dike swarm

APPENDIX D.9: ELECTRON MICROPROBE ANALYSES OF HORNBLENDE

	RDS-283-020 HB	RDS-283-023 HB	RDS-283-024 HB	RDS-283-025 HB	RDS-283-026 HB
SiO_2	40.57	40.66	41.21	41.18	39.67
Al_2O_3	12.94	12.83	12.10	12.74	13.15
TiO_2	4.07	3.95	3.89	3.81	3.99
MgO	13.64	13.00	14.21	14.49	13.72
FeO	12.06	13.11	11.23	10.62	11.85
MnO	0.07	0.18	0.14	0.11	0.11
Na_2O	2.27	2.36	2.23	2.21	2.27
CaO	11.68	11.76	11.82	11.95	11.83
K_2O	1.47	1.22	1.42	1.51	1.46
F	0.31	0.42	0.27	0.41	0.64
Cl	0.02	0.03	0.00	0.02	0.02
	99.10	99.52	98.50	99.05	98.70
-O=F,Cl	0.13	0.18	0.11	0.18	0.27
Total	98.97	99.34	98.39	98.88	98.42
Numbers of ions on the basis of 23O					
Si	5.9524	5.9641	6.0570	6.0034	5.8536
Al	2.2376	2.2173	2.0952	2.1894	2.2875
Ti	0.4489	0.4361	0.4295	0.4181	0.4424
Mg	2.9839	2.8434	3.1128	3.1487	3.0178
Fe^{2+}	1.4791	1.6085	1.3803	1.2944	1.4620
Mn	0.0086	0.0222	0.0174	0.0131	0.0134
Na	0.6467	0.6714	0.6363	0.6257	0.6498
Ca	1.8356	1.8479	1.8612	1.8667	1.8694
K	0.2745	0.2287	0.2653	0.2803	0.2742
F	0.1419	0.1964	0.1232	0.1897	0.2997
Cl	0.0045	0.0064	0.0000	0.0047	0.0045
Total	16.0138	16.0425	15.9783	16.0341	16.1743

HB: hornblende porphyry dike west of the Riley dike swarm

APPENDIX E: Electron Microprobe Standard Analyses

	Orthoclase n=48			Kaersuitite (amphibole) n=47			Albite n=48		
	Accepted	Measured	1σ	Accepted	Measured	1σ	Accepted	Measured	1σ
SiO_2	64.79	64.87	0.27	39.30	38.59	0.86	68.24	68.66	0.30
TiO_2				4.14	4.17	0.11			
Al_2O_3	16.72	16.71	0.11	15.37	15.05	0.46	19.90	20.23	0.16
FeO*	1.88	1.80	0.06	8.90	8.49	0.31			
MnO				0.10	0.09	0.02			
MgO				13.89	13.92	0.31			
CaO				12.54	12.12	0.31	0.03	0.05	0.05
Na_2O	0.91	0.92	0.02	2.36	2.24	0.36	11.94	11.81	0.09
K_2O	15.49	15.58	0.21	1.36	1.26	0.05	0.04	0.02	0.01
P_2O_5				0.40					
SO_2									
BaO	0.05	0.07	0.03						
SrO									
F				0.26	0.31**	0.05			
Cl									
Cr_2O_3									

**n=11

	Anorthite n=48			Biotite-3 n=26			Magnetite n=42		
	Accepted	Measured	1σ	Accepted	Measured	1σ	Accepted	Measured	1σ
SiO_2	44.17	44.14	0.18	38.62	38.20	1.26	6.90	0.11	0.03
TiO_2				2.26	2.19	0.09	0.02	0.04	0.02
Al_2O_3	34.95	34.92	0.27	10.72	10.98	0.51	0.38	0.39	0.24
FeO*	0.57	0.39	0.03	18.13	18.26	0.62	92.73	93.34	1.29
MnO				0.95	0.96	0.07	0.07	0.05	0.02
MgO				14.01	13.41	0.64	0.12	0.10	0.08
CaO	18.63	18.51	0.18			0.02			
Na_2O	0.79	0.63	0.06	0.69	0.58	0.17			
K_2O	0.05	0.02	0.01	9.21	9.15	0.35			
P_2O_5									
SO_2									
BaO				0.11					
SrO									
F				3.30	3.55	0.39			
Cl									
Cr_2O_3							0.01	0.01	0.01

APPENDIX E: Electron Microprobe Standard Analyses

	VG2 (basalt glass) n=30			kakanui (amphibole) n=48			beeap (apatite) n=4		
	Accepted	Measured	1σ	Accepted	Measured	1σ	Accepted	Measured	1σ
SiO_2	50.81	50.19	0.40	40.37	40.59	0.21	0.11	0.06	0.02
TiO_2	1.85	1.83	0.07	4.72	4.74	0.08			
Al_2O_3	14.06	14.19	0.17	14.90	14.40	0.35			
FeO*	11.82	12.03	0.20	10.89	11.00	0.24	0.04	0.02	0.02
MnO	0.22	0.21	0.04	0.09	0.09	0.02			
MgO	6.71	6.84	0.09	12.80	12.68	0.24			
CaO	11.12	10.83	0.16	10.30	10.15	0.21	54.31	54.16	0.40
Na_2O	2.62	2.78	0.05	2.60	2.61	0.13			
K_2O	0.19	0.20	0.02	2.05	2.11	0.05			
P_2O_5	0.2	0.22	0.04				40.93	41.13	0.35
SO_2									
BaO									
SrO							0.20	0.44	0.02
F							3.67	5.61	0.14
Cl									
Cr_2O_3									

	usnm (olivine) n=8		
	Accepted	Measured	1σ
SiO_2	40.81	40.93	0.12
TiO_2			
Al_2O_3			
FeO*	9.55	10.07	0.27
MnO	0.14	0.12	0.02
MgO	49.42	49.02	0.26
CaO			
Na_2O			
K_2O			
P_2O_5			
SO_2			
BaO			
SrO			
F			
Cl			
Cr_2O_3			

APPENDIX F: XRF AND ICP-MS GEOCHEMICAL ANALYSES

	RDS-211	MDS-32	RDS-009	RDS-5	MDS-15	MDS-15 duplicate 1	MDS-15 duplicate 2
SiO2 (wt%)	48.04	48.91	48.06	46.88	50.55	50.56	50.54
TiO2	1.11	1.15	1.13	1.27	1.28	1.28	1.27
Al2O3	12.61	12.58	12.62	13.47	13.68	13.71	13.72
FeO	8.71	9.19	8.66	9.33	8.89	8.90	8.89
MnO	0.17	0.14	0.15	0.17	0.16	0.16	0.15
MgO	11.16	11.05	11.00	10.39	10.27	10.26	10.25
CaO	11.98	10.27	11.56	11.62	8.86	8.85	8.86
Na2O	3.29	2.70	2.82	3.94	2.50	2.51	2.51
K2O	2.25	3.40	3.27	2.07	3.13	3.11	3.12
P2O5	0.69	0.61	0.72	0.85	0.67	0.67	0.67
Total	100.00	100.00	100.00	100.00	100.00	100.00	100.00
LOI	3.90	2.87	5.50	5.55	1.06	1.06	1.06
An. Total	94.80	96.36	93.58	93.35	98.44	98.40	98.19
mg#	56	55	56	53	54	54	54
Sc^ (ppm)	32.1	-	31.8	31.3	-	-	-
Sc~	36.7	-	36.4	35.0	-	-	-
V	220.0	227.0	219.4	250.3	249.8	247.5	251.5
Cr	519.1	539.0	477.1	443.8	571.3	555.4	585.6
Ni	169.4	152.0	151.6	147.4	189.4	188.0	189.1
Cu	103.9	93.0	100.0	101.7	90.5	89.3	89.7
Zn	87.5	83.0	89.2	90.0	88.8	88.4	87.9
Ga	12.4	15.0	13.1	15.6	18.1	17.4	17.4
As	-	1.0	-	-	2.4	0.0	1.2
Rb^	77.5	62.0	93.3	52.9	83.5	84.5	83.6
Rb~	77.4	-	92.0	51.6	-	-	-
Sr^	919.6	869.0	638.2	1023.2	1136.1	1137.7	1135.9
Sr~	959.5	-	647.3	1051.6	-	-	-
Y^	45.7	38.0	45.7	45.8	31.5	31.2	31.7
Y~	46.1	-	45.2	46.7	-	-	-
Zr^	308.9	266.0	304.4	315.8	257.1	258.5	259.4
Zr~	308.7	-	298.2	309.5	-	-	-
Nb^	6.2	8.0	6.7	5.9	5.7	6.0	6.1
Nb~	6.3	-	6.1	6.2	-	-	-
Mo	-	2.0	-	-	0.0	0.0	0.0
Cs	6.3	-	5.8	13.0	-	-	-
Ba^	623.6	994.0	608.1	702.4	1185.3	1191.8	1186.6
Ba~	612.1	-	593.9	693.0	-	-	-
La^	54.7	-	54.3	63.5	-	-	-
La~	54.8	-	54.1	65.0	-	-	-
Ce^	120.0	-	117.9	141.5	-	-	-
Ce~	121.6	-	120.7	142.1	-	-	-
Pr	17.9	-	17.9	20.9	-	-	-

Total Fe reported as FeO. Fe_2O_3 for MDS samples recalculated to FeO.
Major oxides normalized to 100%.
mg# = 100*MgO/(MgO+FeO)
^XRF
~ICP-MS

APPENDIX F: XRF AND ICP-MS GEOCHEMICAL ANALYSES

	RDS-211	MDS-32	RDS-009	RDS-5	MDS-15	MDS-15 duplicate 1	MDS-15 duplicate 2
Nd^ (ppm)	76.6	-	78.0	88.6	-	-	-
Nd~	77.7	-	78.0	90.1	-	-	-
Sm	18.9	-	19.0	21.4	-	-	-
Eu	5.1	-	5.2	5.6	-	-	-
Gd	16.6	-	16.8	18.1	-	-	-
Tb	2.2	-	2.2	2.3	-	-	-
Dy	10.7	-	10.8	11.1	-	-	-
Ho	1.8	-	1.7	1.8	-	-	-
Er	4.2	-	4.0	4.1	-	-	-
Tm	0.5	-	0.5	0.5	-	-	-
Yb	3.0	-	2.9	2.9	-	-	-
Lu	0.4	-	0.4	0.4	-	-	-
Hf	7.9	-	7.8	8.0	-	-	-
Ta	0.6	-	0.3	0.4	-	-	-
Pb^	8.2	12.0	7.4	7.5	11.9	12.2	13.5
Pb~	7.1	-	6.9	6.6	-	-	-
Th^	8.5	6.0	5.9	6.5	3.6	4.4	5.4
Th~	7.0	-	6.7	7.2	-	-	-
U	2.8	5.0	2.1	2.9	3.0	3.4	3.6

^XRF
~ICP-MS

APPENDIX F: XRF AND ICP-MS GEOCHEMICAL ANALYSES

	MDS-12	RDS-130	RDS-130 duplicate	MDS-31	MDS-11	MDS-14	RDS-013A
SiO2 (wt%)	51.50	50.63	-	51.39	52.10	54.37	51.63
TiO2	1.15	1.60	-	1.26	1.24	1.21	1.18
Al2O3	15.09	15.00	-	14.69	14.69	15.32	14.95
FeO	8.03	10.29	-	8.67	8.18	8.54	8.15
MnO	0.15	0.17	-	0.10	0.15	0.14	0.16
MgO	9.13	8.72	-	8.68	8.51	8.23	7.50
CaO	7.70	8.59	-	6.95	6.97	5.74	8.93
Na2O	4.01	3.06	-	3.03	4.64	3.15	3.11
K2O	2.69	1.47	-	4.63	2.92	2.85	3.84
P2O5	0.55	0.48	-	0.60	0.60	0.47	0.56
Total	100.00	100.00	-	100.00	100.00	100.00	100.00
LOI	3.32	1.95	-	1.52	1.91	1.44	3.07
An. Total	96.09	97.13	-	98.04	97.67	98.18	96.31
mg#	53	46	-	50	51	49	48
Sc^ (ppm)	-	25.2	-	-	-	-	26.4
Sc~	-	27.3	27.6	-	-	-	31.2
V	204.1	230.2	-	188.0	200.3	210.0	212.2
Cr	252.1	381.6	-	241.0	324.2	164.0	319.8
Ni	85.0	188.0	-	83.0	107.8	54.0	108.2
Cu	79.7	64.2	-	80.0	84.3	90.0	83.7
Zn	87.5	100.2	-	86.0	75.0	83.0	82.0
Ga	19.2	18.8	-	18.0	17.8	19.0	16.0
As	0.0	-	-	0.0	7.4	2.0	-
Rb^	153.5	26.8	-	175.0	149.7	117.0	139.8
Rb~	-	26.4	26.5				138.9
Sr^	907.4	698.4	-	872.0	961.8	820.0	990.1
Sr~	-	703.9	710.9				1007.9
Y^	39.0	29.3	-	40.0	35.1	39.0	35.5
Y~	-	29.3	29.5				36.4
Zr^	333.4	207.7	-	319.0	349.6	333.0	331.5
Zr~	-	202.5	204.1				327.1
Nb^	9.4	11.4	-	12.0	10.5	10.0	12.6
Nb~	-	11.1	11.2				12.4
Mo	1.3	-	-	2.0	1.0	1.0	-
Cs	-	0.9	0.9				9.9
Ba^	1007.4	852.1	-	1085.0	1029.9	1014.0	885.9
Ba~	-	829.6	835.6	-	-	-	860.1
La^	-	37.6	-	-	-	-	55.7
La~	-	37.9	38.3	-	-	-	56.2
Ce^	-	79.4	-	-	-	-	116.6
Ce~	-	76.2	77.0	-	-	-	116.5
Pr	-	9.6	9.8	-	-	-	15.1

Total Fe reported as FeO. Fe_2O_3 for MDS samples recalculated to FeO.
Major oxides normalized to 100%.
mg# = 100*MgO/(MgO+FeO)
^XRF
~ICP-MS

APPENDIX F: XRF AND ICP-MS GEOCHEMICAL ANALYSES

	MDS-12	RDS-130	RDS-130 duplicate	MDS-31	MDS-11	MDS-14	RDS-013A
Nd^ (ppm)	-	39.2	-	-	-	-	59.4
Nd~	-	39.4	39.6	-	-	-	60.0
Sm	-	8.2	8.3	-	-	-	12.7
Eu	-	2.3	2.4	-	-	-	3.2
Gd	-	7.1	7.3	-	-	-	10.7
Tb	-	1.1	1.1	-	-	-	1.5
Dy	-	6.1	6.2	-	-	-	7.7
Ho	-	1.2	1.2	-	-	-	1.4
Er	-	3.0	3.1	-	-	-	3.5
Tm	-	0.4	0.4	-	-	-	0.5
Yb	-	2.5	2.5	-	-	-	2.9
Lu	-	0.4	0.4	-	-	-	0.4
Hf	-	5.2	5.3	-	-	-	8.2
Ta	-	0.7	0.7	-	-	-	0.9
Pb^	15.3	9.9	-	15.0	16.3	19.0	15.8
Pb~	-	9.3	9.4	-	-	-	13.4
Th^	12.5	3.4	-	8.0	13.6	17.0	13.5
Th~	-	6.2	6.3	-	-	-	14.5
U	4.3	1.2	1.2	6.0	5.2	6.0	3.8

^XRF
~ICP-MS

APPENDIX F: XRF AND ICP-MS GEOCHEMICAL ANALYSES

	RDS-19	RDS-191	MDS-32 duplicate 1	MDS-32 duplicate 2	02-77-11-1	02-77-11-1 duplicate	MDS-16
SiO2 (wt%)	51.99	54.38	-	-	54.62	54.67	52.48
TiO2	1.26	1.22	-	-	1.22	1.22	1.25
Al2O3	14.75	15.22	-	-	15.38	15.35	15.61
FeO	7.98	8.61	-	-	8.59	8.60	8.10
MnO	0.15	0.15	-	-	0.15	0.15	0.24
MgO	6.89	5.61	-	-	5.33	5.31	4.39
CaO	8.56	8.12	-	-	8.19	8.16	12.95
Na2O	3.25	3.07	-	-	2.92	2.93	3.02
K2O	4.57	3.17	-	-	3.14	3.14	1.60
P2O5	0.61	0.47	-	-	0.47	0.47	0.37
Total	100.00	100.00	-	-	100.00	100.00	100.00
LOI	2.13	2.85	-	-	0.30	-	10.32
An. Total	96.13	95.94	-	-	99.10	99.2	89.14
mg#	46	39	-	-	38	-	35
Sc^ (ppm)	24.5	25.4	-	-	-	-	-
Sc~	27.8	29.4	-	-	-	-	-
V	204.0	211.5	213.0	209.0	224.3	-	181.0
Cr	230.8	156.2	502.0	508.0	181.2	-	432.0
Ni	90.1	56.3	153.0	153.0	54.2	-	191.0
Cu	78.6	91.3	93.0	93.0	93.7	-	57.0
Zn	88.8	87.4	84.0	82.0	91.3	-	71.0
Ga	18.0	17.8	15.0	14.0	19.9	-	19.0
As	-	-	1.0	3.0	1.0	-	0.0
Rb^	174.4	113.6	62.0	60.0	115.8	-	23.0
Rb~	176.6	113.8	-	-	-	-	-
Sr^	964.1	794.1	866.0	867.0	827.4	-	672.0
Sr~	996.1	824.8	-	-	-	-	-
Y^	38.2	37.8	38.0	38.0	38.8	-	23.0
Y~	39.1	38.7	-	-	-	-	-
Zr^	314.6	317.5	264.0	265.0	335.8	-	174.0
Zr~	316.0	315.4	-	-	-	-	-
Nb^	10.8	11.3	8.0	8.0	10.4	-	6.0
Nb~	10.9	12.1	-	-	-	-	-
Mo	-	-	2.0	2.0	1.2	-	0.0
Cs	9.8	2.1	-	-	-	-	-
Ba^	914.7	895.4	977.0	984.0	975.2	-	883.0
Ba~	915.4	888.1	-	-	-	-	-
La^	53.5	51.4	-	-	-	-	-
La~	52.9	50.5	-	-	-	-	-
Ce^	113.0	107.8	-	-	-	-	-
Ce~	111.7	105.4	-	-	-	-	-
Pr	14.9	13.4	-	-	-	-	-

Total Fe reported as FeO. Fe_2O_3 for MDS samples recalculated to FeO.
Major oxides normalized to 100%.
mg# = 100*MgO/(MgO+FeO)
^XRF
~ICP-MS

APPENDIX F: XRF AND ICP-MS GEOCHEMICAL ANALYSES

	RDS-19	RDS-191	MDS-32 duplicate 1	MDS-32 duplicate 2	02-77-11-1	02-77-11-1 duplicate	MDS-16
Nd^ (ppm)	62.0	49.9	-	-	-	-	-
Nd~	60.6	52.4	-	-	-	-	-
Sm	13.3	10.7	-	-	-	-	-
Eu	3.5	2.6	-	-	-	-	-
Gd	11.5	9.2	-	-	-	-	-
Tb	1.6	1.4	-	-	-	-	-
Dy	8.5	7.7	-	-	-	-	-
Ho	1.5	1.5	-	-	-	-	-
Er	3.8	4.0	-	-	-	-	-
Tm	0.5	0.6	-	-	-	-	-
Yb	3.0	3.4	-	-	-	-	-
Lu	0.5	0.5	-	-	-	-	-
Hf	8.1	8.3	-	-	-	-	-
Ta	0.8	1.3	-	-	-	-	-
Pb^	12.7	16.6	14.0	12.0	17.1	-	12.0
Pb~	12.4	15.1	-	-	-	-	-
Th^	9.0	14.7	7.0	5.0	15.7	-	5.0
Th~	9.9	15.6	-	-	-	-	-
U	2.6	3.8	5.0	4.0	5.5	-	2.0

^XRF
~ICP-MS

APPENDIX G.1: ICP-MS PRECISION

Sample: TED, n=54

Element	Average	Std. Dev.
La (ppm)	4.2	0.1
Ce	9.8	0.2
Pr	1.6	0.0
Nd	8.2	0.2
Sm	3.0	0.1
Eu	1.2	0.0
Gd	4.0	0.1
Tb	0.7	0.0
Dy	5.0	0.1
Ho	1.1	0.0
Er	3.1	0.1
Tm	0.5	0.0
Yb	2.9	0.0
Lu	0.5	0.0
Ba	71.2	1.6
Th	0.4	0.0
Nb	2.6	0.1
Y	28.9	0.7
Hf	1.9	0.0
Ta	0.2	0.0
U	0.1	0.0
Pb	0.9	0.1
Rb	4.1	0.3
Cs	0.1	0.0
Sr	208.4	3.5
Sc	47.3	1.8
Zr	60.7	1.0

Precision for samples with prefix "RDS"
Samples analyzed at Washington State University GeoAnalytical Lab

APPENDIX G.2: XRF PRECISION

	R^2	Std. Dev.		R^2	Std. Dev.
Unnormalized Major Elements (Weight %)			**Trace Elements (ppm)**		
SiO_2	0.99929	0.58	Ni	0.9992	3.5
TiO_2	0.99992	0.017	Cr	0.9998	3
Al_2O_3	0.99949	0.16	Sc	0.997	1.6
FeO*	0.99948	0.2	V	0.9996	5
MnO	0.99983	0.002	Ba	0.9997	11.7
MgO	0.99994	0.076	Rb	0.9998	1.7
CaO	0.99976	0.064	Sr	0.99992	4.6
Na_2O	0.99981	0.045	Zr	0.99994	3.9
K_2O	0.99992	0.031	Y	0.9987	1.2
P_2O_5	0.9999	0.005	Nb	0.99987	1.2
			Ga	0.955	2.7
			Cu	0.994	7.4
Normalized Major Elements (Weight %)			Zn	0.9991	3.3
SiO_2	0.99992	0.19	Pb	0.9966	2.6
TiO_2	0.99996	0.012	La	0.9941	5.7
Al_2O_3	0.99987	0.082	Ce	0.996	7.9
FeO*	0.99956	0.18	Th	0.997	1.6
MnO	0.99988	0.002	Nd	0.992	4.3
MgO	0.99994	0.073	U	0.983	2.7
CaO	0.99998	0.043	Bi	0.758	2
Na_2O	0.99989	0.036	Cs	0.365	5.1
K_2O	0.99998	0.015			
P_2O_5	0.99996	0.003			

Precision for samples with prefix "RDS"
Samples analyzed at Washington State University GeoAnalytical Lab
*FeO = Total Fe

APPENDIX H: $^{40}AR/^{39}AR$ ANALYTICAL DATA

	ID	Temp (°C)	$^{40}Ar/^{39}Ar$	$^{37}Ar/^{39}Ar$	$^{38}Ar/^{39}Ar$ (x 10^{-3})	$^{39}Ar_K$ x 10^{-15} mol)	K/Ca	$^{40}Ar^*$ (%)	^{39}Ar (%)	Age (Ma)	±1σ (Ma)
Basaltic samples											
	RDS-1, groundmass concentrate, 26.67 mg, J=0.000878±0.19%, D=1.0055±0.001, NM-183BB, Lab#=55209-01										
xi	A	650	175.7	3.568	532.9	6.21	0.14	10.5	4.5	29.1	1.1
x	B	725	25.60	1.480	22.81	7.90	0.34	74.1	10.3	29.80	0.13
	C	775	20.90	1.519	8.677	6.45	0.34	88.3	15.0	29.00	0.13
	D	825	20.79	1.583	8.868	12.9	0.32	88.0	24.4	28.75	0.10
	E	900	20.19	0.8886	6.420	18.7	0.57	90.9	38.1	28.834	0.079
	F	1000	22.90	0.4399	15.15	29.1	1.2	80.6	59.3	28.970	0.085
	G	1100	27.04	0.4384	28.32	38.7	1.2	69.1	87.6	29.34	0.11
	H	1275	30.15	1.035	39.34	11.6	0.49	61.6	96.1	29.19	0.18
x	I	1725	47.50	3.819	95.69	5.41	0.13	41.0	100.0	30.68	0.30
	Integrated age ± 2σ			n=9		137.1	0.49		K2O=2.25%	**29.19**	**0.26**
	Plateau ± 2σ	steps C-H		n=6	MSWD=4.25	117.6	0.86 ±0.78		85.8	28.97	0.20
	Isochron±2σ	steps B-I		n=8	MSWD=4.23		$^{40}Ar/^{36}Ar$=	309.5±3.8		28.72	0.17
	02-77-11-1, groundmass concentrate, 15.00 mg, J=0.0016388±0.10%, D=1.0052±0.00172, NM-156, Lab#=53418-01										
xi	A	625	725.1	0.6209	2445.7	0.9	0.82	0.3	0.6	6.9	16.2
xi	B	700	72.27	0.5209	212.1	4.5	0.98	13.3	3.2	28.2	1.7
x	C	750	24.05	0.4304	45.57	7.9	1.2	44.2	7.8	31.14	0.53
x	D	800	16.87	0.4285	23.39	12.0	1.2	59.2	14.9	29.30	0.32
x	E	875	12.27	0.4346	8.773	27.1	1.2	79.2	30.9	28.51	0.15
x	F	975	10.51	0.3809	3.326	41.2	1.3	90.9	55.3	28.047	0.094
x	G	1075	10.95	0.4171	5.397	33.8	1.2	85.8	75.2	27.57	0.12
x	H	1250	11.67	1.581	8.852	32.7	0.32	78.7	94.6	26.97	0.14
x	I	1650	13.50	8.547	17.10	9.2	0.060	67.8	100.0	27.03	0.27
	Integrated age ± 2σ			n=9		169.2	0.47		K2O=2.64%	**27.89**	**0.46**
	Plateau ± 2σ	steps H-I		n=2	MSWD=0.04	41.904			24.8	26.98	0.050
	Isochron±2σ	steps C-I		n=7	MSWD=19.83		$^{40}Ar/^{36}Ar$=	314.6±7		27.48	0.19
	MDS-14 gm, groundmass concentrate, 15.32 mg, J=0.0016392±0.10%, D=1.0052±0.00172, NM-156, Lab#=53417-01										
x	A	625	15591.1	0.6963	52887.9	0.0	0.73	-0.3	0.0	-123.1	397.9
x	B	700	417.5	0.8335	1380.1	1.3	0.61	2.3	0.7	28.5	10.0
x	C	750	89.23	0.6459	264.1	2.9	0.79	12.6	2.2	32.9	2.1
	D	800	24.23	0.5922	49.13	7.8	0.86	40.3	6.4	28.64	0.43
	E	875	12.74	0.6930	11.35	24.6	0.74	74.1	19.6	27.74	0.16
	F	975	10.52	0.3842	3.570	45.0	1.3	90.3	43.7	27.881	0.084
	G	1075	11.29	0.2705	6.467	47.8	1.9	83.3	69.3	27.61	0.11
	H	1250	10.34	0.8831	3.498	27.8	0.58	90.7	84.1	27.54	0.10
	I	1650	11.03	3.998	6.652	29.6	0.13	85.2	100.0	27.66	0.13
	Integrated age ± 2σ			n=9		186.8	0.48		K2O=2.86%	27.81	0.44
	Plateau ± 2σ	steps E-I		n=5	MSWD=2.03	174.8	1.1 ±1.4		93.6	**27.70**	**0.15**
	Isochron±2σ	steps A-I		n=9	MSWD=2.25		$^{40}Ar/^{36}Ar$=	297.8±2.7		27.68	0.12
	MDS-15, groundmass concentrate, 14.72 mg, J=0.0016438±0.10%, D=1.0052±0.00172, NM-156, Lab#=53415-01										
xi	A	625	402.9	0.6998	1347.3	0.9	0.73	1.2	0.5	14.2	10.1
xi	B	700	92.50	0.4112	282.9	3.0	1.2	9.6	2.0	26.3	2.4
x	C	750	34.55	0.3012	82.14	4.0	1.7	29.8	4.0	30.30	0.83
x	D	800	18.47	0.2251	31.26	7.1	2.3	50.1	7.5	27.23	0.33
x	E	875	13.99	0.1993	15.22	16.9	2.6	68.0	16.0	27.99	0.20
	F	975	11.24	0.3055	6.950	23.9	1.7	82.0	28.0	27.13	0.13
	G	1075	11.08	0.3686	7.040	31.8	1.4	81.5	44.0	26.60	0.12
	H	1250	10.31	1.020	5.182	96.4	0.50	86.0	92.3	26.122	0.087
	I	1650	12.45	5.331	12.45	15.3	0.096	74.0	100.0	27.23	0.18
	Integrated age ± 2σ			n=9		199.3	0.49		K2O=3.16%	**26.63**	**0.35**
	Plateau ± 2σ	steps F-I		n=4	MSWD=19.59	167.3			84.0	26.56	0.520
	Isochron±2σ	steps C-I		n=7	MSWD=11.90		$^{40}Ar/^{36}Ar$=	318.5±5.9		26.16	0.19

APPENDIX H: $^{40}AR/^{39}AR$ ANALYTICAL DATA

	ID	Temp (°C)	$^{40}Ar/^{39}Ar$	$^{37}Ar/^{39}Ar$	$^{36}Ar/^{39}Ar$ (x 10^{-3})	$^{39}Ar_K$ x 10^{-15} mol)	K/Ca	$^{40}Ar^*$ (%)	^{39}Ar (%)	Age (Ma)	±1σ (Ma)
	MDS-16, groundmass concentrate, 15.85 mg, J=0.0016417±0.10%, D=1.0052±0.00172, NM-156, Lab#=53416-01										
x	A	625	17871.9	1.874	60932.6	0.0	0.27	-0.8	0.0	-460.4	704.2
x	B	700	83.43	1.285	237.8	1.7	0.40	15.9	1.6	38.9	2.3
	C	750	16.24	1.112	21.81	1.3	0.46	60.9	2.8	29.1	1.1
	D	800	12.00	0.9505	7.289	4.2	0.54	82.7	6.8	29.17	0.34
	E	875	10.18	0.9250	1.981	12.7	0.55	95.0	19.0	28.45	0.13
	F	975	9.749	0.8035	0.5630	19.7	0.63	99.0	37.8	28.370	0.097
	G	1075	10.24	0.5602	2.277	22.9	0.91	93.9	59.7	28.266	0.099
	H	1250	11.08	0.6107	5.285	33.0	0.84	86.4	91.3	28.14	0.12
	I	1650	14.07	1.532	15.53	9.1	0.33	68.3	100.0	28.26	0.29
	Integrated age ± 2σ			n=9		104.6	0.65		K2O=1.54%	28.45	0.29
	Plateau ± 2σ	steps C-I		n=7	MSWD=1.72	102.9	0.72 ±0.41		98.4	**28.33**	**0.15**
	Isochron±2σ	steps A-I		n=9	MSWD=3.72		$^{40}Ar/^{36}Ar$=	300.4±4.2		28.30	0.13
	Highly altered basaltic samples										
	RDS-4, groundmass concentrate, 31.2 mg, J=0.0008987±0.41%, D=1.0055±0.001, NM-183C, Lab#=55218-01										
x	A	650	261.8	0.6934	797.9	5.66	0.74	9.9	32.0	41.5	1.7
	B	725	36.77	0.4204	61.54	3.93	1.2	50.6	54.2	29.88	0.26
	C	775	29.66	0.7870	37.94	0.701	0.65	62.4	58.2	29.73	0.73
	D	825	27.24	0.6559	33.68	0.717	0.78	63.6	62.3	27.86	0.70
	E	900	25.84	1.680	31.50	0.782	0.30	64.5	66.7	26.81	0.63
	F	1000	24.51	0.5181	20.02	1.97	0.98	76.0	77.8	29.93	0.28
	G	1100	35.57	0.6402	57.67	2.46	0.80	52.2	91.7	29.82	0.36
xi	H	1275	137.2	1.342	361.4	0.519	0.38	22.1	94.6	48.6	1.8
xi	I	1725	351.0	2.287	1011.7	0.949	0.22	14.8	100.0	82.3	2.6
	Integrated age ± 2σ			n=9		17.7	0.67		K2O=0.24%	36.9	1.5
	Plateau ± 2σ	steps B-G		n=6	MSWD=5.79	10.557	0.939±0.616		59.7	29.59	0.784
	Isochron±2σ	steps A-G		n=7	MSWD=5.27		$^{40}Ar/^{36}Ar$=	305.2±2.8		**28.93**	**0.46**
	RDS-6, groundmass concentrate, 27.55 mg, J=0.0008877±0.37%, D=1.0055±0.001, NM-183G, Lab#=55239-01										
x	A	650	151.8	0.3517	458.0	40.3	1.5	10.7	37.0	25.91	0.97
	B	725	104.8	1.007	307.6	18.2	0.51	13.2	53.7	22.07	0.65
	C	775	69.99	4.406	197.5	3.76	0.12	17.0	57.1	18.99	0.53
	D	825	30.09	3.582	68.67	4.28	0.14	33.4	61.0	16.05	0.25
	E	900	31.08	3.774	67.30	3.76	0.14	36.9	64.5	18.30	0.32
i	F	1000	44.43	0.9648	98.84	3.98	0.53	34.3	68.1	24.25	0.40
i	G	1100	33.63	1.226	62.36	12.8	0.42	45.4	79.9	24.30	0.20
xi	H	1275	117.2	8.394	326.6	19.9	0.061	18.1	98.2	33.84	0.70
xi	I	1725	918.4	12.92	2968.2	2.01	0.039	4.5	100.0	65.6	6.2
	Integrated age ± 2σ			n=9		109.0	0.19		K2O=1.71%	26.5	1.4
	Plateau ± 2σ	steps B-G		n=6	MSWD=166.8	46.750			42.9	20.93	3.200
	Isochron±2σ	steps A-E		n=5	MSWD=10		$^{40}Ar/^{36}Ar$=	309±4		15.40	0.90
	Analcime-bearing samples, Spears Ranch Dike										
	RDS-2, groundmass concentrate, 29.12 mg, J=0.0008783±0.40%, D=1.0055±0.001, NM-183C, Lab#=55219-01										
x	A	650	88.25	0.2731	258.4	40.6	1.9	13.4	10.1	18.59	0.54
x	B	725	25.14	0.0735	27.54	24.2	6.9	67.6	16.1	26.69	0.11
x	C	775	24.89	0.0716	24.71	9.86	7.1	70.6	18.5	27.60	0.14
x	D	825	25.48	0.0845	25.43	13.6	6.0	70.5	21.9	28.20	0.12
x	E	900	22.37	0.0903	15.97	25.3	5.6	78.9	28.2	27.704	0.083
x	F	1000	20.81	0.0828	11.39	42.4	6.2	83.8	38.7	27.385	0.069
x	G	1100	20.37	0.1057	13.25	63.5	4.8	80.8	54.4	25.842	0.071
	H	1275	21.74	1.261	20.11	156.9	0.40	73.1	93.3	24.993	0.083
	I	1725	25.79	4.326	34.52	26.9	0.12	61.7	100.0	25.10	0.11
	Integrated age ± 2σ			n=9		403.3	0.60		K2O=6.06%	**25.21**	**0.30**
	Plateau ± 2σ	steps H-I		n=2	MSWD=0.58	183.8	0.363±0.406		45.6	25.03	0.239
	Isochron±2σ	steps A-I		n=9	MSWD=160		$^{40}Ar/^{36}Ar$=	276±16		27.20	0.60

APPENDIX H: $^{40}AR/^{39}AR$ ANALYTICAL DATA

	ID	Temp (°C)	$^{40}Ar/^{39}Ar$	$^{37}Ar/^{39}Ar$	$^{36}Ar/^{39}Ar$ (x 10^{-3})	$^{39}Ar_K$ x 10^{-15} mol)	K/Ca	$^{40}Ar^*$ (%)	^{39}Ar (%)	Age (Ma)	±1σ (Ma)
	MDS-11, groundmass concentrate, 13.96 mg, J=0.0016409±0.10%, D=1.0052±0.00172, NM-156, Lab#=53419-01										
xi	A	625	507.6	1.024	1703.1	0.5	0.50	0.9	0.1	12.9	15.4
xi	B	700	27.58	0.1753	66.37	7.5	2.9	28.9	2.4	23.46	0.57
x	C	750	14.72	0.0991	18.66	6.8	5.1	62.6	4.4	27.06	0.27
x	D	800	12.87	0.0840	12.31	11.9	6.1	71.8	8.0	27.15	0.18
x	E	875	11.37	0.0982	7.114	26.6	5.2	81.6	16.1	27.25	0.13
x	F	975	10.70	0.1605	5.361	30.5	3.2	85.3	25.8	26.81	0.11
x	G	1075	10.41	0.1244	5.543	38.7	4.1	84.4	38.4	25.82	0.11
	H	1250	10.63	0.2868	7.208	120.3	1.8	80.2	81.3	25.072	0.097
	I	1650	10.93	3.169	9.015	48.0	0.16	78.0	100.0	25.12	0.11
	Integrated age ± 2σ			n=9		290.8	0.73		K2O=4.88%	**25.63**	**0.24**
	Plateau ± 2σ	steps-H-I		n=2	MSWD=0.09	168.363			61.6	25.09	0.160
	Isochron±2σ	steps C-I		n=7	MSWD=63.82		$^{40}Ar/^{36}Ar$=	335.4±13.7		25.18	0.30
	MDS 31, groundmass concentrate, 21.71 mg, J=0.0007318±0.00%, D=1.0058±0.001, NM-172, Lab#=54428-01										
xi	A	625	677.2	1.635	2259.5	0.6	0.31	1.4	0.4	12.4	5.1
xi	B	700	53.01	0.2474	116.6	8.7	2.1	35.0	5.3	24.35	0.30
xi	C	750	31.27	0.2193	36.05	3.5	2.3	66.0	7.2	27.04	0.24
xi	D	800	29.91	0.1857	30.43	12.2	2.7	70.0	14.1	27.42	0.13
xi	E	875	30.68	0.1773	32.91	15.4	2.9	68.3	22.8	27.47	0.14
xi	F	975	28.49	0.1819	27.11	19.6	2.8	71.9	33.9	26.85	0.12
	G	1075	25.33	0.1263	17.64	25.6	4.0	79.5	48.4	26.382	0.085
	H	1250	24.88	0.4602	17.11	59.3	1.1	79.8	81.9	26.044	0.077
	I	1700	25.86	2.873	20.57	32.1	0.18	77.4	100.0	26.285	0.091
	Integrated age ± 2σ			n=9		177.1	0.67		K2O=4.28%	**26.34**	**0.17**
	Plateau ± 2σ	steps G-I		n=3	MSWD=4.64	117.1			66.1	26.22	0.270
	Isochron±2σ	steps D-I		n=6	MSWD=1.97		$^{40}Ar/^{36}Ar$=	361±12.8		24.69	0.37
	MDS 32, groundmass concentrate, 22.27 mg, J=0.000738±0.10%, D=1.0058±0.001, NM-172, Lab#=54430-01										
x	A	625	1322.2	0.5149	4463.0	1.2	0.99	0.2	1.0	3.9	8.5
x	B	700	83.33	0.0939	218.7	8.4	5.4	22.4	7.5	24.70	0.47
x	C	750	56.66	0.1140	122.7	3.2	4.5	36.0	10.0	26.94	0.52
x	D	800	76.16	0.0813	189.6	6.5	6.3	26.4	15.1	26.59	0.49
x	E	875	63.61	0.0931	143.2	9.3	5.5	33.5	22.3	28.13	0.35
x	F	975	34.39	0.0843	46.58	16.4	6.1	60.0	35.1	27.25	0.18
x	G	1075	26.78	0.1000	24.36	17.9	5.1	73.1	49.1	25.89	0.10
	H	1250	24.76	0.9651	20.11	42.1	0.53	76.3	82.0	24.997	0.082
	I	1700	27.22	6.026	29.38	23.1	0.085	69.9	100.0	25.27	0.12
	Integrated age ± 2σ			n=9		128.2	0.35		K2O=3.00%	**25.61**	**0.39**
	Plateau ± 2σ	steps H-I		n=2	MSWD=3.78	65.2			51.9	26.04	0.13
	Isochron±2σ	steps A-I		n=9	MSWD=29		$^{40}Ar/^{36}Ar$=	299±5		26.40	0.40
	Analcime-bearing sample, other										
	RDS-5, groundmass concentrate, 27.37 mg, J=0.0008784±0.44%, D=1.0055±0.001, NM-183C, Lab#=55220-01										
x	A	650	212.8	0.7030	663.5	16.0	0.73	7.8	11.3	26.0	1.4
x	B	725	45.97	0.6051	75.03	6.37	0.84	51.8	15.9	37.34	0.28
x	C	775	45.41	0.9111	72.67	3.73	0.56	52.8	18.5	37.60	0.31
x	D	825	40.36	0.6971	55.95	6.81	0.73	59.1	23.3	37.40	0.25
x	E	900	35.51	0.2058	41.34	16.4	2.5	65.6	34.9	36.50	0.16
x	F	1000	24.59	0.1639	15.12	24.4	3.1	81.9	52.2	31.58	0.10
	G	1100	21.54	0.4290	9.684	17.3	1.2	86.8	64.5	29.374	0.084
	H	1275	23.87	4.541	18.46	45.3	0.11	78.7	96.6	29.580	0.089
	I	1725	53.94	11.23	121.6	4.82	0.045	35.0	100.0	29.87	0.39
	Integrated age ± 2σ			n=9		141.1	0.24		K2O=2.25%	**31.31**	**0.53**
	Plateau ± 2σ	steps G-I		n=3	MSWD=1.92	67.428	0.384±1.284		47.8	29.48	0.306
	Isochron±2σ	steps A-I		n=9	MSWD=340		$^{40}Ar/^{36}Ar$=	330±20		30.30	1.20

APPENDIX H: $^{40}AR/^{39}AR$ ANALYTICAL DATA

	ID	Temp (°C)	$^{40}Ar/^{39}Ar$	$^{37}Ar/^{39}Ar$	$^{36}Ar/^{39}Ar$ (x 10^{-3})	$^{39}Ar_K$ x 10^{-15} mol)	K/Ca	$^{40}Ar^*$ (%)	^{39}Ar (%)	Age (Ma)	±1σ (Ma)
Minette samples											
	RDS-3, groundmass concentrate, 9.15 mg, J=0.0008649±0.11%, D=1.0055±0.001, NM-183E, Lab#=55230-01										
Xi	A	650	123.5	0.4013	403.0	1.68	1.3	3.5	0.8	6.7	1.0
Xi	B	750	67.74	1.490	187.7	1.43	0.34	18.2	1.6	19.13	0.73
	C	850	29.30	0.0339	37.19	23.3	15.0	62.4	13.2	28.28	0.12
	D	920	23.63	0.0400	16.67	31.9	12.7	79.1	29.1	28.910	0.077
	E	1000	20.98	0.0295	7.688	28.0	17.3	89.2	43.1	28.919	0.060
	F	1075	20.84	0.0126	6.442	39.0	40.6	90.8	62.7	29.259	0.055
	G	1110	19.60	0.0173	3.943	23.6	29.5	94.0	74.5	28.497	0.047
	H	1180	19.58	0.0195	4.067	30.9	26.2	93.9	89.9	28.408	0.051
	I	1210	19.84	0.0599	5.244	10.7	8.5	92.2	95.3	28.271	0.076
	J	1250	19.03	0.0175	2.136	6.82	29.2	96.7	98.7	28.438	0.086
	K	1300	20.61	0.1252	7.442	2.23	4.1	89.4	99.8	28.46	0.21
	L	1725	193.8	9.380	592.2	0.435	0.054	10.0	100.0	30.2	1.9
	Integrated age ± 2σ			n=12		200.0	8.3		K2O=9.71%	28.48	0.14
	Plateau ± 2σ	steps C-L		n=10	MSWD=25.11	196.872	23.513±25.612		98.4	28.67	0.233
	Isochron±2σ	steps C-L		n=10	MSWD=27.68		$^{40}Ar/^{36}Ar$=	298.5±3.1		28.643	0.085
	RDS-106, Biotite, 7.53 mg, J=0.0013612±0.07%, D=1.002±0.001, NM-202H, Lab#=56755-01										
xi	A	650	30.42	0.2514	86.24	3.36	2.0	16.3	3.0	12.10	0.42
xi	B	750	54.01	1.373	121.7	3.17	0.37	33.6	5.8	44.04	0.55
xi	C	850	30.20	0.0651	24.56	8.04	7.8	76.0	13.0	55.47	0.19
xi	D	920	17.09	0.0149	5.718	11.8	34.3	90.1	23.6	37.416	0.089
i	E	1000	14.95	0.0127	3.748	18.7	40.3	92.6	40.2	33.657	0.071
i	F	1075	15.21	0.0114	2.965	21.8	44.7	94.2	59.6	34.835	0.062
i	G	1110	14.58	0.0161	2.218	10.9	31.7	95.5	69.4	33.863	0.076
i	H	1180	14.63	0.0261	2.989	8.62	19.6	94.0	77.1	33.417	0.091
i	I	1210	14.28	0.0203	1.854	8.46	25.2	96.2	84.6	33.395	0.089
xi	J	1250	13.87	0.0127	2.930	11.5	40.1	93.8	94.9	31.634	0.074
xi	K	1300	13.03	0.0119	2.972	5.13	42.8	93.3	99.5	29.56	0.12
xi	L	1700	20.12	0.4660	45.35	0.593	1.1	33.5	100.0	16.50	0.97
	Integrated age ± 2σ			n=12		112.2	7.7		K2O=4.20%	35.01	0.15
	Plateau ± 2σ	steps E-I		n=5	MSWD=73.06	68.473			61.1	37.40	0.300
	Isochron±2σ	no isochron									

APPENDIX H: $^{40}AR/^{39}AR$ ANALYTICAL DATA

	ID	$^{40}Ar/^{39}Ar$	$^{37}Ar/^{39}Ar$	$^{36}Ar/^{39}Ar$ (x 10^{-3})	$^{39}Ar_K$ (x 10^{-15} mol)	K/Ca	$^{40}Ar^*$ (%)	Age (Ma)	±1σ (Ma)
	RDS-3, biotite, J=0.00086±1.00%, D=1.0063±0.001, NM-183E, Lab#=55230								
	07A	52.95	0.1294	119.9	0.696	3.9	33.1	26.97	0.66
	04B	18.80	0.0209	3.437	0.632	24.5	94.6	27.34	0.31
	16	24.22	-0.0047	21.15	0.760	-	74.2	27.62	0.36
	13	19.48	0.0438	4.995	3.015	11.7	92.4	27.68	0.11
	10	21.54	0.0359	11.71	0.672	14.2	83.9	27.80	0.32
	06B	18.57	0.0428	1.568	0.631	11.9	97.5	27.84	0.32
	14	20.38	0.0037	7.536	4.595	138.1	89.1	27.909	0.085
	12	21.54	-0.0022	11.05	2.686	-	84.8	28.09	0.13
	03B	18.60	0.0114	0.9396	1.015	44.7	98.5	28.17	0.22
	06A	20.09	-0.0047	5.921	1.296	-	91.3	28.19	0.22
	05A	21.83	0.0085	11.80	3.466	59.8	84.0	28.20	0.12
	17	20.97	0.0476	8.791	0.939	10.7	87.6	28.25	0.26
	03A	20.95	0.0157	8.627	4.225	32.4	87.8	28.28	0.11
	04A	21.16	0.0831	9.342	3.693	6.1	87.0	28.29	0.13
	15	28.73	0.0328	34.86	2.056	15.6	64.1	28.33	0.19
	08A	41.20	0.0922	76.86	0.553	5.5	44.9	28.44	0.51
	05B	19.26	0.0047	2.518	0.554	107.7	96.1	28.46	0.32
	02B	19.25	0.0091	2.378	0.956	55.9	96.4	28.50	0.24
	02A	25.61	0.0232	23.85	3.163	22.0	72.5	28.53	0.15
	11	24.79	0.0194	21.02	1.361	26.3	74.9	28.56	0.21
	07B	21.04	0.0595	8.317	0.612	8.6	88.3	28.57	0.33
	09	21.33	0.0020	9.209	2.448	255.5	87.2	28.60	0.15
	18	35.32	0.0281	54.93	0.970	18.1	54.0	29.33	0.34
#	08B	21.25	0.0658	1.253	0.114	7.8	98.3	32.1	1.5
	Mean age ± 2σ				43.7 ±113.7			**28.16**	**0.58**
			n=23	MSWD=3.64					

Isotopic ratios corrected for blank, radioactive decay, and mass discrimination, not corrected for interfering reactions.
Errors quoted for individual analyses include analytical error only, without interfering reaction or J uncertainties.
Integrated age calculated by summing isotopic measurements of all steps.
Integrated age error calculated by quadratically combining errors of isotopic measurements of all steps.
Plateau age is inverse-variance-weighted mean of selected steps.
Plateau age error is inverse-variance-weighted mean error (Taylor, 1982) times root MSWD where MSWD>1.
Plateau error is weighted error of Taylor (1982).
Mean age is weighted mean age of Taylor (1982). Mean age error is weighted error of the mean (Taylor, 1982), multiplied by the root of the MSWD where MSWD>1, and also incorporates uncertainty in J factors and irradiation correction uncertainties.
Decay constants and isotopic abundances after Steiger and Jäger (1977).
x-symbol preceding sample ID denotes analyses excluded from plateau age calculations.
i-symbol preceding sample ID denotes analyses excluded from isochron age calculations.
#-synmbol preceding sample ID denotes analysis excluded from mean age calculations.
Weight percent K_2O calculated from ^{39}Ar signal, sample weight, and instrument sensitivity.
Ages calculated relative to FC-2 Fish Canyon Tuff sanidine interlaboratory standard at 28.02 Ma
Decay Constant (LambdaK (total)) = 5.543e-10/a
Correction factors for respective irradiation numbers:

NM-156

$(^{39}Ar/^{37}Ar)_{Ca}$ = 0.0007 ± 2e-05
$(^{36}Ar/^{37}Ar)_{Ca}$ = 0.00028 ± 5e-06
$(^{38}Ar/^{39}Ar)_{K}$ = 0.01077
$(^{40}Ar/^{39}Ar)_{K}$ = 0.0002 ± 0.0003

NM-183

$(^{39}Ar/^{37}Ar)_{Ca}$ = 0.00077 ± 2e-05
$(^{36}Ar/^{37}Ar)_{Ca}$ = 0.000276 ± 5e-06
$(^{38}Ar/^{39}Ar)_{K}$ = 0.0127
$(^{40}Ar/^{39}Ar)_{K}$ = 0.03 ± 0.002

NM-166

$(^{39}Ar/^{37}Ar)_{Ca}$ = 0.0007 ± 2e-05
$(^{36}Ar/^{37}Ar)_{Ca}$ = 0.00028 ± 5e-06
$(^{38}Ar/^{39}Ar)_{K}$ = 0.01077
$(^{40}Ar/^{39}Ar)_{K}$ = 0.0002 ± 0.0003

NM-202

$(^{39}Ar/^{37}Ar)_{Ca}$ = 0.0007 ± 5e-05
$(^{36}Ar/^{37}Ar)_{Ca}$ = 0.00028 ± 1e-05
$(^{38}Ar/^{39}Ar)_{K}$ = 0.01077
$(^{40}Ar/^{39}Ar)_{K}$ = 0 ± 0.0004

NM-172

$(^{39}Ar/^{37}Ar)_{Ca}$ = 0.0007 ± 5e-05
$(^{36}Ar/^{37}Ar)_{Ca}$ = 0.00028 ± 1e-05
$(^{38}Ar/^{39}Ar)_{K}$ = 0.01077
$(^{40}Ar/^{39}Ar)_{K}$ = 0 ± 0.0004

APPENDIX I $^{40}AR/^{39}AR$ GEOCHRONOLOGY OF TWO DIKES OUTSIDE THE RILEY DIKE SWARM

The ages of two dikes outside the Riley Dike Swarm were analyzed by the $^{40}Ar/^{39}Ar$ method. Both dikes contain K-bearing phases: one dike is sanidine-bearing and the second is a hornblende porphyry. The sanidine-bearing dike near Pie Town, New Mexico, west of Riley, is also part of the MRDS. The hornblende porphyry dike west of Riley was recognized by Tonking (1957). The mineral assemblage—hornblende, biotite, plagioclase, and quartz—of the hornblende porphyry dike is unusual for the MRDS. The unusual mineralogy and freshness of the outcrops of the hornblende porphyry dike suggest that it is not part of the MRDS.

I.1 Hornblende porphyry dike

Hornblende separated from the hornblende porphyry dike for $^{40}Ar/^{39}Ar$ dating was also probed for mineral chemistry. This dike also contains abundant biotite, feldspar, and quartz with reaction rims suggesting the quartz is xenocrystic.

A hornblende separate from the hornblende porphyry dike (RDS-283) west of the Riley area was analyzed by bulk furnace step-heating. Early steps show significant scatter in age, 40Ar*, and K/Ca (Fig. 72). Steps E-I have relatively high $^{40}Ar^*$, a relatively constant K/Ca of ~0.15, and form a plateau of age 24.41±0.15 Ma with an acceptable MSWD of 2.01.

The plateau is concordant with the integrated age and the isochron age. Steps D-I form an isochron of age 24.47±0.20 Ma, an atmospheric intercept (292.7±7.7), and an MSWD of 1.81. An isochron formed using all 10 steps has an age of 24.39±0.13 Ma, an

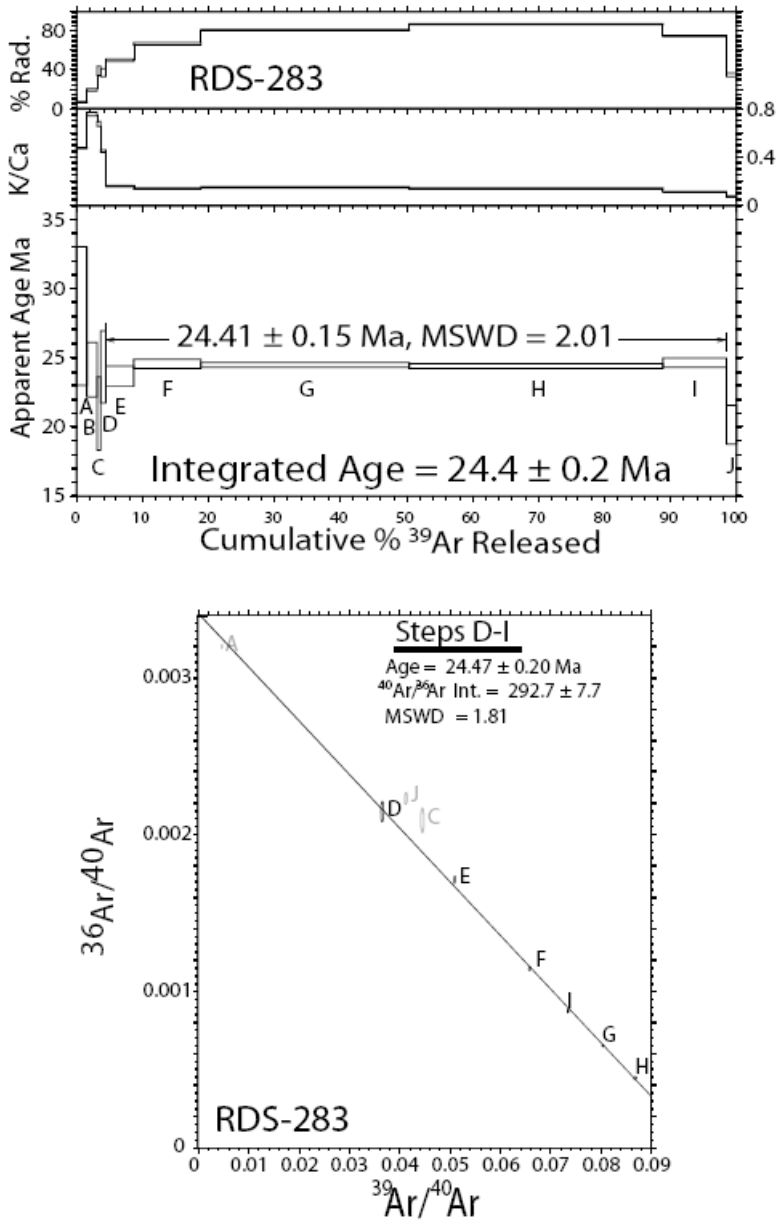

Figure 72. Age spectrum and isochron diagram for hornblende separate sample RDS-283.

intercept of 295.0±2.6, but an elevated MSWD of 6.45. Steps C and J are disturbed and fall off the isochron.

I.2 Sanidine-bearing dike

One dike from the Pie Town subswarm of the MRDS west of Riley contains sanidine xenocrysts. These sanidine crystals appear partially resorbed which suggests that their argon gas content, and therefore age, has been reset to the age of dike emplacement. Feldspar crystals from this dike were picked and analyzed for composition and suitability for $^{40}Ar/^{39}Ar$ age determination. The dike contains plagioclase in addition to sanidine.

Sample MDS-26 from the Pie Town subswarm west of the Riley subswarm of the MRDS was analyzed as groundmass concentrate by furnace step-heating and as a sanidine mineral separate by CO_2 laser fusion and bulk CO_2 laser step-heating.

Age spectra of the groundmass concentrate and sanidine separate are different—the groundmass sample has a hump-shaped spectrum—but some middle steps appear concordant at ~27 Ma (Fig. 73). The integrated age of the mineral separate is ~3 Ma older than the integrated age of the groundmass concentrate. Both samples are highly radiogenic but the $^{40}Ar^*$ of the sanidine separate is slightly higher. K/Ca values for the sanidine separate are much lower than expected for pure sanidine. K/Ca values of the two samples are opposites; values for the groundmass are higher than those for sanidine in the early steps and lower than sanidine in later steps. This must be caused by the presence of pyroxene and other phases in the groundmass sample. Neither sample is isochronous.

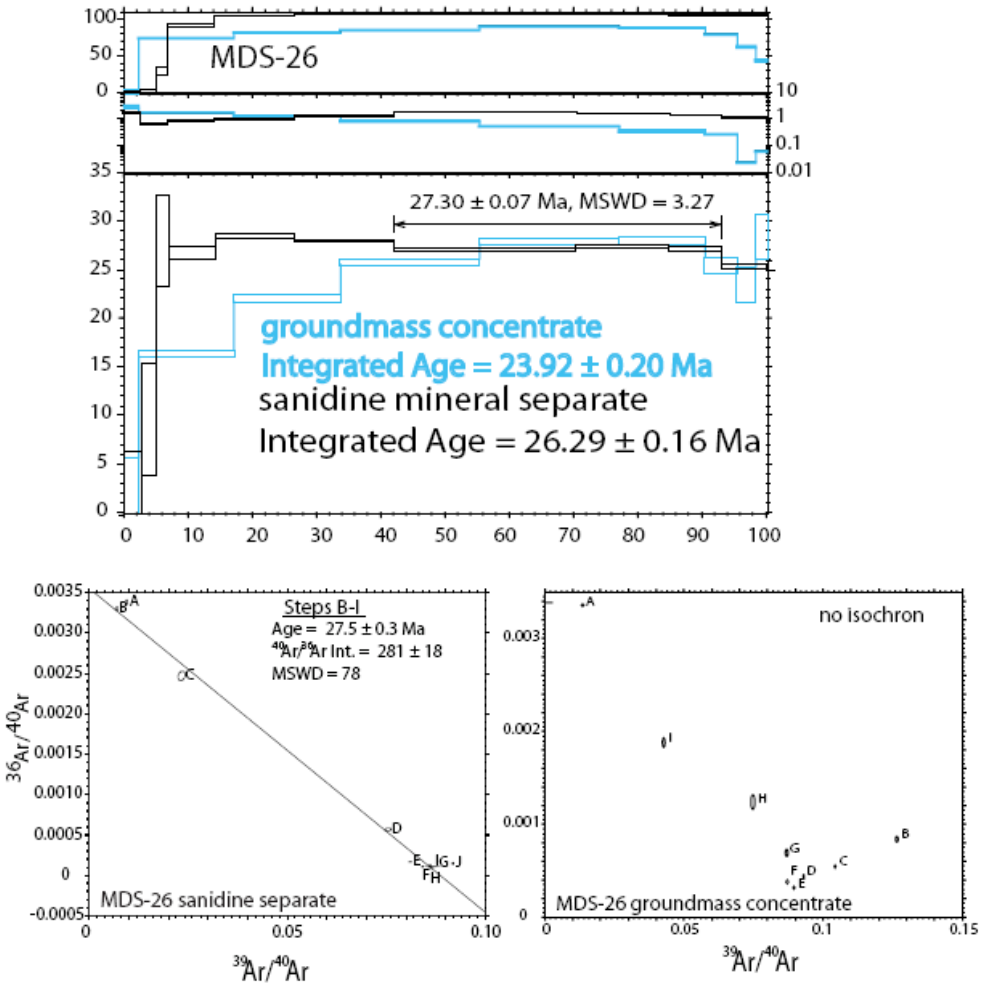

Figure 73. Age spectra and isochron diagrams for the sanidine-bearing dike MDS-26.

Laser fusion analysis of four individual feldspar crystals reveal an impure sanidine separate (Fig. 74). One crystal has a typical sanidine K/Ca of 59.2 and K/Ca values of the other three crystals are less than 10. Two crystals with K/Ca values of 6.1 and 9.0 may be unclean sanidine with adhered groundmass. The fourth crystal is likely plagioclase. The plagioclase and one other crystal have negative $^{36}Ar/^{39}Ar$ values and ^{40}Ar over 100% and are removed from the age calculation.

I.3 Conclusions

The hornblende separate contains only 0.89 wt% K_2O but provides a more precise age than even the sanidine separate. The hornblende porphyry dike is ~3 Ma younger than the Riley dikes, is west of the Riley area, and has a mineral assemblage not seen in the Riley area and probably has a completely different petrogenetic history. Though the sanidine-bearing dike is not from Riley, it is expected to have a similar age to the Riley dikes because it is part of the MRDS. The low amount of K_2O in the sanidine separate (1.67 wt%) is not much higher than the groundmass concentrate from the same sample (1.05 wt%) and indicates that it is impure and diluted by a phase such as plagioclase.

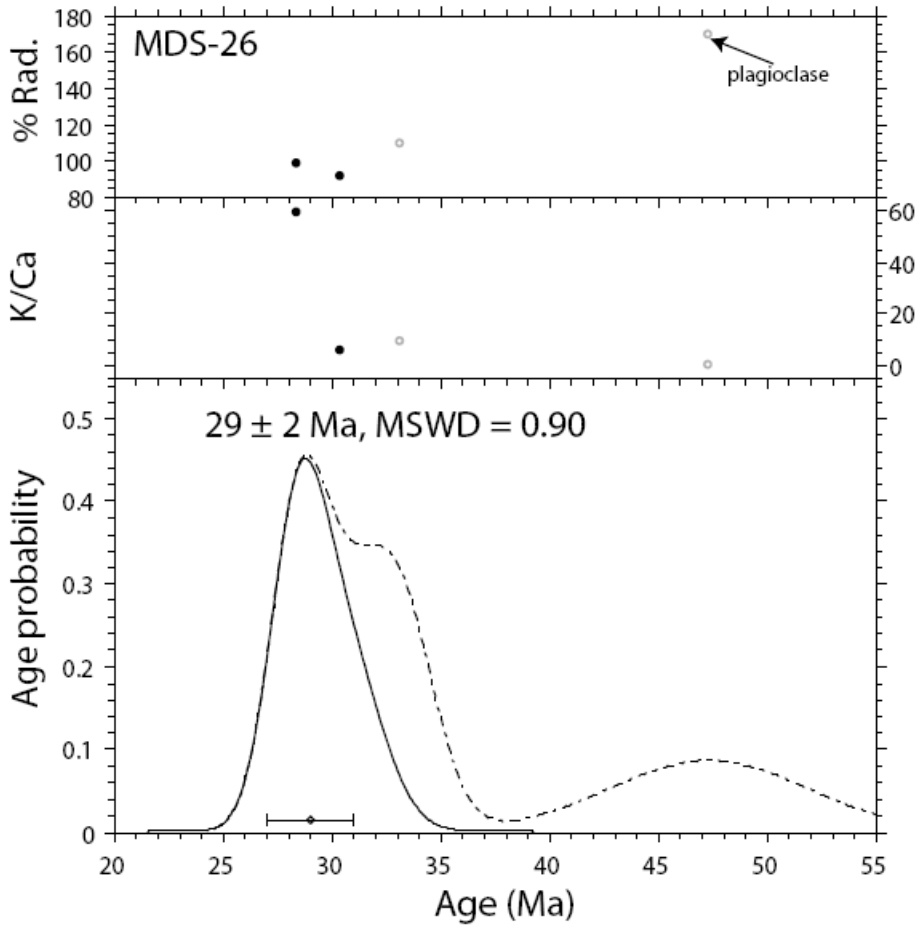

Figure 74. Age probability diagram for single crystal laser fusion analyses of sanidine mineral separate from sample MDS-26.

Plate 1: Geologic map of Oligocene mafic dikes near Riley, Socorro County, New Mexico

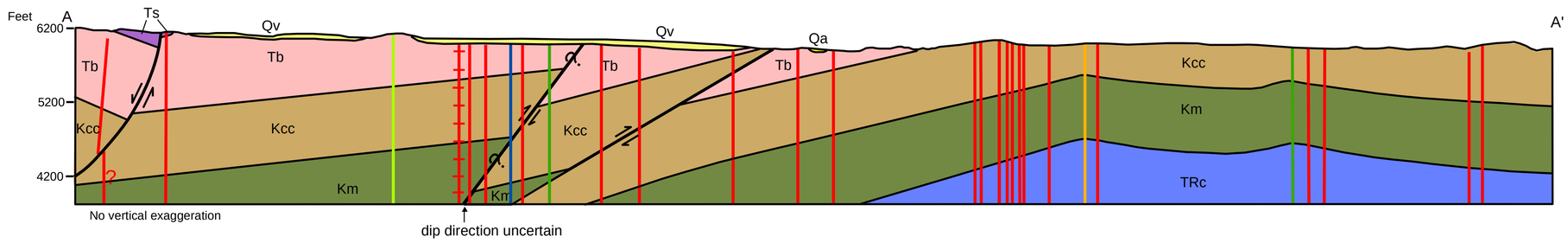

Legend

Geologic Units

Qa	Intermittent stream deposits (Holocene).
Qco	Colluvium. Dike collapse deposits (Pleistocene).
Qv	Alluvial valley deposits (Middle to late Pleistocene).
QTsp	Tan, moderately cemented alluvial gravels and sandstones. Piedmont facies of the Sierra Ladrones Formation (Pliocene to early Pleistocene).
Tis	Basaltic sills
Ts	Spears Formation: purplish gray volcaniclastic sediments.
Tb	Baca Formation: red to tan coarse- to fine-grained sandstones and arkosic conglomerates.
Kcc	Crevasse Canyon Formation: tan shaley siltstone, sandstone, and minor coal.
Km	Pre-Crevasse Canyon Cretaceous strata, mostly marine Thickness from Massingill (1979; in cross section only)
TRc	Chinle Group, from Massingill (1979; in cross section only)

Map Symbols

- Formation contact
- Thrust fault
- Thrust fault, inferred
- Monocline
- Monocline, approximate
- Anticline
- Syncline
- Fault, concealed
- Fault, approximately located
- U / D — Normal fault, relative movement up (U) or down (D), ball and bar on downthrown block
- Dike, pyroxene porphyry
- Dike, basaltic (undifferentiated)
- Dike with wide contact metamorphic aureole, interpreted as a feeder dike for the La Jara Peak Basaltic Andesite
- Dike, basaltic with significant biotite
- Dike, minette
- Dike, analcime-bearing
- Dike, analcime-bearing, speckled texture

May 2008

by

Melissa Dimeo

New Mexico Institute of Mining and Technology

Base map from U.S. Geological Survey 1984, from photographs taken 1976, field checked in 1976, edited in 1984.
1927 North American datum, UTM projection -- zone 13
1000-meter Universal Transverse Mercator grid, zone 13, shown in red

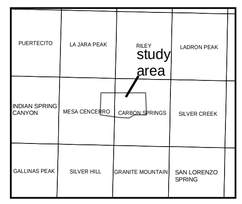

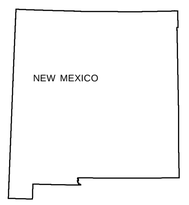

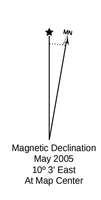

QUADRANGLE LOCATION

1:12,000

0.4 0.2 0 0.4 MILE

500 0 500 1000 1500 2000 2500 3000 3500 FEET

0.6 0.3 0 0.6 KILOMETER

MESA CENCERRO CONTOUR INTERVAL 40 FEET
CARBON SPRINGS CONTOUR INTERVAL 20 FEET
NATIONAL GEODETIC VERTICAL DATUM OF 1929